

Distribution Agreement

In presenting this thesis or dissertation as a partial fulfillment of the requirements for an advanced degree from Emory University, I hereby grant to Emory University and its agents the non-exclusive license to archive, make accessible, and display my thesis or dissertation in whole or in part in all forms of media, now or hereafter known, including display on the world wide web. I understand that I may select some access restrictions as part of the online submission of this thesis or dissertation. I retain all ownership rights to the copyright of the thesis or dissertation. I also retain the right to use in future works (such as articles or books) all or part of this thesis or dissertation.

Signature:

Kathryn Crotty

Date

Alveolar Macrophage Oxidative Stress and Metabolic Dysfunction During Chronic Alcohol Use

By

Kathryn M. Crotty

Doctor of Philosophy

Graduate Division of Biological and Biomedical Science
Molecular & Systems Pharmacology

Samantha M. Yeligar, M.S., Ph.D.
Advisor

Eric Ortlund, Ph.D.
Committee Member

Kathy Griendling, Ph.D.
Committee Member

Roy Sutliff, Ph.D.
Committee Member

Accepted:

Kimberly Jacob Arriola, Ph.D., M.P.H.

Dean of the James T. Laney School of Graduate Studies

Date

**Alveolar Macrophage Oxidative Stress and Metabolic Dysfunction During Chronic
Alcohol Use**

By

Kathryn Crotty, B.S.

Florida State University

Advisor: Samantha M. Yeligar, M.S., Ph.D.

An abstract of a dissertation submitted to the Faculty of the James T. Laney School of Graduate Studies of Emory University in partial fulfillment of the requirements for the degree of Doctor of Philosophy in Graduate Division of Biological and Biomedical Science, Molecular & Systems Pharmacology

2024

Abstract

Alveolar Macrophage Oxidative Stress and Metabolic Dysfunction During Chronic Alcohol Use

By Kathryn Crotty, B.S.

Nearly 11% of the adult population in the United States have an alcohol use disorder (AUD), characterized by an inability to resist alcohol use despite adverse effects. Chronic alcohol consumption is injurious across multiple tissues and the causes of cellular injury due to chronic alcohol exposure are multifactorial. Alcohol misuse severely impairs many aspects of immune regulation and immune cell function, which predisposes people with AUDs to acute or chronic diseases. Alveolar macrophages are the first line of defense against pathogens in the lower respiratory tract, but alcohol misuse decreases alveolar macrophage function, leading to increased risk of pneumonia and acute respiratory distress syndrome in people with AUDs. Mechanisms of decreased alveolar macrophage function due to alcohol misuse include diminished phagocytic capacity and cellular and mitochondrial oxidative stress. These studies use alveolar macrophages isolated from humans with AUDs and various models of chronic alcohol exposure in combination with agents meant to either decrease oxidative stress or reverse metabolic bioenergetics dysfunction. The extent of metabolic impairment due to chronic alcohol exposure was characterized and included alcohol-induced alterations in glycolysis, hexosamine biosynthesis, and oxidation of pyruvate, glutamine, or long chain fatty acids that are preferred for cellular energy generation. Impaired alveolar macrophage phagocytosis was reversed through improved bioenergetic phenotype using the peroxisome-proliferator activated receptor gamma ligand, pioglitazone. These studies have demonstrated that targeting AM metabolic or bioenergetic dysfunction is a viable strategy to improve AM phagocytosis during chronic alcohol misuse. This work in alcohol misuse expands on the knowledge of alveolar macrophage oxidative stress pathways and mitochondrial biology, since alcohol misuse impairs mitochondrial metabolism pathways necessary for bioenergetics. These approaches can be applied to other pathological conditions characterized by mitochondrial dysfunction, resulting in dysregulation of lung immunity.

**Alveolar Macrophage Oxidative Stress and Metabolic Dysfunction During Chronic
Alcohol Use**

By

Kathryn Crotty, B.S.

Florida State University, 2019

Advisor: Samantha M. Yeligar, M.S., Ph.D.

A dissertation submitted to the Faculty of the James T. Laney School of Graduate
Studies of Emory University in partial fulfillment of the requirements for the degree of
Doctor of Philosophy in Graduate Division of Biological and Biomedical Science,
Molecular & Systems Pharmacology

2024

Acknowledgements

In my four and a half years at Emory University in the Molecular and Systems Pharmacology Program I discovered a great deal about pharmacology and the biomedical sciences, but I learned so much more about myself than I ever anticipated. This program and our community went above and beyond to support my scientific and personal needs. Every PhD had its challenges, but my world changed between the time I started in 2019 with the COVID-19 pandemic, the death of my parents and other family members, and the mental health challenges that persisted throughout. With that being said, I would not have been able to finish this degree without the love and support of several people. You all are more important to me than you know.

In particular, Dr. Samantha Yeligar was instrumental in all aspects of my progress and allowed me to develop as an independent scientist in my own unique way. You let me take all the mental health days I needed, and I am incredibly grateful because your support was exactly what I needed to stay in the program. Your lab was a safe space for me to express what I needed without having my ideas restricted and I am still in shock at how much freedom I was given when developing my F31 project (go naked mole rats!). I hope that you can use this data and these ideas for many more successful grant applications and rotation student projects.

To the person who can read me like no other, Sarah Chang, you deserve all of the happiness and pets (kind of the same thing really) in the world. I would not be the scientist I am without your help in the lab. You gave me the foundation I needed to perform a lot of the cellular and microbiology techniques that did not come naturally to me. Our La Parilla lunch trips are precious to me and a much-needed break from the

stressors of life. We WILL be continuing our lunch outings in the future, and I cannot wait to have you as a bridesmaid in my wedding!

Shayaan Kabir – you are a GOAT undergrad and assistant to me. You deserve an honorary honors thesis for the work you contributed toward these projects. I know it was frustrating at times, but we had a lot of fun in the process, and I am so happy to have been your mentor these past few years. Any medical school will be lucky to have you. Additionally, Caitlin Reisner, Nicholas Harbin, and Elijah Ullman created a space like no other to talk about science in the home. You all are some of the best roommates I have ever had and an invaluable resource for the science and life problems that inevitably come up. Our dynamic is diverse and continues to make me question the norm; I hope we all continue to grow together in the years to come.

To my family, I love you all so much and I do not express it enough. Lee, Shayla, and Daniel were the only people I cared about for a long time, but they helped me learn to live again. Lee, you are an understanding, compassionate, and loving fiancé and I am proud to be Dr. Brave in the months to come. Charlie gets the biggest thanks in proportion to her size (32 lbs. already!) for being the best unofficial emotional support dog on the planet. On a similar note, my MSP family has provided much needed relief during SIP events and Bachelor/Bachelorette nights. A special thanks to my committee members for challenging me with their questions, and special thanks to Roy for allowing us to use materials from his time at Emory after his departure. P.S. I got better at cardiac punctures and think of your words of wisdom every time. Eric and Kathy, your dedication to research inspires me to be a better scientist and to meet and exceed your standards. Thank you for all your feedback throughout the past three years.

And finally, my parents provided unconditional love and support at a level that I will never experience again. They never got to see me fully develop into a real scientist but believed in my potential far before I did. To my dad, I know I was your pride and joy, and I should have gotten to know you better as you got to know me. To my mom, you were my best friend when you died. I think about you every day and how hard you worked to get your degree and post-baccalaureate classes while supporting our family. It hurts me thinking that you never got to experience the second chance in life that you wanted. I will live for you. Thank you and I love you all.

Table of Contents

List of Figures & Tables	1
List of Abbreviations	7
Chapter 1: Introduction	15
1.1 A Critical Review of Recent Knowledge Gained on Alcohol’s Effects on the Immunological Response in Different Tissues	18
Abstract	20
Introduction	21
Alcohol-Associated Neuroinflammation	22
Alcohol Misuse and Advanced Age	24
Alcohol-Induced Lung Dysfunction	26
Alcohol-Mediated Liver Inflammation and Disease	30
Alcohol’s Effects on the Gut and Organ Crosstalk	33
Conclusion	38
Chapter 2: Clinical Evaluation of Oral Zinc, S-adenosylmethionine (S-AdoMet), or Combination Supplementation to Improve Alveolar Macrophage Function in People with Alcohol Use Disorders	41
2.1 Evaluation of Oral Zinc, S-Adenosylmethionine, or Combination Therapy to Decrease Alveolar Macrophage Oxidative Stress in Participants with Alcohol Use Disorders: Blinded and Randomized Clinical Trial	43
Abstract	44

Introduction	46
Materials & Methods	48
Results.....	53
Discussion	56
Tables & Figures.....	60
2.2 Conclusions	76
Chapter 3: Application of Pioglitazone to Improve Alcohol-Induced Alveolar Macrophage Metabolic and Phagocytic Dysfunction.....	77
3.1 Alcohol-Induced Glycolytic Shift in Alveolar Macrophages Is Mediated by Hypoxia- Inducible Factor-1 Alpha	79
Abstract	80
Introduction	82
Materials & Methods.....	84
Results.....	92
Discussion	97
Figures.....	104
Supplementary Material.....	125
3.2 Pioglitazone Reverses Alcohol-Induced Alterations in Alveolar Macrophage Mitochondrial Phenotype	128
Abstract	130

Introduction	132
Materials & Methods	135
Results.....	143
Discussion	148
Tables & Figures.....	156
Supplemental Figures.....	174
3.3 Conclusions	178
Chapter 4: Other Alterations in Pulmonary Cell Function due to Changes in	
Metabolism	180
4.1 Hyaluronic Acid Dynamics Affect Alveolar Macrophage Mitochondrial and Phagocytic Function.....	184
4.1.1 Excerpt from: New Insights into the Mechanism of Alcohol-Mediated Organ Damage via its Impact on Immunity, Metabolism, and Repair Pathways: A Summary of the 2021 Alcohol and Immunology Research Interest Group (AIRIG) Meeting.	185
4.1.2 Excerpt from: Alcohol and Immunology: Mechanisms of Multi-Organ Damage. Summary of the 2022 Alcohol and Immunology Research Interest Group (AIRIG) Meeting	193
4.2 Preliminary Data: Chronic Alcohol Exposure Increases Lung Hyaluronic Acid ..	201
Abstract	202
Introduction	204
Methods & Materials	207

Results.....	213
Discussion	217
Tables & Figures.....	219
Supplemental Figures.....	227
4.3 Hyaladherins May be Implicated in Alcohol-Induced Susceptibility to Bacterial Pneumonia.....	230
Abstract	231
Introduction	232
Extracellular Matrix in the Lung.....	232
Hyaluronic Acid Signaling: Hyaladherins and Hyaluronic Acid-Protein Interactions	233
Discussion	241
Controversies in the Hyaluronic Acid Field	242
Therapeutic Potential.....	244
Figures.....	247
4.4 Application of Hyaluronic Acid in Pulmonary Hypertension.....	248
4.4. Conclusions	251
Chapter 5: Perspectives & Contributions Toward Other Fields	253
5.1 Perspectives	253
5.2 Collaborations & Contributions to Other Fields	256

5.2.1 Regulator of G protein Signaling 14 Affects Mitochondrial Function in Human Embryonic Kidney 293T Cells.....	257
5.2.2 Activation of ATP-Dependent Clp protease (ClpXP) Affects Mitochondrial Function in Human Aortic Smooth Muscle Cells.....	262
5.3 Conclusions	266
Chapter 6: Discussion & Future Directions	267
6.1 Discussion.....	267
6.2 Future Directions.....	274
References.....	278

List of Figures & Tables

Chapter 1

Figure 1.1: Alcohol mediated multi-organ immune dysfunction.

Chapter 2

Table 2.1: Demographics from participants with alcohol use disorders (AUDs).

Figure 2.1: Consolidated Standards of Reporting Trials (CONSORT) flow diagram for subjects recruited into the Examination of Zinc, S-adenosylmethionine (SAME) and Combination Therapy Versus Placebo in People with Alcohol Use Disorders.

Figure 2.2: The Alcohol Use Disorders Identification Test (AUDIT) questionnaire.

Figure 2.3: Short Michigan Alcohol Screening Test (SMAST) questionnaire.

Figure 2.4: Oral zinc decreases reactive oxygen species in alveolar macrophages (hAMs) isolated from people with alcohol use disorders (AUDs).

Figure 2.5: Oral zinc decreases mitochondrial superoxide in alveolar macrophages (hAMs) isolated from people with alcohol use disorders (AUDs).

Figure 2.6: Mitochondrial health dependent on membrane potential and mass does not change in response to supplementation with zinc, S-adenosylmethionine (SAME), or combination in alveolar macrophages (hAMs) isolated from people with alcohol use disorders (AUDs).

Figure 2.7: Phagocytic index does not change in response to supplementation with zinc, S-adenosylmethionine (SAME), or combination in alveolar macrophages (hAMs) isolated from people with alcohol use disorders (AUDs).

Figure 2.8: Oxidative stress is not correlated with phagocytic index in alveolar macrophages (hAMs) isolated from people with alcohol use disorders (AUDs) who did not undergo treatment.

Chapter 3

Chapter 3.1

Table 3.1.1: Primer sequences to measure mRNA levels using qRT-PCR.

Figure 3.1.1: Ethanol (EtOH) induces glycolysis in mouse alveolar macrophages (mAM).

Figure 3.1.2: Ethanol (EtOH) induces glycolysis in MH-S cells.

Figure 3.1.3: Ethanol (EtOH) increases expression of glycolytic proteins and lactate levels in MH-S.

Figure 3.1.4: Ethanol (EtOH) induces hypoxia-inducible factor-1 alpha (HIF-1 α) in mouse alveolar macrophages (mAM) and MH-S.

Figure 3.1.5: Stabilization of hypoxia-inducible factor-1 alpha (HIF-1 α) *in vitro* via cobalt chloride (CoCl₂) mimics ethanol (EtOH)-mediated derangements in MH-S.

Figure 3.1.6: Cobalt chloride (CoCl₂) induces expression of glycolytic proteins and lactate levels and causes phagocytic dysfunction in MH-S.

Figure 3.1.7: Hypoxia-inducible factor-1 alpha (HIF-1 α) modulates ethanol (EtOH)-induced glycolysis and phagocytic function in MH-S.

Figure 3.1.8: Pioglitazone (PIO) treatment reverses ethanol (EtOH)-induced hypoxia-inducible factor-1 alpha (HIF-1 α) levels.

Figure 3.1.9: Pioglitazone (PIO) treatment reverses ethanol (EtOH)-induced glycolysis in MH-S.

Figure 3.1.10: Pioglitazone (PIO) treatment reverses ethanol (EtOH)-induced glycolysis in mouse alveolar macrophages (mAM).

Supplemental Figure 3.1.1: Ethanol (EtOH) induces glucose transporter 1 (GLUT1) in mouse lung tissue.

Supplemental Figure 3.1.2: Cobalt chloride (CoCl₂) stabilizes hypoxia-inducible factor-1 alpha (HIF-1 α) in MH-S.

Supplemental Figure 3.1.3: Hypoxia-inducible factor-1 alpha (HIF-1 α) regulates ethanol (EtOH)-induced glycolysis in MH-S.

Chapter 3.2

Table 3.2.1: Inclusion and exclusion criteria and drinking history questionnaire for selection of participants with AUD.

Table 3.2.2: Demographics of alcohol use disorder (AUD) participants, whose alveolar macrophages (hAMs) were collected and treated with or without pioglitazone (PIO) *ex vivo*.

Figure 3.2.1: Pioglitazone (PIO) decreases mitochondrial superoxide in isolated human alveolar macrophages (hAMs).

Figure 3.2.2: Pioglitazone (PIO) improves phagocytic capacity and decreases mitochondrial superoxide in isolated mouse alveolar macrophages (mAMs).

Figure 3.2.3: Pioglitazone (PIO) improves metabolism of glucose (GLC), long chain fatty acids (FA), and glutamine (GLN) to meet baseline cellular

oxidation rates in mouse alveolar macrophages (mAMs) following chronic ethanol (EtOH) feeding.

Figure 3.2.4: Hypoxia-inducible factor-1 alpha (HIF-1 α) knock-down *in vitro* further decreases glucose (GLC) capacity and flexibility and decreases glutamine (GLN) dependency following chronic ethanol (EtOH) exposure.

Figure 3.2.5: Pioglitazone (PIO) improves glucose (GLC) oxidation in MH-S cells following chronic ethanol (EtOH) exposure.

Figure 3.2.6: Chronic ethanol (EtOH) decreases ATP-linked and maximal respiration derived from long chain fatty acid (FA) oxidation in MH-S cells.

Figure 3.2.7: Pioglitazone (PIO) and chronic ethanol (EtOH) increase ability to compensate for loss of glutamine (GLN) oxidation in MH-S cells.

Figure 3.2.8: Graphical summary of alcohol-induced alterations in alveolar macrophage (AM) metabolic phenotype and reversal by pioglitazone (PIO).

Supplementary Figure 3.2.1: *Ex vivo* pioglitazone (PIO) in alveolar macrophages isolated (hAMs) from people with alcohol use disorders (AUD) does not change proliferator-activated receptor gamma (PPAR γ) or superoxide dismutase 2 (SOD2) protein levels.

Supplementary Figure 3.2.2: Pioglitazone (PIO) improves phagocytic capacity and decreases mitochondrial superoxide in ethanol (EtOH)-fed mouse alveolar macrophages (mAMs).

Supplementary Figure 3.2.3: Knock down of hypoxia-inducible factor-1 alpha (HIF-1 α) in MH-S cells.

Chapter 4

Figure 4.1: Simplified pathway of hyaluronic acid (HA) production from the hexosamine biosynthetic pathway.

Figure 4.2: Simplified illustration of high and low molecular weight hyaluronic acid (HA) synthesis, fragmentation, and signaling.

Chapter 4.1

Table 4.1.1: Summary of new findings related to alcohol-induced organ damage.

Chapter 4.2

Table 4.2.1: Summary of mouse primers used for qRT-PCR used for mRNA detection of genes important for mitochondrial function and hyaluronic acid (HA) metabolism.

Figure 4.2.1: Effect of ethanol (EtOH) *in vitro* or peroxisome proliferator-activated receptor 1 gamma (PPAR γ) knock out *in vitro* in MH-S or *in vivo* mouse lungs on mRNAs associated with mitochondrial function and hyaluronic acid (HA) metabolism.

Figure 4.2.2: *In vitro* hyaluronic acid (HA)-related protein expression may influence HA release.

Figure 4.2.3: High molecular weight hyaluronic acid (HMW HA, 1000 kD) decreases the alveolar macrophage (AM) phagocytosis and mitochondrial bioenergetic profile *in vitro*.

Supplemental Figure 4.2.1: Representative western blot membranes from control and ethanol (EtOH) treated MH-S cells.

Supplemental Figure 4.2.2: MH-S cell internalization of fluorescently labeled *Staphylococcus aureus*.

Chapter 4.3

Figure 4.3.1: Alcohol affects hyaladherin signaling in the lung.

Chapter 4.4

Figure 4.4.1: Measurement of human pulmonary artery smooth muscle cells (HPASMC) apoptosis Annexin-V staining, corresponding to intermediate-to-late apoptosis, determined by flow cytometry.

Chapter 5

Chapter 5.2

Figure 5.2.1: Regulator of G-protein signaling 14 (RGS14) decreases mitochondrial respiration *in vitro*.

Figure 5.2.2: ClpXP chaperone protein (CLPX) decreases human aortic smooth muscle cell (HASMC) mitochondrial respiration and shifts cells toward a quiescent phenotype.

Figure 5.2.3: ATP-dependent Clp protease (ClpXP) loss-of-function inhibits respiration and induces glycolytic reprogramming in human aortic smooth muscle cell (HASMC).

List of Abbreviations

Abbreviation	Definition
2-DG	2-deoxy-glucose
4-MU	4-methylumbelliferone, Hyaluronic acid synthase inhibitor
AD	Alzheimer's disease
Ad_CLPX	Overexpression of CLPX with an adenovirus
AH	Alcohol-associated hepatitis
AIRIG	Alcohol and Immunology Research Interest Group
ALD	Alcohol-associated liver disease
AM/s	Alveolar Macrophage/s
ANOVA	Analysis of variance
ARDS	Acute respiratory distress syndrome
aSMase	Acid sphingomyelinase
ATII	Alveolar epithelial type II cells
ATP	Adenosine triphosphate
AUD/s	Alcohol use disorder/s
AUDIT	Alcohol Use Disorders Identification Test
B1	BAL 1, before supplementation
B2	BAL 2, after supplementation
BAL	Bronchoalveolar lavage
BCA	Bicinchoninic acid
BPTES	Bis-2-(5-phenylacetamido-1,2,4-thiadiazol-2-yl) ethyl sulfide
C57BL/6J	Mouse strain commonly used in animal experiments

Cap	Fuel capacity
CCCP	Carbonyl cyanide m-chlorophenyl hydrazone
CD	Cluster of differentiation
CD44	Cluster of differentiation 44
CHI3L1	Chitinase-3 like-protein-1
ClpP	Proteasome-like protease associated with ClpXP
CLPX	Chaperone protein associated with ClpXP
ClpXP	ATP-Dependent Clp protease
CMXRos	Chloromethyl X rosamine
CoCl ₂	Cobalt (II) chloride hexahydrate
CON or Con	Control
CONSORT	Consolidated Standards of Reporting Trials
CTR/s	C-type lectin receptors
CX3CR1	C-X3-C Motif Chemokine Receptor 1
DAMP/s	Danger associated molecular pattern/s
DAPI	4',6-diamidino-2-phenylindole
DCFH-DA	2',7'-dichlorodihydrofluorescein diacetate
Dep	Fuel Dependency
Drp1	Dynamin-related protein 1
ECAR	Extracellular acidification rate
ESP	Electron paramagnetic (spin) resonance
ELISA	Enzyme-linked immunosorbent assay
Eto	Etomoxir, inhibition of long chain fatty acid oxidation

EtOH	Ethanol
ExZACTO	Examination of Zinc, S-adenosylmethionine (SAME), and Combination Therapy Versus Placebo in Alcoholics
FA	Long chain fatty acid
FBS	Fetal bovine serum
FCCP	Carbonilcyanide p-triflouromethoxyphenylhydrazone
FDA	Federal drug administration
Flex	Fuel flexibility
GAPDH	Glyceraldehyde-3-phosphate dehydrogenase
gC1qR	aka HABP1 or p32
GLC	Glucose, pyruvate oxidation
GlcA	Glucuronic acid
GlcNAC	N-acetylglucosamine
GLN	Glutamine
GLUT1	Glucose transporter 1
GLUT4	Glucose transporter 4
Glyco	Glycolytic
GM-CSF	Granulocyte-macrophage colony stimulating factor
GP96	Glycoprotein 96
Grp75	75 kD glucose-related protein
GSH	Glutathione
GSSG	Glutathione disulfide
HA	Hyaluronic acid

HA10	10 kD hyaluronic acid
HA100	100 kD hyaluronic acid
HA1000	1000 kD hyaluronic acid
HABP1	Hyaluronic acid binding protein 1, aka P32 or gC1qR
HABP2	Hyaluronic acid binding protein 2
HABPs	Hyaluronic acid binding protein/s
hAM	Human alveolar macrophage
HAS	Hyaluronic acid synthase
HAS1	Hyaluronic acid synthase 1
HAS2	Hyaluronic acid synthase 2
HAS3	Hyaluronic acid synthase 3
HASMC/s	Human aortic smooth muscle cell/s
HEK293	Human embryonic kidney cells
HIF-1 α	Hypoxia-inducible factor 1 alpha
HIF-1 β	Hypoxia-inducible factor 1 beta
HMGB1	High mobility group box 1
HMW HA	High molecular weight hyaluronic acid (> 1000 kD)
HPASMC/s	Human pulmonary artery smooth muscle cell/s
HYAL/s	Hyaluronidases
HYAL1	Hyaluronidase 1
HYAL2	Hyaluronidase 2
IaI	Inter- α -trypsin-inhibitor
IgG	Immunoglobulin G

IgM	Immunoglobulin M
IL-18	Interleukin 18
IL-1B	Interleukin-1 beta
IL-22	Interleukin 22
IL-6	Interleukin 6
LC-MS	Liquid chromatography mass spectrometry
LMW HA	Low molecular weight hyaluronic acid (<200 kD)
LPS	lipopolysaccharide
LYVE-1	Lymphatic vessel endothelial cell receptor 1
mAM/s	Primary mouse alveolar macrophage/s
MFN2	Mitofusin 2
M-GP96KO	Myeloid-specific GP96 knock out in mice
MH-S	Murine alveolar macrophage cell line
miRNA	Micro RNA
Mito	Mitochondrial
MLE-12	Murine alveolar epithelial cell line
MnSOD	Manganese-dependent superoxide dismutase aka SOD2
mRNA	Messenger ribonucleic acid
miRNA	Micro RNA
MT	Mitochondrial
MV/s	Microvesicles
NAD	Nicotinamide adenine dinucleotide
NADH	Nicotinamide adenine dinucleotide (NAD) + hydrogen (H)

NADPH	Nicotinamide adenine dinucleotide phosphate
NFkB	Nuclear factor kappa B
NIAAA	National Institute of Alcohol and Alcoholism
NK	Natural killer (cells)
NLRP3	NOD-, LRR- and pyrin domain-containing protein 3
NOX	NADPH oxidase protein
Nox4	NADPH oxidase 4
Nrf2	Nuclear factor erythroid 2-related factor 2
ns	Not significant ($p > 0.05$)
OCR	Oxygen consumption rate
Oligo	Oligomycin, ATP synthase inhibitor
P2RY12	Purinergic Receptor P2Y12
P32	Hyaluronic acid binding protein 1; Mitochondrial protein 32; aka HABP1 or gClqR
PAF	Platelet-activating factor
PAR	Protease-activated receptors
PAMP/s	Pattern associated molecular pattern/s
PBMC/s	Peripheral blood mononuclear cell/s
PBS	Phosphate buffered saline
PDK-1	Pyruvate dehydrogenase kinase 1
PEI	Polyethyleneimine
Pfkfb3	6-phosphofructo-2-kinase/fructose-2-bisphosphate-3
PH	Pulmonary hypertension

PI	Principle investigator
PI	Propidium iodide, Ch. 4.4
PIO	Pioglitazone
PKM2	Pyruvate kinase M2
PPAR γ	Peroxisome proliferator-activated receptor gamma
PTSD	Post traumatic stress syndrome
PTX3	Pentraxin-related protein
PU-WS13	GP96 specific inhibitor
qRT-PCR	Quantitative real time polymerase chain reaction
R/A	Rotenone and Antimycin A
RFUs	Relative fluorescence units
RGS14	Regulator of G protein signaling 14
RHAMM	Receptor for hyaluronic acid mediated motility
Rip3	Receptor-interacting protein kinase 3
ROS	Reactive oxygen species
RSV	Respiratory syncytial virus
SAMe	S-adenosylmethionine
SCFA	Short chain fatty acid
siSCR or siScr	Scrambled (siRNA)
scRNA-seq	Single cell RNA sequencing
SD	Standard deviation
SEM	Standard error of the mean
siRNA	Silencing RNA

SIRT2	Sirtuin 2
SMAST	Short Michigan Alcohol Screening Test
SOD2	Superoxide dismutase 2
TBST	Tween + tris buffered saline
TFAM	Mitochondrial transcription factor A
TFB1M	Mitochondrial transcription factor 1
TGFb or TGFB1	Transforming growth factor beta
TLR/s	Toll-like receptor/s
TLR2	Toll-like receptor 2
TLR4	Toll-like receptor 4
TLR6	Toll-like receptor 6
Tmem119	Transmembrane protein 119
TNF- α	Tumor necrosis factor alpha
TSG-6	Tumor necrosis factor-stimulated gene-6
UDP	Uridine diphosphate glucose
UK5099	Inhibitor of pyruvate entry into the mitochondria
VA	Veteran's Affairs
VDAC	Voltage dependent anion channel
Veh	Vehicle
w/v	Weight by volume
WT	Wild type

Chapter 1: Introduction

People have been drinking alcohol to gain an altered state of consciousness for a minimum of 10,000 years, and likely many millennia longer. By the late 19th century, physicians knew that chronic alcohol use resulted in extreme liver injury and neurological impairment¹. Shortly after, chronic alcohol use was observed to increase the risk of pulmonary diseases². However, impaired pulmonary function due to long-term drinking remained understudied for decades. Today, there is a large collection of research supporting the idea that alcohol misuse increases morbidity and mortality, including lessened quality of life due to lung injury³⁻¹¹. In fact, alcohol-related deaths are increasing and now rank as the fourth leading cause preventable deaths in the United States, only trumped by obesity, smoking, and high blood pressure according to the World Health Organization^{11,12}. Further, the number of people diagnosed with alcohol use disorders (AUDs) doubled between 2018 and 2021^{13,14}.

This dissertation builds on the rich body of knowledge gained previously from other investigators about the detrimental effects of alcohol on immunity, with a specific focus on how alcohol affects lung immunity. My mentor, Dr. Samantha Yeligar, has spent nearly two decades unraveling mechanisms underlying alcohol-induced liver and lung disorders. It has been a privilege to continue this legacy and aid in the discovery of novel therapeutics to reverse organ damage due to alcohol use. Here I highlight my contributions to the alcohol and immunity field and span multiple foundational, pre-clinical/translational, and clinical studies with the goal of improving outcomes in people with AUDs.

To begin, this chapter will feature recent advancements in the alcohol and immunology field covering active investigations on alcohol's effect on different tissues and current gaps in knowledge others should address in future studies. Chapter 2 and 3 will delve into potential supplements and therapeutics to improve pulmonary immunity in people with AUDs, including potential mechanisms of diminished lung immune cell function. Chapter 4 expands on Chapter 3 by characterizing how the extracellular environment contributes toward alcohol-induced immune cell dysfunction.

The bulk of Chapters 2-4 highlight several oxidative stress and metabolism pathways including zinc, glutathione, and superoxide dismutase maintenance of redox homeostasis, cellular bioenergetics pathways (glycolysis, pyruvate oxidation, glutaminolysis, long chain fatty acid oxidation, oxidative phosphorylation) necessary for ATP generation, and the impact of the extracellular matrix synthesis on immune cell phenotype. I highlight the idea that cells must be able to switch metabolic phenotype to maintain normal functions. Importantly, cells have differing levels of dependency on "fuels" (e.g., glucose, glutamine, or fatty acids) but have a level of flexibility whereby the cell can switch usage of a fuel to regulate cellular metabolism. Redox imbalance persistence, and impaired flexibility or dependency of a cell to use certain fuels impacts cell functions, which may result in disease.

Overall, this dissertation addresses several gaps in knowledge, including the identification of several aberrant redox and metabolic pathways caused by chronic alcohol exposure that can be reversed pharmacologically. Finally, Chapter 5 gives perspectives on how the mechanisms and methods of discovery explained in Chapters

2-4 aid in studying additional disorders in other tissues. Discussion of a summary of the results presented in this dissertation and next steps are in Chapter 6.

1.1 A Critical Review of Recent Knowledge Gained on Alcohol's Effects on the Immunological Response in Different Tissues

Kathryn Crotty, BS^{1*}, Paige Anton, BS^{2,3*}, Leon G. Coleman, MD, PhD⁴, Niya L. Morris, MS, PhD¹, Sloan A. Lewis, PhD⁵, Derrick R. Samuelson, PhD⁶, Rachel H. McMahan, PhD^{3,7}, Phillipp Hartmann, MD⁸, Adam Kim, PhD⁹, Anuradha Ratna, PhD¹⁰, Pranoti Mandrekar, PhD¹¹, Todd A. Wyatt, PhD¹², Mashkooor A. Choudhry, PhD¹³, Elizabeth J. Kovacs, PhD^{3,7,14}, Rebecca McCullough, PhD^{3,2}, Samantha M. Yeligar, MS, PhD¹

¹Department of Medicine, Emory University, Atlanta, GA 30322 and Atlanta Veterans Affairs Health Care System, Decatur, GA 30033

²Department of Pharmaceutical Sciences, University of Colorado Anschutz Medical Campus, Aurora, CO 80045

³Alcohol Research Program, University of Colorado Denver, Anschutz Medical Campus, Aurora, CO, United States

⁴Department of Pharmacology, Bowles Center for Alcohol Studies, University of North Carolina at Chapel Hill, Chapel Hill, NC 27599

⁵Department of Molecular Biology and Biochemistry, University of California, Irvine, CA 92697

⁶Department of Internal Medicine, University of Nebraska Medical Center, Omaha, NE 68198

⁷Department of Surgery, University of Colorado Anschutz Medical Campus, Aurora, CO 80045

⁸Department of Pediatrics, University of California San Diego, La Jolla, CA 92093

⁹Lerner Research Institute, Cleveland Clinic, Cleveland, Ohio 44195

¹⁰Department of Medicine, University of Massachusetts Chan Medical School, Worcester, MA 01655

¹¹Department of Medicine, University of Massachusetts Medical School, Worcester, MA, USA

¹²Department of Environmental, Agricultural & Occupational Health, University of Nebraska Medical Center, Omaha, NE, United States; Veterans Affairs Nebraska-Western Iowa Health Care System, Omaha, NE, United States

¹³Alcohol Research Program, Burn and Shock Trauma Research Institute, Department of Surgery, Loyola University Chicago Health Sciences Campus, Maywood, IL, United States

¹⁴Rocky Mountain Regional Veterans Affairs (VA) Medical Center, Aurora, CO, United States.

Full Citation: Crotty, Kathryn et al. "A critical review of recent knowledge of alcohol's effects on the immunological response in different tissues." *Alcohol, clinical & experimental research* vol. 47,1 (2023): 36-44. doi:10.1111/acer.14979

Abstract

Alcohol misuse contributes to dysregulation of immune responses across various tissues and multi-organ dysfunction, which are associated with higher risk of morbidity and mortality in people with alcohol use disorders (AUDs). Organ-specific immune cells, including microglia in the brain, alveolar macrophages in the lungs, and Kupffer cells in the liver, play vital functions in host immune defense through tissue repair and maintaining homeostasis. However, binge-drinking and chronic alcohol misuse impair these immune cells' abilities to regulate inflammatory signaling and metabolism, thus contributing towards multi-organ dysfunction. To further complicate these delicate systems, immune cell dysfunction during alcohol misuse is exacerbated by aging and gut barrier leakage. This critical review delves into recent advances made in elucidating the potential mechanisms by which alcohol misuse leads to derangements in host immunity and highlights current gaps in knowledge that may be the focus of future investigations.

Introduction

Alcohol misuse is linked to end-organ injury in the brain, lungs, liver, and gut due, in part, to dysregulated immune responses across these tissues. A status report on alcohol and health conducted by the World Health Organization estimates that alcohol misuse is associated with about 14 percent of total deaths among people ages 20 to 39¹⁵. In the United States, over fifteen million people are diagnosed with alcohol use disorders (AUDs), and over 95,000 people die per year due to alcohol-related causes¹⁶. Additionally, alcohol-related healthcare costs, including emergency room and physician office visits, total more than \$249 billion annually in the United States¹⁷.

The toxic effects of alcohol can directly and negatively impact the immune system, particularly organ-specific immune cells. Overall, the critical functions of immune cells that maintain host defense are impaired as alcohol misuse is associated with non-resolving inflammation and perturbations in cellular metabolism¹⁸. More co-morbidities, including advanced age, appear to have heightened sensitivity to alcohol and worsened immune cell dysfunction. Despite this knowledge, there are still significant gaps in knowledge related to the specific health impacts of alcohol misuse on host immunity. Accordingly, this critical review delves into recent advances in elucidating potential mechanisms by which alcohol misuse leads to derangements in immunity at the cellular, organ-specific, and organismal level.

The mechanisms involved in alcohol-related organ damage are multifactorial, thus effective therapeutic strategies are limited. In this review, we will outline exciting and novel approaches used to identify mechanisms underlying organ-specific alcohol-

associated abnormalities in immune cell signaling. We will additionally highlight areas that are ripe for future investigation regarding current gaps in knowledge.

Alcohol-Associated Neuroinflammation

Alcohol is a direct neurotoxicant, and chronic alcohol misuse leads to neurodegeneration and cognitive dysfunction¹⁹. Persistent neuroimmune activation (i.e., neuroinflammation) facilitates alcohol-induced neurodegeneration through generation of danger associated molecular patterns (DAMPs) and activation of microglia, the resident macrophages of the brain²⁰⁻²². Human alcohol and animal ethanol (EtOH) consumption studies show neuroinflammatory responses to EtOH are mediated via Toll-like receptor (TLR) signaling: post-mortem brain tissue from people with AUD exhibit increased TLR expression compared to healthy controls²³, and TLR knock out mice are protected from inductions in pro-inflammatory factor release and neuronal injury after chronic EtOH exposure^{24,25}. Although these studies indicate mitigating neuroinflammation will protect against alcohol-induced neurotoxicity, the inter- and intracellular factors that facilitate alcohol-induced neuroinflammation have not been fully elucidated.

Despite limited knowledge on alcohol-induced neuroinflammation, newer studies are beginning to define the specific impact of alcohol on innate immunity in the brain. Extracellular vesicles are emerging as key intercellular signaling mediators that carry signaling proteins, mRNAs, and microRNAs^{26,27}, but the role of extracellular vesicles in alcohol-induced neuroimmune activation has not been extensively explored²⁸. Recent studies have revealed microglia-derived microvesicles (MVs), extracellular vesicles (0.1-1 μ m diameter) released from the cell surface of somatic cells, to be pro-inflammatory mediators of neuroimmune signaling in response

to EtOH^{20,29}. Activation of microglia leads to augmented release of pro-inflammatory cytokines interleukin-1 beta (IL-1 β) and tumor necrosis factor alpha (TNF- α) that amplify neuroinflammation and accelerate alcohol-related neuronal death^{30,31}.

Using primary organotypic brain slice cultures and sequential ultracentrifugation for MV isolation, studies by Crews *et al.* demonstrate that MVs drive temporal pro-inflammatory gene production in EtOH challenged animal brain slices³¹, including TNF- α and IL-1 β , concomitant with decreased homeostatic microglia Tmem119, and changes in other microglia-specific genes (i.e., P2RY12, CX3CR1). It was also found that blocking MV secretion using an inhibitor of acid-sphingomyelinase, imipramine, blunted pro-inflammatory activation by EtOH³¹. Further, microglia depletion with a colony-stimulating factor-1 receptor inhibitor prevented the EtOH-induced production of pro-inflammatory MVs, without diminishing the total number of extracellular vesicles in media. Together, these findings implicate MVs as mediators of neuroimmune signaling in response to EtOH. While these seminal findings identify MVs as critical drivers of neuroinflammation by EtOH, it will be important for future studies to explore the cellular mechanisms underlying EtOH-MV effects as well as the therapeutic potential of blocking EtOH-induced MVs *in vivo* to reduce AUD-associated neuropathology.

Alcohol Misuse and Advanced Age

Age-related exacerbation of alcohol-induced neurological diseases is a concern considering that binge-drinking is becoming increasingly common among older (>65 years of age) populations³²⁻³⁴. Advanced age and alcohol use can cause neuroinflammation via microglial activation and pro-inflammatory cytokine production, leading to neurodegeneration^{21,22}. However, the synergistic effects of advanced age and binge alcohol exposure on neuroinflammation and neurodegeneration are not well defined, and there is a current lack of validated animal models to explore age-related susceptibilities to the effects of binge-EtOH exposure. Novel rodent models are being developed to accurately reflect alterations in human microglia activation and cytokine production between young and aged alcohol-exposed brain.

Still, the contribution of alcohol misuse to age-related neurodegenerative diseases, such as Alzheimer's disease and (AD) and AD-Related Dementias has not been fully characterized. The aged brain may be more vulnerable to alcohol-related neuroinflammation and damage due to neuronal "inflamm-aging," as evidenced by baseline increases in microglia polarization to a pro-inflammatory state and elevated TNF- α and IL-1 β production that are further elevated upon exposure to TLR agonists like lipopolysaccharide (LPS)^{35,36}. These data suggest the aged brain may respond to binge EtOH exposure with greater neuroinflammation and resulting degeneration, yet there is a gap in research defining the specific changes associated with alcohol misuse, neuroinflammation, and advanced age.

To address these gaps in knowledge, an animal model was developed to measure changes in EtOH-induced microglia activation and cytokine production

between the young and aged brain. Using an intermittent binge EtOH exposure model, aged mice have heightened neuroinflammatory response to EtOH compared to their younger counterparts. Eighteen hours after final exposure, *TNF α* , *IL-1 β* , and *IL-6* mRNA levels in aged, EtOH exposed animals were elevated compared to young control and EtOH exposed animals. These data also identify specific differences in EtOH metabolism, like previously published data³⁷: aged animals exhibited significantly higher blood EtOH concentrations (380 mg/dL) compared to young animals (280mg/dL) 30 minutes after final gavage. This induction pattern is like that of aged adults compared to young adults after consuming equal amounts of EtOH³⁸. These studies suggest that advanced age sensitizes the brain to binge EtOH-related neuroinflammation and that the consequences of these responses on age-related neurodegeneration and cognitive dysfunction should be explored in future studies. This novel model of intermittent binge-EtOH exposure can be used to investigate age-related susceptibility to EtOH-induced microglia activation and associated neuronal injury.

Alcohol-Induced Lung Dysfunction

In contrast to the pro-inflammatory state of the brain during chronic alcohol consumption, AUDs profoundly increase the risk of respiratory infections in part due to diminished alveolar macrophage phagocytic capacity³⁹ and impaired mucociliary clearance^{40,41}, resulting in lung damage and acute respiratory distress syndrome^{4,42}. Further, like alcohol-associated gut barrier dysfunction, inflammasome activation diminishes tight junction protein levels and barrier integrity of the lung epithelium⁴³⁻⁴⁵, but the molecular mechanisms leading to these alcohol-induced immune derangements need to be further clarified. We will discuss recent studies that highlight the role of extracellular matrix, bacterial metabolites, and inflammasome activation in regulating immune function in the lung following alcohol use.

In studies of chronic alcohol misuse in humans and mice, alcohol has been shown to impair the ability of alveolar macrophages to phagocytose pathogens^{10,39,46,47} via increased oxidative stress⁴⁸, mitochondrial redox imbalance⁴⁹ and impaired mitochondrial bioenergetics⁵⁰. Chronic alcohol drinking is associated with increased susceptibility to infection as well as decreased wound healing and tissue repair capacity⁵¹⁻⁵³.

Recent studies suggest that alveolar macrophages from alcohol drinking rhesus macaques demonstrate chromatin reorganization and accessibility changes lead to functional deficits in the macrophages and limit their ability to respond properly to pathogens. A study conducted by Lewis, et al. aimed to uncover the physiological mechanisms by which alcohol disrupts monocyte/macrophage function. One year of chronic alcohol drinking in rhesus macaques results in systematic rewiring of circulating

monocytes and splenic macrophages, affecting their ability to respond to bacterial products such as LPS *ex vivo*⁵⁴. Additionally, transcriptional analysis of the response to respiratory syncytial virus (RSV) indicated that while inflammatory, the alcohol exposed macrophage response was lacking in critical antiviral response genes, including interferons^{54,55}. Even without a secondary stimulation, alveolar macrophages demonstrated heightened cellular oxidative stress levels⁵⁴ and intensified mitochondrial potential. To assess potential mechanisms for these altered functional states with alcohol, single cell level transcriptomics and epigenetics were performed on isolated alveolar macrophages. A new subset of macrophage chromatin reorganization and accessibility changes with alcohol were identified that bolsters the hypothesis that macrophages have limited ability to respond properly to pathogens.

Hyaluronic acid (HA) is an extracellular matrix glycosaminoglycan of variable molecular weight that can function as a pro- or anti-inflammatory signaling molecule. For example, HA synthesis and fragmentation are increased in chronic respiratory diseases and in the bronchoalveolar lavage fluid of acute respiratory distress syndrome (ARDS) patients⁵⁶, potentially through amplified hyaluronidase activity and oxidant generation during inflammation^{57,58}. *In vitro* and *in vivo* models of EtOH exposure include a murine alveolar macrophage cell line, MH-S cells, treated with 0.08% EtOH for three days or a 12-week EtOH feeding model (20% w/v in drinking water) in C57BL/6J mice⁵⁹. Preliminary data gathered by the Yeligar lab showed that alcohol or 1000 kD high molecular weight HA treatment diminished mitochondrial bioenergetics measured by an extracellular flux analyzer *in vitro*. Additionally, alcohol altered HA-binding protein expression *in vitro* and induced reactive oxygen species in bronchoalveolar lavage fluid

in vivo, which was attenuated with pioglitazone (PIO), a synthetic peroxisome proliferator-activated receptor gamma (PPAR γ) thiazolidinedione ligand with antioxidant effects⁶⁰. These findings suggest that alcohol alters HA dynamics, and that targeting oxidant stress may improve alveolar macrophage dysfunction. Future studies will continue to explore alterations in HA dynamics resulting in alveolar macrophage immune dysfunction.

Alveolar epithelial barrier disruption and subsequent pulmonary leakage are major contributors to ARDS^{43,45}. However, the relationship between inflammasome activation and chronic alcohol-induced lung barrier dysfunction has not previously been examined. NOD-, LRR- and pyrin domain-containing protein 3 (NLRP3) inflammasome activation diminishes tight junction protein levels and barrier integrity^{61,62}. Also, earlier findings have demonstrated that inflammasome activation is suppressed by activation of PPAR γ ^{63,64}. Recent data suggest that chronic alcohol exposure increases inflammasome activation, resulting in barrier impairment in lung epithelial cells and that activation of PPAR γ with a synthetic thiazolidinedione ligand reverses these derangements.

An additional study expands on the use of thiazolidinedione ligands in alcohol use lung dysfunction. A mouse alveolar epithelial cell line, MLE-12 cells, was used to examine the role of PPAR γ in alcohol-induced alveolar epithelial inflammasome activation and lung barrier dysfunction. MLE-12 cells were treated with 0.08% EtOH for three days followed by treatment with PIO (10 μ M) during the final day of alcohol exposure. Preliminary data showing that chronic EtOH increased Nlrp3 mRNA levels and stimulated the expression of the downstream effector proteins IL-1 β and IL-18

suggest that chronic alcohol exposure enhanced inflammasome activation *in vitro*.

Chronic EtOH exposure also decreased transepithelial electrical resistance and expression of the tight junction proteins claudin-1, occludin, and zonula occludens-1.

Treatment of MLE-12 cells with PIO reversed alcohol-induced inflammasome activation and barrier impairment in lung epithelial cells. These findings suggest that therapeutic intervention with PIO may diminish pulmonary barrier disruption in people with a history of AUDs.

Alcohol-Mediated Liver Inflammation and Disease

Acute and chronic alcohol consumption modulates the innate immune system, leading to increased systemic and liver inflammation, and alcohol-associated liver disease (ALD). ALD is characterized by steatosis or fatty liver, steatohepatitis, and fibrosis which can progress to cirrhosis and hepatocellular carcinoma. Chronic insults including alcohol exposure disturb cellular homeostasis and induce heat shock proteins in the endoplasmic reticulum⁶⁵ and cytoplasm⁶⁶. Recent studies highlight the pathogenic role of cytosolic heat shock protein 90 and therapeutic potential of its endoplasmic reticulum paralog, glycoprotein 96 (GP96), in liver macrophages during ALD⁶⁷. GP96 is required for the folding, processing, and trafficking of several client proteins including TLRs⁶⁸. Further, the role of GP96 has been identified in metabolic diseases and cancer but not in ALD.

Preliminary data from Ratna, et al. suggests that GP96 may be of clinical relevance during alcohol-induced hepatitis, prominently in liver macrophages. Preliminary evidence suggests the prevention of chronic alcohol-mediated liver injury, steatosis, and inflammation in a murine myeloid-specific GP96 knock out model (M-GP96KO)⁶⁸. Utilizing this model, this same group found higher expression of anti-inflammatory genes and markers of restorative macrophages in livers of M-GP96KO mice compared to wild type (WT) mice. M-GP96KO mice additionally showed alterations in hepatic lipid homeostasis and endoplasmic reticulum stress. Finally, a cell permeable GP96 specific inhibitor, PU-WS13, and GP96-siRNA markedly decreased pro-inflammatory cytokine production in primary murine macrophages, thus confirming a vital role for GP96 in macrophage activation. These findings highlight a novel and

critical role for a liver macrophage endoplasmic reticulum resident chaperone, GP96, in ALD and GP96 targeted inhibition represents a promising therapeutic approach in ALD.

Alcohol-associated hepatitis (AH) is a severe inflammatory disease that can superimpose the spectrum of ALD and leads to significant mortality. In a model of AH, gut-derived LPS acts as an initial signal, and C-type lectin receptor (CTR) upregulation serves as a secondary immune surveillance to detect other gut-derived commensal bacteria, virus, and fungi. CTRs are a family of pattern recognition receptors that sense a diverse array of bacteria, fungi, viruses, and DAMPs⁶⁹. However, the role of CTRs in modulating myeloid-derived cells, including human peripheral monocytes and murine macrophages during AH, was largely unknown. Research has recently revealed that CTRs engage in cell-cell communications between immune effector cells, indicating that modeling signaling dysfunction could supply further targetable pathways for treating AH.

While myeloid cells have low basal CTR expression, it was newly discovered that these genes are robustly induced by TLR signaling in myeloid-derived cells, including human peripheral monocytes and murine macrophages^{70,71}. Using single-cell RNA-seq (scRNA-seq) of peripheral blood mononuclear cells (PBMCs) from patients, CTRs were found to be upregulated and sensitized monocytes to a wider array of pathogen-associated molecular patterns (PAMPs) and DAMPs⁷⁰. Interestingly, CTR genes were clustered together in the genome into a cassette on chromosome 12 called the NK gene receptor complex. Using the scRNA-seq data, CTR genes including Mincle, Dectin-2, and Dectin-3 were discovered to have highly coordinated expression in monocytes. Likewise implicated in AH, Dectin-1⁷², was upregulated at baseline in monocytes, while CTRs involved in cell-cell communication between monocytes, natural killer (NK)-cells,

and CD8 T-cells were similarly dysregulated. Overall, these findings highlight the need for more studies investigating the role of CTRs and other pattern recognition receptors and their specific role as potential drivers of host immune dysfunction and alcohol-mediated liver damage, particularly as the field embraces an ever-growing appreciation that perturbations in the microbiome and epithelial cell barriers change with chronic alcohol misuse.

Alcohol's Effects on the Gut and Organ Crosstalk

Alcohol misuse additionally disturbs intestinal barriers^{73,74} and the gut microbiota, leading to exacerbated immune responses in humans and mouse models^{75,76}. Thus, acute and chronic alcohol consumption and microbial metabolites may modulate the innate immune system, leading to increased systemic and liver inflammation⁷⁷. Chronic alcohol drinking is additionally associated with a heightened incidence of ALD⁷⁸⁻⁸⁰ characterized by steatosis or fatty liver, steatohepatitis, and fibrosis which can progress to cirrhosis and hepatocellular carcinoma⁸¹. However, study designs are complicated by multi-organ communication, and the lack of adequate models to control for complex variable changes. Herein, we highlight a few studies attempting to elucidate the effect of moderate alcohol consumption and aging on the gut-lung and gut-liver axis.

Alcohol and the gut-lung axis

The intestinal microbiota generates many different metabolites which are associated with disease pathogenesis and immune homeostasis^{75,76}. Chronic alcohol consumption can change intestinal microbial community structure and functional homeostasis. Intestinal microbiota has been recently highlighted as a major driver of alcohol-induced tissue injury to other organs, including the lungs and liver⁸². Yet, little is known about the role of alcohol-associated dysbiosis on host defense against bacterial pneumonia. The specific effects of alcohol on the intestinal microbiome are still being explored, but together with increased permeability of the intestinal barrier⁸³, gut dysbiosis, and bacterial overgrowth⁸⁴⁻⁸⁶, new insights into the mechanisms associated with alcohol and the gut have recently been highlighted.

Bacterial species that produce indole derivatives of tryptophan catabolism, which normally exert beneficial effects to the host⁸⁷, are lost during chronic alcohol exposure and influence epithelial integrity⁸⁸ in part, via the cytokine IL-22^{89,90}. Indole derivatives can affect host immunity and defense outside of the gut⁷⁵. Indeed, patients with AUD are more frequently infected with highly virulent respiratory pathogens (e.g., *Klebsiella pneumoniae*) and experience elevated morbidity and mortality^{3,91,92}. These clinical observations have been replicated in rodent models whereby EtOH-fed mice have elevated *K. pneumoniae* lung burden that can be alleviated with oral supplementation of indole⁷⁵. Importantly, the protective effects of indole are exerted via aryl hydrocarbon receptors to improve leukocyte trafficking and killing of *K. pneumoniae* in the lung while also re-establishing pulmonary and intestinal permeability⁷⁵. Interestingly, indole treatment preferentially improved pulmonary recruitment of NK cells in EtOH-fed mice.

However, if NK cells are required for host defense in indole-treated mice or if indole works directly or indirectly on NK cells remains to be answered. These seminal studies have highlighted that targeting the gut microbiome and their associated metabolites may serve as potential therapeutic targets for alcohol-associated diseases. Further, manipulation of tryptophan catabolism and, therefore, aryl hydrocarbon receptor signaling should be further explored as novel therapeutic approaches for the prevention of alcohol-associated pneumonia.

Alcohol and the gut-liver axis

As previously mentioned, excessive alcohol use and associated gut damage can also influence the pathogenesis of ALD^{82,84}. A handful of clinical and animal studies examining dysbiosis of the gut microbiome reveal a dramatic shift in the fecal microbiome in patients with ALD^{93,94} and animals chronically exposed to alcohol-containing diets^{95,96}, characterized by pathobiont expansion, reduced diversity and loss of beneficial microbes⁸². The changes in microbial diversity induced by alcohol can directly cause early organ damage, as demonstrated in fecal transplant studies of donor stool from ALD patients and alcohol-fed rodents into naïve recipients⁹⁷. In addition to bacteria, the gut microbiome also consists of archaea, viruses, protists, and fungi, which represent understudied areas in ALD pathogenesis^{98,99}. Fungi are opportunistic pathogens capable of causing highly lethal blood-borne infections; for example, more than half of individuals with *Candida* bloodstream infections who also have cirrhosis will succumb to the infection¹⁰⁰.

Recent advances have revealed a differential fungal microbiome (i.e., mycobiome) in subjects with progressive and non-progressive ALD, including elevations in genera *Candida*, *Debaryomyces*, *Pichia*, *Kluyveromyces*, and *Issatchenkia*, which positively correlate with liver damage markers including caspase-dependent cleavage products of cytokeratin 18¹⁰¹. Two weeks of alcohol abstinence significantly ameliorated liver disease markers caspase-cleaved and intact cytokeratin 18 concentrations and controlled attenuation parameters in subjects with AUDs, which was accompanied by significantly lower contributions of the genera *Candida*, *Malassezia*, *Pichia*, *Kluyveromyces*, *Issatchenkia*, and the species *Candida albicans* and *Candida*

zeylanoides. Moreover, anti-*C. albicans* immunoglobulin G (IgG) and M (IgM) are acutely increased in AUD patients and taper off after two weeks of alcohol abstinence, while the genus *Malassezia* is elevated in AUD patients with progressive liver disease¹⁰¹, suggesting mycobiome components may also be additional biomarkers for alcohol misuse. Overall, alcohol abstinence ameliorates liver disease in subjects with AUDs, which is associated with lower intestinal contributions of *Candida* and *Malassezia*, and lower serum anti-*Candida albicans* IgG titers. These data add to the limited number of publications in the field^{72,102,103}, but collectively demonstrate that there is much to be discovered related to the mycobiome and if it is a causal factor for ALD.

Conclusion

Excessive alcohol facilitates multi-organ immune dysfunction, as shown in **Figure 1.1**. Overall, there remains much to be discovered regarding the specific health effects of alcohol on people of all ages, but these early studies identify possible links to the exacerbated toxicity and immune response to alcohol. In addition to drinking patterns (e.g., heavy, binge-drinking, chronic), additional host factors, including genetics, sex, co-morbidities, environmental exposures, and age all contribute to alcohol-related organ damage and multi-organ damage¹⁰⁴. In fact, individuals over the age of 65 consist of the fastest growing demographic of increasing alcohol consumers in the United States, particularly among female individuals^{33,105,106}. As such, there are significant gaps of knowledge related to specific health impacts of alcohol misuse in subpopulations of people with AUD. Further studies must be done to target especially vulnerable populations, while continuing to investigate mechanisms underlying biological dysfunction in those with AUD.

Acknowledgements

This work was supported in part by grants from: the National Institute on Alcohol Abuse and Alcoholism (F31AA029938) to KMC (ORCID ID: 0000-0002-9461-4032), (R01AA026086) to SMY (ORCID ID: 0000-0001-9309-0233), (R00AA025386, R00AA025386-05S) to RM (ORCID ID: 0000-0001-5341-7326), (R00-AA026336) to DRS (ORCID ID: 0000-0002-5356-1413). (R13AA020768) to EJK/MAC (ORCID ID: 0000-0002-1152-7145), and (R21AA026295) to EJK. Additional support was granted from: the National Institute of General Medical Sciences (T32GM008602) to Randy A. Hall and (R35 GM131831) to EJK (ORCID ID: 000-0002-9459-9928), and from the Department of Veterans Affairs: (I01 BX004335) to EJK, and a Research Career Scientist Award (IK6 BX005962) to TAW. Further, the National Institutes of Health (K12HD85036), University of California San Diego Altman Clinical and Translational Research Institute (ACTRI)/NIH grant (KL2TR001444), and Pinnacle Research Award in Liver Diseases Grant (PNC22-159963) from the American Association for the Study of Liver Diseases Foundation to PH, and (R01AG018859) to EJK. The contents of this report do not represent the views of the Department of Veterans Affairs or the US Government. Finally, we thank Shayaan Kabir for his contribution toward Figure 1.1.

Figure 1.1

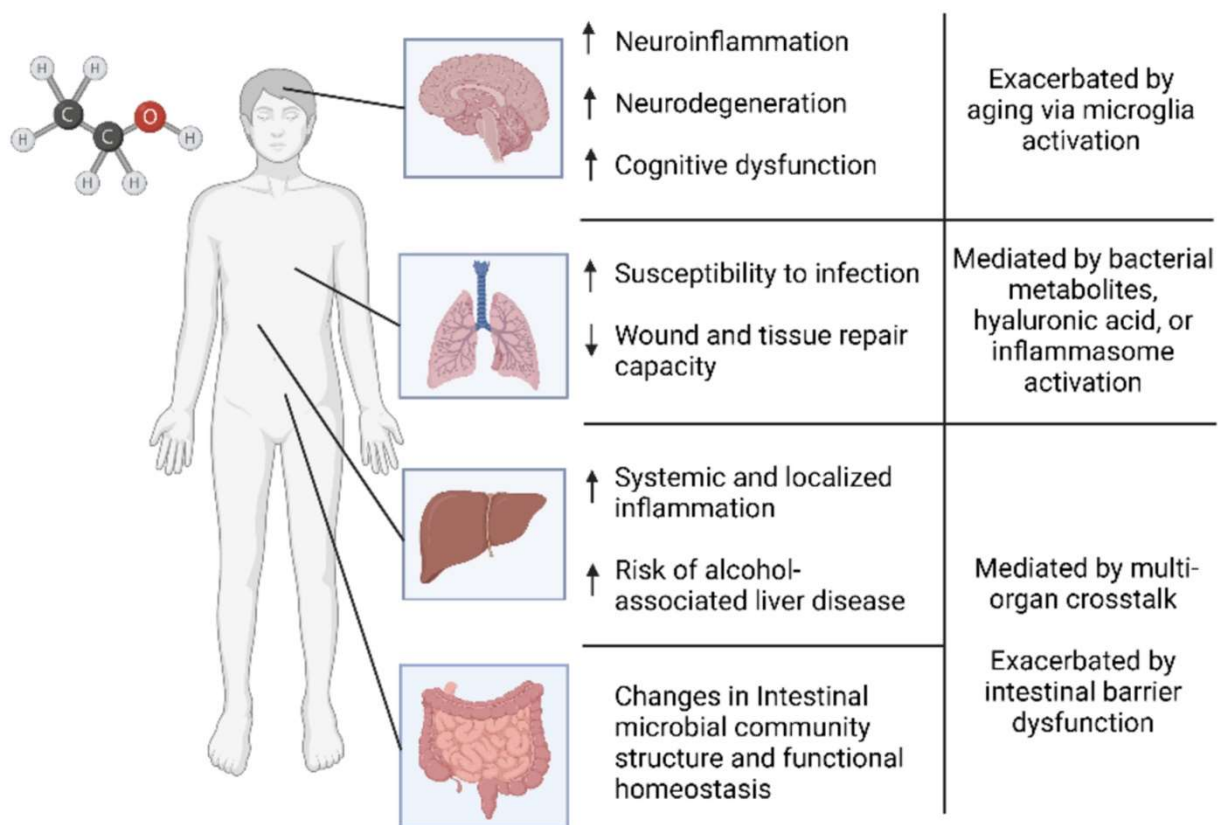


Figure 1.1: Alcohol mediated multi-organ immune dysfunction. Excessive alcohol induces neuroinflammation, neurodegeneration and cognitive dysfunction, which is worsened by microglia activation during aging. Pulmonary immunity is compromised by alcohol-induced alterations in bacterial metabolites, hyaluronic acid and inflammasome activation. Gut and liver immunity is diminished, resulting in systematic and localized inflammation and changes in microbial community structure, resulting in intestinal barrier dysfunction. Figure created using BioRender.com.

Chapter 2: Clinical Evaluation of Oral Zinc, S-adenosylmethionine (S-AMe), or Combination Supplementation to Improve Alveolar Macrophage Function in People with Alcohol Use Disorders

Alcohol misuse causes multi-organ damage, however the focus of the Yeligar lab is on how chronic alcohol impacts pulmonary immunity. As I highlighted in Chapter 1, alcohol use increases the incidence of pulmonary diseases including pneumonia, sepsis, and ARDS. Yet, there are no differences in clinical treatment for people with AUDs with pulmonary disease presentation. Multiple clinical trials held at Emory University and the Atlanta Veteran's Affairs Healthcare System have aimed to test the efficacy of drugs and supplements to improve pulmonary immunity in people with AUDs. While I was not yet part of Emory for the onset of these studies, I was able to meet several objectives of one study aimed to improve AM oxidative stress and phagocytosis through oral zinc, S-adenosylmethionine (S-AMe), or combination supplementation. We hypothesized that oral zinc, S-AMe, or combination in participants with AUDs would improve alcohol-induced cellular and mitochondrial oxidative stress in isolated AMs, which would correlate with improved mitochondrial health and phagocytosis.

AUDs disproportionately affect the United States Veteran population¹⁰⁷ and increase the risk of pulmonary diseases, like pneumonia and acute respiratory distress syndrome (ARDS)^{4,7,45}. AMs are the first line of defense against pathogens in the lower respiratory tract, but AM phagocytic capacity, redox homeostasis, and zinc levels are impaired following chronic alcohol use *in vitro* and *in vivo*. People with AUDs that enrolled in the Atlanta Veterans Hospital Substance Abuse and Treatment Program met the active drinking criteria for study enrollment (n=95) and underwent a bronchoalveolar

lavage (BAL) procedure to isolate AMs. Randomly assigned participants took double placebo, zinc placebo + active S-AdoMet, S-AdoMet placebo + active zinc, or active S-AdoMet + active zinc supplements for 14 days followed by a final BAL. Plated AMs were imaged and quantified by fluorescence microscopy for *in vitro Staphylococcus aureus* internalization, cellular and mitochondrial reactive oxygen species, and mitochondrial health. Zinc supplementation improved AM cellular and mitochondrial oxidative stress, but combination of treatments was unable to improve phagocytic index. AM oxidative stress and phagocytic index were not significantly correlated. Subsequent chapters examine alternative therapeutic strategies to improve AM phagocytosis in people with AUDs and models of chronic alcohol exposure.

My contributions toward the primary and secondary objectives of this study are described here. One co-author paper including the phagocytic index data I collected is in preparation. I intend to publish a second first-author manuscript with the remaining data from this chapter upon acceptance of the manuscript including the primary objectives. My role in the preparation of these manuscripts was to image, analyze, and summarize my findings for the pre-stained slides for quantification of alveolar macrophage phagocytosis and oxidative stress before and after supplementation with double placebo, zinc sulfate, S-adenosylmethionine, or combination therapy. Drs. Ashish Mehta and Samantha Yeligar assisted in the statistical analysis and interpretation of these findings, while other secondary objectives, to be published with the primary objectives, were analyzed by Dr. Samantha Yeligar, Dr. Lou Ann Brown, and their respective labs prior to my time at Emory University.

2.1 Evaluation of Oral Zinc, S-Adenosylmethionine, or Combination Therapy to Decrease Alveolar Macrophage Oxidative Stress in Participants with Alcohol Use Disorders: Blinded and Randomized Clinical Trial

Kathryn M. Crotty BS^{1,2}, Ashish J. Mehta MSc, MD^{1,2}, Samantha M. Yeligar MS, PhD^{1,2}

¹ Department of Medicine, Emory University, Atlanta, Georgia, USA.

² Atlanta Veterans Affairs Health Care System, Decatur, Georgia, USA.

Correspondence

Samantha Yeligar, MS, PhD. Department of Medicine, Emory University, and USA
Atlanta VA Medical Center, 1670 Clairmont Rd. 12C 104, Decatur, GA 30033. Phone:
(404) 321-6111 ext. 202518. Email: samantha.yeligar@emory.edu

Acknowledgements

This work was supported by the National Institute on Alcohol Abuse and Alcoholism, Grant/Award Number: F31AA029938 (KMC), R01AA026086 (SMY); National Institute of General Medical Sciences, Grant/Award Number: T32GM008602 (RH); National Institute of Health Veterans Affairs, Grant/Award Number: 1K2CX000643 (AJM). We further acknowledge Dr. David Guidot and Amy Anderson for their help recruiting participants for this clinical trial. The contents of this report do not represent the views of the Department of Veterans Affairs or the United States Government.

Abstract

Background: In 2021, 28.6 million people over 18 years old had an alcohol use disorder (AUD), accounting for over 11% of the United States population. Loss of pulmonary immunity due to alcohol use occurs in part by human alveolar macrophage (hAM) mitochondrial and phagocytic dysfunction, but there are no current approved therapeutics for people with AUD to improve hAM or lung immune function during chronic alcohol use. Previous work showed that *ex vivo* zinc or glutathione treatment of hAMs decreased alcohol-induced oxidative stress and phagocytic dysfunction. We hypothesized that oral supplementation of zinc or S-adenosylmethionine in participants with AUDs will improve hAM cellular and mitochondrial oxidative stress, which would subsequently improve hAM mitochondrial health and phagocytosis.

Methods: Otherwise healthy participants (n=113) with AUDs were recruited from the Atlanta Veterans Affairs Substance Abuse and Treatment Program. Assignments to supplementation group and analyses of endpoints were randomized and blinded. Each participant underwent a bronchoalveolar lavage for isolation of hAMs before and after daily two-week supplementation with oral double placebo, S-adenosylmethionine (SAME) placebo + 220 mg zinc sulfate 1x, zinc placebo + 400 mg SAME 2x, or active SAME + zinc. All samples were stained 24 hours after hAM isolation for fluorescence microscopy imaging of cellular oxidative species, mitochondrial-derived superoxide, mitochondrial health dependent on mitochondrial mass and membrane potential. Additionally, hAM phagocytic index was determined by internalized and cleared pHrodo-labeled *Staphylococcus aureus*.

Results: Only daily supplementation with zinc (n=17-22) decreased hAM cellular oxidative species and mitochondrial superoxide in participants with AUD ($p < 0.05$, Multiple Wilcoxon Matched Pairs Test) but did not change mitochondrial health, as a measure of mitochondrial mass and membrane potential, or phagocytic index ($p > 0.05$). Oxidative species, mitochondrial superoxide, mitochondrial health as a measure of mitochondrial mass and membrane potential, or phagocytic index were not significantly different in hAMs from double placebo, SAME, or combination supplementation groups.

Conclusions: Zinc improved hAM oxidative stress in participants with AUDs, however this did not result in a functional change in mitochondrial health dependent on mitochondrial mass or membrane potential or phagocytic capacity in hAMs.

Understanding and targeting the mechanisms of alcohol-associated hAM dysfunction are important to improve clinical outcomes in people with AUDs that are at greater risk for lung infection and injury.

Keywords: Alcohol use disorder, lung, alveolar macrophage, oxidative stress, zinc, S-adenosylmethionine

Introduction

Approximately 11% of the adult population in the United States had an alcohol use disorder (AUD) in 2021 despite the known unfavorable social, behavioral, and physiological effects of alcohol misuse¹⁰⁸. In fact, alcohol is the fourth leading cause of preventable deaths in the U.S. despite the number of alcohol-related deaths increasing annually^{11,12}, there are few pharmacological therapeutics available to improve clinical outcomes in people with AUDs. An especially understudied area of research includes alcohol's effect on pulmonary immunity, even though alcohol misuse increases the risk of community-acquired pneumonia and acute respiratory distress syndrome (ARDS) by 2-4-fold^{4,45}. Further, individuals admitted to hospitals with community-acquired pneumonia commonly have an AUD^{3,5}.

Alveolar macrophages (AMs), essential resident immune cells, assist with preventing pneumonia progression by recognition, internalization, and clearance of potentially infectious particles and pathogens¹⁰⁹. Following chronic alcohol exposure, AMs have perturbed redox balance⁴⁹ and cellular bioenergetics^{50,59,110,111}, which contribute toward diminished AM phagocytic capacity^{46,59,112,113}. Yet, there are no available therapeutics for people with AUD and pneumonia to limit morbidity and mortality due to loss of AM phagocytic function. This manuscript describes the investigation of two supplements aimed to decrease alcohol-induced oxidative stress in human AMs (hAMs) and improve hAM function as a blinded and randomized clinical trial: Examination of Zinc, S-adenosylmethionine (SAME), and Combination Therapy Versus Placebo in Alcoholics (ExZACTO; ClinicalTrials.gov identifier: NCT01899521).

Alcohol-induced hAM dysfunction and loss of pulmonary immunity is due in part to dysregulated oxidative stress, resulting in the loss of pathogen clearance. Thus, people with AUDs have higher mortality rates^{11,114}, making the need to find, report, and review therapeutics targeting oxidative stress, as in the ExZACTO clinical trial, of foremost importance. In people with AUDs, intracellular hAM zinc and alveolar pools of reduced glutathione (GSH) are lessened, and GSH homeostasis is perturbed toward a more oxidized redox state (glutathione disulfide, GSSG)^{43,49,112,115-118}. Additionally, *ex vivo* supplementation of hAMs with zinc, GSH, or combination of zinc and GSH improved hAM intracellular zinc as well as phagocytic index, a measure of internalization and lysosomal clearance of *Staphylococcus aureus*¹¹⁹⁻¹²¹. Therefore, the researchers expected that supplementation with oral zinc or the GSH precursor (SAME) will decrease total cellular oxidative stress and mitochondrial (MT)-derived superoxide in hAMs isolated from Veterans with AUDs recruited from the ExZACTO study. We hypothesized that the decrease in hAM oxidative stress will correlate with MT health and phagocytic capacity, and that zinc or SAME or combination will be able to improve hAM phagocytosis. If successful, these results would call for further investigations into usage of antioxidant supplements for the treatment of AUD-induced co-morbidities in the lung, like pneumonia and ARDS.

Materials & Methods

Trial Design: The Atlanta Veterans Affairs Healthcare System Research and Development Committee and Emory University Institutional Review Board reviewed and approved all procedures and protocols. Participants (n=113) recruited from the Atlanta Veterans Hospital Substance Abuse and Treatment Program enrolled in the Examination of Zinc, SAME, and Combination Therapy Versus Placebo in Alcoholics (ExZACTO; ClinicalTrials.gov identifier: NCT01899521) clinical trial. Clinicians assessed history of alcohol consumption based on the Alcohol Use Disorders Identification Test (AUDIT, **Fig. 2.2**), the Short Michigan Alcohol Screening Test (SMAST, **Fig. 2.3**), and drinking history questionnaires (not shown). The ExZACTO study is a randomized, placebo-controlled trial of daily dietary supplements zinc sulfate and SAME intended to determine if either supplement or combination of supplements can restore lung immune defenses in Veterans with AUDs, thereby minimizing the risk of lung infection and injury. This trial had an interventional, parallel assignment design with equal randomized allocation of treatment groups (see Randomization below) and triple masking (Statistician, Participant, Care Provider, Investigator). Only the statistician generating the randomization list and pharmacist were unblinded to the treatment groups. Study onset and completion was May 1, 2013 – July 31, 2017. All medical procedures were performed at the Atlanta Veterans Affairs (VA) Medical and Rehab Center, Decatur, GA, United States, 30033. Data collection occurred at the Atlanta VA Healthcare System and Emory University in Decatur, GA, United States.

Inclusion / Exclusion Criteria: Participants were male and female Veterans between 18-60 years of age with active AUDs who last ingested alcohol < 8 days prior to

bronchoscopy. The ExZACTO study did not include healthy volunteers. Exclusion criteria included: any active and uncontrolled medical problem(s) not successfully treated with medication; known zinc deficiency; primary substance misuse of not alcohol; abnormal chest x-ray; HIV-positive status; any blood coagulation disorder or current treatment with anti-coagulants (inc. warfarin, heparin, direct thrombin inhibitors, and anti-platelet agents other than Aspirin); daily use of vitamins / nutritional supplements; renal impairment with glomerular filtration rate $< 60 \text{ mL / min / } 1.73 \text{ m}^2$; active bipolar disorder; active Parkinson's disease; current pregnancy; contraindication to treatment with zinc or SAME; inability to give informed consent (i.e., limited cognitive capacity); and non-English speaking.

Interventions: Participants underwent a procedure to instill isotonic saline in a sub-segment of the right middle lobe or lingula using a flexible fiberoptic bronchoscopy followed by suction to obtain bronchoalveolar lavage (BAL) fluid, which contains hAMs. Standard conscious sedation techniques were employed. After initial evaluation for inclusion and exclusion criteria and BAL procedure, randomization of participants decided the 14-day supplementation protocol for placebo and intervention groups:

- i. SAME placebo 2x per day + zinc sulfate placebo 1x per day (double placebo).
- ii. SAME placebo 2x per day + 220 mg zinc sulfate 1x per day.
- iii. Zinc sulfate placebo 1x per day + 400 mg SAME 2x per day.
- iv. 400 mg SAME 2x per day + 220 mg zinc sulfate 1x per day.

The investigational drug services and dispensing pharmacist at the VA maintained study medication inventory and were the only investigators unblinded to participant grouping. Continued evaluation for inclusion and exclusion criteria and participant health occurred

during this period. 2-3 weeks following the onset of supplementation, participants received a second BAL procedure for hAM isolation.

Outcomes: Primary and secondary outcome measures included serum and intracellular zinc levels, redox potential in the alveolar space, hAM granulocyte macrophage-colony stimulating factor receptor expression (all published separately), and hAM response to *S. aureus* (by determining phagocytic index). However, we show only phagocytic index in this chapter, and this study reports additional outcomes: hAM oxidative stress and mitochondrial health dependent on membrane potential and mass before and after two-week supplementation of double placebo, zinc, SAME, or combination intervention.

Human Alveolar Macrophage Culture: Following bronchoscopies, ~150-180 mL samples were centrifuged at 1200 rpm for 5 min to pellet remaining cells, which contain hAMs. BAL fluid was removed for separate storage and remaining cell pellets were washed with 5 mL ddH₂O for red blood cell lysis. Centrifugation was repeated and cell density was determined upon resuspension in 5 mL 1x PBS. Cells were then centrifuged and resuspended at 1×10^6 cells / mL in hAM medium: RPMI 1640 medium containing 2% FBS, 1% penicillin / streptomycin, and 8 µg / mL gentamycin. hAMs were then cultured in 16-well chamber slides for 24 h before staining with fluorescent probes. The full hAM isolation protocol has been described previously^{48,113} and have confirmed that this isolation technique generates a >90% macrophage population by Diff-Quik staining (Dade Behring)¹²².

Fluorescence Microscopy: All fluorescent probes were made according to manufacturer's protocols and diluted in hAM medium before incubation with hAMs at 37°C in a dark incubator. Cultured cells were stained with 5 µM 2',7'-

dichlorodihydrofluorescein diacetate (DCFH-DA, Invitrogen, Waltham, MA) for 30 min to measure cellular reactive oxygen species. To measure mitochondrial-derived superoxide, hAMs were incubated with 5 μ M MitoSOX (Invitrogen) for 10 min. Mitochondrial health dependent on membrane potential and mass was measured by incubating hAMs with 500 nM MitoTracker Chloromethyl X rosamine (CMXRos, Invitrogen, Waltham, MA) for 30 min. Phagocytic capacity in MH-S was measured using a pH-sensitive fluorophore-labeled bacteria, pHrodo *Staphylococcus aureus* BioParticles conjugate (Invitrogen, Waltham, MA). Following staining, cells were washed twice with 1x PBS, fixed to chamber slides in 4% paraformaldehyde for 20 min, washed twice more in 1x PBS, and stored in 1x PBS in the dark. Fluorescence was detected using the BZ-X800 imaging software (Keyence Corporation, Osaka, Japan). Quantification of relative fluorescence units (RFUs) per cell was performed using ImageJ (National Institutes of Health). RFUs were measured in at least 10 cells per image with no less than 100 cells imaged total per technical duplicate. All images were deconvoluted for measurement RFUs via ImageJ software (National Institute of Health, Bethesda, MD). Cells with internalized *S. aureus* were considered positive for phagocytosis. Phagocytic capacity was quantified as phagocytic index: RFUs of pHrodo per cell multiplied by the number of cells positive for internalized bacteria divided by total number of cells.

Sample Size: Data from previous animal studies were used to determine sample size, where the change in the primary endpoint (phagocytic index) following treatment changed between 20-40% relative to baseline values. A correlation coefficient of 0.85 and a 30% change in endpoint value in treatment groups was assumed, predicting no

change in placebo treated participants. Based on these assumptions, 19 AUD participants were needed per group to detect a difference between groups at the two-sided 5% significance level. Participant dropout was anticipated, therefore 25-30 participants per group were enrolled to ensure statistical power was maintained. No interim analyses were planned or used, as participants were monitored for adverse events throughout the supplementation phase of the trial.

Randomization: Randomization was performed by an otherwise uninvolved statistician who provided a randomization list based on a computerized pseudo-random number generator with permuted-block randomization (block size 8 and allocation ratio of 2:2:2:2). Unequal smoker to non-smoker ratio was expected based on pilot information with ~85-90% smokers expected; therefore, randomization was stratified to ensure equal smoker and non-smoker representation between treatment groups. Additionally, participants were only assigned to supplementation groups based on the randomization list following the initial BAL procedure to ensure inclusion / exclusion criteria were met.

Statistical Methods: Non-parametric statistical testing for multiple pairwise groups (Multiple Wilcoxon Matched Pairs Test) were used in the final analyses for the experiments outlined in this study due to non-normal distribution of data (Shapiro-Wilk Test for normality $p < 0.05$). Outliers in data were removed based on $1.5 * \text{interquartile range}$ of lognormal data before statistical testing. Results are reported as RFUs / cell before (B1) and after (B2) supplementation period.

Results

Trial Set Up & Participant Demographics: Participant flow diagram adapted from the Consolidated Standards of Reporting Trials (CONSORT) ¹²³ is in **Figure 2.1**. Groups were allocated into equal sizes (± 1) but were not equal after participant or Principal Investigator requested withdrawal from the study. Based on initial power analysis the study was slightly underpowered, with the double placebo group having 17 participants rather than the suggested 19. As a requirement of enrollment, all participants needed to have a history of alcohol misuse. Alcohol use disorder screening included obtaining AUDIT and SMAST questionnaire scores to grade alcohol consumption. The AUDIT and SMAST questionnaires for determining risk of AUDs and gauging drinking history are in **Figure 2.2** and **Figure 2.3**. Importantly, all participants included had a history of AUD by the Principal Investigator and had an alcoholic drink within 8 days of bronchoscopy (using alcohol at the time of the study). A summary of participant characteristics, AUDIT and SMAST scores, and participant demographics are in **Table 2.1**. There were no significant differences seen between age, weight, height, BMI, AUDIT, or SMAST score ($p > 0.05$ by ANOVA with Dunn's post-hoc). The only difference between group demographics that was significant was illegal drug use, where less of the active SAME group used illegal drugs. Notably, all groups had about 80-90% of people identifying as Male or Black/African American and under 10% identifying as Hispanic or Latino.

Oxidative stress in human alveolar macrophages: Previous studies have shown that people with AUDs have increased BAL and hAM oxidative stress occurring due to impaired redox homeostasis^{60,117}. hAMs isolated from people with AUDs have two-fold

higher generation of cellular reactive oxygen species and extracellular release of H_2O_2 ^{59,60}. Additionally, hAM oxidative stress may be due to loss of intracellular zinc and loss of reduced glutathione¹²¹, but zinc and glutathione precursor, SAME, supplements have not been investigated clinically for alcohol-induced hAM dysfunction until now. Participants with AUD had hAMs isolated for fluorescence microscopy before (B1) and after (B2) oral supplementation with either double placebo, SAME, zinc, or SAME + zinc combination, as described above in the Interventions methods section. **Figure 2.4** shows that people with AUDs who received two weeks of either oral zinc or oral zinc + SAME supplements have decreased cellular reactive oxygen species as measured by DCF fluorescence ($p < 0.05$ by multiple pairwise t-tests). Further, zinc decreased hAM mitochondrial superoxide levels as measured by MitoSOX fluorescence (**Figure 2.5**, $p < 0.05$ by multiple pairwise t-tests). Representative images have been included showing DCF and MitoSOX fluorescence at 40x. There was no difference found between any groups before supplementation, or in the double placebo and SAME only groups for either DCF or MitoSOX levels after supplementation.

Mitochondrial health dependent on mitochondrial mass and membrane potential and phagocytosis in human alveolar macrophages: hAMs isolated from people with AUDs have decreased phagocytic abilities⁶⁰, predicted to be in part caused by diminished MT function^{49,50,124}. MT health that is dependent on MT mass and membrane potential, as measured by MitoTracker CMX-Ros, was not significantly different in any of the supplementation groups (**Figure 2.6**). Phagocytic index, calculated by internalization and clearance of fluorescently labeled *S. aureus*, did not change after oral supplementation in any groups (**Figure 2.7**). While zinc was able to improve cellular

and MT oxidative stress (**Figures 2.4 and 2.5**), these biochemical changes did not result in improved MT health dependent on MT mass and membrane potential or phagocytic function in this study. Upon further evaluation, cellular reactive oxygen species and MT superoxide in pre-treatment B1 samples were significantly correlated ($p < 0.05$, **Figure 2.8A, 2.8B**), and MT superoxide levels correlated to mitochondrial health dependent on mitochondrial mass and membrane potential (**Figure 2.8C**). However, cellular reactive oxygen species, MT superoxide, and mitochondrial health dependent on MT mass and membrane potential were not correlated with phagocytic index (**Figure 2.8D-2.8F**).

Discussion

The major objective of ExZACTO was to evaluate if zinc, SAME or a combination of both supplements could improve biologically relevant outcomes in Veterans with AUDs through restoration of hAM function. Zinc and SAME are inexpensive and readily available supplements that, if effective, could decrease mortality and economic burden in this participant population. While the primary objectives noted no changes in hAM mitochondrial health or phagocytic index following 14 days of daily supplementation of zinc, SAME, or zinc + SAME, the hypothesis that zinc would decrease extracellular, cellular, and mitochondrial-derived oxidative species in AUD hAM was true. Zinc is a trace element and essential micronutrient that has been recognized as an antioxidant element for nearly 25 years¹²⁵, yet zinc does not directly interact with oxidative species. We propose two mechanisms of alcohol-induced oxidative stress dependent loss of zinc for future investigation:

1) Loss of intracellular zinc decreases zinc-driven antioxidant enzyme activity. While preliminary studies did not find that chronic alcohol use decreased serum zinc levels in a similar participant population, chronic alcohol did decrease AM intracellular zinc¹²¹. Zinc acts as a cofactor for the antioxidant enzymes superoxide dismutase and catalase, which convert superoxide and hydrogen peroxide into less reactive species, but loss of zinc may result in loss of SOD or catalase activity. AM zinc transporter and storage proteins, zinc transporter 4, metallothionein 1, metallothionein 2, were lessened following chronic ethanol *in vivo*¹²⁰, thus potentially decreasing available cellular zinc for antioxidant activity. Unfortunately, a limitation of this study is the lack of antioxidant enzyme activity data due to priority of the physiological

endpoints, MT health and phagocytic index. Ongoing studies using the same participant samples will aim to publish alveolar space redox potential as measured by GSH:GSSG ratio, as well as serum and hAM zinc levels, but studies could evaluate mRNA or protein levels of hAM antioxidant enzymes if sample quantity permits.

GSH is both intracellular and extracellular in the lung, and its depletion towards more of the oxidized form of GSH, GSSG, occurs in end-stage pulmonary diseases, such as interstitial lung disease^{122,126}, pulmonary fibrosis^{53,127-129}, and ARDS⁴⁵. We expected the GSH precursor, SAME, to decrease oxidative stress and improve hAM function in people with AUDs. SAME, however, is not only a precursor for GSH. SAME can also donate a methyl group to macromolecules including DNA, proteins, and phospholipids, thereby enforcing chromatin remodeling, protein activity, or membrane structure. GSH cannot be ruled out as a potential therapeutic to decrease alcohol-induced AM oxidative stress since SAME may not directly result in increased GSH levels or activity.

Even if SAME uptake did result in increased GSH levels, zinc and GSH have a complicated relationship. Zinc has a binding affinity for biomolecules containing O, S, or N, and prevents oxidative damage in part by preventing oxidation of sulfhydryl groups¹²⁵. However, this includes the conversion of GSH to glutathione disulfide (GSSG), which is a well-known cycle to decrease hydrogen peroxide via reduction to water^{130,131}. In fact, zinc may be a competitive antioxidant with GSH by inhibiting GSH reductase activity thus decreasing GSH antioxidant capacity. This interplay was not considered when designing the clinical trial since *ex vivo* treatment with GSH and zinc were able to improve hAM phagocytic function but could potentially explain why the

combination of a GSH precursor and zinc did not significantly decrease mitochondrial superoxide. Yet, GSH was not given orally in this study due to its low bioavailability and high oxidation in the gut. Therefore, alternative therapeutic strategies may improve oxidative stress, mitochondrial health, and phagocytosis in AMs isolated from people with AUDs.

2) Loss of intracellular zinc alters the AM transcriptome involved in redox balance. Current clinical trials using pioglitazone are in progress to determine if loss of transcriptional control of key antioxidant and metabolic regulators drive hAM alcohol-associated oxidative stress and phagocytic dysfunction. Chronic alcohol suppresses nuclear factor erythroid 2-related factor 2 (Nrf2), a transcription factor dependent on zinc that controls antioxidant responses through an antioxidant response element, and peroxisome proliferator-activated receptor gamma (PPAR γ), a transcription factor involved in metabolic regulation crucial for mitochondrial function. PPAR γ regulates Nrf2, and the PPAR γ ligand, pioglitazone, improves AM oxidative stress and phagocytic index *in vivo* in mice given chronic ethanol and *ex vivo* in hAMs isolated from people with AUDs^{60,119,132}.

Interestingly, our studies have shown that chronic alcohol depresses AM mitochondrial respiration, including the ability of AMs to use mitochondrial fuels (glucose, glutamine, or long chain fatty acids) to make ATP, meaning that disrupted mitochondrial metabolism may be central to the alcohol-induced AM phenotype. Some of these results could be explained by altered NAD:NADH ratio, as alcohol metabolism increases NADH and increased NADH is linked to higher mitochondrial superoxide levels. However, mitochondrial dysfunction goes beyond NADH-associated oxidative

stress, and we suspect that without improving PPAR γ transcription of metabolic proteins including regulation of glycolysis and fatty acid metabolism, mitochondrial respiration rates will not improve.

There may be multiple mechanisms of impaired AM phenotype, but we posit that a therapeutic strategy must involve targeting alcohol-associated oxidative stress and metabolic dysfunction together in order to improve AM phenotype. As alternative to SAME, a formulation of liposomal GSH that is more bioavailable could potentially be effective at decreasing AM oxidative stress and improving phagocytic index, but this formulation has never been tested in humans¹³³. Pioglitazone may be a more promising therapeutic because supplementation has improved multiple disrupted endpoints (oxidative stress, mitochondrial respiration, and phagocytosis)^{59,60,110}, whereas supplementation with zinc only improved oxidative stress in hAMs. Overall, there may not be one true mechanism of alcohol-induced alterations in AM phenotype, but many of the observations seen revolve around pathways related to the loss of zinc and PPAR γ . Combining zinc and/or pioglitazone may decrease the risk of pulmonary disease and improve clinical outcomes in people with AUDs with AM dysfunction.

Tables & Figures

Table 2.1

	Mean of group (SD)	Double Placebo	Active SAME	Active Zinc	Zinc + SAME	Significance
	Age (yrs.)	43 (10)	47 (9)	45 (9)	48 (10)	ns
	Weight (lbs.)	188 (43)	190 (27)	193 (34)	186 (34)	ns
	Height (in.)	69 (3)	69 (3)	70 (4)	69 (4)	ns
	BMI	28 (5)	28 (5)	28 (6)	27 (4)	ns
	AUDIT	22 (6)	20 (8)	19 (7)	21 (8)	ns
	SMAST	6 (4)	7 (3)	6 (4)	7 (3)	ns
Demographic	% of group	Double Placebo	Active SAME	Active Zinc	Zinc + SAME	
Sex	Male	88	81	86	79	ns
	Female	12	19	14	21	
Race	Black or African American	82	81	81	89	ns
	More than one race	12	10	14	5	
	White	6	10	5	5	
Ethnicity	Hispanic or Latino	6	5	0	5	ns
	Not Hispanic or Latino	94	95	100	95	
Smoking Status	Do not smoke	41	43	43	26	ns
	Smoke some days	18	10	10	11	
	Smoke every day	47	48	48	63	
Drug Use	Use illegal drugs	65	19	43	53	* p = 0.0387
	Do not use illegal drugs	35	81	57	47	

Table 2.1: Demographics from participants with alcohol use disorders (AUDs).

Demographics from participant samples (n=80) used from the Examination of Zinc, S-adenosylmethionine (SAME), and Combination Therapy Versus Placebo in People with Alcohol Use Disorders (ExZACTO, ClinicalTrials.gov identifier: NCT01899521) clinical trial. Results are expressed as mean (SD) or as percentage. Significance (*p < 0.05) was calculated using one-way AVOVA with Dunn's *post hoc* or by Chi-squared testing.

Figure 2.1

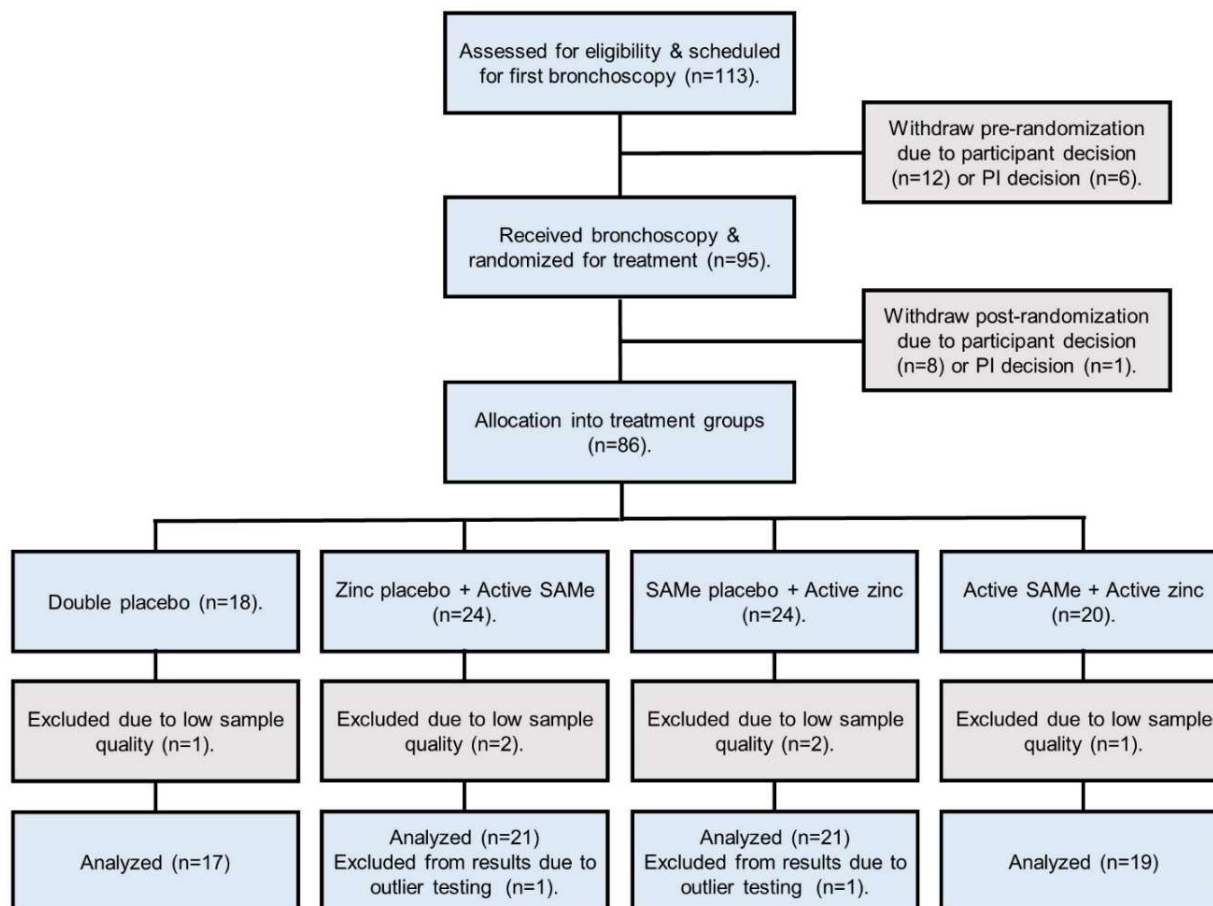


Figure 2.1: Consolidated Standards of Reporting Trials (CONSORT) flow diagram for subjects recruited into the Examination of Zinc, S-adenosylmethionine (SAME) and Combination Therapy Versus Placebo in People with Alcohol Use Disorders.

ClinicalTrials.gov identifier: NCT01899521.

Figure 2.2

<h3>The Alcohol Use Disorders Identification Test: Interview Version</h3> <p>Read questions as written. Record answers carefully. Begin the AUDIT by saying "Now I am going to ask you some questions about your use of alcoholic beverages during this past year." Explain what is meant by "alcoholic beverages" by using local examples of beer, wine, vodka, etc. Code answers in terms of "standard drinks". Place the correct answer number in the box at the right.</p>	
<p>1. How often do you have a drink containing alcohol?</p> <p>(0) Never [Skip to Qs 9-10] (1) Monthly or less (2) 2 to 4 times a month (3) 2 to 3 times a week (4) 4 or more times a week</p> <input type="text"/>	<p>6. How often during the last year have you needed a first drink in the morning to get yourself going after a heavy drinking session?</p> <p>(0) Never (1) Less than monthly (2) Monthly (3) Weekly (4) Daily or almost daily</p> <input type="text"/>
<p>2. How many drinks containing alcohol do you have on a typical day when you are drinking?</p> <p>(0) 1 or 2 (1) 3 or 4 (2) 5 or 6 (3) 7, 8, or 9 (4) 10 or more</p> <input type="text"/>	<p>7. How often during the last year have you had a feeling of guilt or remorse after drinking?</p> <p>(0) Never (1) Less than monthly (2) Monthly (3) Weekly (4) Daily or almost daily</p> <input type="text"/>
<p>3. How often do you have six or more drinks on one occasion?</p> <p>(0) Never (1) Less than monthly (2) Monthly (3) Weekly (4) Daily or almost daily</p> <p><i>Skip to Questions 9 and 10 if Total Score for Questions 2 and 3 = 0</i></p> <input type="text"/>	<p>8. How often during the last year have you been unable to remember what happened the night before because you had been drinking?</p> <p>(0) Never (1) Less than monthly (2) Monthly (3) Weekly (4) Daily or almost daily</p> <input type="text"/>
<p>4. How often during the last year have you found that you were not able to stop drinking once you had started?</p> <p>(0) Never (1) Less than monthly (2) Monthly (3) Weekly (4) Daily or almost daily</p> <input type="text"/>	<p>9. Have you or someone else been injured as a result of your drinking?</p> <p>(0) No (2) Yes, but not in the last year (4) Yes, during the last year</p> <input type="text"/>
<p>5. How often during the last year have you failed to do what was normally expected from you because of drinking?</p> <p>(0) Never (1) Less than monthly (2) Monthly (3) Weekly (4) Daily or almost daily</p> <input type="text"/>	<p>10. Has a relative or friend or a doctor or another health worker been concerned about your drinking or suggested you cut down?</p> <p>(0) No (2) Yes, but not in the last year (4) Yes, during the last year</p> <input type="text"/>
<p style="text-align: right;">Record total of specific items here <input type="text"/></p> <p><i>If total is greater than recommended cut-off, consult User's Manual.</i></p>	

Figure 2.2: The Alcohol Use Disorders Identification Test (AUDIT) questionnaire.

AUDIT scores determined alcohol consumption and risk for alcohol use disorders (AUDs) in participants screened for the Examination of Zinc, S-adenosylmethionine (SAME), and Combination Therapy Versus Placebo in People with Alcohol Use Disorders (ExZACTO, ClinicalTrials.gov identifier: NCT01899521) clinical trial. Form copied from the Study Protocol and Statistical Analysis pdf found at ClinicalTrials.gov.

Figure 2.3

SHORT MICHIGAN ALCOHOL SCREENING TEST (SMAST)

NAME: _____

Date: _____

The following questions concern information about your involvement with alcohol during the past 12 months. Carefully read each countymnt and decide if your answer is "YES" or "NO". Then, check the appropriate box beside the question.

Please answer every question. If you have difficulty with a countymnt, then choose the respons that is mostly right.

These questions refer to the past 12 months only.

YES NO

- | | YES | NO |
|---|--------------------------|--------------------------|
| 1. Do you feel that you are a normal drinker? (by normal we mean do you drink less than or as much as most other people.)..... | <input type="checkbox"/> | <input type="checkbox"/> |
| 2. Does your wife, husband, a parent, or other near relative ever worry or complain about your drinking?..... | <input type="checkbox"/> | <input type="checkbox"/> |
| 3. Do you ever feel guilty about your drinking?..... | <input type="checkbox"/> | <input type="checkbox"/> |
| 4. Do friends or relatives think you are a normal drinker?..... | <input type="checkbox"/> | <input type="checkbox"/> |
| 5. Are you able to stop drinking when you want to?..... | <input type="checkbox"/> | <input type="checkbox"/> |
| 6. Have you ever attended a meeting of Alcoholics Anonymous (AA)?..... | <input type="checkbox"/> | <input type="checkbox"/> |
| 7. Has your drinking ever created problems between you and your wife, husband, a parent or other near relative?..... | <input type="checkbox"/> | <input type="checkbox"/> |
| 8. Have you ever gotten into trouble at work because of your drinking?..... | <input type="checkbox"/> | <input type="checkbox"/> |
| 9. Have you ever neglected your obligations, your family, or your work for two or more days in a row because you were drinking?..... | <input type="checkbox"/> | <input type="checkbox"/> |
| 10. Have you ever gone to anyone for help about your drinking?..... | <input type="checkbox"/> | <input type="checkbox"/> |
| 11. Have you ever been in a hospital because of drinking?..... | <input type="checkbox"/> | <input type="checkbox"/> |
| 12. Have you ever been arrested for drunken driving, driving while intoxicated, or driving under the influence of alcoholic beverages?..... | <input type="checkbox"/> | <input type="checkbox"/> |
| 13. Have you ever been arrested, even for a few hours, because of other drunken behaviors?..... | <input type="checkbox"/> | <input type="checkbox"/> |

* SMAST Score.....

* See scoring instructions for correct scoring procedures.

Figure 2.3: Short Michigan Alcohol Screening Test (SMAST) questionnaire.

SMAST scores determined alcohol consumption and risk for alcohol use disorders (AUDs) in participants screened for the Examination of Zinc, S-adenosylmethionine (SAME), and Combination Therapy Versus Placebo in People with Alcohol Use Disorders (ExZACTO, ClinicalTrials.gov identifier: NCT01899521) clinical trial. Form copied from the Study Protocol and Statistical Analysis pdf found at ClinicalTrials.gov.

Figure 2.4

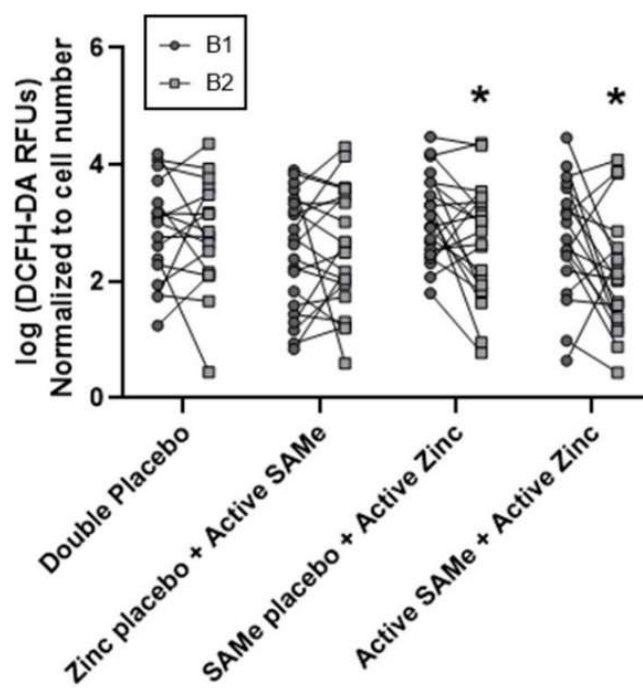
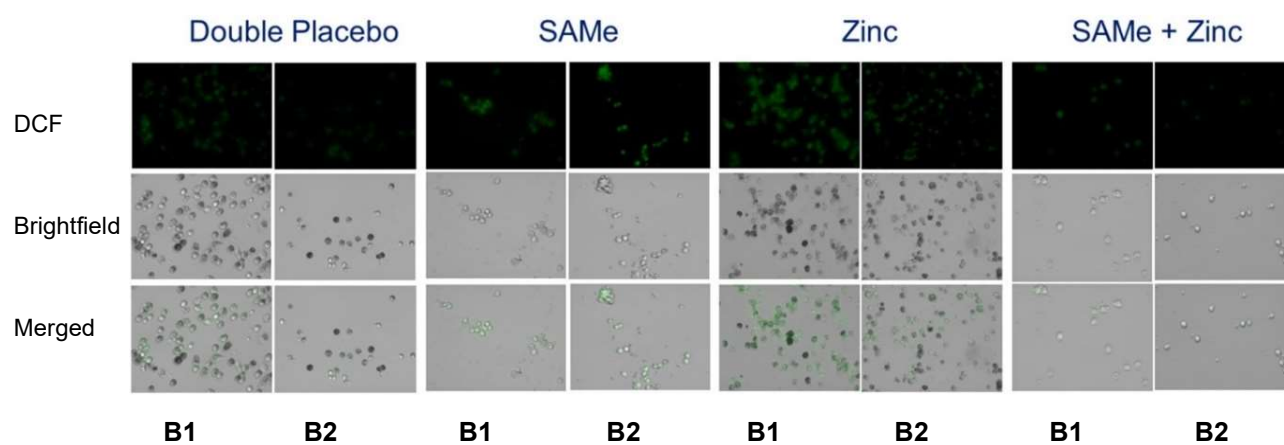


Figure 2.4: Oral zinc decreases reactive oxygen species in alveolar macrophages (hAMs) isolated from people with alcohol use disorders (AUDs). Human alveolar macrophages (hAMs) after 24 h of culture were stained with DCFH-DA and imaged for relative fluorescence. hAMs from lavage of participants who received 14 days of oral double placebo (n=17), zinc placebo + active S-adenosylmethionine (S-AMe, n=21), S-AMe placebo + active zinc (n=21), or active S-AMe + active zinc (n=19) were used. Top: Representative images of hAMs before and after 14 days of placebo or oral supplementation taken at 40x. Bottom: Quantification of RFUs before (B1) and after (B2) oral supplementation. Points shown are paired measures of RFUs. * $p < 0.05$ vs. B1 (paired t-test).

Figure 2.5

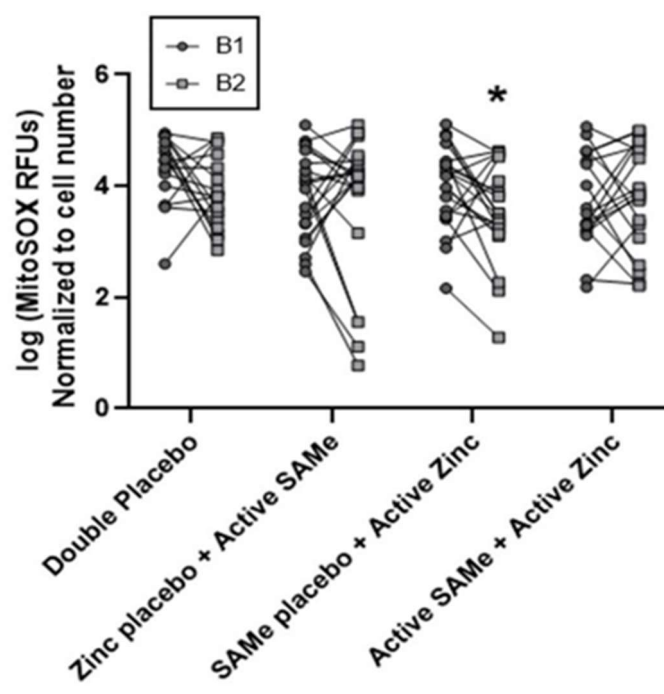
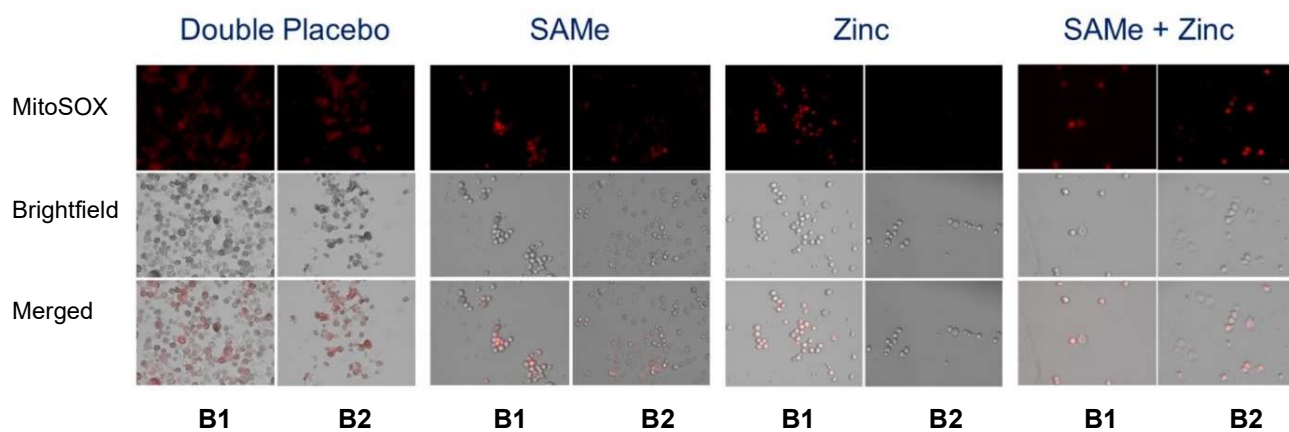


Figure 2.5: Oral zinc decreases mitochondrial superoxide in alveolar macrophages (hAMs) isolated from people with alcohol use disorders (AUDs).

Human alveolar macrophages (hAMs) after 24 h of culture were stained with MitoSOX and imaged for relative fluorescence. hAMs from lavage of participants who received 14 days of oral double placebo (n=17), zinc placebo + active S-adenosylmethionine (SAME, n=21), SAME placebo + active zinc (n=21), or active SAME + active zinc (n=19) were used. Top: Representative images of hAMs before and after 14 days of placebo or oral supplementation taken at 40x. Bottom: Quantification of RFUs before (B1) and after (B2) oral supplementation. Points shown are paired measures of RFUs. * $p < 0.05$ vs. B1 (paired t-test).

Figure 2.6

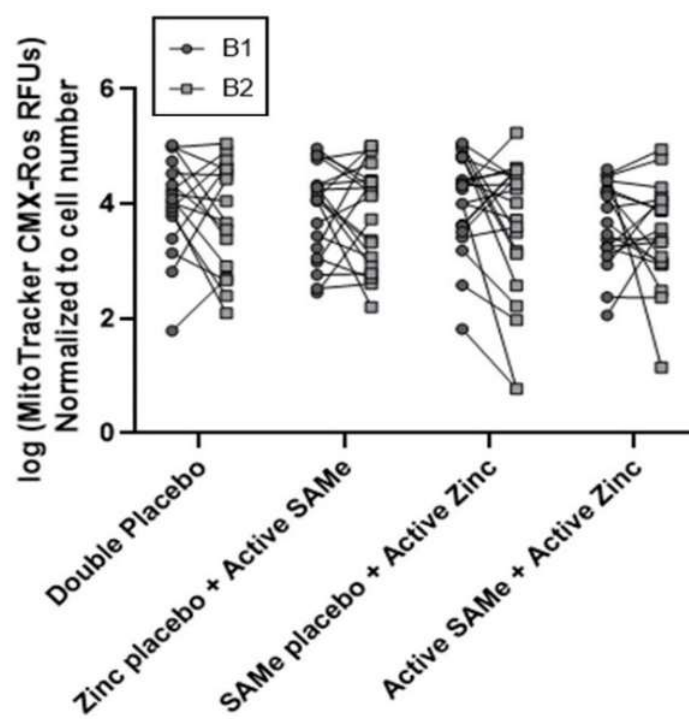
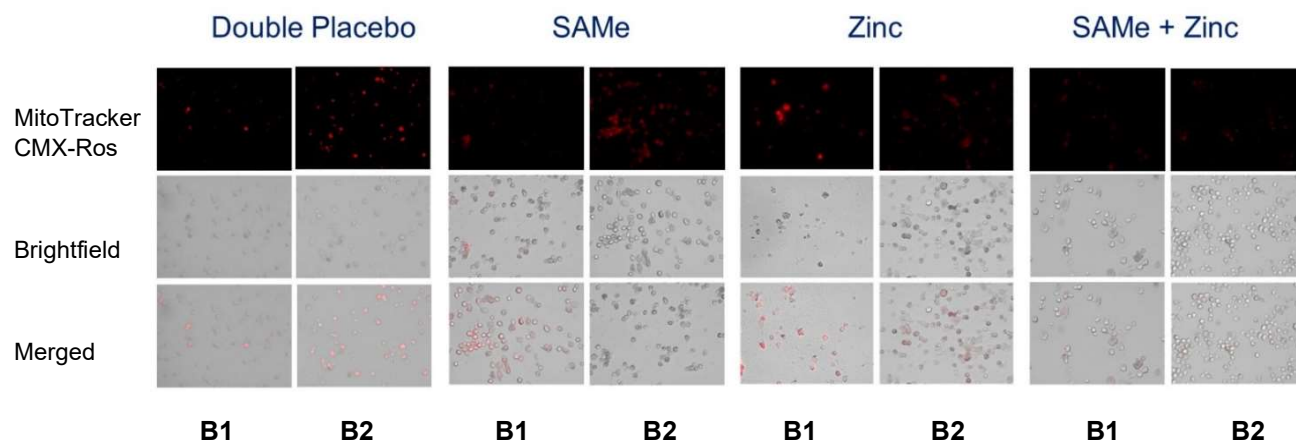


Figure 2.6: Mitochondrial health dependent on membrane potential and mass does not change in response to supplementation with zinc, SAME, or combination in alveolar macrophages (hAMs) isolated from people with alcohol use disorders (AUDs). Human alveolar macrophages (hAMs) after 24 h of culture were stained for MitoTracker CMXRos and imaged for relative fluorescence. hAMs from lavage of participants who received 14 days of oral double placebo (n=17), zinc placebo + active S-adenosylmethionine (SAME, n=21), SAME placebo + active zinc (n=21), or active SAME + active zinc (n=19) were used. Top: Representative images of hAMs before and after 14 days of placebo or oral supplementation taken at 40x. Bottom: Quantification of RFUs before (B1) and after (B2) oral supplementation. Points shown are paired measures of RFUs. * $p < 0.05$ vs. B1 (paired t-test).

Figure 2.7

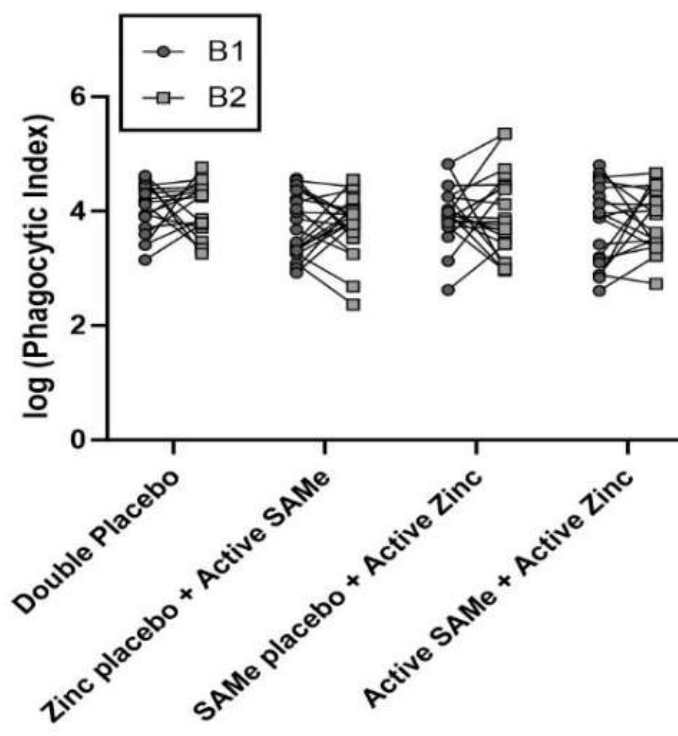
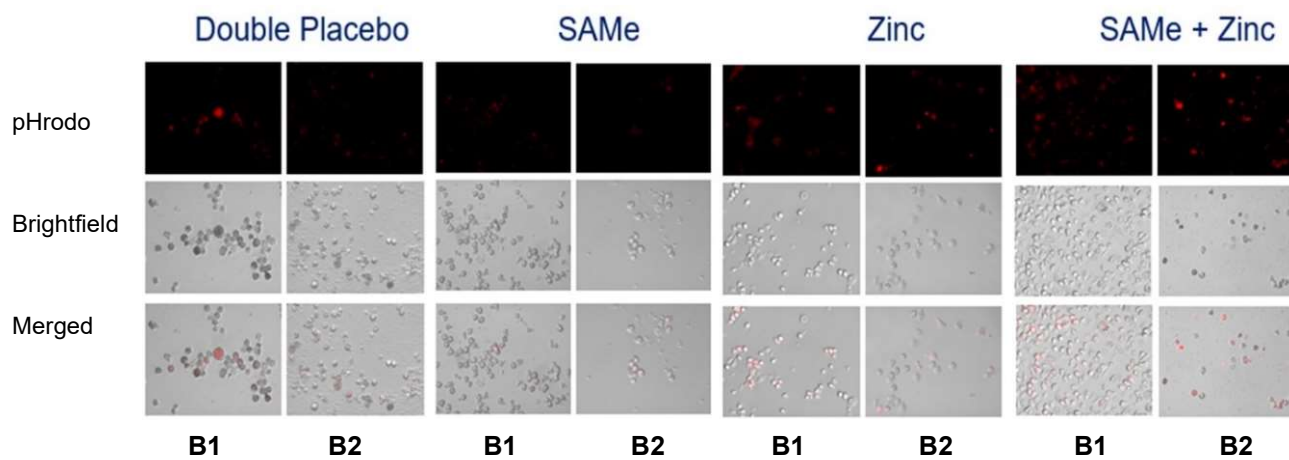


Figure 2.7: Phagocytic index does not change in response to supplementation with zinc, S-adenosylmethionine (SAME), or combination in alveolar macrophages (hAMs) isolated from people with alcohol use disorders (AUDs). Human alveolar macrophages (hAMs) after 24 h of culture were stained for pHrodo *Staphylococcus aureus* and imaged for relative fluorescence. hAMs from lavage of participants who received 14 days of oral double placebo (n=17), zinc placebo + active S-adenosylmethionine (SAME, n=21), SAME placebo + active zinc (n=21), or active SAME + active zinc (n=19) were used. Top: Representative images of hAMs before and after 14 days of placebo or oral supplementation taken at 40x. Bottom: Quantification of phagocytic index (RFUs * number of cells positive for *S. aureus* uptake / total cells) before (B1) and after (B2) oral supplementation. Points shown are paired measures of phagocytic index. * p < 0.05 vs. B1 (paired t-test).

Figure 2.8

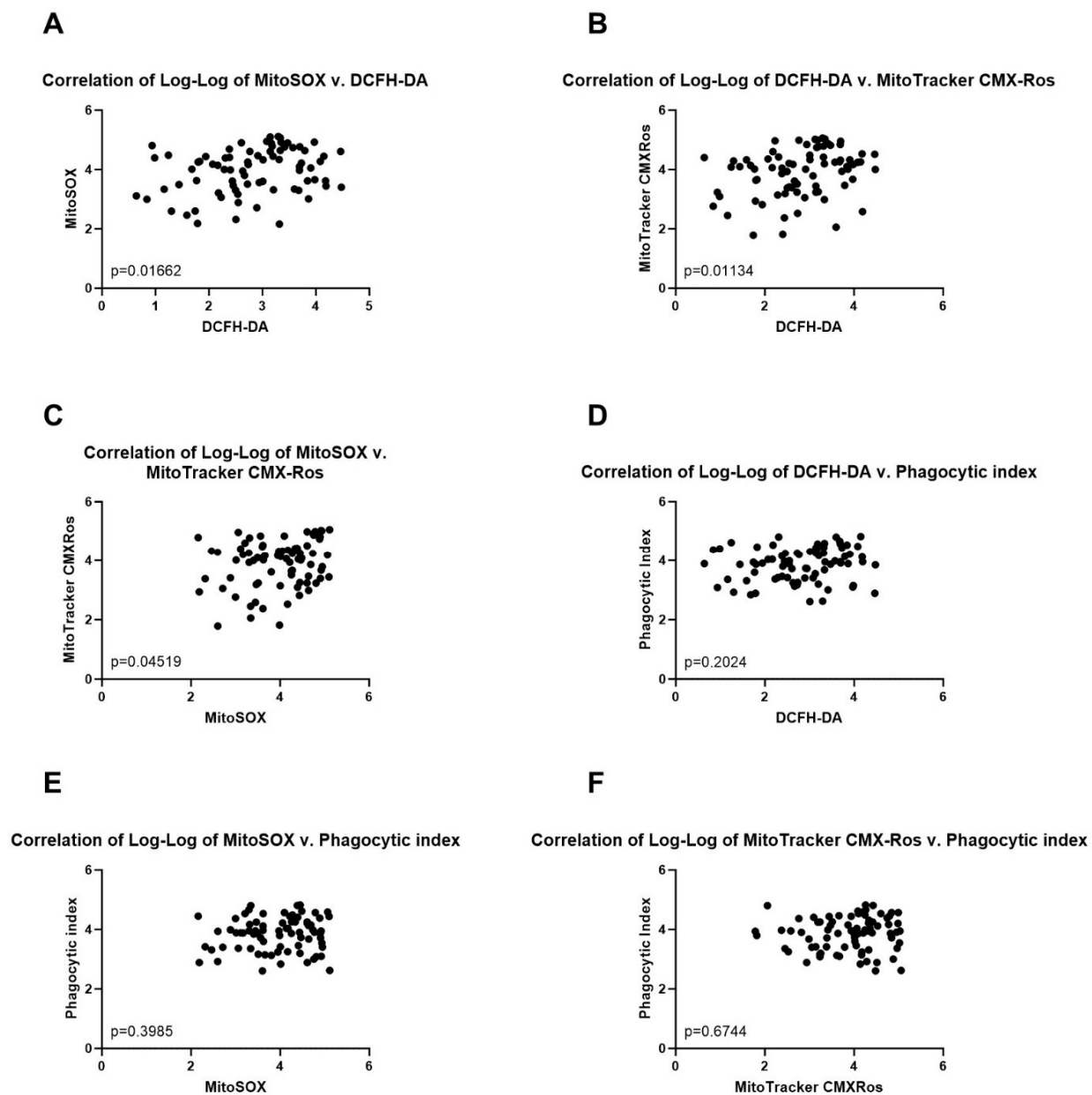


Figure 2.8: Oxidative stress is not correlated with phagocytic index in alveolar macrophages (hAMs) isolated from people with alcohol use disorders (AUDs) who did not undergo treatment. A-C) Markers of oxidative stress and mitochondrial health dependent on mitochondrial mass and membrane potential are correlated in hAMs from people with alcohol use disorders who did not undergo treatment (n=78, $p < 0.05$). **D-F)** hAM phagocytic index is not correlated with cellular reactive oxygen species, mitochondrial superoxide levels, or mitochondrial health dependent on mitochondrial mass and membrane potential in people with alcohol use disorders (n=78) who did not undergo treatment.

2.2 Conclusions

This chapter contributed toward the field by showing that oral zinc sulfate decreases cellular and mitochondrial oxidative species in AMs isolated from people with AUDs. Yet, at this time point and concentration of zinc, this decrease in oxidative stress did not result in improved AM phagocytic capacity. Rather, cellular ROS or mitochondrial superoxide were not correlated with phagocytic index. These conclusions challenge the previously thought idea that alcohol-induced AM phagocytic dysfunction is due to increased oxidative stress. Moving forward, these results need future confirmation and a causal relationship between loss of phagocytosis will need to be linked to specific molecular mechanisms. The following chapters include further characterization of the alcohol-induced AM phenotype to better predict these underlying molecular mechanisms and target them for treatment.

Chapter 3: Application of Pioglitazone to Improve Alcohol-Induced Alveolar Macrophage Metabolic and Phagocytic Dysfunction

Alcohol diminishes AM phagocytosis in part by promoting MT dysfunction. The previous chapter described one approach to restoring AM function by improving oxidative stress. While oxidative stress and loss of AM phagocytic capacity are features of an altered AM phenotype during chronic alcohol exposure, AMs also demonstrate a metabolic shift whereby cells exhibit diminished MT-derived ATP-linked respiration⁵⁹. This chapter includes two published manuscripts that further characterize the shift in AM energy metabolism during chronic ethanol exposure. One co-author manuscript (copied here from PMID: 35634337) details AM metabolic dysfunction potentiated by hypoxia-inducible factor-1 alpha (HIF-1 α) stabilization and promotion of glycolysis rather than oxidative phosphorylation. Pioglitazone (PIO), the PPAR γ ligand with antioxidant effects, reverses EtOH-dependent shift toward glycolysis *in vitro* and *in vivo*.

I contributed toward this manuscript by assisting with mouse experiments, collecting, and processing *in vivo* and *in vitro* samples, performing experiments using these samples, and analyzing the data collected from experiments. In this first co-author manuscript, I supplied data for Figures 3.1.1A-F, 3.1.6C, 3.1.10A-F, and Supplemental Fig. 3.1.3A-D. For Figures 3.1.1 and 3.1.10 I performed seahorse assays to measure cell energy phenotype and glycolytic rate in mouse AMs from one cohort of animals (n= 3-5 per group). I helped with SOP development, animal husbandry, chronic EtOH feeding, sacrifice, and AM isolation in the months prior to these experiments. The results of Figure 3.1.1 indicate that chronic EtOH feeding in mice shifts AMs toward a glycolytic phenotype. Additionally, for Figure 3.1.6 I imaged and analyzed phagocytic

capacity in murine AMs (MH-S cell line) treated with and without cobalt chloride (CoCl₂), a stabilizer of hypoxia-inducible factor-1 alpha (HIF-1α) levels. Further, for supplemental Figure 3.1.3 I cultured, transfected, and performed and analyzed seahorse assays in MH-S cells treated with and without chronic EtOH (0.08%, 72 h). In combination with Figure 3.1.5, we determined that stabilization of HIF-1α using CoCl₂ mimics the phenotypic shift seen in AMs exposed to chronic EtOH (increased glycolysis and decreased phagocytosis), and that this EtOH-induced shift is in part dependent on HIF-1α.

3.1 Alcohol-Induced Glycolytic Shift in Alveolar Macrophages Is Mediated by Hypoxia-Inducible Factor-1 Alpha

Niya L. Morris^{1,2}, David N. Michael^{1,2}, Kathryn M. Crotty^{1,2}, Sarah S. Chang^{1,2} and Samantha M. Yeligar^{1,2*}

¹ Department of Medicine, Division of Pulmonary, Allergy, Critical Care and Sleep Medicine, Emory University, Atlanta, GA, United States, ² Atlanta Veterans Affairs Health Care System, Decatur, GA, United States

*Correspondence: Samantha M. Yeligar, syeligar@emory.edu

Full Citation: Morris NL, Michael DN, Crotty KM, Chang SS, Yeligar SM. Alcohol-induced Glycolytic Shift in Alveolar Macrophages Is Mediated by Hypoxia-Inducible Factor-1 Alpha. *Front Immunol.* 2022 May 11;13:865492. doi: 10.3389/fimmu.2022.865492. PMID: 35634337; PMCID: PMC9130492.

Author Contributions: NLM designed experiments, obtained samples from animal experiments, analyzed experiments, and prepared the manuscript; DNM, KMC, and SSC obtained samples from animal experiments and analyzed experiments; SMY designed and analyzed experiments and prepared the manuscript. All authors contributed to the article and approved the submitted version.

Abstract

Excessive alcohol use increases the risk of developing respiratory infections partially due to impaired alveolar macrophage (AM) phagocytic capacity. Previously, we showed that chronic ethanol (EtOH) exposure led to mitochondrial derangements and diminished oxidative phosphorylation in AM. Since oxidative phosphorylation is needed to meet the energy demands of phagocytosis, EtOH mediated decreases in oxidative phosphorylation likely contribute to impaired AM phagocytosis. Treatment with the peroxisome proliferator-activated receptor gamma (PPAR γ) ligand, pioglitazone (PIO), improved EtOH-mediated decreases in oxidative phosphorylation likely contribute to impaired AM phagocytosis. Treatment with the peroxisome proliferator-activated receptor gamma (PPAR γ) ligand, pioglitazone (PIO), improved EtOH-mediated decreases in oxidative phosphorylation. In other models, hypoxia-inducible factor-1 alpha (HIF-1 α) mediates the switch from oxidative phosphorylation to glycolysis; however, the role of HIF-1 α in chronic EtOH mediated derangements in AM has not been explored. We hypothesize that AMs undergo a metabolic shift from oxidative phosphorylation to a glycolytic phenotype in response to chronic EtOH exposure. Further, we speculate that HIF-1 α is a critical mediator of this metabolic switch. To test these hypotheses, primary mouse AM (mAM) were isolated from a mouse model of chronic EtOH consumption, and a mouse AM cell line (MH-S) was exposed to EtOH *in vitro*. Expression of HIF-1 α , glucose transporters (Glut1 and 4), and components of the glycolytic pathway (Pfkfb3 and PKM2), were measured by qRT-PCR and western blot. Lactate levels (lactate assay), cell energy phenotype (extracellular flux analyzer), glycolysis stress tests (extracellular flux analyzer), and phagocytic function (fluorescent

microscopy) were conducted. EtOH exposure increased expression of HIF-1 α , Glut1, Glut4, Pfkfb3, and PKM2 and shifted AM to a glycolytic phenotype. Pharmacological stabilization of HIF-1 α via cobalt chloride treatment *in vitro* mimicked EtOH-induced AM derangements (increased glycolysis and diminished phagocytic capacity). Further, PIO treatment diminished HIF-1 α levels and reversed glycolytic shift following EtOH exposure. These studies support a critical role for HIF-1 α in mediating the glycolytic shift in energy metabolism of AM during excessive alcohol use.

Keywords: alveolar macrophage; energy metabolism; ethanol; glycolysis; hypoxia-inducible factor-1 alpha.

Introduction

Over 15 million people in the United States have been diagnosed with alcohol use disorders¹³⁴. Excessive alcohol use increases morbidity and mortality⁷ and increases risk of developing respiratory infections⁹, which is largely linked to immune dysfunction in alveolar macrophages (AMs)^{46,112,113,121}. AMs initiate the immune response to pathogens in the lower airway¹⁰⁹, but excessive alcohol use impairs AM phagocytic capacity and bacterial clearance^{112,135}. Phagocytosis requires high energy demands, and mitochondrial-dependent oxidative phosphorylation is the most efficient method of generating cellular ATP. Our laboratory has established that chronic alcohol exposure results in AM mitochondrial dysfunction (e.g., mitochondrial fragmentation, morphological alteration, and derangements in mitochondrial bioenergetics)⁵⁹. Further, treatment with the peroxisome proliferator-activated receptor gamma (PPAR γ) ligand, pioglitazone (PIO), improved AM phagocytic dysfunction^{46,60} and oxidative phosphorylation⁵⁹ during ethanol (EtOH) exposure.

One mechanism employed by cells to meet their energy demands in the absence of oxidative phosphorylation is glycolysis¹³⁶. Glycolysis is a metabolic pathway that converts glucose into pyruvate utilizing enzymatic proteins, such as 6-phosphofructo-2-kinase/fructose-2,6-bisphosphatase 3 (Pfkfb3) and pyruvate kinase M2 (PKM2), to generate energy^{136,137}. Blocking key glycolytic proteins such as Pfkfb3 and PKM2 has been shown to mitigate acute lung injury^{138,139}. The effect of EtOH on these glycolytic proteins in AM has not been explored.

Stabilization of hypoxia-inducible factor (HIF)-1 α and subsequent formation of HIF-1 (comprised of the inducible HIF-1 α and constitutive HIF-1 β) increases the

transcription of numerous genes including those in the glycolytic pathway, such as glucose transporters (GLUT) 1 and 4 and pyruvate dehydrogenase kinase 1 (PDK-1)¹⁴⁰⁻¹⁴². Mounting evidence suggests that HIF-1 α may act as a “metabolic switch”, shifting cells from relying on oxidative phosphorylation towards glycolysis instead¹⁴¹⁻¹⁴³. The availability of glucose needed for glycolysis is in part regulated by glucose transporters which transport glucose into the cell¹³⁶. HIF-1 α (with GLUT and PDK-1) have been shown in other models to contribute to lung injury¹⁴⁴⁻¹⁴⁶. Further, numerous studies have shown a direct relationship between HIF-1 α and EtOH-mediated pathologies in the brain¹⁴⁷, adipose tissue¹⁴⁸, and liver¹⁴⁹. The findings from these studies showed that EtOH-induced HIF-1 α can occur during oxidative stress or elevated inflammation.

The relationship between HIF-1 α and these metabolic derangements in the context of chronic EtOH-induced AM phagocytic dysfunction, however, has not been examined and is the focus of the current study. Our data demonstrate that HIF-1 α is a critical mediator of EtOH-mediated energy derangements in AM, suggesting a key role of HIF-1 α in EtOH-mediated lung pathobiology. Further, PIO attenuated EtOH-induced HIF-1 α , which could provide a novel therapeutic strategy in the treatment of alcohol use disorders in the lung and decrease susceptibility to respiratory infections.

Materials & Methods

Mouse Model of Chronic Ethanol Ingestion

Animal studies were carried out in accordance with the National Institutes of Health guidelines as outlined in the Guide for the Care and Use of Laboratory Animals. Additionally, all protocols were reviewed and approved by the Atlanta VA Health Care System Institutional Animal Care and Use Committee. 8- to 10-week-old male C57BL/6J mice purchased from Jackson Laboratory (Bar Harbor, Maine, United States) were fed standard laboratory chow ad libitum. Mice were randomly divided into two groups (control and EtOH). EtOH fed mice received increases of EtOH (5% w/v every 3-4 days) in their drinking water for 2 weeks until the EtOH concentration reached 20% w/v and this concentration was maintained for 10 weeks, resulting in a 0.12% blood alcohol level^{46,48,113}. During the last week of ethanol ingestion, mice were administered PIO (10 mg / kg / day in 100- μ L methylcellulose vehicle) or vehicle alone via oral gavage⁴⁶. Following euthanasia, tracheas were cannulated, and a tracheotomy was performed to collect bronchoalveolar lavage fluid. Bronchoalveolar lavage fluid was centrifuged at 8000 RPM for 5 minutes to isolate mouse alveolar macrophages (mAM). Isolated mAM were resuspended in RPMI-1640 culture medium (2% fetal bovine serum and 1% penicillin/streptomycin) for 24 hours for further experimentation^{46,113}. Lung tissue was harvested and homogenized for RNA isolation.

***In Vitro* Ethanol Exposure of MH-S Cells**

The mouse alveolar macrophage cell line (MH-S) was purchased from American Type Culture Collection (Manassas, VA, United States). MH-S cells were cultured in RPMI-1640 medium (10% fetal bovine serum, 1% penicillin/streptomycin, 11.9 mM

sodium bicarbonate, gentamicin (40mg/ml) and 0.05 mM 2mercaptoethanol) in the presence or absence of 0.08% EtOH for 72 hours (media changed daily) at 37°C in a humidified incubator in 5% CO₂¹¹². In a subset of experiments, MH-S were treated with PIO (10 mM; last 24 hours of EtOH exposure) (Cayman Chemicals, Ann Arbor, Michigan, United States).

Cell Energy Phenotype Test

Cell energy phenotype tests were performed to evaluate the metabolic phenotypes of mAM and MH-S using either an XFe96 (Catalog number: 103325-100) or an XFp extracellular flux analyzer (Catalog number: 103275-100) (Agilent Seahorse Bioscience Inc.; Billerica, MA, United States). Oxygen consumption rate (OCR) and extracellular acidification rate (ECAR) were measured in mAM and MH-S over time in XF Base Medium supplemented with 1 mM of sodium pyruvate, 10 mM glucose, and 2 mM of L-glutamine followed by a single injection of 2 mM oligomycin (ATP synthase inhibitor) + 0.5 mM carbonilcyanide p-triflouromethoxyphenylhydrazone (FCCP; a mitochondrial uncoupling agent). XFp plates were precoated with collagen (~4 hours) and washed with PBS and media prior to addition of mAM cells to promote mAM adherence to the plates. Raw OCR and ECAR were determined using the XF Wave 2.1 software. OCR and ECAR values were calculated, normalized to cell protein concentration in the same sample, and were expressed as mean of biological replicates ± standard error of the mean (SEM).

Glycolysis Stress Test

Glycolysis stress tests were performed using either an XFe96 or an XFp extracellular flux analyzer (Agilent Seahorse Bioscience Inc.) to evaluate the parameters of glycolytic flux. ECAR was measured in mAM and MH-S over time in XF Base Medium supplemented with 2 mM L-glutamine followed by sequential injections of 10 mM glucose (saturating concentration of glucose to promote glycolysis), 2 mM oligomycin (ATP synthase inhibitor), and 50 mM 2-deoxy-glucose (2-DG; a glucose analog that inhibits glycolysis). To maximize mAM adherence to XFp microculture plates, wells were precoated with collagen (~4 hours) and were subsequently washed with PBS and media before addition of cells. Glycolysis, glycolytic capacity, glycolytic reserve, and non-glycolytic acidification were determined using the XF Wave 2.1 software. Raw ECAR was determined using the XF Wave 2.1 software. Glycolysis, glycolytic capacity, glycolytic reserve, and non-glycolytic acidification ECAR values were calculated, normalized to cell protein concentration in the same sample, and were expressed as mean of biological replicates \pm SEM.

RNA Isolation and Quantitative RT-PCR (qRT-PCR)

TRIzol reagent (Catalog number:15596026, Invitrogen, Waltham, MA, United States) was used to isolate total RNA. Primer sequences outlined in **Table 3.1.1** were used to measure and quantify target mRNA levels by qRT-PCR with iTaq Universal SYBR Green One-Step kit (Catalog number: 1725151, Bio-Rad, Hercules, CA, United States) using the Applied Biosystems ABI Prism 7500 version 2.0.4 sequence detection system^{46,113}. Target mRNA values were normalized to 9S or glyceraldehyde-3-phosphate dehydrogenase (GAPDH). mRNA levels were expressed as fold-change of mean \pm SEM, relative to control samples.

TABLE 3.1.1 | Primer sequences to measure mRNA levels using qRT-PCR.

	Gene	Forward Sequence (5' to 3')	Reverse Sequence (5' to 3')
Mouse	GAPDH	GGATTTGGTCGTATTGGG	GGAAGATGGTGATGGGATT
Mouse	Glut1	CTCCTGCCCTGTTGTGTATAG	AAGGCCACAAAGCCAAAGAT
Mouse	Glut4	AAAAGTGCCTGAAACCAGAG	TCACCTCCTGCTCTAAAAGG
Mouse	HIF-1 α	CTCAAAGTCGGACAG	CCCTGCAGTAGGTTT
Mouse	Pfkfb3	TCTAGAGGAGGTGAGATCAG	CCTGCCACTCTTATCTTCTG
Mouse	Pkm2	GAGGCCTCCTTCAAGTGCT	CCAGACTTGGTGAGGACGAT
Mouse	9S	ATCCGCCAGCGCCATA	TCGATGTGCTTCTGGGAATCC

GAPDH; glyceraldehyde 3-phosphate dehydrogenase, Glut1; glucose transporter 1, Glut4; glucose transporter 4, HIF-1 α ; hypoxia-inducible factor-1 alpha, Pfkfb3; 6-phosphofructo-2kinase/fructose-2,6-bisphosphatase 3, PKM2; pyruvate kinase M2.

Cytoimmunostaining and Phagocytosis by Fluorescent Microscopy

HIF-1 α protein was measured in mAM isolated from control and EtOH-fed mice. mAMs were fixed with 4% paraformaldehyde and incubated with a HIF-1 α rabbit monoclonal antibody (1:500, Cell Signaling Technology, Danvers, MA, United States) for 1 hour, washed, and incubated with fluorescent-labeled antirabbit secondary antibody (1:1000) for 1 hour. Protein values were normalized to 4',6-diamidino-2-phenylindole (DAPI) nuclear stain.

In vitro phagocytic capacity in MH-S was determined using pHrodo *Staphylococcus aureus* BioParticles conjugate (Catalog number: A10010, Invitrogen). MH-S (1.2×10^5 cells) were incubated with 1×10^6 particles of pH-sensitive fluorescent labeled *S. aureus* for 2 hours. Following the incubation, cells were fixed with 4% paraformaldehyde. Cells with internalized *S. aureus* were considered positive for phagocytosis. Phagocytic capacity was quantified as phagocytic index: cells positive for internalized bacteria multiplied by the relative fluorescent units (RFU) of *S. aureus* per cell. Phagocytic index is expressed as foldchange of mean \pm SEM, relative to control samples^{46,60}.

Fluorescence for HIF-1 α cytoimmunostaining and phagocytosis of *S. aureus* was measured using FluoView (Olympus, Melville, New York, United States) and are expressed as fold-change of mean relative fluorescent units RFU per cell \pm SEM, relative to control samples. RFU were evaluated in at least 10 cells per field, with 10 fields per experimental condition. Gain and gamma microscope settings were constant for each field and experimental condition. ImageJ was used to deconvolute and analyze images^{59,145}.

Western Blot

Proteins were isolated from MH-S using SESSA lysis buffer and quantified using the Pierce bicinchoninic acid (BCA) Protein Assay Kit (Catalog number for Pierce BCA Protein Assay Reagent A: 23228 and Catalog number for Pierce BCA Protein Assay Reagent B: 23224, Thermofisher, Waltham, Massachusetts, United States). Equal amounts of protein from cell lysates were loaded on NuPAGE Novex 10% Bis-Tris Protein Gels (Catalog number: NP0301BOX, Fisher Scientific, Hampton, NH, United States) subsequent to being transferred onto nitrocellulose membranes. The membranes were blocked in 5% non-fat milk and TBST for 1 hour and then incubated with primary antibodies for HIF-1 α rabbit monoclonal antibody (Catalog number: 14179S, 1:500, Cell Signaling Technology) or GAPDH rabbit polyclonal antibody (Catalog number: G9545-100UL, 1:20,000, GAPDH, Sigma-Aldrich, St. Louis, MO, United States) overnight at 4°C. Following this incubation, the membranes were washed and incubated with 1:10,000 anti-rabbit IRDye800CW Secondary Antibodies (Catalog number: 926-32211, Li-COR Biosciences, Lincoln, NE, United States) for 1 hour at room temperature. Odyssey Infrared Imaging System (LI-COR Biosciences) was used to image the membranes. Image J software (NIH, Bethesda, MD, United States) was used to measure densitometry. HIF-1 α protein values were normalized to GAPDH and expressed as foldchange of mean \pm SEM, relative to control samples.

Lactate Assay

Lactate levels in MH-S were determined using a lactate assay kit (Catalog number: MAK064, Sigma Aldrich) according to the manufacturer's instructions. Lactate

values were normalized to protein concentration in the same sample and were expressed as fold-change of mean \pm SEM, relative to control samples.

Cobalt Chloride Treatment of MH-S

MH-S were treated with the HIF-1 α stabilizer cobalt (II) chloride hexahydrate (Catalog number: C8661-25g, 25 mM, CoCl₂, Sigma-Aldrich) in PBS vehicle or PBS alone for 4 hours. CoCl₂ increases HIF-1 α expression (28) and stabilizes HIF-1 α by inhibiting the binding of von Hippel Lindau E3 ubiquitin ligase, preventing HIF-1 α ubiquitination and subsequent degradation¹⁵⁰.

Transient Transfection of MH-S

HIF-1 α was silenced in MH-S using transient transfection of a HIF-1 α siRNA (Catalog number: sc-35562, Santa Cruz, Dallas, TX, United States), and HIF-1 α was induced in MH-S using transient transfection of HIF-1 α lysate (Catalog number: sc120778, Santa Cruz). MH-S were resuspended in 100 mL of Amaxa Mouse Macrophage Nucleofector Kit solution (Catalog number: VPA-1009, Lonza, Alpharetta, GA, United States) containing 100 nM of control scrambled (Catalog number: sc37007, control-scr, Santa Cruz), siRNA for HIF-1 α (siHIF-1 α), or HIF-1 α lysate (HIF-1 α) followed by nucleofection according to the manufacturer's protocol using program Y-001. Following transfection, MH-S were washed with media and cultured with or without 0.08% EtOH for 3 days (media changed daily).

Statistical Analysis

Data are presented as mean \pm SEM. A Student's t-test was used in studies with two groups. In studies, with more than two groups, statistical significance was

calculated using one-way analysis of variance (ANOVA) followed by Tukey-Kramer *post hoc* (GraphPad Prism version 9, San Diego, CA). In the event that the data was not normally distributed, a non-parametric statistical analysis using Kruskal-Wallis test was used. $P < 0.05$ was considered significant.

Results

Ethanol Shifts AM to a Glycolytic Metabolic Phenotype

Previously, we have shown that EtOH exposure alters mitochondrial morphology and negatively impacts mitochondrial bioenergetics⁵⁹. To assess whether EtOH exposure increased glycolysis, we evaluated the cell energy phenotype of mAM isolated from control and EtOH-fed mice. mAM from EtOH-fed mice shifted to a glycolytic phenotype in response to the oligomycin + FCCP stressors (**Figure 3.1.1A**). To provide further evidence that EtOH resulted in glycolytic shift, we performed a glycolysis stress test on mAM from control and EtOH fed mice. Compared with mAM from control mice, mAM from EtOH fed mice exhibited increased glycolytic profiling (**Figure 3.1.1B**), glycolysis (**Figure 3.1.1C**), glycolytic capacity (**Figure 3.1.1D**), glycolytic reserve (**Figure 3.1.1E**), and non-glycolytic acidification (**Figure 3.1.1F**). Similar to our *in vivo* studies, glycolytic bioenergetics were elevated in EtOH-treated MH-S (**Figure 3.1.2**) compared to control. Assessment of the cell energy phenotype of EtOH treated MH-S exhibited a glycolytic shift compared to control (**Figure 3.1.2A**). Additionally, EtOH treated MH-S displayed increased glycolytic profiling compared to control (**Figure 3.1.2B**). Finally, glycolysis (**Figure 3.1.2C**), and glycolytic capacity (**Figure 3.1.2D**) were also elevated in EtOH-treated MH-S compared to controls. We did not observe any differences in glycolytic reserve (**Figure 3.1.2E**) or non-glycolytic acidification (**Figure 3.1.2F**) between the groups. Collectively, these data illustrate that AMs exhibit a glycolytic energy phenotype in response to EtOH.

Ethanol Increases Glycolytic Proteins in Mouse Lungs and MH-S

As we observed increases in glycolytic flux following EtOH exposure in AM, we assessed expression of the glucose transporters, Glut1 and Glut4, and key enzymes of the glycolytic pathway, Pfkfb3 and PKM2. mRNA levels of Glut1, Glut4, Pfkfb3, and PKM2 increased in response to EtOH (**Figure 3.1.3A**). Additionally, EtOH induced mRNA expression of Glut1 in mouse lung homogenates (**Supplementary Figure 3.1.S1**). Since lactate levels correlate with generation of ECAR during glycolysis¹⁵¹, we investigated the effect of EtOH on AM lactate levels. EtOH elevated lactate in response to EtOH in MH-S (**Figure 3.1.3B**). These results further suggest that EtOH induces glycolysis in mouse lungs and AM.

Ethanol Induces HIF-1 α in mAM and MH-S

We sought to investigate the mechanism by which EtOH increased parameters of glycolytic flux in AM. HIF-1 α , a component of the transcription factor HIF-1, can act as a “metabolic switch”. HIF-1 increases the transcription of some genes in the glycolytic pathway and has been shown in other models to be increased by EtOH exposure^{147-149,152}. Here, we examined how EtOH affected hypoxia-inducible factor (HIF)-1 α in AM. mRNA and protein levels of HIF-1 α were measured in control and EtOH mAM. EtOH feeding elevated mAM HIF-1 α mRNA (**Figure 3.1.4A**) and protein (**Figure 3.1.4B**) expression. Similarly, we observed increases in HIF-1 α mRNA (**Figure 3.1.4C**) and protein (**Figure 3.1.4D**) in MH-S exposed to EtOH compared to control. Collectively, these data show that EtOH induces HIF-1 α in AM.

HIF-1 α Mediates Ethanol-Induced Derangements in AM Glycolytic Shift in MH-S

To establish whether HIF-1 α is implicated in EtOH-mediated glycolytic shift in AM, control MH-S were treated with cobalt chloride, a HIF-1 α stabilizer. Treatment of

MH-S with cobalt chloride mimicked the increase in HIF-1 α mRNA (**Supplementary Figure 3.1.2A**) and protein (**Supplementary Figure 3.1.2B**) seen in AM exposed to EtOH (**Figure 3.1.4**). Cobalt chloride exposed MH-S exhibited increases in components of glycolytic profiling (**Figure 3.1.5A**), glycolysis (**Figure 3.1.5B**), and glycolytic capacity (**Figure 3.1.5C**) similar to our EtOH studies of AM (**Figures 3.1.1 & 3.1.2**). Similar to our *in vitro* studies (**Figure 3.1.2**), we did not observe changes in glycolytic reserve (**Figure 3.1.5D**) and non-glycolytic capacity (**Figure 3.1.5E**) with cobalt chloride treatment. Concomitantly, treatment of MH-S with HIF-1 α lysate increased glycolytic profiling (**Supplementary Figure 3.1.3A**), glycolysis (**Supplementary Figure 3.1.3B**), glycolytic capacity (**Supplementary Figure 3.1.3C**), and glycolytic reserve (**Supplementary Figure 3.1.3D**). Glut4, Pfkfb3, and PKM2 (**Figure 3.1.6A**) mRNA levels and lactate levels (**Figure 3.1.6B**) increased in response to cobalt chloride, similar EtOH-treated MH-S (**Figure 3.1.3**). As cobalt chloride is a mimetic for HIF-1 α , these data suggest that EtOH-induced HIF-1 α mediates the glycolytic shift observed in AM. Further, similar to our EtOH studies^{46,60}, treatment with cobalt chloride led to AM phagocytic dysfunction (**Figure 3.1.6C**).

HIF-1 α Modulates EtOH-Induced Glycolysis and Phagocytic Function in MH-S

To further implicate HIF-1 α in modulating EtOH-induced glycolysis, we knocked down HIF-1 α in the presence and absence of EtOH. We determined that knockdown of HIF-1 α prevented EtOH-mediated glycolytic shift (**Figure 3.1.7A**). Further, these improvements coincided with improved phagocytic index in MH-S lacking HIF-1 α in the presence of EtOH (**Figure 3.1.7B**). Collectively, these data show that HIF-1 α plays a

key role in EtOH-mediated increases in AM glycolysis and impaired phagocytic capacity.

Pioglitazone Treatment Reverses Ethanol-Induced HIF-1 α

The PPAR γ ligand, PIO, has been previously reported to improve EtOH-mediated mitochondrial derangements⁵⁹, and phagocytic dysfunction^{46,60}. As such, we sought to delineate whether PIO may affect EtOH-induced AM HIF-1 α . PIO treatment diminished HIF-1 α mRNA (**Figure 3.1.8A**) and protein (**Figure 3.1.8B**) levels. Collectively, these data identify PIO as a therapeutic strategy to mitigate EtOH-induced HIF-1 α in AM.

Pioglitazone Treatment Reverses EtOH-Induced Glycolysis

As treatment with PIO improved mitochondrial derangements due to EtOH exposure (**Figure 3.1.10**), here we sought to determine if PIO affected glycolysis in MH-S in the presence of EtOH. As demonstrated previously, EtOH induced a glycolytic shift in response to oligomycin + FCCP stressors. However, PIO treatment prevented the EtOH-induced glycolytic shift in MH-S (**Figure 3.1.9A**). Treatment with PIO also reversed EtOH-induced increases in the MH-S glycolytic bioenergetics parameters, glycolytic profiling (**Figure 3.1.9B**), glycolysis (**Figure 3.1.9C**), glycolytic capacity (**Figure 3.1.9D**), glycolytic reserve (**Figure 3.1.9E**), and non-glycolytic acidification (**Figure 3.1.9F**). Similarly, PIO treatment prevented the glycolytic shift in mAM isolated from EtOH-fed mice (**Figure 3.1.10A**). Treatment with PIO also reversed EtOH-induced increases in the mAM glycolytic bioenergetics parameters, glycolytic profiling (**Figure 3.1.10B**), glycolysis (**Figure 3.1.10C**), glycolytic capacity (**Figure 3.1.10D**), glycolytic reserve (**Figure 3.1.10E**), and non-glycolytic acidification (**Figure 3.1.10F**). Collectively,

these data show that PIO treatment reverses AM glycolytic energy phenotype in response to EtOH.

Discussion

One of the hallmark immune functions of AM is to phagocytose invading pathogens in the lower respiratory tract¹⁰⁹. In order to meet the high energy demands of phagocytosis, oxidative phosphorylation is the most efficient process utilized for cellular ATP generation. Previously, we have demonstrated that EtOH exposure severely diminishes the ability of AM to phagocytose and clear pathogens^{46,112,113,121}. Further, we have shown that EtOH altered mitochondria morphology and diminished oxidative phosphorylation in MH-S. Additionally, we demonstrated that the PPAR γ ligand, PIO, partially reversed EtOH-induced AM mitochondrial derangements⁵⁹ and improved EtOH-induced AM phagocytic dysfunction⁶⁰. However, the mechanisms by which EtOH alters AM metabolism have not been fully elucidated. This study aimed to evaluate whether HIF-1 α has a role in EtOH-mediated energy derangements in AM. Our findings provide evidence that EtOH shifts AM to a glycolytic metabolic phenotype, which is mediated by EtOH-induced HIF-1 α . Also, PIO treatment diminishes EtOH-induced HIF-1 α , providing HIF-1 α as a molecular mechanism by which PIO improves AM phagocytic function. This study establishes HIF-1 α as a critical modulator of chronic EtOH-mediated metabolic derangements in AM.

This study provides a mechanistic understanding of our previous study⁵⁹ by showing that EtOH-mediated decreases in oxidative phosphorylation are due to a glycolytic shift. One method of meeting the metabolic requirements of the cell in the absence of oxidative phosphorylation is glycolysis. Glucose transporters transport glucose into the cell, providing some of the glucose needed for glycolysis¹³⁶. Glycolysis is a multistep process which utilizes proteins such as Pfkfb3 and PKM2^{136,137}. Our

findings herein show that EtOH increases glycolysis (**Figures 3.1.1 & 3.1.2**). The variance in EtOH-induced alterations in ECAR in mAM (**Figure 3.1.1B**) versus MH-S (**Figure 3.1.2B**) may be due to the difference in duration of EtOH exposure (mAM isolated from mice fed EtOH for 12 weeks versus MH-S exposed to 0.08% EtOH *in vitro* for 72 hours) and systemic, physiological effects of EtOH. However, the glycolysis bioenergetics profiles for glycolysis and glycolytic capacity were comparable between these mAMs *in vivo* (**Figures 3.1.1C, D**) and MH-S *in vitro* (**Figures 3.1.2C, D**) models. Further, we observed elevated mRNA levels of glucose transporters (GLUT1 and GLUT 4) following EtOH exposure (**Figure 3.1.3**). Further, EtOH induced Pfkfb3, PKM2, and lactate in AM (**Figure 3.1.3**). Together, these data demonstrate that EtOH shifts AM to a glycolytic phenotype.

Other studies have described a direct relationship between HIF-1 α and EtOH-mediated pathologies^{147-149,152}. These studies have demonstrated that EtOH-induced HIF-1 α occurs under conditions of elevated inflammation or oxidative stress. Other models have investigated the role of HIF-1 α in chronic lung injury^{144,145}. HIF-1 α was activated *in vitro* in human pulmonary artery smooth muscle cells, demonstrating the role of HIF-1 α in pulmonary hypertension pathogenesis¹⁴⁴. HIF-1 α has been branded a “metabolic switch”, shifting cells from utilizing oxidative phosphorylation to glycolysis¹⁴¹⁻¹⁴³. However, the relationship between HIF-1 α and metabolic derangements in the context of chronic EtOH-induced AM phagocytic dysfunction have not been established until now and are supported by the data presented herein. This study illustrates that chronic EtOH exposure increases HIF-1 α expression (**Figure 3.1.4**). Further, as shown in **Figures 3.1.5** and **3.1.6**, treatment with the HIF-1 α mimetic, cobalt chloride, causes

AM derangements similar to EtOH. Knockdown of HIF-1 α in the presence of EtOH prevented EtOH induced glycolytic shift and glycolytic profiling (**Figures 3.1.7A, B**). Taken together, these data suggest that HIF-1 α is a critical modulator of EtOH-induced glycolytic phenotype in AM. Interestingly, Kang et al¹⁵³. showed that EtOH did not alter glycolysis in bone marrow derived macrophages. The group did, however, conclude that EtOH increased glycolytic capacity, glycolytic reserve, and non-glycolytic acidification. HIF-1 α expression and activity was also increased due to EtOH exposure¹⁵³. The slight variance in results between our studies could be due to the differences in experimental models using bone marrow-derived macrophages to model the AM phenotype. AM may be tissue-resident or recruited cells with key differential functions in host defense¹⁵⁴. However, the current study provides evidence of the critical role for HIF-1 α in mediating the glycolytic shift in AM due to EtOH exposure using an AM cell line and AM isolated from *in vivo* EtOH-fed mice. As HIF-1 α is a component of the transcription factor HIF-1; elevated levels could have effects not related to glycolysis. One limitation of the current study is that it does not explore non glycolytic effects of HIF-1 α . As described above, previous reports have shown that HIF-1 α is elevated as a response to inflammation or oxidative stress^{147-149,152}, and our lab has shown that oxidative stress contributes to AM phagocytic impairments^{46,59,60}. Modulation of HIF-1 α could alleviate EtOH-mediated oxidative stress, thus improving phagocytic dysfunction.

Since HIF-1 is a transcription factor with numerous targets, other targets may be of future interest. For example, the HIF-1 target PDK-1 can repress mitochondrial function and oxygen consumption. PDK-1-mediated phosphorylation inhibits pyruvate dehydrogenase, preventing the use of pyruvate in oxidative phosphorylation and

resulting in decreased mitochondrial oxygen consumption¹⁵⁵. Additionally, other mechanisms, such as fatty acid oxidation, may be involved in meeting the energy demands of the cell due to EtOH exposure. However, studies in the liver suggest that chronic alcohol exposure promotes hepatic injury but does not increase the rate of fatty acid β -oxidation through inhibition of mitochondrial β -oxidation¹⁵⁶⁻¹⁵⁸.

Previously, our lab has shown that alcohol-mediated decreases in PPAR γ cause AM dysfunction⁴⁶. PPAR γ is activated by synthetic ligands, such as PIO. This results in heterodimerization of PPAR γ with a retinoid receptor and subsequent binding to the PPAR response element in the promoter region of its target genes. The response to this binding is dependent on whether the heterodimerization results in recruitment of coactivators (increases gene expression) or corepressors (decreases gene expression)¹⁵⁹. Our lab has shown that treatment with PPAR γ ligands diminished oxidative stress following chronic EtOH exposure^{46,59,60}. Interestingly, decreased expression of PPAR γ impaired AM phagocytic capacity following chronic EtOH exposure⁴⁶. However, the mechanism by which PPAR γ mediates these effects is not known. Other models which generate reactive oxygen species (ROS) have determined that there is an inverse relationship between PPAR γ and HIF-1 α and that PPAR γ ligand treatment decreased hypoxia-induced HIF-1 α expression^{144,160}. Here, we show that treatment PIO attenuated EtOH-induced HIF-1 α (**Figure 3.1.8**). It is unclear however, if PPAR γ mediates its action on HIF-1 α in a direct (binding to HIF-1 α promoter) or indirect (reduction of ROS) manner. As shown in **Figures 3.1.5** and **3.1.6**, the HIF-1 α mimetic, cobalt chloride produced results similar to EtOH-induced metabolic derangements. Collectively, these data demonstrated that EtOH-mediated phagocytic dysfunction is in part linked to

increased HIF-1 α levels, which is mitigated with PIO treatment. Further, PIO treatment reversed EtOH-induced glycolytic bioenergetics (**Figures 3.1.9, 3.1.10**).

The current study fills a gap in knowledge by providing a mechanistic understanding to earlier studies which demonstrate that chronic EtOH exposure results in phagocytic dysfunction^{46,112,113,121} and decreases oxidative phosphorylation⁵⁹ in AM. Together, our previous studies suggest that AM has diminished phagocytic capacity due to an inability to meet the energy requirements for phagocytosis. Using both *in vitro* and *in vivo* approaches, we identified HIF-1 α as a critical mediator of EtOH-mediated metabolic derangements in AM. These studies establish HIF-1 α as a potential therapeutic target for PIO (approved for clinical use in the treatment of type 2 diabetes), which could mitigate the risk of developing respiratory infections in people with a history of alcohol use disorders.

Data Availability Statement

The original contributions presented in the study are included in the article/Supplementary Material. Further inquiries can be directed to the corresponding author.

Ethics Statement

The animal study was reviewed and approved by Atlanta Veterans Affairs Health Care System Institutional Animal Care and Use Committee.

Funding

This work was supported in part by grants from the National Institute on Alcohol Abuse and Alcoholism (R01AA026086) to SMY (ORCID ID: 0000-0001-9309-0233) and the National Heart, Lung, and Blood Institute (T32HL116271) to David M. Guidot, Lou Ann S. Brown, and C. Michael Hart. The contents of this report do not represent the views of the Department of Veterans Affairs or the US Government.

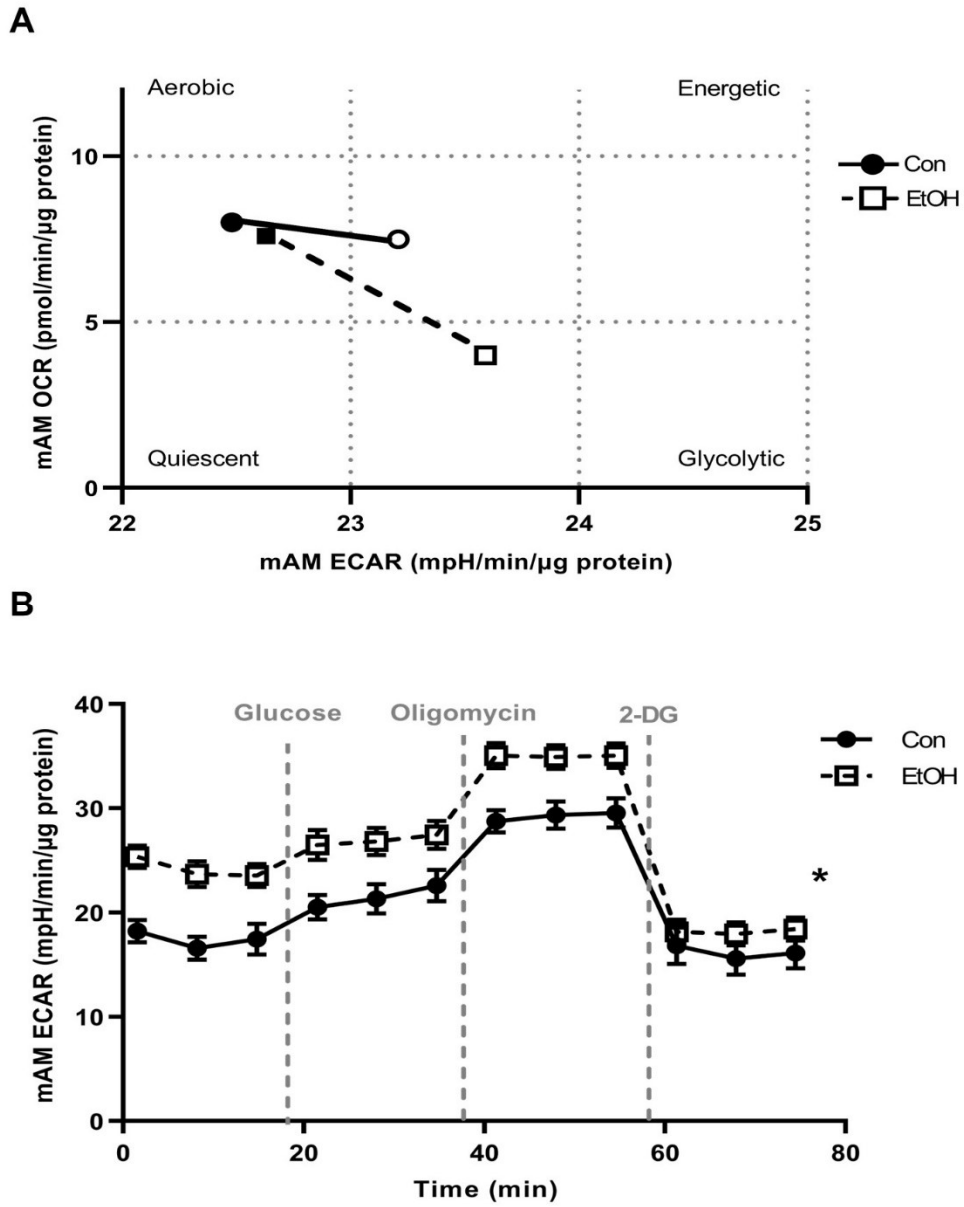
Conflict of Interest: The authors declare that the research was conducted in the absence of any commercial or financial relationships that could be construed as a potential conflict of interest.

Publisher's Note: All claims expressed in this article are solely those of the authors and do not necessarily represent those of their affiliated organizations, or those of the publisher, the editors and the reviewers. Any product that may be evaluated in this article, or claim that may be made by its manufacturer, is not guaranteed or endorsed by the publisher.

Copyright © 2022 Morris, Michael, Crotty, Chang and Yeligar. This is an open-access article distributed under the terms of the Creative Commons Attribution License (CC BY). The use, distribution or reproduction in other forums is permitted, provided the original author(s) and the copyright owner(s) are credited and that the original publication in this journal is cited, in accordance with accepted academic practice. No use, distribution or reproduction is permitted which does not comply with these terms.

Figures

Figure 3.1.1



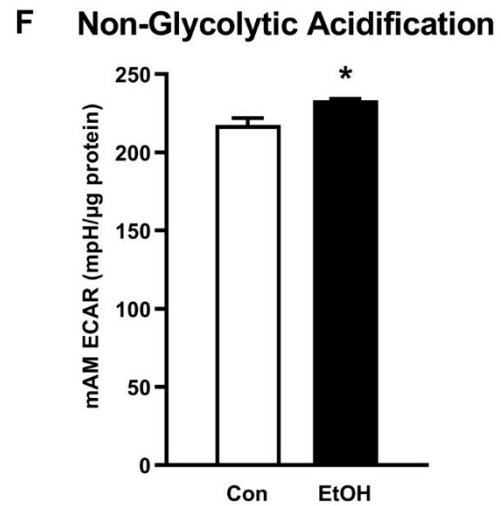
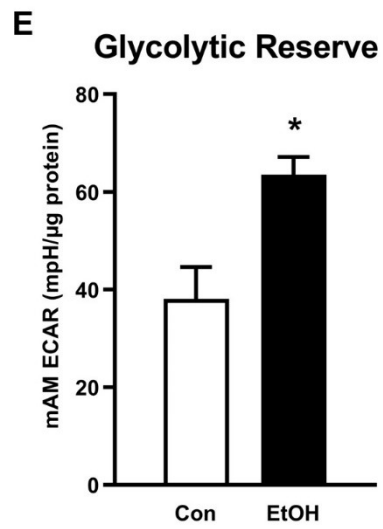
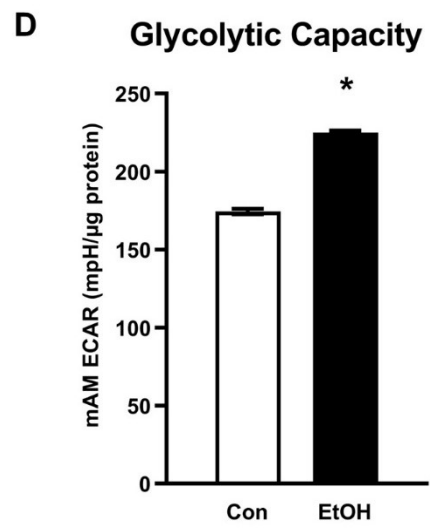
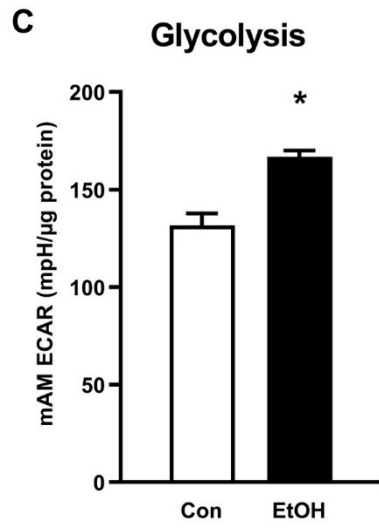
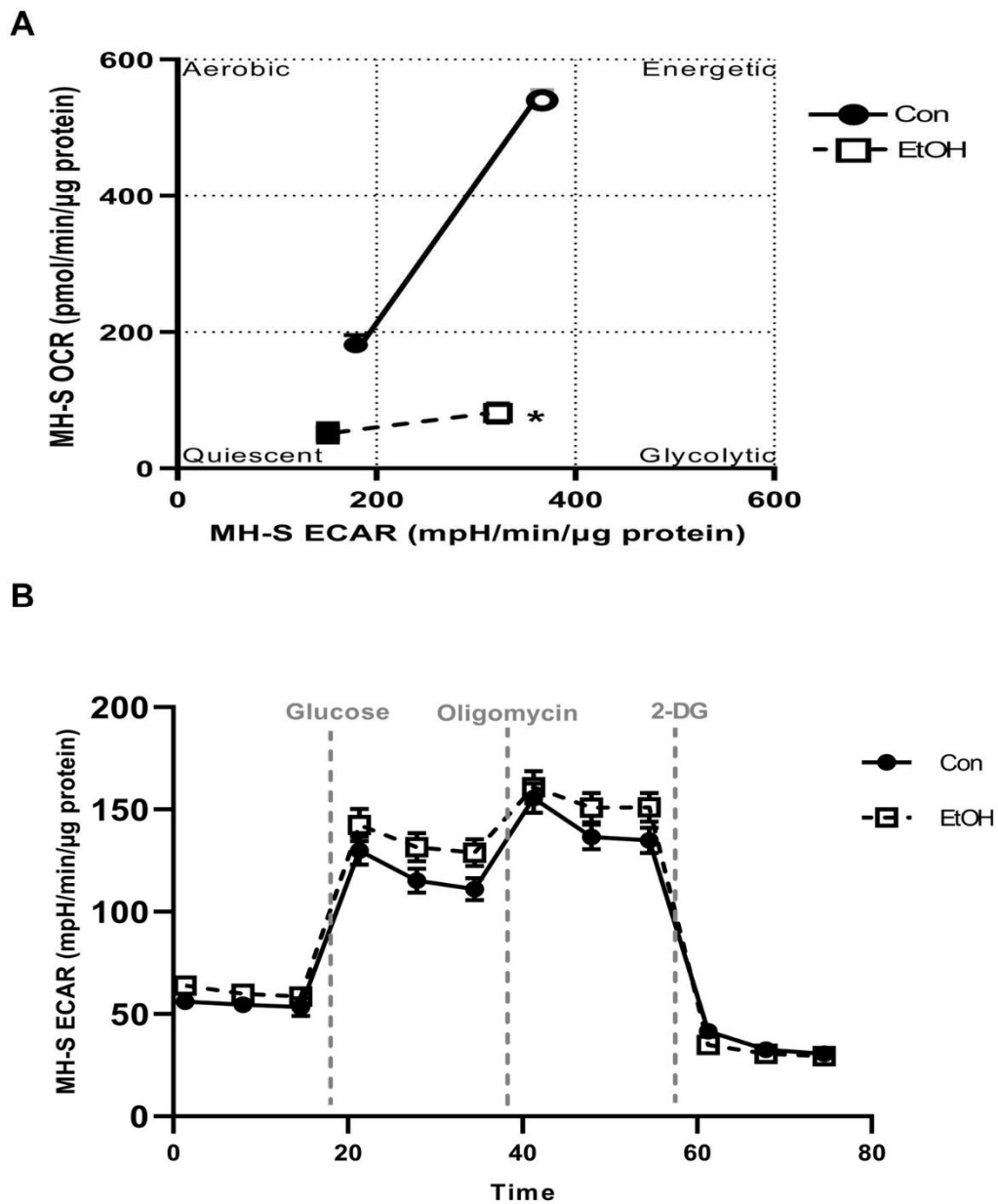
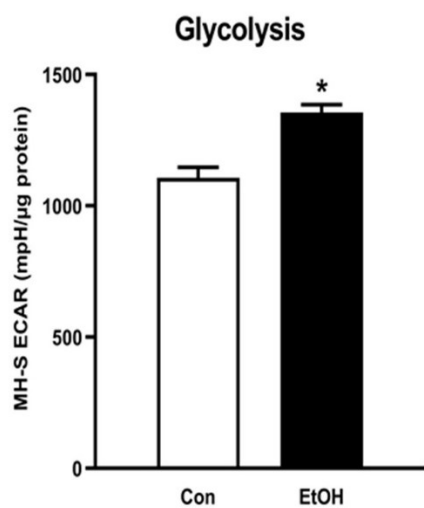


Figure 3.1.1: Ethanol (EtOH) induces glycolysis in mouse alveolar macrophages (mAM). Mouse alveolar macrophages (mAM) were isolated from mice fed either control (Con) or ethanol (EtOH; 20% v/w in drinking water, 12 weeks). (A) Oxygen consumption rates (OCR) and extracellular acidification rates (ECAR) were measured in response to an injection mixture of oligomycin (oligo; mitochondrial complex V inhibitor) and carbonilcyanide p-triflouromethoxyphenylhydrazone (FCCP; ATP synthase inhibitor and proton uncoupler) using an extracellular flux analyzer. Cell energy phenotype was measured, normalized to protein levels, and are expressed as mean \pm SEM (n = 4-5). Closed symbols are cells at baseline and open symbols are after Oligo / FCCP injection, aka after “stressor.” ECAR were measured in response to sequential injections of glucose (saturating concentration of glucose to promote glycolysis), oligomycin (ATP synthase inhibitor), and 2-deoxy-glucose (2-DG; a glucose analog that inhibits glycolysis) using an extracellular flux analyzer. OCR measures are pmol over time and ECAR measures are mpH over time, normalized to total protein in the same sample well, and are expressed as mean \pm SEM. Parameters of glycolytic function (B), glycolysis (C), glycolytic capacity (D), glycolytic reserve (E), and non-glycolytic acidification (F) are expressed as mean \pm SEM, relative to control (n = 12-14). *p < 0.05 verses control.

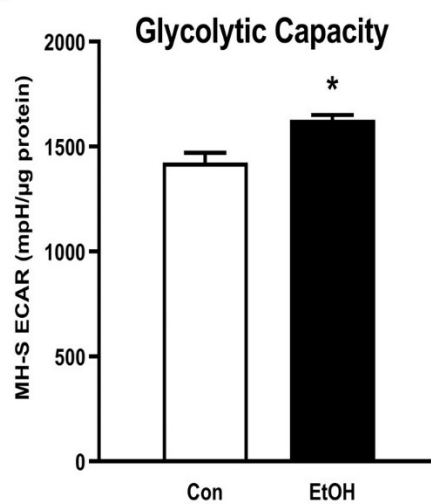
Figure 3.1.2



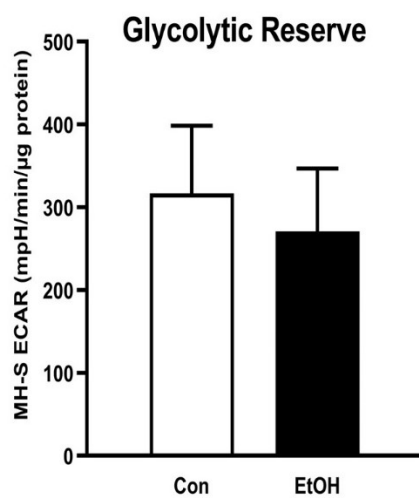
C



D



E



F

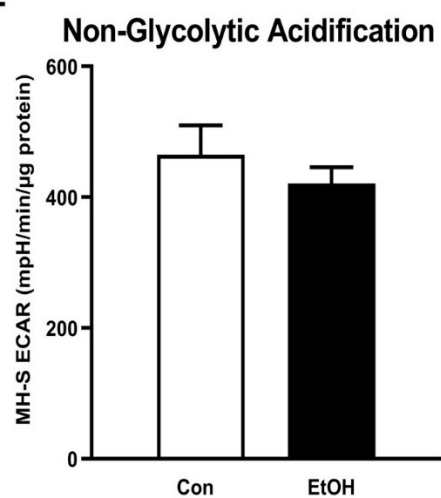


Figure 3.1.2: Ethanol (EtOH) induces glycolysis in MH-S cells. MH-S were exposed to either control (Con) or ethanol (EtOH; 0.08%) for 72 hours. (A) Oxygen consumption rates (OCR) and extracellular acidification rates (ECAR) were measured in response to an injection mixture of oligomycin (oligo; mitochondrial complex V inhibitor), carbonilcyanide p-triflouromethoxyphenylhydrazone (FCCP; ATP synthase inhibitor and proton uncoupler) using an extracellular flux analyzer. Cell energy phenotype was measured, normalized to protein levels, and are expressed as mean \pm SEM (n = 3). Closed symbols are cells at baseline and open symbols are after Oligo / FCCP injection, aka after “stressor.” ECAR were measured in response to sequential injections of glucose (saturating concentration of glucose to promote glycolysis), oligomycin (ATP synthase inhibitor), and 2-deoxy-glucose (2-DG; a glucose analog that inhibits glycolysis) using an extracellular flux analyzer. OCR measures are pmol over time and ECAR measures are mpH over time, normalized to total protein in the same sample well, and are expressed as mean \pm SEM. Parameters of glycolytic function (B), glycolysis (C), glycolytic capacity (D), glycolytic reserve (E), and non-glycolytic acidification (F) are expressed as mean \pm SEM, relative to control (n = 6). *p < 0.05 verses control.

Figure 3.1.3

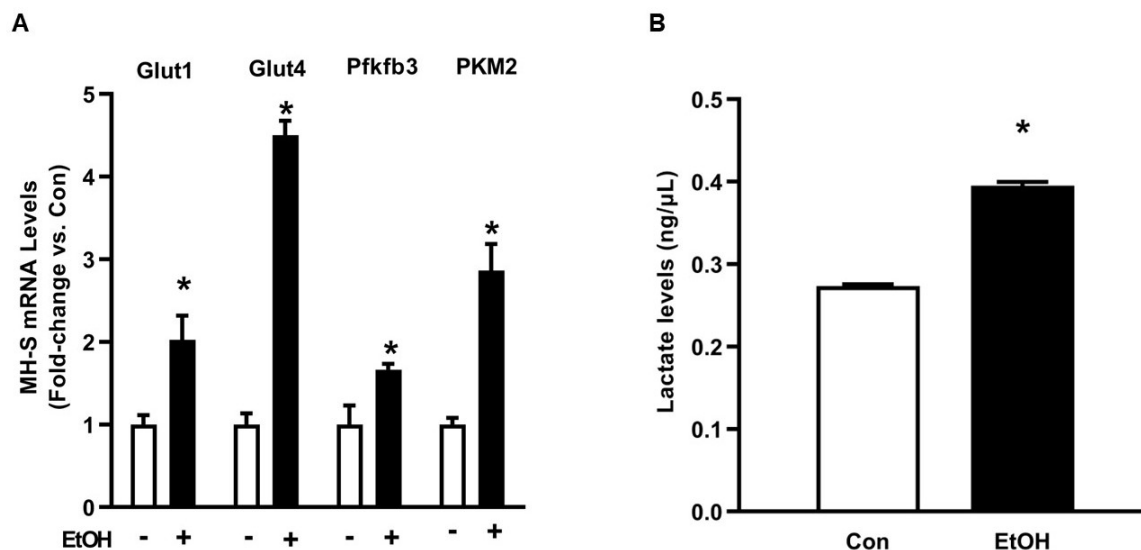


Figure 3.1.3: Ethanol (EtOH) increases expression of glycolytic proteins and lactate levels in MH-S. MH-S were exposed to either control (Con) or ethanol (EtOH; 0.08%) for 72 hours. (A) mRNA levels of glucose transporter (Glut)1, Glut4, 6-phosphofructo-2-kinase/fructose-2,6-bisphosphatase 3 (Pfkfb3), and pyruvate kinase 2 (PKM2) were measured by qRT-PCR, in duplicate, normalized to GAPDH, and are expressed as mean \pm SEM, relative to control. (B) Protein isolated from MH-S cells was used to evaluate lactate levels via lactate assay kit and are expressed as mean \pm SEM, relative to control (n = 4-6). *p < 0.05 versus control.

Figure 3.1.4

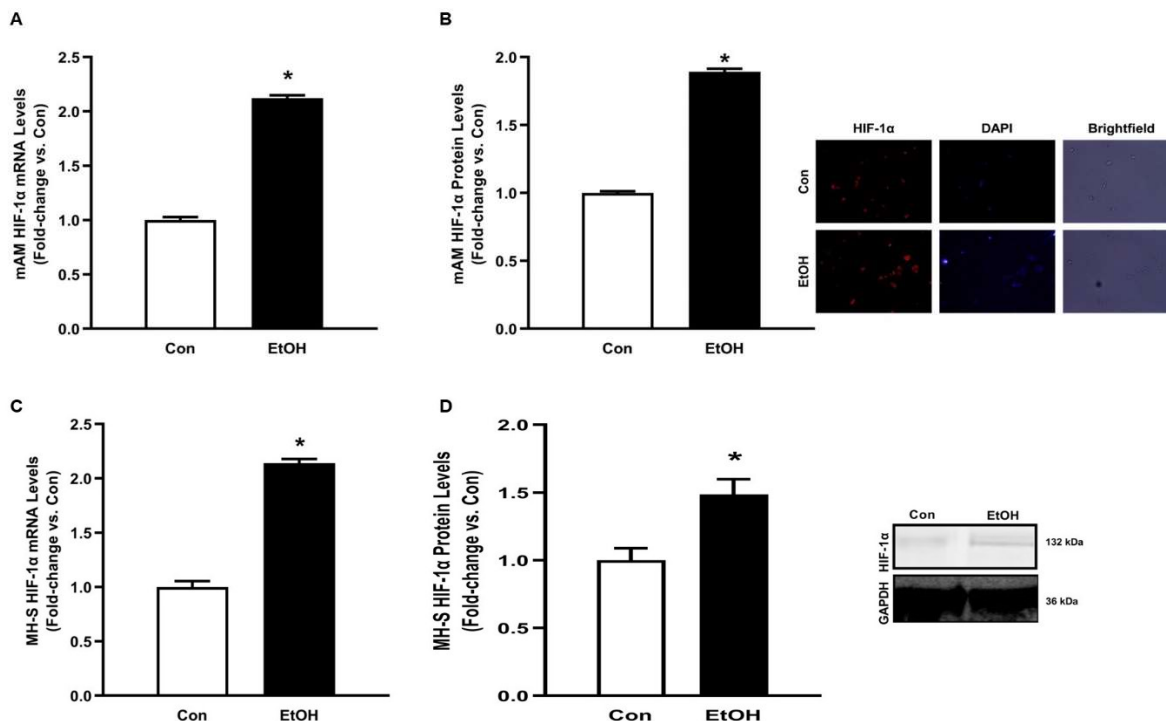


Figure 3.1.4: Ethanol (EtOH) induces hypoxia-inducible factor-1 alpha (HIF-1 α) in mouse alveolar macrophages (mAM) and MH-S. (A, B) Mouse alveolar macrophages (mAM) were isolated from mice fed either control (Con) or ethanol (EtOH; 20% v/w in drinking water, 12 weeks). (A) HIF-1 α mRNA levels were measured by qRT-PCR, in duplicate, normalized to 9S, and expressed as mean \pm SEM, relative to control. (B) HIF-1 α protein levels were measured by fluorescence microscopy (10 fields/condition), normalized to DAPI, and are expressed as mean RFU \pm SEM, relative to control. Representative microscopy images have been provided. (C, D) MH-S were exposed to either control (Con) or ethanol (EtOH; 0.08%) for 72 hours. (C) HIF-1 α measured by qRT-PCR, in duplicate, normalized to GAPDH, and expressed as mean \pm SEM, relative to control (n = 6). (D) HIF-1 α protein levels were evaluated via western blot, normalized to GAPDH protein, and densitometry is expressed as mean \pm SEM, relative to control (n = 4). Representative western blot images have been provided. *p < 0.05 versus control.

Figure 3.1.5

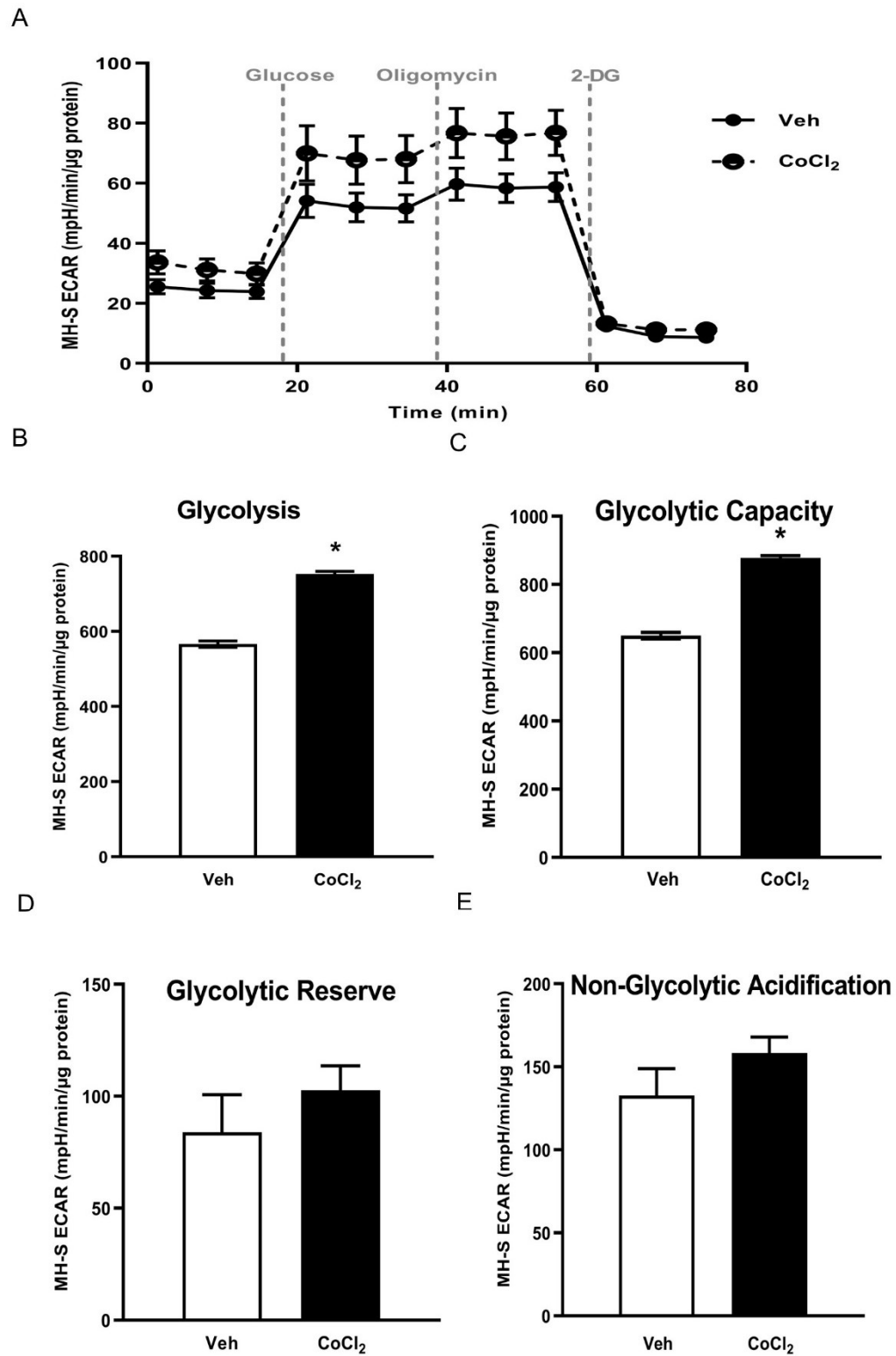


Figure 3.1.5: Stabilization of hypoxia-inducible factor-1 alpha (HIF-1 α) *in vitro* via cobalt chloride (CoCl₂) mimics ethanol (EtOH)-mediated derangements in MH-S.

MH-S were exposed to either vehicle (Veh) or cobalt chloride (CoCl₂, 25 μ M) for 4 hours. Extracellular acidification rates (ECAR) were measured in response to sequential injections of glucose (saturating concentration of glucose to promote glycolysis), oligomycin (ATP synthase inhibitor), and 2-deoxy-glucose (2-DG; a glucose analog that inhibits glycolysis) using an extracellular flux analyzer. ECAR from glycolytic profiling, normalized to protein levels, and are expressed as mean \pm SEM (A), glycolysis (B), glycolytic capacity (C), glycolytic reserve (D), and non-glycolytic acidification (E) are expressed as mean \pm SEM, relative to vehicle (n = 6). *p < 0.05 versus vehicle.

Figure 3.1.6

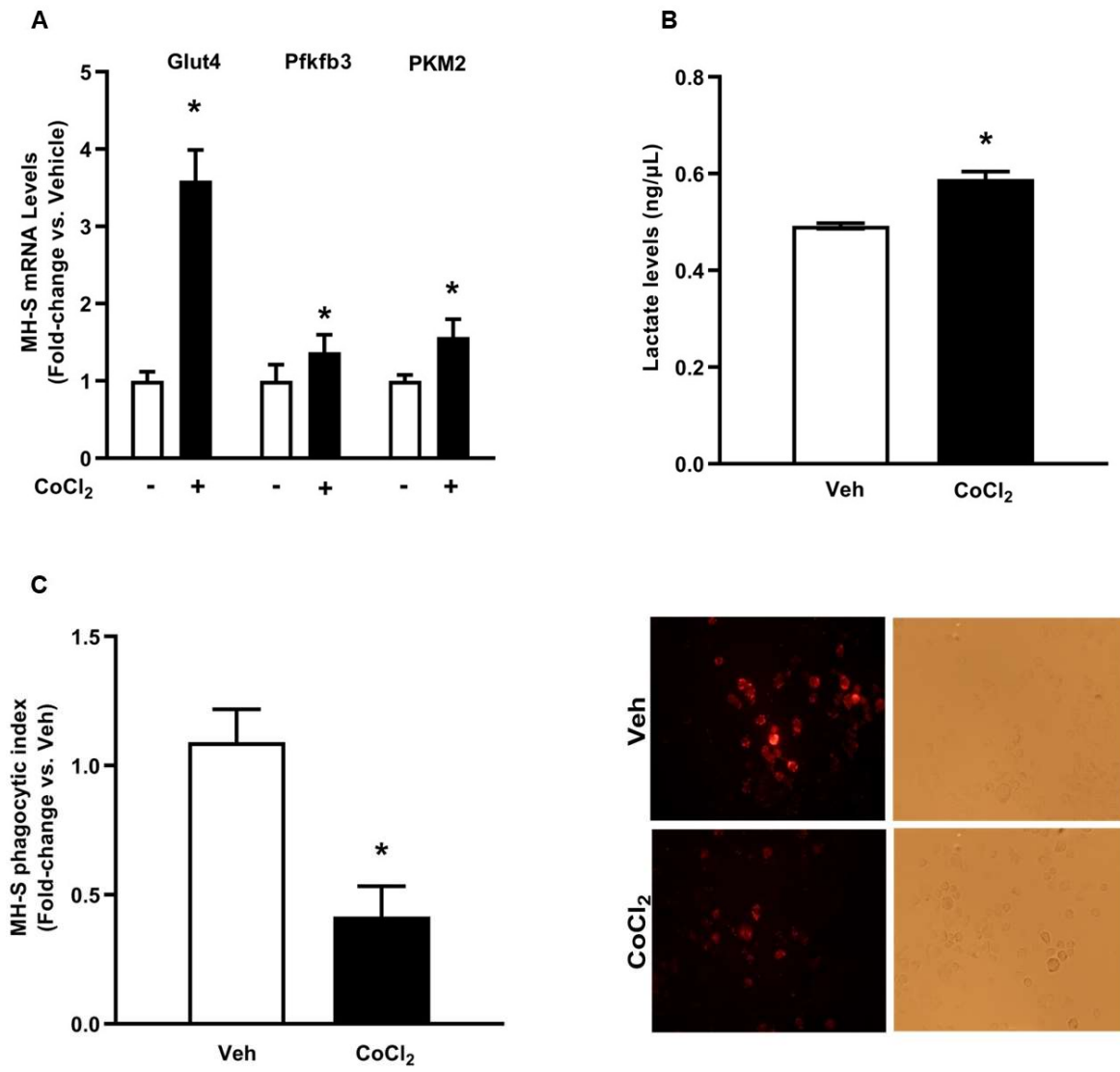


Figure 3.1.6: Cobalt chloride (CoCl₂) induces expression of glycolytic proteins and lactate levels and causes phagocytic dysfunction in MH-S. MH-S were exposed to either vehicle (Veh) or cobalt chloride (CoCl₂, 25 μM) for 4 hours. (A) mRNA levels of glucose transporter (Glut4), 6-phosphofructo-2-kinase/fructose-2,6-bisphosphatase 3 (Pfkfb3), and pyruvate kinase 2 (PKM2) were measured by qRT-PCR, in duplicate, normalized to GAPDH, and are expressed as mean ± SEM, relative to control (n = 4-6). (B) Protein isolated from MH-S was used to evaluate lactate levels via lactate assay kit and are expressed as mean ± SEM, relative to vehicle (n = 6). *p < 0.05 versus vehicle. (C) Phagocytic index was calculated from the percentage of cells positive for bacterial uptake multiplied by the RFU of *S. aureus* per cell. Values are expressed as mean ± SEM relative to vehicle (n = 5). Representative fluorescent and brightfield images have been provided. *p < 0.05 versus vehicle.

Figure 3.1.7

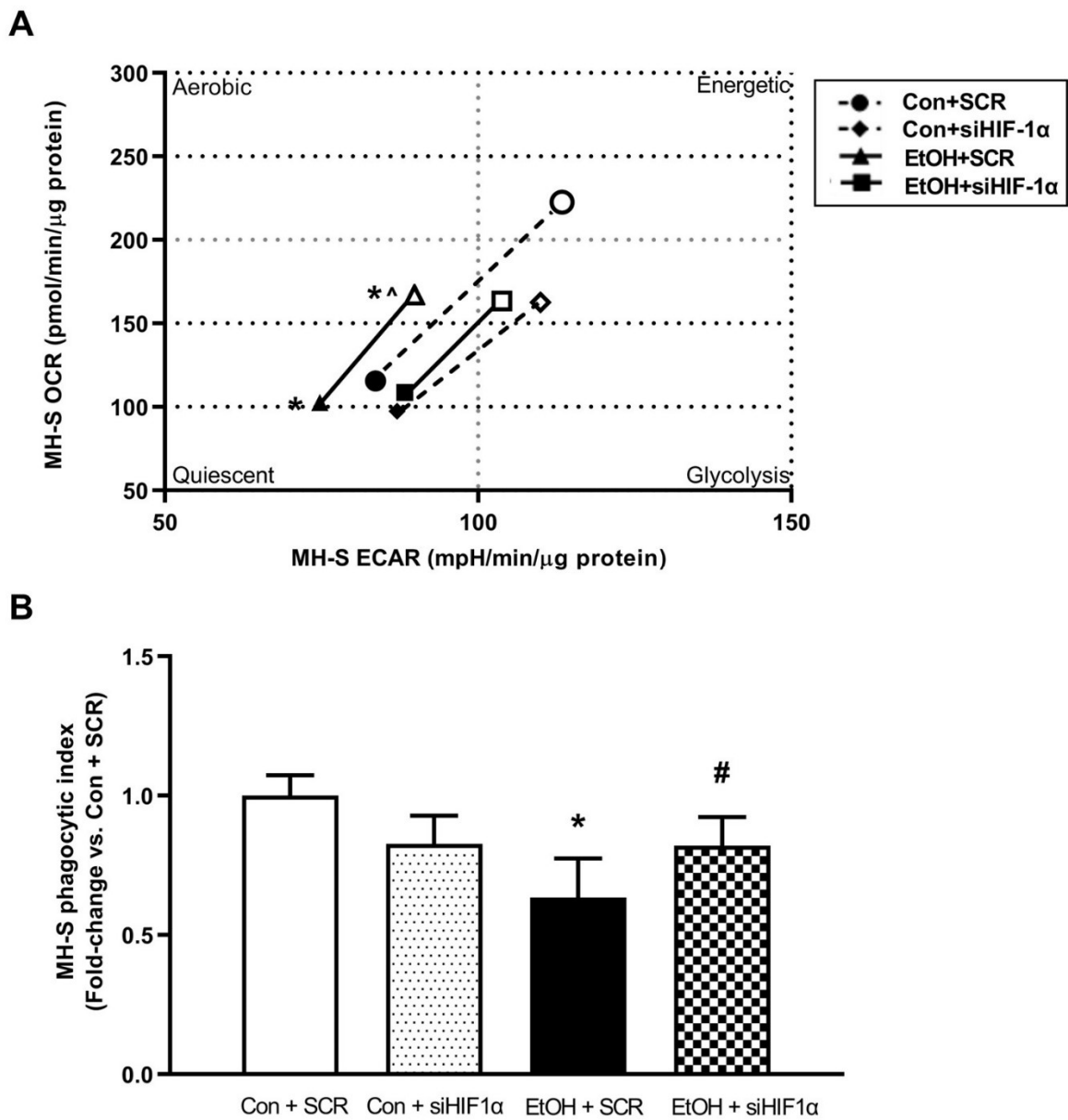


Figure 3.1.7: Hypoxia-inducible factor-1 alpha (HIF-1 α) modulates ethanol (EtOH)-induced glycolysis and phagocytic function in MH-S. MH-S transiently transfected with control scramble (SCR) or siRNA against HIF-1 α (siHIF1 α) were exposed to either Con or EtOH (0.08%) for 72 hours. (A) Oxygen consumption rates (OCR) and extracellular acidification rates (ECAR) were measured in response to an injection mixture of oligomycin (oligo; mitochondrial complex V inhibitor) and carbonilcyanide p-trifluoromethoxyphenylhydrazine (FCCP; ATP synthase inhibitor and proton uncoupler) using an extracellular flux analyzer. Cell energy phenotype was measured, normalized to protein levels, and are expressed as mean \pm SEM (n = 5). Closed symbols are cells at baseline and open symbols are after Oligo / FCCP injection, aka after “stressor.” ECAR were measured in response to sequential injections of glucose (saturating concentration of glucose to promote glycolysis), oligomycin (ATP synthase inhibitor), and 2-deoxy-glucose (2-DG; a glucose analog that inhibits glycolysis) using an extracellular flux analyzer. OCR measures are pmol over time and ECAR measures are mpH over time, normalized to total protein in the same sample well, and are expressed as mean \pm SEM. (B) Phagocytic index was calculated from the percentage of cells positive for bacterial uptake multiplied by the RFU of *S. aureus* per cell. Values are expressed as mean \pm SEM relative to vehicle (n = 6). *p < 0.05 versus control; # p < 0.05 versus ethanol.

Figure 3.1.8

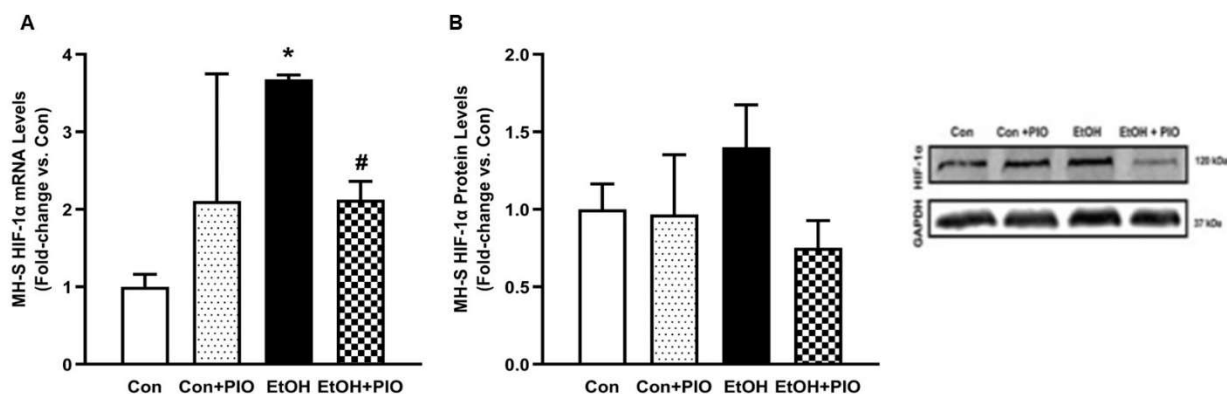


Figure 3.1.8: Pioglitazone (PIO) treatment reverses ethanol (EtOH)-induced

hypoxia-inducible factor-1 alpha (HIF-1α) levels. MH-S exposed to either control

(Con) or ethanol (EtOH; 0.08%) for 72 hours ± pioglitazone (PIO; 10 μM, last 24 hours

of EtOH exposure). (A) HIF-1α mRNA levels were measured by qRT-PCR, in triplicate,

normalized to GAPDH, and expressed as mean ± SEM, relative to control (n = 3). *p <

0.05 versus control; # p < 0.05 versus EtOH. (B) HIF-1α protein levels were evaluated

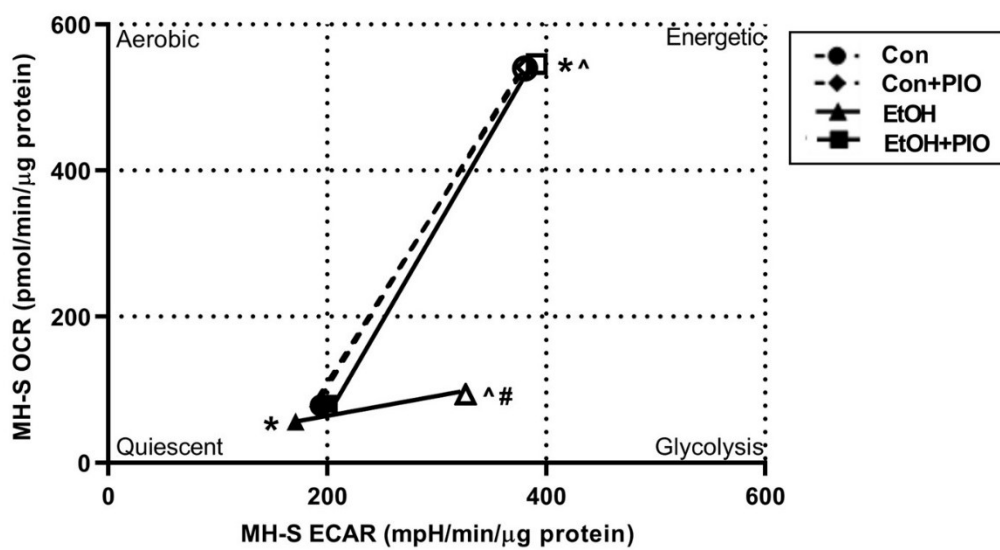
via western blot, normalized to GAPDH protein, and densitometry is expressed as

mean ± SEM, relative to control (n = 3). Representative western blot images have been

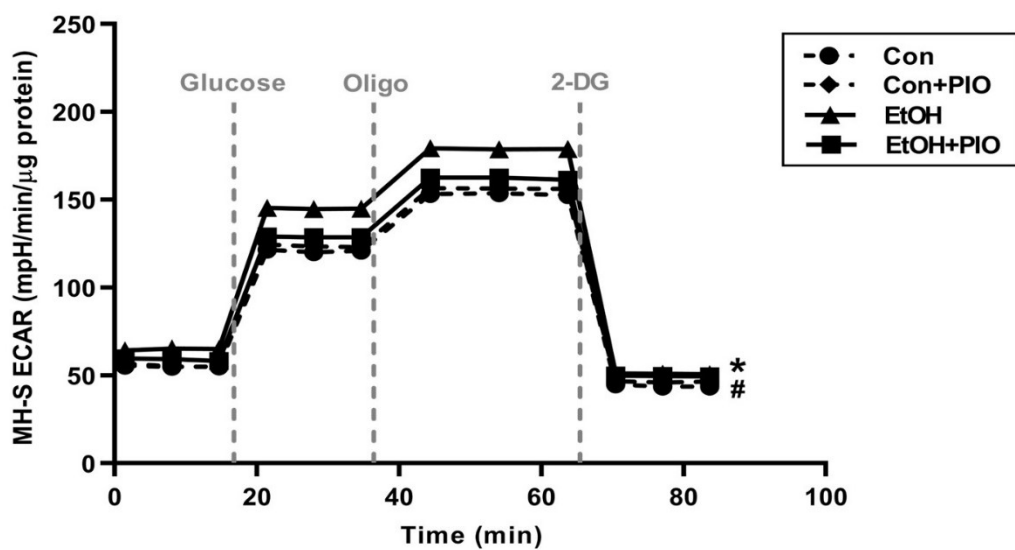
provided. *p < 0.05 versus control; # p < 0.05 versus ethanol.

Figure 3.1.9

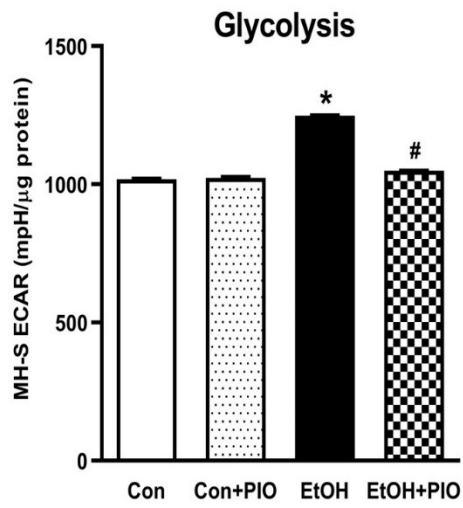
A



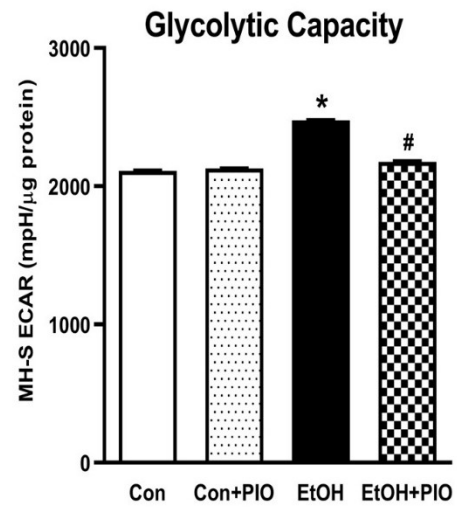
B



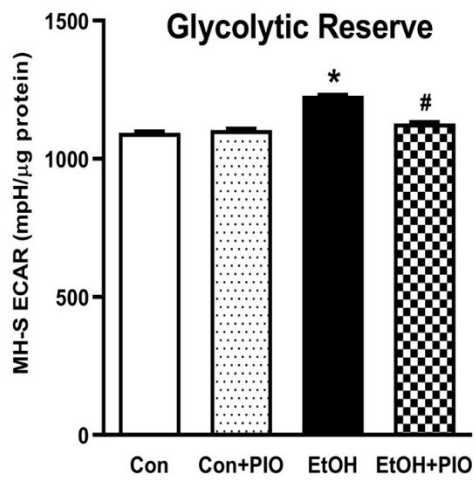
C



D



E



F

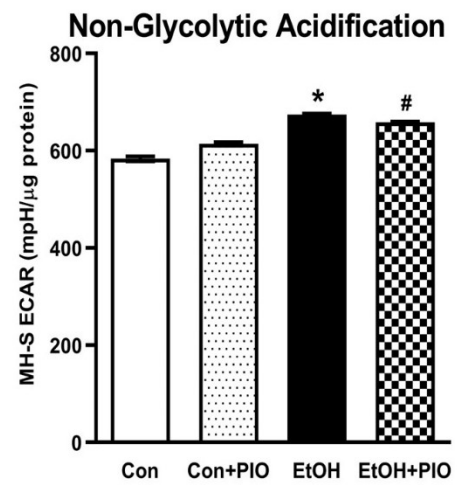
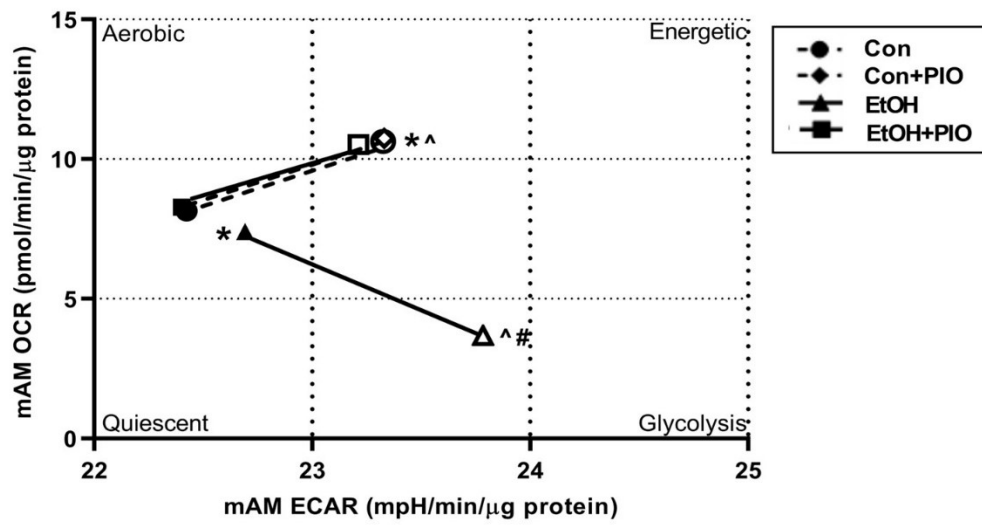


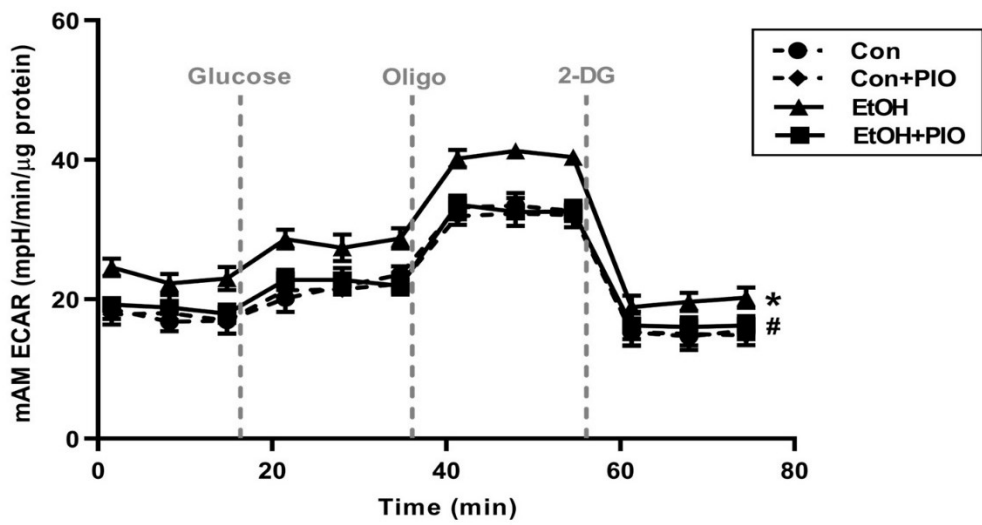
Figure 3.1.9: Pioglitazone (PIO) treatment reverses ethanol (EtOH)-induced glycolysis in MH-S. MH-S were exposed to either control (Con) or ethanol (EtOH; 0.08%; 72 hours) \pm pioglitazone (PIO, last day of ethanol). (A) Oxygen consumption rates (OCR) and extracellular acidification rates (ECAR) were measured in response to an injection mixture of oligomycin (oligo; mitochondrial complex V inhibitor), carbonilcyanide p-triflouromethoxyphenylhydrazone (FCCP; ATP synthase inhibitor and proton uncoupler) using an extracellular flux analyzer. Cell energy phenotype was measured, normalized to protein levels, and are expressed as mean \pm SEM (n = 15). Closed symbols are cells at baseline and open symbols are after Oligo / FCCP injection, aka after “stressor.” ECAR were measured in response to sequential injections of glucose (saturating concentration of glucose to promote glycolysis), oligomycin (ATP synthase inhibitor), and 2-deoxy-glucose (2-DG; a glucose analog that inhibits glycolysis) using an extracellular flux analyzer. OCR measures are pmol over time and ECAR measures are mpH over time, normalized to total protein in the same sample well, and are expressed as mean \pm SEM. Parameters of glycolytic function (B), glycolysis (C), glycolytic capacity (D), glycolytic reserve (E), and non-glycolytic acidification (F) are expressed as mean \pm SEM, relative to control (n = 15). *p < 0.05 verses control; # p < 0.05 versus ethanol; ^p < 0.05 versus control stressed.

Figure 3.1.10

A



B



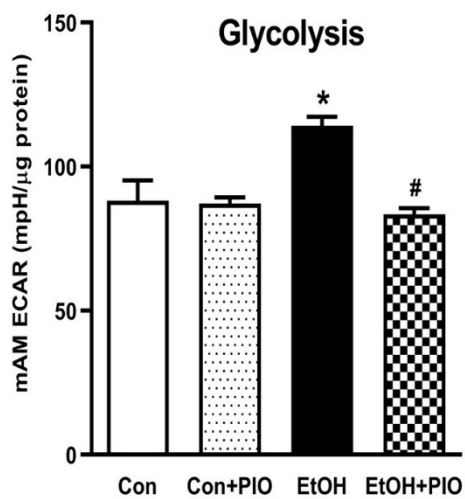
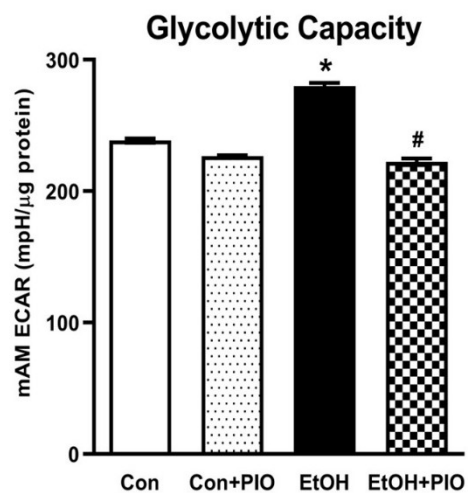
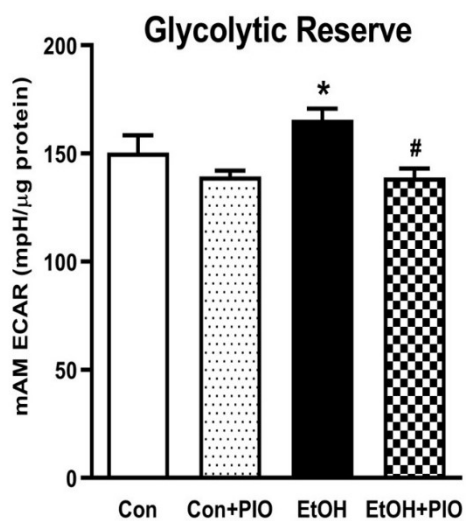
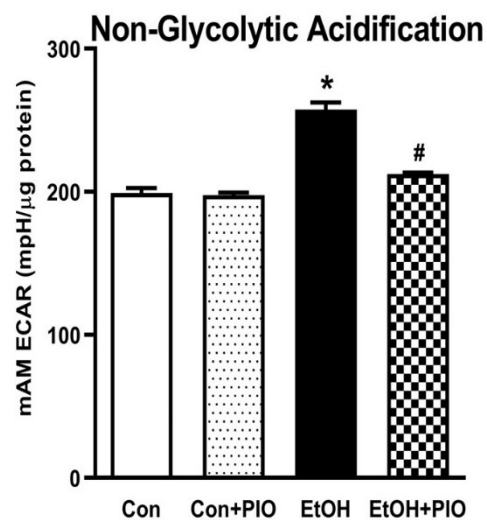
C**D****E****F**

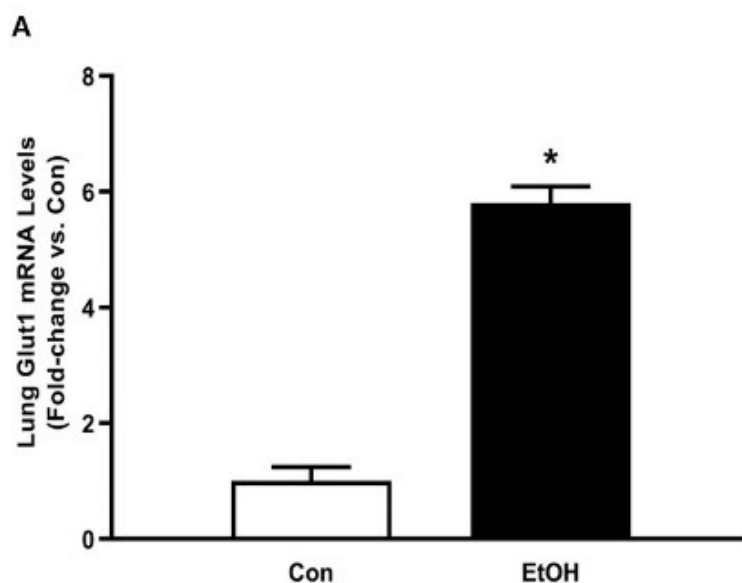
Figure 3.1.10: Pioglitazone (PIO) treatment reverses ethanol (EtOH)-induced glycolysis in mouse alveolar macrophages (mAM). Mouse alveolar macrophages (mAM) were isolated from mice fed either control (Con) or ethanol (EtOH; 20% v/w in drinking water) ± oral pioglitazone (PIO, last 7 days of ethanol). (A) Oxygen consumption rates (OCR) and extracellular acidification rates (ECAR) were measured in response to an injection mixture of oligomycin (oligo; mitochondrial complex V inhibitor) and carbonilcyanide p-trifluoromethoxyphenylhydrazone (FCCP; ATP synthase inhibitor and proton uncoupler) using an extracellular flux analyzer. Cell energy phenotype was measured, normalized to protein levels, and are expressed as mean ± SEM (n = 10-12). Closed symbols are cells at baseline and open symbols are after Oligo / FCCP injection, aka after “stressor.” ECAR were measured in response to sequential injections of glucose (saturating concentration of glucose to promote glycolysis), oligomycin (ATP synthase inhibitor), and 2-deoxy-glucose (2-DG; a glucose analog that inhibits glycolysis) using an extracellular flux analyzer. OCR measures are pmol over time and ECAR measures are mpH over time, normalized to total protein in the same sample well, and are expressed as mean ± SEM. Parameters of glycolytic function (B), glycolysis (C), glycolytic capacity (D), glycolytic reserve (E), and non-glycolytic acidification (F) are expressed as mean ± SEM, relative to control (n = 11-14). *p < 0.05 versus control; # p < 0.05 versus ethanol; ^p < 0.05 versus control stressed.

Supplementary Material

The Supplementary Material for this article can be found online at:

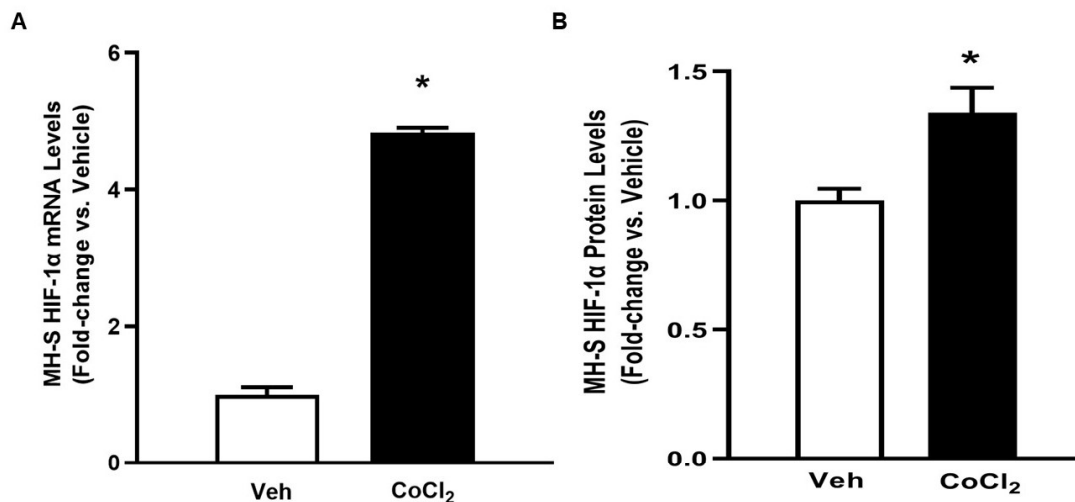
<https://www.frontiersin.org/articles/10.3389/fimmu.2022.865492/full#supplementary-material>.

Supplemental Figure 3.1.1: Ethanol (EtOH) induces glucose transporter 1 (GLUT1) in mouse lung tissue.



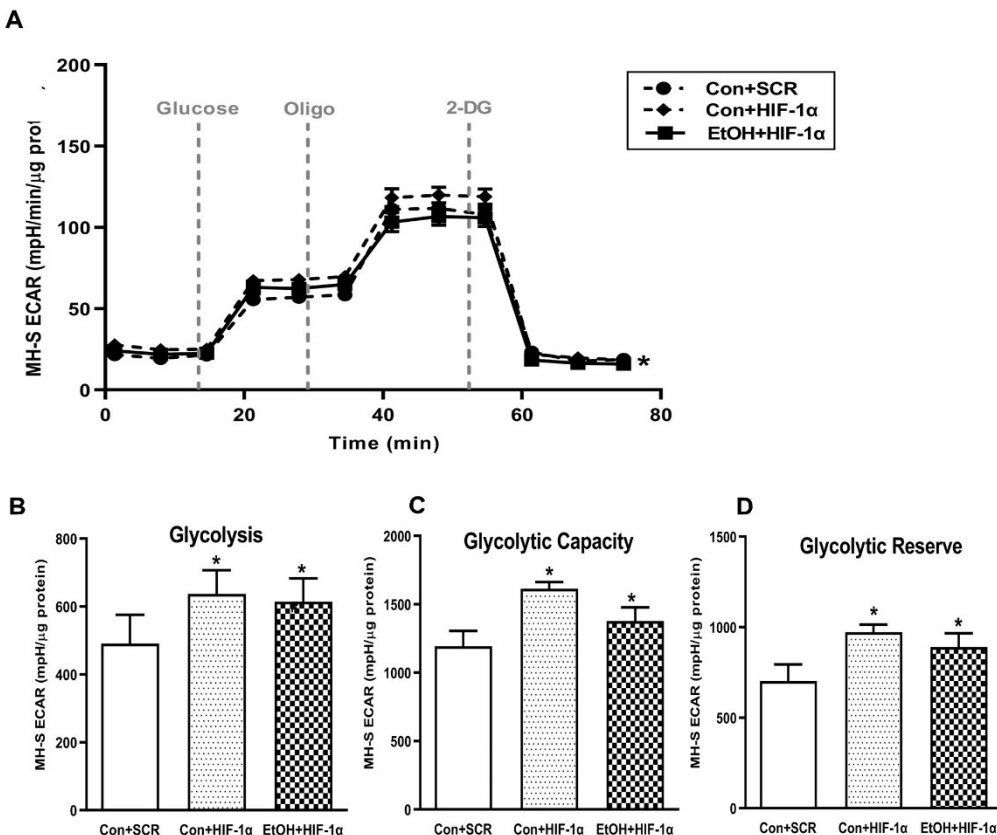
Supplemental Figure 1. Ethanol induces GLUT1 in mouse lung tissue. Mouse lung tissue (mLung) was harvested from mice fed either control (Con) or ethanol (EtOH; 20% v/w in drinking water, 12 weeks). GLUT1 mRNA levels were measured in mouse lung homogenates by qRT-PCR, in duplicate, normalized to 9S, and expressed as mean \pm SEM, relative to control (n=6). * $p < 0.05$ versus control.

Supplemental Figure 3.1.2: Cobalt chloride (CoCl₂) hypoxia-inducible factor-1 alpha (HIF-1 α) in MH-S.



Supplemental Figure 2. Cobalt chloride stabilizes HIF-1 α in MH-S. MH-S were exposed to either vehicle (Veh) or cobalt chloride (CoCl₂, 25 μ M) for 4 hours (n = 3-6). (A) HIF-1 α and were measured by qRT-PCR, in duplicate, normalized to GAPDH, and expressed as mean \pm SEM, relative to vehicle. (B) HIF-1 α protein levels were evaluated via western blot, normalized to GAPDH protein, and densitometry is expressed as mean \pm SEM, relative to vehicle. * p < 0.05 versus vehicle.

Supplemental Figure 3.1.3: Hypoxia-inducible factor-1 alpha (HIF-1 α) regulates ethanol (EtOH)-induced glycolysis in MH-S.



Supplemental Figure 3: HIF-1 α regulates EtOH-induced glycolysis

in MH-S. MH-S transiently transfected with control scramble (Con+scr) or HIF-1 α lysate (HIF1 α) were exposed to either Con or EtOH (0.08%) for three days. Extracellular acidification rates (ECAR) were measured in response to sequential injections of glucose (saturating concentration of glucose to promote glycolysis), oligomycin (ATP synthase inhibitor), and 2-deoxy-glucose (2-DG; a glucose analog that inhibits glycolysis) using an extracellular flux analyzer. ECAR measures are mpH over time, normalized to total protein in the same sample well, and are expressed as mean \pm SEM. Parameters of glycolytic function (**A**), glycolysis (**B**), glycolytic capacity (**C**), and glycolytic reserve (**D**) are expressed as mean \pm SEM, relative to control (n=5). * $p < 0.05$ versus control.

3.2 Pioglitazone Reverses Alcohol-Induced Alterations in Alveolar Macrophage Mitochondrial Phenotype

The completion of my part in the ExZACTO clinical trial (Chapter 2) and my contributions to the manuscript by Morris et al. set the foundation for the preparation of a submitted first-author manuscript entitled “Pioglitazone reverses alcohol-induced alterations in alveolar macrophage mitochondrial phenotype.” The training I received to develop protocols to measure mitochondrial glucose, long chain fatty acid, and glutamine oxidation in AMs is highlighted here, in addition to microbiology techniques including fluorescence microscopy, quantitative PCR, and western blotting. Ultimately, my co-authors and I were able to describe further a mechanism of chronic alcohol-induced AM metabolic dysfunction that can be alleviated by acute application of the FDA approved therapeutic, pioglitazone (PIO).

We aimed to investigate the effect the PPAR γ ligand, PIO, on AM MT substrate oxidation in human and animal models of chronic alcohol exposure to determine their therapeutic potential for targeting these pathways. We found that *ex vivo* PIO improved MT superoxide in human AMs from people with AUDs and improved male and female mouse AM phagocytic index and MT superoxide levels. Additionally, PIO reversed EtOH-induced AM heightened dependency on glutamine and fatty acid oxidation while decreasing dependency on glycolytic-derived ATP and glucose oxidation. Further understanding of PIO's mechanism will help to repurpose current metabolic-targeted therapeutics to decrease morbidity and mortality due to loss of AM immune function in people with AUDs. Ultimately, we hope to improve clinical outcomes in people with AUDs, who are 2-4x more susceptible to respiratory infections and pulmonary damage.

**Pioglitazone reverses alcohol-induced alterations in alveolar macrophage
mitochondrial phenotype**

Kathryn M. Crotty, BS a,b, Shayaan A. Kabir, BS a,b, Sarah S. Chang, BS a,b, Ashish J. Mehta, MD a,b, Samantha M. Yeligar, MS, PhD a,b*

a Department of Medicine, Division of Pulmonary, Allergy, Critical Care and Sleep Medicine, Emory University, Atlanta, GA, United States.

b Atlanta Veterans Affairs Health Care System, Decatur, GA, United States.

***Corresponding author:** Samantha Yeligar, MS, PhD. Atlanta VA Medical Center (VHA) 1670 Clairmont Rd. 12C 104. Phone: (404) 321-6111 ext. 202518. Email: samantha.yeligar@emory.edu

Sources of support: This work was supported by NIAAA R01-AA026086 to SMY, NIGMS T32-GM008602 to Randy Hall, Department of Pharmacology and Chemical Biology, Emory University, NIAAA F31-F31AA029938 to KMC, and 1K2CX000643 to AJM.

Data availability: The data that support the findings of this study are available from Emory Dataverse upon reasonable request. Emory Dataverse is the open generalist data repository supported by Emory University in partnership with the Odum Institute Data Archive at UNC Chapel Hill.

Declarations of interest: none

Full Citation (pending): Accepted to Alcohol: Clinical and Experimental Research (ACER) Feb. 2024.

Abstract

Background: People with alcohol use disorder (AUD) have increased risk for developing pneumonia and pulmonary diseases. Alveolar macrophages (AMs) are lower respiratory tract resident immune cells necessary for clearance of pathogens. However, alcohol causes AM oxidative stress, mitochondrial damage and dysfunction, and diminished phagocytic capacity, leading to lung injury and immune suppression.

Methods: AMs were isolated by bronchoalveolar lavage from people with AUD and male and female C57BL/6J mice given chronic ethanol (20% w/v, 12 wks.) in drinking water. The peroxisome-proliferator activated receptor γ ligand, pioglitazone, was used to treat human AMs *ex vivo* (10 μ M, 24 h) and mice *in vivo* by oral gavage (10 mg/kg/day). Levels of AM mitochondrial superoxide and hypoxia-inducible factor-1 alpha (HIF-1 α) mRNA, a marker of oxidative stress, were measured by fluorescence microscopy and RT-qPCR, respectively. Mouse AM phagocytic capacity was determined by internalized *Staphylococcus aureus*, and mitochondrial capacity, dependency, and flexibility for glucose, long chain fatty acid, and glutamine oxidation were measured using an extracellular flux analyzer. *In vitro* studies using a murine AM cell line, MH-S (\pm 0.08% ethanol, 72 h) investigated mitochondrial fuel oxidation and ATP-linked respiration.

Results: Pioglitazone treatment improved mitochondrial superoxide in AMs from people with AUD and ethanol-fed mice and decreased HIF-1 α mRNA in ethanol-fed mouse lungs. Pioglitazone also reversed mouse AM glutamine oxidation and glucose or long-chain fatty acid flexibility to meet basal oxidation needs. *In vitro*, ethanol decreased AM

mitochondrial and total ATP production rate, and pioglitazone improved changes in glucose and glutamine oxidation.

Conclusions: Pioglitazone reversed chronic alcohol-induced oxidative stress in human AM and mitochondrial substrate oxidation flexibility and superoxide levels in mouse AM. Decreased ethanol-induced AM HIF-1 α mRNA with pioglitazone suggests that this pathway may be a focus for metabolic-targeted therapeutics to improve morbidity and mortality in people with AUD.

Keywords: immunometabolism; alcohol use disorder; oxidative stress; mitochondria; pulmonary

Introduction

Alcohol use disorder (AUD) impacts over 11% of the United States adult population¹⁴. Alcohol-related emergency department visits and deaths have increased between 25-50% within the last 15 years, primarily attributable to chronic conditions, including community-acquired pneumonia^{11,162}. In fact, the severity of alcohol-associated lung damage often goes unnoticed until secondary lung diseases persist longer than in non-AUD participants¹⁶³. AUD elevates the risk of community-acquired pneumonia and acute respiratory distress syndrome, and negatively impacts innate immunity in the lung^{4,9,42,163}. Yet, people with AUD do not receive alternative treatments to improve pulmonary immunity upon hospital admission. Addressing the need for supplemental therapeutics in those with AUD requires understanding the impact of alcohol on innate immune defenses in the lung.

Alveolar macrophages (AMs) are responsible for uptake and clearance of pathogens or damaged cells and engage in the resolution of inflammation during wound repair. AMs have diminished function following chronic alcohol use in humans and models of chronic ethanol (EtOH) consumption in mice. Previous studies show that AMs exhibit impaired pathogen recognition receptor action, diminished phagocytic capacity, suppressed proinflammatory cytokine expression, and increased extracellular and intracellular oxidative stress following chronic alcohol exposure^{113,165-166}. Further, phagocytosis and clearance of pathogens are high-energy processes, but alcohol decreases AM mitochondrial (MT)-dependent ATP-linked respiration⁵⁹. MT dysfunction is gaining interest as a marker for disease risk¹⁶⁷, but the depth of MT impairment

during chronic alcohol use and irregularities in related metabolic pathways is undetermined.

Alcohol shifts AM MT metabolism toward glycolysis rather than oxidative phosphorylation, and this shift is dependent on hypoxia-inducible factor-1 alpha (HIF-1 α)¹¹⁰. This metabolic shift is well characterized in cancer cells, but there are few therapeutics to reverse an aberrant glycolytic phenotype, and it is unknown how alcohol impacts pyruvate oxidation in AMs despite the evident shift toward glycolysis. Additionally, alcohol use negatively impacts AM cysteine homeostasis thereby increasing cellular and MT-oxidative stress and increasing pulmonary disease risk^{45,49,116}, but how chronic alcohol use impacts MT glutamine oxidation for cellular respiration is unknown. Lastly, like HIF-1 α , peroxisome-proliferator activated receptor gamma (PPAR γ), a regulator of lipid metabolism, is implicated in the metabolic shift of AMs during chronic alcoholic conditions^{46,60,110}. Alcohol decreases PPAR γ levels in AM and knock down of PPAR γ diminished AM phagocytic function while increasing oxidative stress⁴⁶. Further, the PPAR γ ligand, pioglitazone (PIO) improves AM redox homeostasis, cellular oxidative stress, MT dysfunction, and phagocytosis^{59,60,110}. Recently, alcohol has been shown to increase HIF-1 α in AMs, and HIF-1 α may regulate PPAR γ expression indirectly¹⁶⁸. In all, loss of PPAR γ activity dysregulates AM redox balance and MT metabolism^{46,49,59,110}, justifying further investigation into mechanisms underlying AM MT dysfunction.

The aim of this study is to further characterize MT-impairment in cell culture and mouse models of chronic alcohol use by quantifying AM MT-oxidative stress and AM use of glucose, glutamine, or long chain fatty acid oxidation for MT-dependent

respiration. We hypothesize that the proposed antioxidant and metabolic regulator, PIO, has the therapeutic potential to reverse AM phagocytic and metabolic dysfunction seen in chronic alcohol exposure.

Materials & Methods

Human samples: All procedures and data collection occurred at the Joseph Maxwell Cleland Atlanta Veterans Affairs Medical Center, Decatur, GA, United States, 30033 and reviewed and approved by the Atlanta Veterans Affairs Healthcare System Research and Development Committee and Emory University Institutional Review Boards. Otherwise healthy participants with AUD recruited from the Atlanta Veterans Hospital Substance Abuse and Treatment Program were already enrolled in research studies already including bronchoalveolar lavage (BAL) fluid collection via a standard bronchoscopy procedure¹⁶⁹. No lung diseases were diagnosed from bronchoscopy procedure. Participants gave informed consent to all procedures performed and VA Pulmonary Disease Repository sample storage. Samples from the biorepository were examined for the effect of PIO *ex vivo* on human AMs (hAMs) isolated.

Inclusion / exclusion criteria: Inclusion and exclusion criteria including drinking history questions are listed in **Table 3.2.1**. All participants had an active AUD at the time of bronchoscopy procedure. Alcohol use was graded based on Alcohol Use Disorders Identification Test (AUDIT) (Aasland et al., 1990) the Short Michigan Alcohol Screening Test (SMAST) (Selzer et al., 1975) and drinking history. A score of 7 on AUDIT (De Silva et al., 2008) and 3 on SMAST (Escobar et al., 1994) was considered an increased risk of AUD or borderline alcohol dependence.

hAM culture: Participants (n=80) underwent a procedure under standard conscious sedation to instill isotonic saline into a sub-segment of the right middle lobe or lingula using a flexible fiberoptic bronchoscopy followed by 6 ~30 mL suction aliquots to obtain BAL fluid containing hAMs. Following BAL procedure, ~150-180 mL samples were

centrifuged at 100 x g for 5 min to pellet remaining cells containing hAMs. Cell pellets were washed with 5 mL diH₂O for red blood cell lysis, centrifugation was repeated, and cell density was determined upon resuspension in 5 mL 1x PBS. Cells were centrifuged and resuspended at 1 x 10⁶ cells / mL in hAM medium: RPMI 1640 medium containing 2% Fetal bovine serum (FBS), 1% penicillin/streptomycin, and 8 µg/mL gentamycin. hAMs were cultured for 24 h with and without *ex vivo* PIO (10 µM in DMSO vehicle, Cayman Chemicals, Ann Arbor, MI) before experiments were performed. This hAM isolation technique generates a >90% macrophage population by Diff-Quik (Dade Behring, Deerfield, IL) staining¹²².

Mouse model of chronic EtOH ingestion & AM isolation: All animal studies were performed in compliance with the Atlanta VA Health Care System Institutional Care and Use Committee and National Institute of Health *Guide for the Care and Use of Laboratory Animals* guideline. Adult male and female C57BL/6J mice (8–10-week-old) were purchased from Jackson Laboratory (Bar Harbor, Maine), fed standard chow *ad libitum*, on a 12 h day/night light cycle, given enrichment with huts and shredding paper, and were acclimated to facilities for 3 weeks in a quarantined environment. Mice were acclimated to EtOH in drinking water bags (6.34 mg / mL or 5% w/v increase every 3-4 days until at 25.35 mg / mL or 20%) for 2 weeks. Mice remained at 20% weight/volume for 10 weeks while control animals received normal water. This mouse model of EtOH consumption is shown to maintain clinically relevant blood alcohol concentration of 0.12% ± 0.03^{48,170}. During the final 7 days of water or EtOH consumption, mice were given PIO (10 mg / kg / day, Cayman Chemicals, Ann Arbor, MI) in 100 µL methylcellulose vehicle or methylcellulose vehicle alone by oral gavage^{46,113}. Mice were

ethanized for tracheotomy and BAL procedure to instill and subsequently suction 1x PBS (1 mL, 4 times). BAL fluid was centrifuged at 200 x g for 5 min, washed with diH₂O to lyse red blood cells, and centrifuged again at 100 x g to isolate mouse AMs (mAMs), previously reported to generate an over 90% AM population by Diff-Quik measurement¹²². Cells were counted and plated in mAM complete media (RPMI-1640 with 5% FBS and 1% penicillin/streptomycin). Cells remained at 37°C in a humidified, 5% CO₂ controlled incubator for 24 h until stabilization for further investigation. Previous studies have shown sustained effects of chronic alcohol use following BAL procedure from AUD participants^{60,347}; therefore, cells were not incubated with additional EtOH.

RT-qPCR: Mouse lungs from all groups were taken and stored in RNA Later (Invitrogen, Waltham, MA) for preservation. Lungs were transferred to liquid nitrogen and pulverized by mortar and pestle for RNA isolation by TRIzol reagent (ThermoFisher Scientific, Rockford IL) and chloroform (200 µL per 1 mL TRIzol). After vortex and 20 min centrifugation at 100 x g the aqueous layer was transferred to a new tube for precipitation (isopropanol and ethanol washes). RNA was quantified by nanodrop, diluted to 100 ng / µL, and RT-qPCR was performed using iTaq Universal SYBR Green One-Step kit (Bio-Rad, Hercules, CA) on the Applied Biosystems 7500 Fast sequence detection system (ThermoFisher Scientific, Rockford IL). Mouse mRNA for PPAR γ (Forward 5' GAGTTCATGCTTGCAAGGATGC 3', Reverse 5' CGATATCACTGGAGATCTCGCC 3'), HIF-1 α (Forward 5' CTCAAAGTCGGACAG 3', Reverse 5' CCCTGCAGTAGGTTT 3'), and GAPDH housekeeping gene (Forward 5' GGATTTGGTCGTATTGGG 3', Reverse 5' GGAAGATGGTGATGGGATT 3') were

measured and quantified using specific mouse primers (Eurofins Genomics, Luxembourg City, Luxembourg) as previously published^{59,171}.

Fluorescence microscopy: All fluorescent probes were made according to manufacture protocols and diluted in hAM or mAM medium before incubation with live cells at 37°C in a dark incubator. hAMs or mAMs were incubated for 30 min in media with 0.5 μ M MitoTracker Red Chloromethyl-X-rosamine (CMXRos, Cell Signaling, Danvers, MA), a lipophilic cationic fluorescent dye dependent on MT membrane potential and mass, or for 10 min in media with 5 μ M MitoSOX (Invitrogen, Waltham, MA), a fluorescent dye dependent on MT superoxide levels. Phagocytic capacity in MH-S was quantified using a pH-sensitive fluorescence-labeled bacteria, pHrodo *Staphylococcus aureus* BioParticles conjugate (Invitrogen, Waltham, MA). mAMs (2×10^5 cells per well) were incubated with 1×10^6 particles pHrodo for 2 hours. Following staining, cells were washed once with 1x PBS, fixed to 16-well chamber slides in 4% paraformaldehyde for 20 min, washed twice more in 1x PBS, and stored in 1x PBS in a dark area. Alternatively, hAMs and mAMs were blocked with BSA (1%, 60 min), permeabilized (0.1% Triton X-100 in PBS for 15 min) for co-staining for PPAR γ or SOD2. hAM PPAR γ protein expression was performed and quantified as previously published⁴⁶ in 4 randomly selected human samples treated with *ex vivo* PIO. Recombinant anti-superoxide dismutase 2 (SOD2)/MnSOD antibody (ab137037, Abcam, Waltham, MA) was used at a 1 / 200 dilution in 1% BSA in PBS, and Goat anti-Rabbit IgG, Alexa Fluor 488 secondary antibody (A-11008, Invitrogen, Waltham, MA) was used at 4 μ g / mL for 60 min with 2 1x PBS washes in between each step.

pHrodo and MitoSOX were visualized by fluorescence imaging at 40x using TRITC parameters on BZ-X800 imaging software (Keyence Corporation, Osaka, Japan) while PPAR γ and SOD2 visualization was performed by BioTek Cytation C10 widefield microscopy at 20X. Relative fluorescence units (RFUs) were measured in at least 10 cells per image with no less than 50 cells imaged total per technical duplicate. All images were deconvoluted for measurement RFUs via ImageJ software (National Institute of Health, Bethesda, MD) or Cytation C10 software. mAM imaging and RFU quantification was performed by a blinded researcher before analysis. Cells with internalized *S. aureus* were considered positive for phagocytosis. Phagocytic capacity was quantified as phagocytic index: RFUs of pHrodo per cell multiplied by the number of cells positive for internalized bacteria / total cells.

***In vitro* model of chronic EtOH exposure:** MH-S cells (American Type Culture Collection, Manassas, VA), were used for all *in vitro* experimentation. MH-S cells were cultured in complete MH-S media (RPMI-1640 with 10% fetal bovine serum, 1% penicillin/streptomycin, 11.9 mM sodium bicarbonate, 40 mg / mL gentamicin and 50 μ M 2-mercaptoethanol) with or without 0.8 mg / mL (0.08%) of EtOH changed every 24 h for 72 h at 37°C with 5% CO₂ in a humidified incubator. EtOH treated cells were incubated separately with 0.08% EtOH in the incubator water for humidification. On the final day of EtOH exposure 10 μ M PIO or DMSO vehicle was given 24 h prior to extracellular flux assays. HIF-1 α was silenced in MH-S cells using 50 μ M siRNA for HIF-1 α (sc-35562, Santa Cruz, Dallas, TX). MH-S cells at 50% confluency for extracellular flux experiments were serum starved with cell media minus FBS for 2 hours followed by incubation with siRNAs for HIF-1 α or scrambled control plus 0.08 μ L Lipofectamine

3000 (ThermoFisher Scientific, Rockford, IL) per well according to manufacturer protocol.

Extracellular flux assays: Assessment of MT oxygen consumption was performed using an Agilent Seahorse XFp extracellular flux analyzer for mAM samples, an Agilent Seahorse XFe96 extracellular flux analyzer for cell fuel flexibility and ATP-rate assays in MH-S cells, and an Agilent Seahorse XF96 Pro (Agilent technologies, Santa Clara, CA) for substrate oxidation assays in MH-S cells. mAMs and MH-S cells were cultured in complete MH-S cell media to ensure 60-80% confluency during experiments. MH-S cells were cultured with or without 0.8 mg / mL (0.08%) EtOH changed every 24 h for 72 h at 37°C with 5% CO₂ in a humidified incubator. Prior to the experiment, media was replaced with Agilent RPMI base medium supplemented with 10 mM glucose, 1 mM sodium pyruvate, and 2 mM GlutaMAX. Following real-time oxygen consumption rate (OCR) measurements, media was removed, cells were washed once with 1x PBS, and cells were lysed with 20 µL cell lysis buffer with protease and phosphatase inhibitors. BCA (ThermoFisher Scientific, Rockford IL) assay was performed to normalize OCR to cellular protein. Calculations were based on Agilent Seahorse user manuals and white pages for the ATP-rate assay, Fuel Flex Test, and Substrate Oxidation Stress Tests (Agilent Technologies, Santa Clara, CA). Data are expressed as mean ATP production rate (pmol / min), mean OCR (pmol / min), mean % oxidation of fuel, or mean OCR (pmol) depending on which test calculation was performed. Due to limitations in sample acquisition, mAM samples were pooled (male and females pooled separately) and data was combined for males and females in statistical analyses.

Statistical methods: All animals were randomly assigned into water or EtOH ± PIO treatment groups before EtOH-feeding. 10 mice per experimental group were used and housed in cages of 5. Male and female mice (80 total) were used based on a priori sample size determinations and were cared for by the same veterinarian staff or investigators weekly for the duration of water or EtOH-feeding. Power analysis was performed to determine this sample size using an alpha value of 0.05, power of 0.80, error of 15%, and assuming a mean difference of 20% between group endpoints. All data was evaluated for normal distribution by a Shapiro-Wilk normality test. Human fluorescence microscopy of untreated and *ex vivo* PIO treated hAMs were log transformed due to non-normal distribution ($p < 0.05$) and confirmed to be normally distributed after transformation to use parametric testing (Paired t test). Outliers in data were removed based on a predetermined 1.5 * interquartile range of data before statistical testing. For human samples, a logistic regression to see the effect of smoking status and illicit drug use on mitochondrial superoxide and mitochondrial health dependent on mass and membrane potential was done to determine their effects as potential confounders. We did not see any significant effect of these potential confounding variables on either of these endpoints ($p < 0.05$). All other *in vivo* and *in vitro* data was analyzed by one-, or two-way ANOVA and Tukey post-hoc testing if normally distributed or Kruskal-Wallis followed by Dunn post-hoc testing if nonparametric. Results are expressed as paired measures overlaid atop bars displaying mean value for human samples or mean ± standard deviation (SD) relative to male Con + Veh for *in vivo* and *in vitro* studies. Otherwise, all normally distributed data is expressed as mean

± SD where significance was determined by Students *t*-test. All statistical analyses were performed using GraphPad Prism 10 (San Diego, CA).

Results

PIO improves phagocytic capacity and decreases MT superoxide in isolated hAMs and mAMs after chronic alcohol exposure.

Participants with AUD were identified and screened from the Atlanta VA Substance Abuse Treatment Program. Demographics for this participant population are shown in **Table 3.2.2**. Male and female (n=95) participants consented to BAL procedure to isolate AMs (**Fig. 3.2.1A, 3.2.1B**). Some participants had chronic lung disorders (**Table 3.2.2**), but these were managed medically, and no new lung diseases were diagnosed from the bronchoscopy procedure. Fluorescence microscopy of hAMs did not show changes in MT health dependent on MT mass and membrane potential after treatment with *ex vivo* PIO (**Fig. 3.2.1C**), however PIO was able to decrease MT superoxide levels in AUD hAMs (**Fig. 3.2.1D**) without changing total cellular PPAR γ or SOD2 levels (**Supplemental Fig. 3.2.1A**).

Oral PIO in male and female mice improved phagocytic capacity (**Fig. 3.2.2A**, representative fluorescence microscopy images in **Supplemental Fig. 3.2.2A-D**) and attenuated MT superoxide levels (**Fig. 3.2.2B**) in mAMs isolated from mice fed EtOH. SOD2 is the primary superoxide dismutase in the mitochondria, but no notable sex differences were observed in SOD2 (**Fig. 3.2.2C**). mAM PPAR γ and HIF-1 α protein levels have been reported previously in this chronic EtOH mouse model^{46,110}, but since there were noted sex differences in mAM phagocytic capacity, mRNA levels for these targets were quantified by RT-qPCR in mouse lungs. EtOH decreased PPAR γ in male but not female mice, but female mice had significantly less PPAR γ levels in Con + Veh mice. There was no impact of PIO on male or female PPAR γ levels relative to all other

groups (**Fig. 3.2.2D**). EtOH increased HIF-1 α mRNA levels in both male and female mouse lungs, whereas PIO treatment in EtOH exposed groups significantly decreased HIF-1 α level (**Fig. 3.2.2E**).

PIO improves metabolism of glucose, long chain fatty acids, and glutamine to meet baseline cellular oxidation rates in mAMs following chronic EtOH exposure.

mAMs isolated from mice given chronic EtOH or standard water were evaluated by an extracellular flux bioanalyzer for pyruvate, long chain fatty acid, and glutamine oxidation. Since MT respiration for ATP generation is dependent on oxygen, measurement of cellular oxygen consumption rate (OCR) before and after pharmacological inhibition of specific fuel metabolism pathways, that would otherwise result in oxidative phosphorylation, will allow for calculation of MT respiration dependent on that fuel pathway. This strategy allows for measurements of specific fuel dependency, capacity, and flexibility to generate baseline MT-respirations, expressed as percentage of baseline OCR. Calculations for quantification of these measurements are shown in **Fig. 3.2.3A** (adapted from Agilent Seahorse XFp Mito Fuel Flex Test Kit User Manual Kit 103270-100, April 2019).

OCR was taken for 3 baseline measurements before sequential injections of inhibitors for pyruvate oxidation (2 μ M UK5099), long chain fatty acid oxidation, Etomoxir (Eto, 4 μ M), and/or glutamine oxidation, Bis-2-(5-phenylacetamido-1,3,4-thiadiazol-2-yl)ethyl sulfide (BPTES, 3 μ M). ; and EtOH exposure decreased mAM capacity (Cap) to use glucose/pyruvate to meet energetic demand while increasing dependency (Dep) on long chain fatty acid (Cap and Dep in **Fig. 3.2.3C**) and glutamine oxidation (Cap and Dep in **Fig. 3.2.3D**). PIO treatment improved alterations in metabolic

demand and increased the ability of mAMs to use other fuels to make up for the loss of one due to EtOH exposure (Flex in **Fig. 3.2.3B-D**).

HIF-1 α knock down *in vitro* further decreases glucose capacity and flexibility and decreases glutamine dependency following chronic EtOH exposure.

Previously our group showed that EtOH shifts AMs toward a glycolytic phenotype that was dependent on increased HIF-1 α expression and activity^{52,110}. Immune cells must shift MT metabolism towards higher ATP production when necessary for sustained immune function, however we have previously shown that EtOH decreased AM MT respiration. MH-S cells were used to further investigate the changes seen in AM metabolic phenotype after chronic EtOH exposure. Following a similar line of thinking as in **Fig. 3.2.3**, inhibitors for glucose, long chain fatty acid, or glutamine oxidation were used to measure metabolic responses of AMs in stressed conditions. Either BPTES (GLN Inh Con), Eto (FA Inh Con), or UK5099 (GLC Inh Con) followed by ATP-synthase inhibitor oligomycin (2 μ M Oligo), MT uncoupler Carbonyl cyanide-p-trifluoromethoxyphenylhydrazone (FCCP, 0.5 μ M), and MT complex I and III inhibitors rotenone and antimycin A, respectively, (0.5 μ M R/A) were injected onto cells for the substrate oxidation assays. Oxidation of fuels was compared to MT respiration profile without inhibition of the target pathway (Media Con).

MH-S cells were primarily dependent on oxidation of glucose/pyruvate to make up maximal MT-dependent respiration compared to long chain fatty acid oxidation or glutamine oxidation (**Fig. 3.2.4A**). Oligo and R/A were used after baseline OCR measurements for the ATP-rate assay, as described by Agilent Seahorse. EtOH decreased MT-derived and total ATP without a change in glycolytic ATP (**Fig. 3.2.4B**).

Knock down of HIF-1 α , confirmed by GFP-reporter and RT-qPCR (Supplemental **Fig. 3.2.3A, 3.2.3B**) decreased AM capacity and flexibility to use glucose for MT-dependent respiration and increased dependency on glutamine, suggesting less MT-dependent glucose oxidation and a possible shift toward glutaminolysis (**Fig. 3.2.4C, E**). No change in long chain fatty acid capacity, dependency, or flexibility was seen after siHIF-1 α *in vitro* (**Fig. 3.2.4D**).

PIO improves basal pyruvate oxidation *in vitro* following chronic EtOH exposure.

Inhibition of pyruvate oxidation decreased maximal MT-dependent respiration *in vitro* relative to cells not given UK5099 inhibitor (Con Media) (**Fig. 3.2.5A**). EtOH decreased basal MT-dependent pyruvate metabolism (**Fig. 3.2.5B**) and ATP-linked respiration due to pyruvate metabolism (**Fig. 3.2.5C**). EtOH + PIO group MT-dependent basal and ATP-linked respiration due to pyruvate was not significantly different than Con + Veh (**Fig. 3.2.5B, 3.2.5C**). No observed differences were seen in EtOH or PIO groups for the loss of maximal MT-dependent respiration due to pyruvate metabolism inhibition or spare capacity (**Fig. 3.2.5D, 3.2.5E**).

Chronic EtOH decreases ATP-linked and maximal MT-dependent respiration derived from long chain fatty acid oxidation *in vitro*.

EtOH decreased maximal MT-dependent respiration after inhibition of long chain fatty acid oxidation in MH-S cells compared to control and PIO treated cells (**Fig. 3.2.6A, 6D**). EtOH additionally decreased MT-dependent ATP-linked respiration derived from long chain fatty acid oxidation, which was not improved by PIO *in vitro* (**Fig. 3.2.6C**). No change due to EtOH or PIO was seen in the loss of basal respiration or

spare respiratory capacity due to inhibition of long chain fatty acid oxidation (**Fig. 3.2.6B, 3.2.6E**).

PIO and chronic EtOH increase the ability to compensate for loss of glutamine oxidation *in vitro*.

Minor change in OCR was measured after inhibition of glutamine oxidation due to EtOH (**Fig. 3.2.7A-E**). Compared to pyruvate and long chain fatty acid MT metabolism, glutamine does not account for a large amount of basal MT-dependent respiration (**Fig. 3.2.7B**) or ATP-linked respiration (**Fig. 3.2.7C**). However, AMs are more dependent on glutamine when stressed with FCCP (**Fig. 3.2.4A**), resulting in a much greater decrease in maximal MT-dependent OCR in Con + Veh cells after BPTES inhibitor (**Fig. 3.2.7D**). Interestingly, EtOH and PIO treated cell maximal MT-dependent respiration was not as greatly impacted by inhibition of glutamine metabolism compared to the loss seen in control cells (**Fig. 3.2.7D**), but no change was observed in spare capacity (**Fig. 3.2.7E**).

Discussion

Collectively, the results of this study suggest that impaired MT oxidative stress and fuel metabolism including altered glucose, long chain fatty acid, and glutamine oxidation are underlying aspects of the pathologic phenotype seen in AMs following chronic alcohol exposure. Increased cellular superoxide levels have been reported *in vitro* and *in vivo* in other models of alcohol misuse^{172,173}; however, changes in MT superoxide levels in hAMs have not been previously reported. Here, PIO treatment decreased MT superoxide levels in hAMs isolated from participants with AUD and mAMs from male and female C57BL/6J mice given chronic EtOH feeding. We report that total cellular SOD2 and PPAR γ levels did not change in AUD hAMs after PIO treatment (**Supplemental Fig. 3.2.1**), potentially indicating that PIO decreases MT superoxide levels, improves AM phagocytic capacity, and reverses metabolic dysregulation potentially by improving PPAR γ activity and MT fuel metabolism. However, we did not report nuclear or mitochondrial localized PPAR γ or SOD2, which could influence protein ability to transcribe genes related to metabolic regulation or neutralization of mitochondrial oxidative stress. Future studies will focus on quantifying localization and activity of PPAR γ and superoxide dismutase activity in hAMs from healthy control people without AUD, people with AUD, and people with AUD treated with PIO.

Community-acquired pneumonia is the most common respiratory disease, and people with AUD have a 2-fold increase in risk for developing community-acquired pneumonia^{11,162}. It was confirmed here and in a past study⁶⁰ that AMs exposed to chronic alcohol or EtOH have diminished phagocytic capacity for pathogens that can be

improved by PIO treatment. Interestingly, we found that female mice had significantly increased phagocytic capacity in all groups compared to male mice, despite similar trends in EtOH and EtOH + PIO groups. In a cross-sectional study of alcohol-related deaths in over 600,000 people spanning over 20 years, male mortality was found to be 2.88 times more likely. Though, incidence of female mortality due to alcohol is increasing, in part due to increased alcohol consumption and incidence of AUD among females¹¹⁴. Further, males had a greater fatality rate compared to females under 60 years old who contracted community-acquired pneumonia. Other studies have postulated that pneumonia-associated mortality is linked to differences in circulating sex hormones and inflammatory cytokine secretion by AMs¹⁷⁴⁻¹⁷⁶. Due to limitations in sample acquisition during this study and since other reported data showed no sex differences, extracellular flux data was combined for males and females and may have contributed to no observable changes in metabolic function. Sex-differences in AM metabolism and phagocytic abilities are a focus of future studies.

Many mechanisms of decreased AM phagocytosis have been proposed previously^{59,110,111,112,172,173,177}. Alcohol negatively impacts MT function and impairs AM phagocytosis, but how MT function is impaired is inconsistent between different model species and alcohol consumption strategies. In general, EtOH is thought to decrease MT content, but our past studies show that EtOH increases MT number while decreasing MT size, indicating more MT fission⁵⁹. In AUD participants, MT health dependent on mass coupled with membrane potential did not change after PIO treatment. It is possible that this negative observation is due to cessation from alcohol due to enrollment in a substance use and treatment program, or variability in participant

population, but previous studies have shown that metabolic dysfunction is sustained following AM isolation from people with AUD⁶⁰. Therefore, three MT bioenergetic pathways were examined in this study to propose a new mechanism of EtOH-induced AM dysfunction: 1) pyruvate oxidation; 2) glutamine oxidation; 3) long chain fatty acid oxidation. These pathways were chosen due to their critical roles in highly efficient ATP production, which is essential for cellular processes like AM internalization and clearance of pathogens. EtOH was found to decrease pyruvate and long chain fatty acid oxidation-dependent ATP, while increasing maximal glutamine oxidation in AMs. These changes directly related to increased dependency and diminished flexibility of AMs for pyruvate and long chain fatty acid oxidation. Further, PIO was able to restore pyruvate-dependent ATP-linked respiration and reverse EtOH-induced changes in pyruvate, long chain fatty acid, and glutamine flexibility by either increasing lost capacity or decreasing dependency on fuel oxidation (**Fig. 3.2.8**).

EtOH in mice decreases MT-dependent respiration^{50,59}, shifting AM metabolic phenotype toward glycolysis (less efficient ATP production) in a HIF-1 α dependent manner, and metabolic phenotype reversal is possible with oral PIO *in vivo*¹¹⁰. Here, we report that chronic alcohol consumption decreases MT-derived ATP through loss of multiple fuel oxidation pathways in AM. Our results support these previous conclusions, since our findings show improvements in EtOH-induced alterations in pyruvate, long chain fatty acid, and glutamine oxidation (**Fig. 3.2.3**) in AMs treated with PIO *in vitro* and *in vivo*.

Further, EtOH and loss of HIF-1 α decreased capacity of AMs to use glucose for MT-dependent respiration, revealing a potential mechanism for the shift away from

glycolysis seen with PIO treatment, since PIO decreases HIF-1 α levels in AMs ¹¹⁰. Knock down of HIF-1 α , previously shown to be crucial in the AM chronic alcohol exposure phenotype ¹¹⁰, did not completely reverse changes in AM MT substrate oxidation, which could indicate that reversal in MT metabolism by PIO is not solely dependent on HIF-1 α . However, knock down of HIF-1 α was incomplete, with siRNA transfection only amounting to a 30% decrease in expression (Supplemental Fig. S3). Post-transcriptional regulation also plays a major role in HIF-1 α activity, which could explain why the slight knock down in expression did not significantly change oxidation of mitochondrial substrates in EtOH-exposed cells. The combination of the loss of PPAR γ activity and stabilization of HIF-1 α together, but not necessarily in sequence, may be in part responsible for AM phagocytic and metabolic dysfunction following chronic alcohol exposure. Further investigation into the role of HIF-1 α is needed for clarification and thus, we could not conclude that these effects were dependent on HIF-1 α alone.

PPAR γ is highly involved in lipid sensing and metabolism ¹⁷⁸⁻¹⁸⁰, so it was anticipated that PIO would reverse EtOH-dependent decreases in MT-dependent long chain fatty acid oxidation. Alcohol use increases fatty acid accumulation and lipogenesis in the liver, resulting in tissue damage and persistent inflammation ^{6,79,81,181-183}. Fatty acid and acylcarnitine levels are increased in BAL fluid from participants with AUD compared to healthy controls, potentially indicating AM metabolic imbalance ¹²⁴. However, the increase in BAL fluid fatty acid concentration alternatively may result from increased surfactant lipids generated from alveolar epithelial cells ¹⁸⁴, and little is understood about AM metabolism of fatty acids following EtOH exposure. Since cell media prior to bioenergetics measurements did not include additional fatty acids in the

current study, further studies are also needed to determine the detailed pathways involved in fatty acid dependency.

PPAR γ is suggested here to be more important for glucose metabolism in AMs, but limitations included limited AM pools from mice and inability to perform MT bioenergetics assays on preserved human samples. Additionally, this study lacked sufficient evidence to show that PIO improved EtOH-associated MT fuel oxidation phenotype through attenuation of HIF-1 α , given the limitations of low knock down efficacy and post-translational regulation of HIF-1 α . Derangements in pyruvate oxidation, as seen with chronic EtOH *in vitro*, may have a greater impact on MT oxygen consumption and ATP-linked respiration. Finally, EtOH increased glutamine oxidation, likely to make up for loss of glucose and fatty acid oxidation in AMs. This is further supported by the increase in dependency for basal glutamine-derived respiration found *in vivo*. Altogether, this study expanded on previous reports showing dysregulated AM immunometabolism following chronic alcohol exposure and posits that a clinically available therapeutic, PIO, can in part reverse these disrupted metabolic phenotypes.

Overall, this study highlighted previously unknown characteristics of AM MT metabolism and how chronic EtOH exposure negatively shifts AM metabolic phenotypes linked to oxidative stress and low phagocytic capacity. There are concerns regarding the potential toxicity in long term use of the PPAR γ ligand rosiglitazone for diabetes management, but PIO has not shown the same level of toxicity as previously used ligands¹⁸⁵⁻¹⁸⁸. Short-term PIO use may be effective in decreasing the risk of respiratory diseases in people with AUD, but additional data is needed from human studies that include non-AUD healthy controls in the future. Preclinical experiments are necessary to

ensure PIO as a therapeutic strategy is sound in clinically relevant disease models, like pneumonia, but the findings in this study provide foundational evidence that treatment with PIO may reverse AM dysfunction in people with AUD and could improve pulmonary immunity in these individuals.

Conclusions: A summary of AM chronic alcohol-induced phenotype is shown in a graphical summary, **Figure 3.2.8**. Chronic alcohol use increases oxidative stress and decreases AM phagocytic capacity in people with AUD, which is restored by PIO⁶⁰, and chronic EtOH exposure models *in vitro* and *in vivo* recapitulate these findings. These results show that chronic EtOH impaired metabolism of three substrates used by mitochondria. Previously, it was shown that EtOH shifted AM to a glycolytic phenotype via a HIF-1 α ¹¹⁰, and we show that EtOH decreased AM capacity and flexibility to oxidize pyruvate. Dependency to make up basal respiration shifted toward long chain fatty acid and glutamine oxidation; however maximal respiration only increased from glutamine-dependent MT respiration. Altogether, EtOH decreased basal MT flexibility to oxidize pyruvate, long chain fatty acids, and glutamine, resulting in an overall decrease in MT and cellular ATP. Activation of PPAR γ with its ligand, PIO, was able to reverse several alterations in MT metabolism of these fuels, most notably by reversing EtOH-induced attenuation of pyruvate oxidation to restore of pyruvate oxidation-derived ATP. Loss of AM PPAR γ in people with AUD has previously been reported, and ligands for PPAR γ restore AM phagocytic capacity while decreasing lung and cellular oxidative stress^{48,60}. Together, these results indicate that PIO provides a pharmacological

approach targeting metabolic dysfunction to improve AM phagocytic dysfunction in people with AUD.

Author contributions

KMC handled conceptualization, investigation, data curation, formal analysis, validation, visualization, interpretation, writing, review, and editing. SAK and SSC handled data curation, visualization, review, and editing. AJM handled human sample acquisition, interpretation, writing, review, and editing. SMY handled conceptualization, investigation, funding acquisition, methodology, project administration, supervision, interpretation, writing, review, and editing. The authors would like to thank David Guidot and Amy Anderson for AUD participant recruitment.

Tables & Figures

Table 3.2.1: Inclusion and exclusion criteria and drinking history questionnaire for selection of participants with AUD.

Inclusion Criteria	Exclusion Criteria
<ul style="list-style-type: none"> • Male or female Veterans. • Between 18-60 years of age. • Active alcohol use disorder (AUD). • Last ingested alcohol < 8 days prior to bronchoscopy. • Consented to all procedures. • History of drinking based on questions (if applicable): <ol style="list-style-type: none"> 1. At what age did you first have 1 or more drinks of alcohol? 2. How old were you when you first became intoxicated? 3. At what age did drinking begin to have an effect on your life, which you did not approve of? At what age did drinking first become a problem for you? 4. Have you ever willingly quit drinking for a period longer than a few days? 5. How many past quit attempts have you had? 6. Have you ever been through alcohol use treatment? If yes, provide details (inpatient, outpatient, years of treatment)? 	<ul style="list-style-type: none"> • Any active and uncontrolled medical problem(s) not successfully treated with medication. • Known zinc deficiency. • Primary non-AUD related substance misuse. • Abnormal chest x-ray. • HIV-positive status. • Any blood coagulation disorder or currently treatment with anti-coagulants (inc. warfarin, heparin, direct thrombin inhibitors, and anti-platelet agents other than Aspirin). • Daily use of vitamins/nutritional supplements. • Renal impairment with glomerular filtration rate < 60 mL / min / 1.73 m². • Active bipolar disorder. • Active Parkinson's disease. • Current pregnancy. • Inability to give informed consent (i.e., limited cognitive capacity). • Non-English speaking.

Table 3.2.2: Demographics of alcohol use disorder (AUD) participants, whose alveolar macrophages (hAMs) were collected and treated with or without pioglitazone (PIO) *ex vivo*.

Participants (n=80)	Demographic	Median	Mean	Min, Max
	Age (yrs.)	48	49	28, 60
	Weight (lbs.)	184	187	117, 296
	Height (in.)	69	69	60, 76
	Body Mass Index (BMI)	27	28	16, 42
	Alcohol Use Disorder Identification Test (AUDIT)	22	21	6, 40
	Short Michigan Alcohol Screening Test (SMAST)	7	7	1, 13
		Count		%
Sex	Male	68		85
	Female	12		15
Race	Black or African American	64		80
	White	8		10
	Other	8		10
Ethnicity	Hispanic or Latino	3		4
	Not Hispanic or Latino	77		96
Smoking status	Some or every day	49		61
	Never	31		39
Illegal drug use	Yes	30		38
	No	49		61
	Not reported	1		1
Other conditions	Yes	72		90
	• Neurological (Depression, PTSD, anxiety, restless leg syndrome)	50		63
	• Cardiovascular (Hypertension, Hypercholesterolemia, hyperlipidemia, hypertrophy, subdural hemorrhage)	41		53
	• Gastroenteric (GERD, colon cancer, elevated folic acid, B12 deficiency, elevated LFTs, hepatitis c)	24		30
	• Orthopedic (Osteoarthritis, extremity / back / neck pain, gout, traumatic arthropathy, spinal stenosis)	23		29
	• Pulmonary / sleep (pleural effusion, pulmonary embolism, asthma, COPD, sleep apnea)	16		24
	• Endocrine (Hypothyroidism, pancreatitis, diabetes)	3		4
	• Reproductive (erectile dysfunction, prostatitis, prostate cancer)	3		4
	• Other (herpes, seasonal allergies, eczema, cataracts, chronic headaches, vitamin D deficiency, anemia, insomnia)	11		14
No other conditions	8		10	

Table 3.2.2: Demographics of alcohol use disorder (AUD) participants, whose alveolar macrophages (hAMs) were collected and treated with or without pioglitazone (PIO) *ex vivo* (n=80). Only participants used in the final analyses were included in these demographics.

Fig. 3.2.1

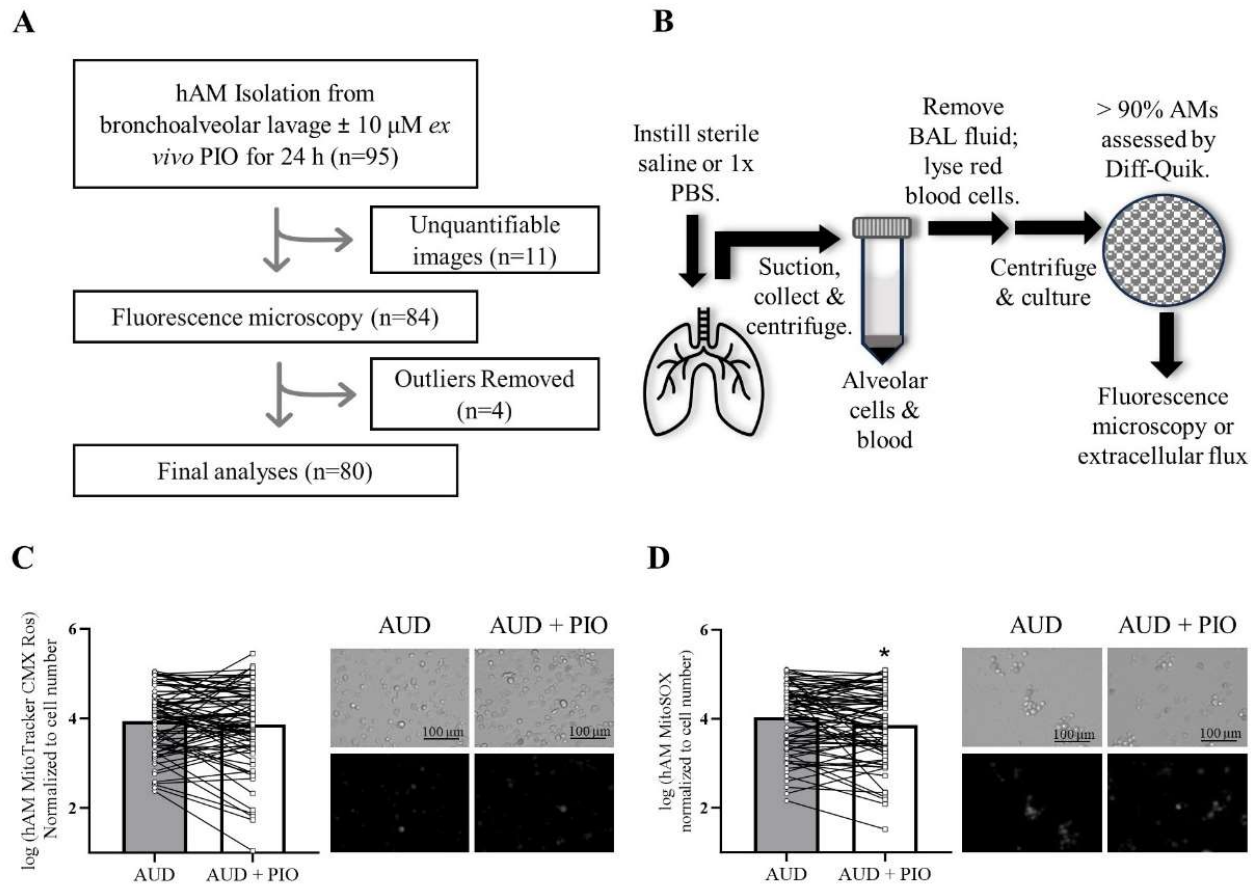


Fig. 3.2.1: Pioglitazone (PIO) decreases mitochondrial superoxide in isolated human alveolar macrophages. A-B) Human participants with alcohol use disorder (AUD, n=95) were screened and selection resulted in n=80 total participants for analysis. **B)** BAL procedure for human and mouse lung fluid to isolate AMs (hAMs). hAMs are isolated in sterile saline and mAMs are isolated in 1x PBS followed by BAL fluid removal, red blood cell lysis with diH₂O, and plating for overnight culture in hAM media prior staining, fixation, and fluorescence microscopy at 40x. hAMs from participants with alcohol use disorder before (AUD) and after treatment with PIO (AUD + PIO, 10 uM for 24 h. *ex vivo* prior to staining) had no change in **C)** mitochondrial health dependent on mass and membrane potential via MitoTracker CMX-Ros and **D)** had decreased mitochondrial superoxide levels via MitoSOX. Bars represented express mean \pm SD (n=80, *p < 0.05, paired t test).

Fig. 3.2.2

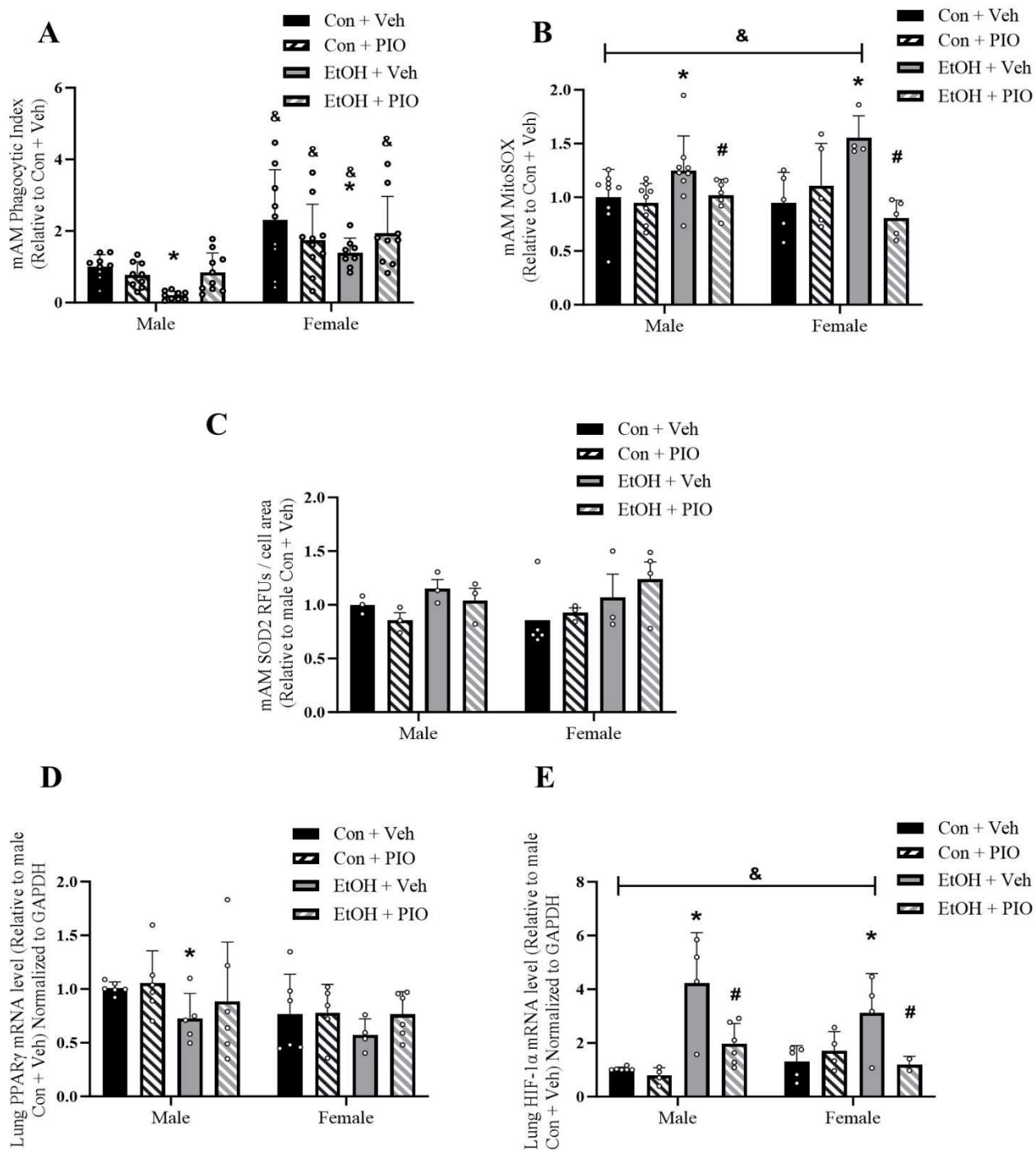


Fig. 3.2.2: Pioglitazone (PIO) improves phagocytic capacity and decreases mitochondrial superoxide in isolated mouse alveolar macrophages (mAMs). **A)** mAMs isolated from EtOH-fed (20% w/v, 12 wks in drinking water) mice had improved phagocytic index following oral PIO treatment (10 mg / kg / day by oral gavage) measured via internalization of pHrodo-labeled *Staphylococcus aureus* in both male (n=9-10) and females (n=8-10). Males had significantly less phagocytic capacity relative to females for all groups. **B)** mAMs had decreased mitochondrial superoxide measured by MitoSOX in male (n=7-9) and females (n=4-5). **C)** Superoxide dismutase 2 protein in male and female mAMs did not change (n=3). **D)** EtOH feeding decreased male mouse lung peroxisome proliferator-activated receptor gamma (PPAR γ) mRNA levels while increasing hypoxia-inducible factor-1 alpha (HIF-1 α) mRNA levels in both sexes. PIO attenuated HIF-1 α levels in EtOH-fed mouse lungs (n=6). Bars represented express mean \pm SD (*p < 0.05 v. Con + Veh, #p < 0.05 v. EtOH + Veh; &p < 0.05 v. Male, Two-way ANOVA with Tukey's *post-hoc*).

Fig. 3.2.3

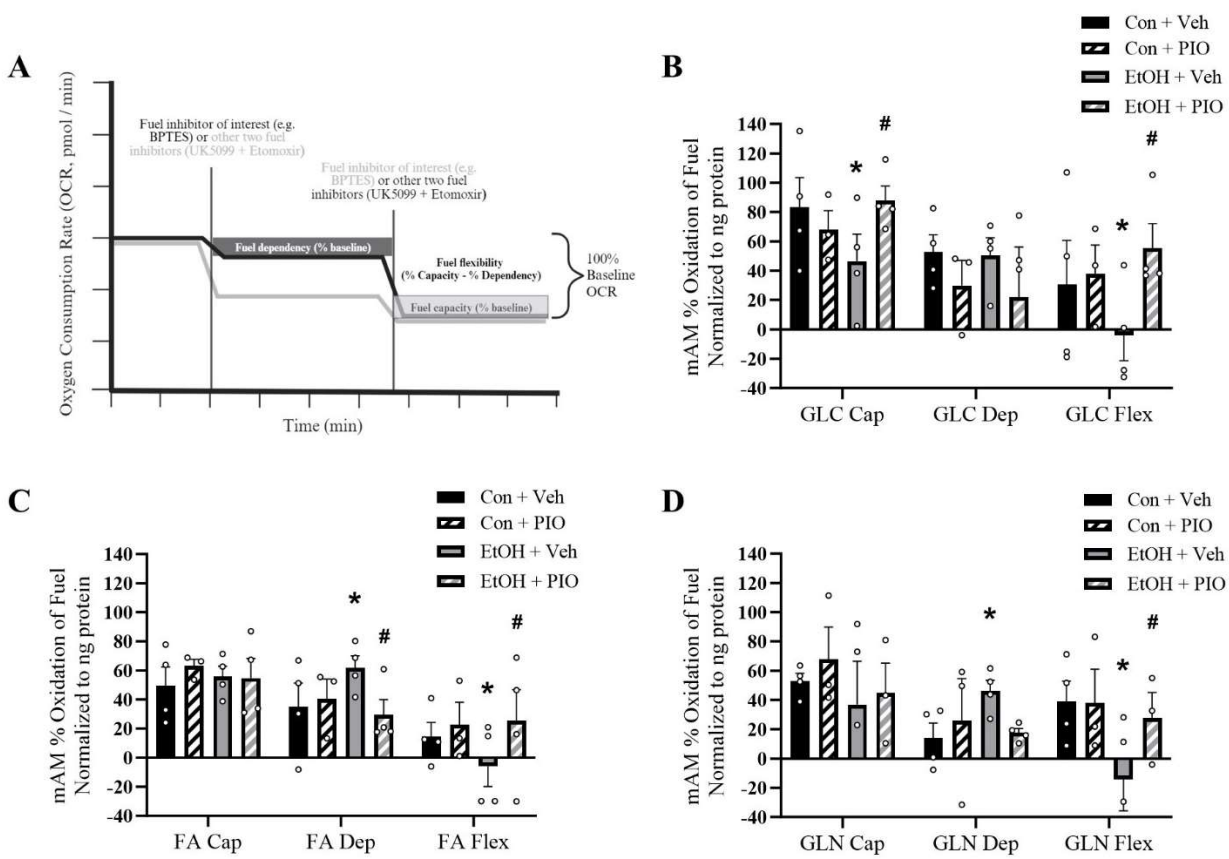


Fig. 3.2.3: Pioglitazone (PIO) improves metabolism of glucose, long chain fatty acids, and glutamine to meet baseline cellular oxidation rates in mouse alveolar macrophages (mAMs) following chronic ethanol (EtOH) feeding. Glucose (GLC), long chain fatty acid (FA), and glutamine (GLN) capacity (Cap), dependency (Dep), and flexibility (Flex) to be oxidized to meet baseline oxygen consumption rate (OCR) in isolated mAMs. **A)** Representative OCR profile measured by an extracellular flux bioanalyzer to calculate Cap, Dep, and Flex in cells given injections of inhibitors for glutamine (3 μ M BPTES), long chain fatty acid (4 μ M Etomoxir), and/or pyruvate (2 μ M UK5099) oxidation in mitochondrion. **B-D)** Male and female mAMs isolated from EtOH-fed (20% w/v, 12 wks in drinking water) mice had improved glucose capacity and flexibility and attenuated long chain fatty acid and glutamine dependency and flexibility following oral PIO treatment (10 mg / kg / day by oral gavage). Bars represented express mean \pm SD (n=3-4 of pooled mAMs (male and female separately pooled) from 4-5 mice per replicate, *p < 0.05 v. Con + Veh, #p < 0.05 v. EtOH + Veh; One-way ANOVA with Tukey's *post-hoc*).

Fig. 3.2.4

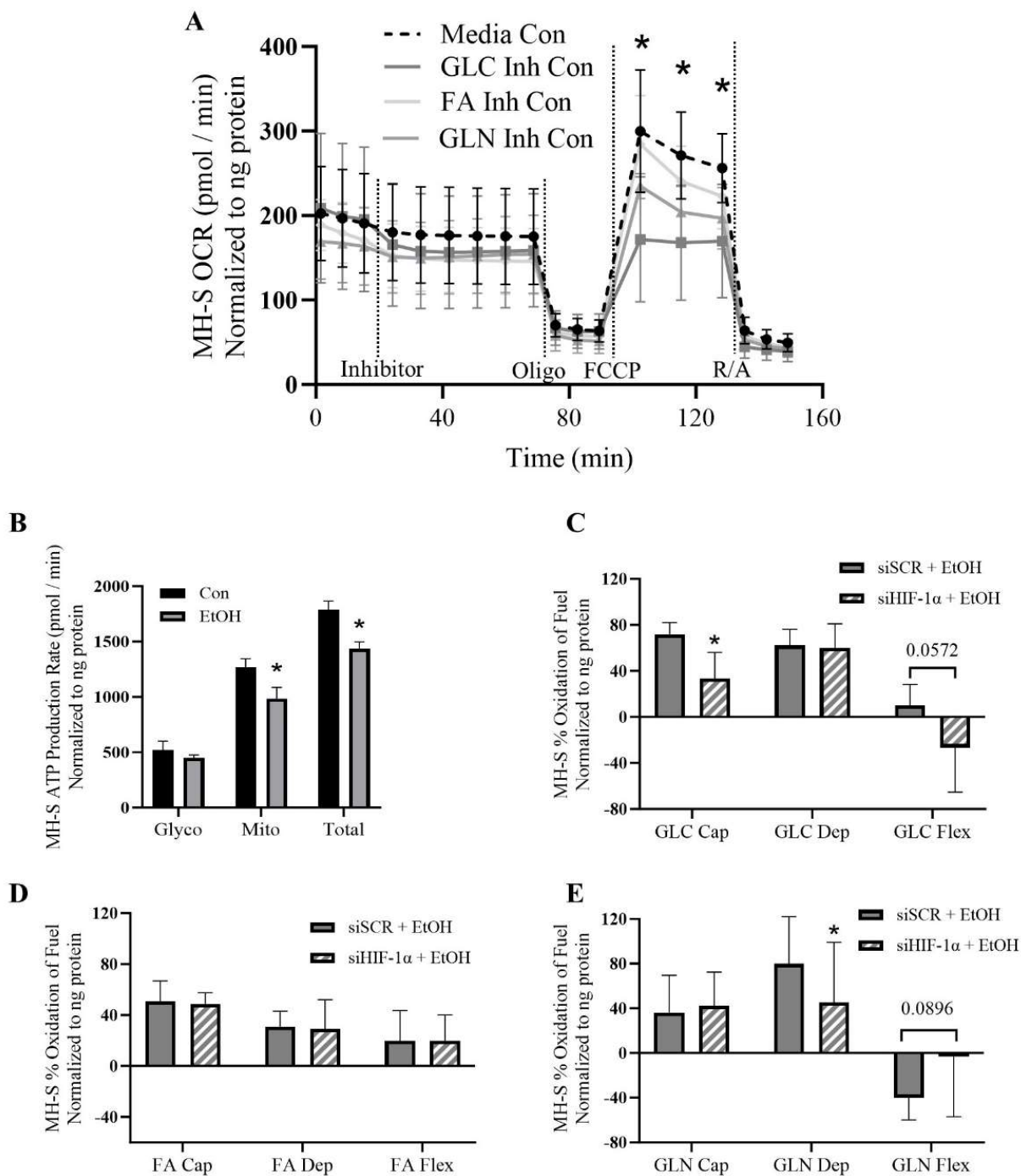


Fig. 3.2.4: Hypoxia-inducible factor-1 alpha (HIF-1 α) knock down *in vitro* further decreases glucose capacity and flexibility and decreases glutamine dependency following chronic ethanol (EtOH) exposure. MH-S cells were given distinct Agilent Seahorse assay injections of inhibitors for glutamine (3 μ M BPTES), long chain fatty acid (4 μ M Etomoxir), and/or pyruvate (2 μ M UK5099) oxidation in mitochondrion to measure oxygen consumption rates related to each pathway separately using an extracellular flux bioanalyzer. **A)** MH-S cells are primarily dependent on glucose, then long chain fatty acid, then glutamine oxidation under stressed conditions. **B)** MH-S cells exposed to EtOH (0.08%, 72 h) have decreased mitochondrial (Mito), and total ATP production but not glycolytic-derived (Glyco) ATP *in vitro* (n=4, *p < 0.05, t-test). **C)** Glucose (GLC), **D)** long chain fatty acid (FA), and **E)** glutamine (GLN) capacity (Cap), dependency (Dep), and flexibility (Flex) to be oxidized to meet baseline oxygen consumption rate (OCR) *in vitro*. Bars represented express mean \pm SD (n=5-6, *p < 0.05 v. siSCR + EtOH; One-way ANOVA with Tukey's *post-hoc*).

Fig. 3.2.5

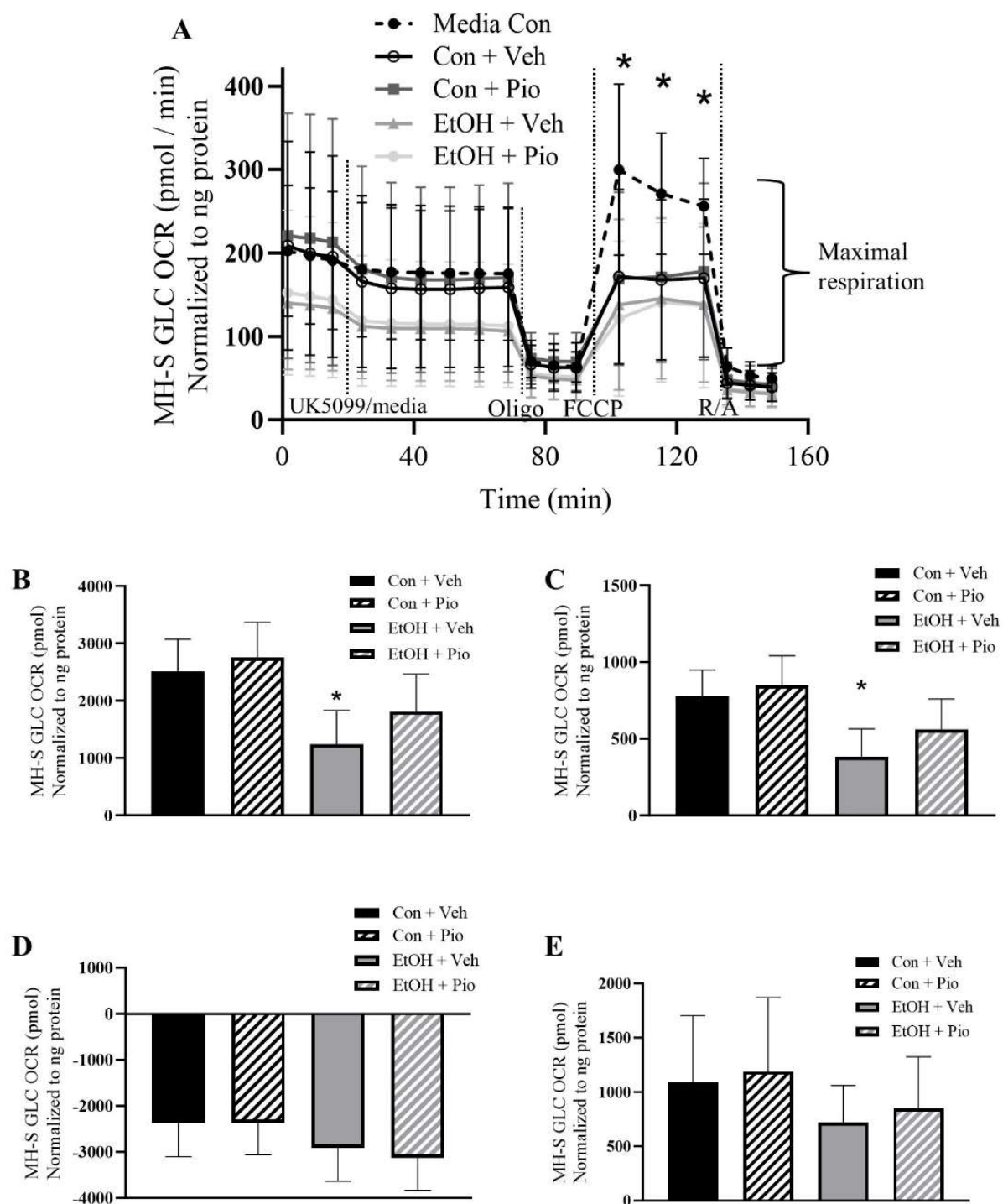


Fig. 3.2.5: Pioglitazone (PIO) improves glucose (GLC) oxidation in MH-S cells following chronic ethanol (EtOH) exposure. MH-S cells were exposed to EtOH (0.08%, 72 h) ± PIO (10 µM last 24 h of EtOH) followed by oxygen consumption rate (OCR) measurements over time by an extracellular flux bioanalyzer before and after injections with limited media or pyruvate oxidation inhibitor (2 µM UK5099), mitochondrial complex V inhibitor (0.5 µM oligomycin, Oligo), mitochondrial uncoupler (0.5 µM FCCP), and mitochondrial complex I and III inhibitors (0.5 µM rotenone / antimycin A, R/A). **A)** OCR profiles used to calculate **B)** pyruvate oxidation resulting in OCR, **C)** change in ATP-linked respiration, **D)** loss of maximal respiration, and **E)** change in spare capacity due to inhibition of pyruvate oxidation. Bars represented express mean ± SD (n=4, *p < 0.05 v. Con + Veh; One-way ANOVA with Tukey's *post-hoc*).

Fig. 3.2.6

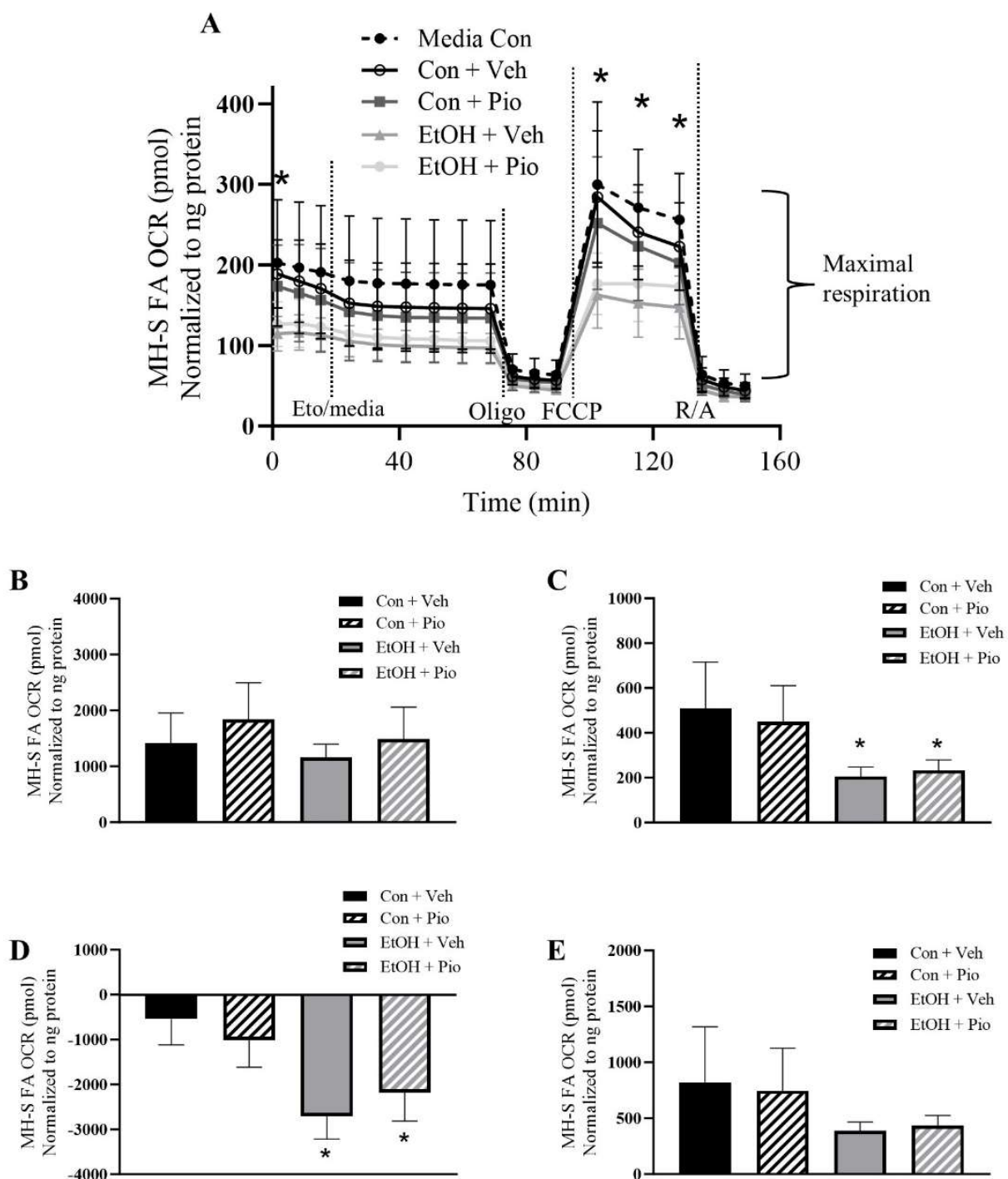


Fig. 3.2.6: Chronic ethanol (EtOH) decreases ATP-linked and maximal respiration derived from long chain fatty acid oxidation in MH-S cells. MH-S cells were exposed to EtOH (0.08%, 72 h) \pm pioglitazone (PIO, 10 μ M last 24 h of EtOH) followed by oxygen consumption rate (OCR) measurements over time by an extracellular flux bioanalyzer before and after injections with limited media or long chain fatty acid oxidation inhibitor (4 μ M Etomoxir, Eto), mitochondrial complex V inhibitor (0.5 μ M oligomycin, Oligo), mitochondrial uncoupler (0.5 μ M FCCP), and mitochondrial complex I and III inhibitors (0.5 μ M rotenone / antimycin A, R/A). **A)** OCR profiles used to calculate **B)** long chain fatty acid oxidation resulting in OCR, **C)** change in ATP-linked respiration, **D)** loss of maximal respiration, and **E)** change in spare capacity due to inhibition of long chain fatty acid oxidation. Bars represented express mean \pm SD (n=4, *p < 0.05 v. Con + Veh, One-way ANOVA with Tukey's *post-hoc*).

Fig. 3.2.7

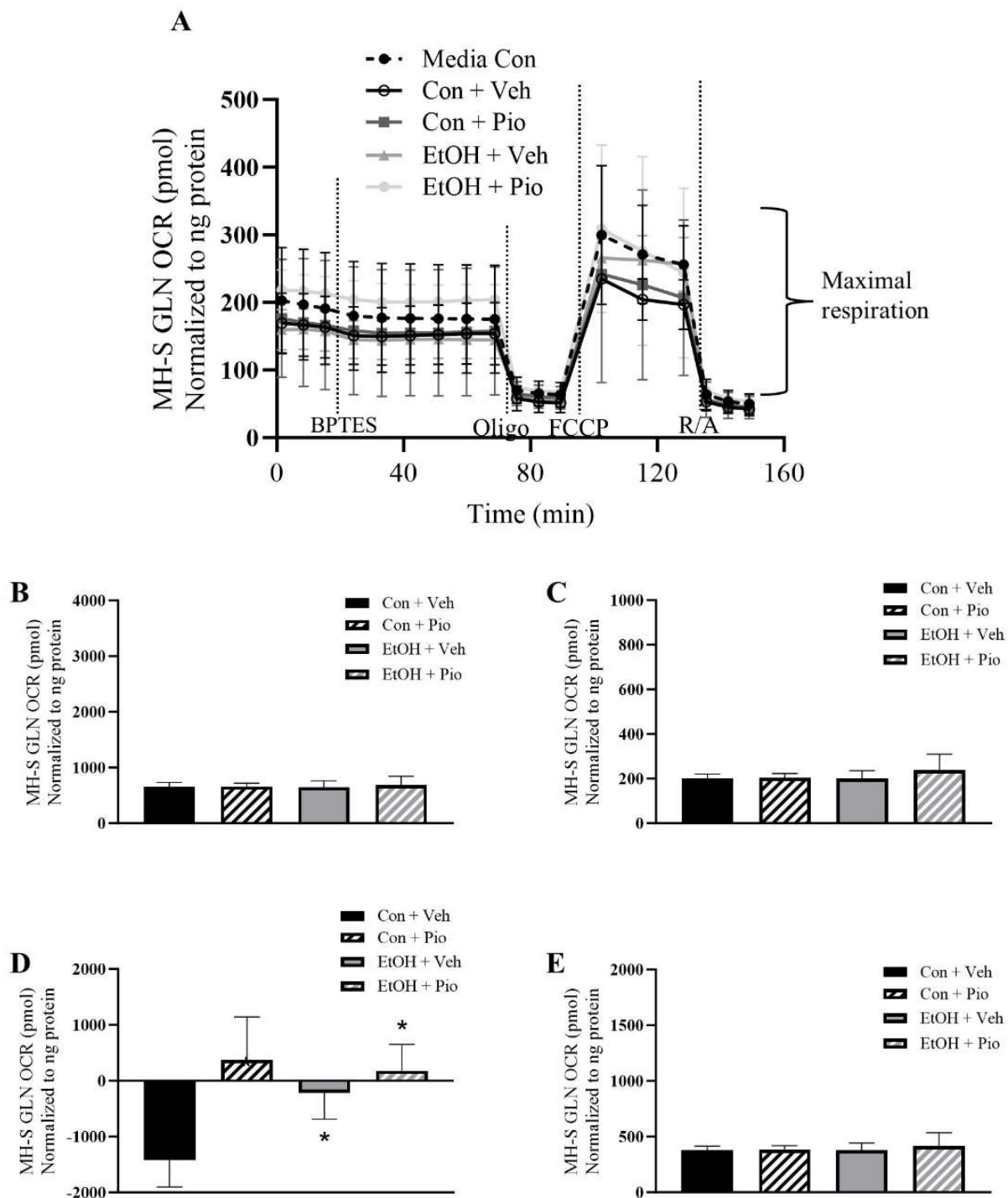


Fig. 3.2.7: Pioglitazone (PIO) and chronic ethanol (EtOH) increase ability to compensate for loss of glutamine oxidation in MH-S cells. MH-S cells were exposed to EtOH (0.08%, 72 h) \pm PIO (10 μ M last 24 h of EtOH) followed by oxygen consumption rate (OCR) measurements over time by an extracellular flux bioanalyzer before and after injections with limited media or glutamine oxidation inhibitor (3 μ M BPTES), mitochondrial complex V inhibitor (0.5 μ M oligomycin, Oligo), mitochondrial uncoupler (0.5 μ M FCCP), and mitochondrial complex I and III inhibitors (0.5 μ M rotenone / antimycin A, R/A). **A)** OCR profiles are used to calculate **B)** glutamine oxidation resulting in OCR, **C)** change in ATP-linked respiration, **D)** loss of maximal respiration, and **E)** change in spare capacity due to inhibition of glutamine oxidation. Bars represented express mean \pm SD (n=4, *p < 0.05 v. Con + Veh, One-way ANOVA with Tukey's *post-hoc*).

Fig. 3.2.8

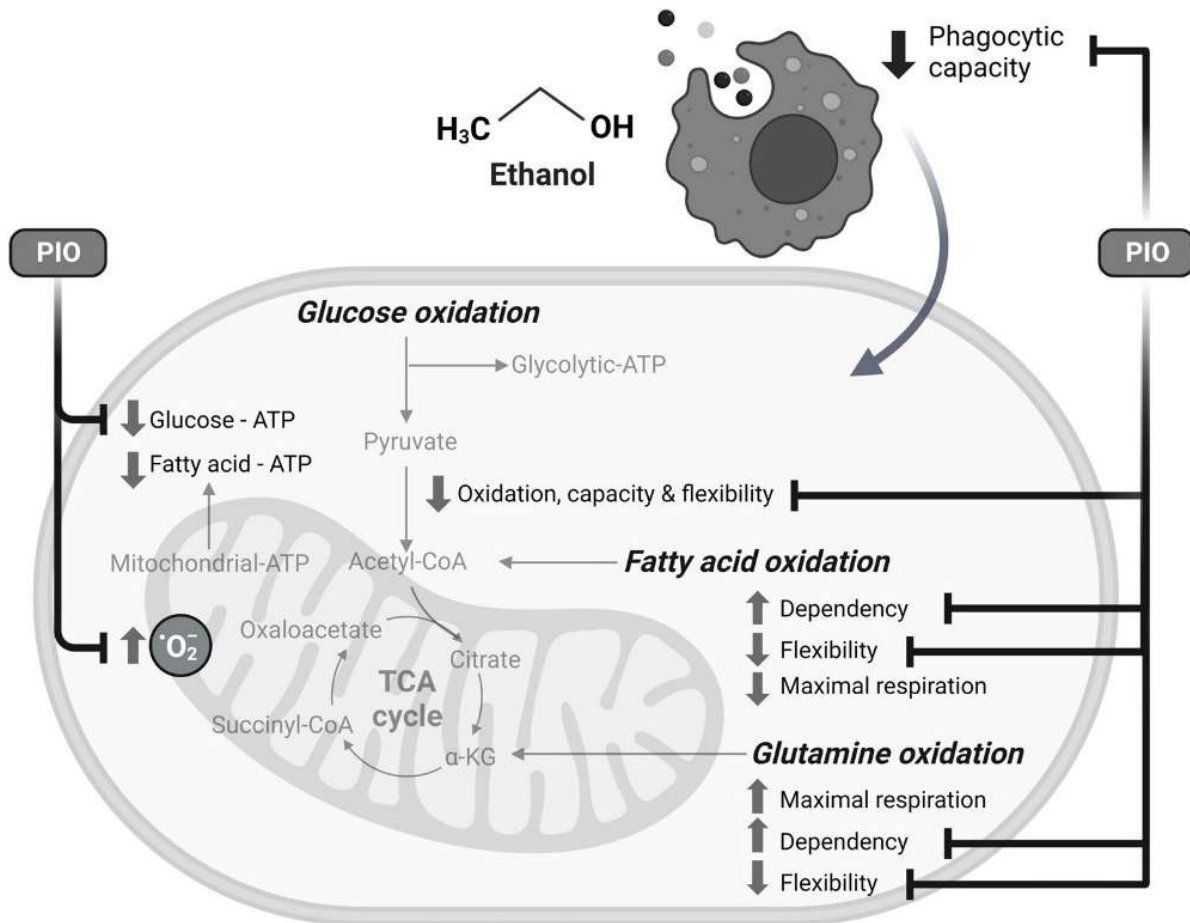
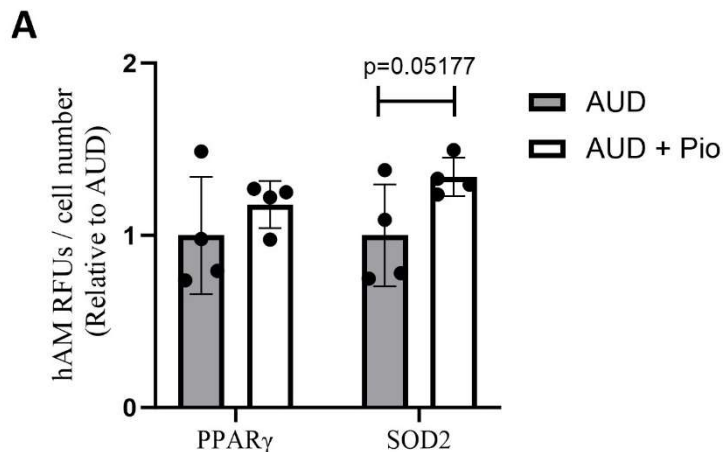


Fig. 3.2.8: Graphical summary of alcohol-induced alterations in alveolar macrophage metabolic phenotype and reversal by pioglitazone (PIO). Created using Biorender.com.

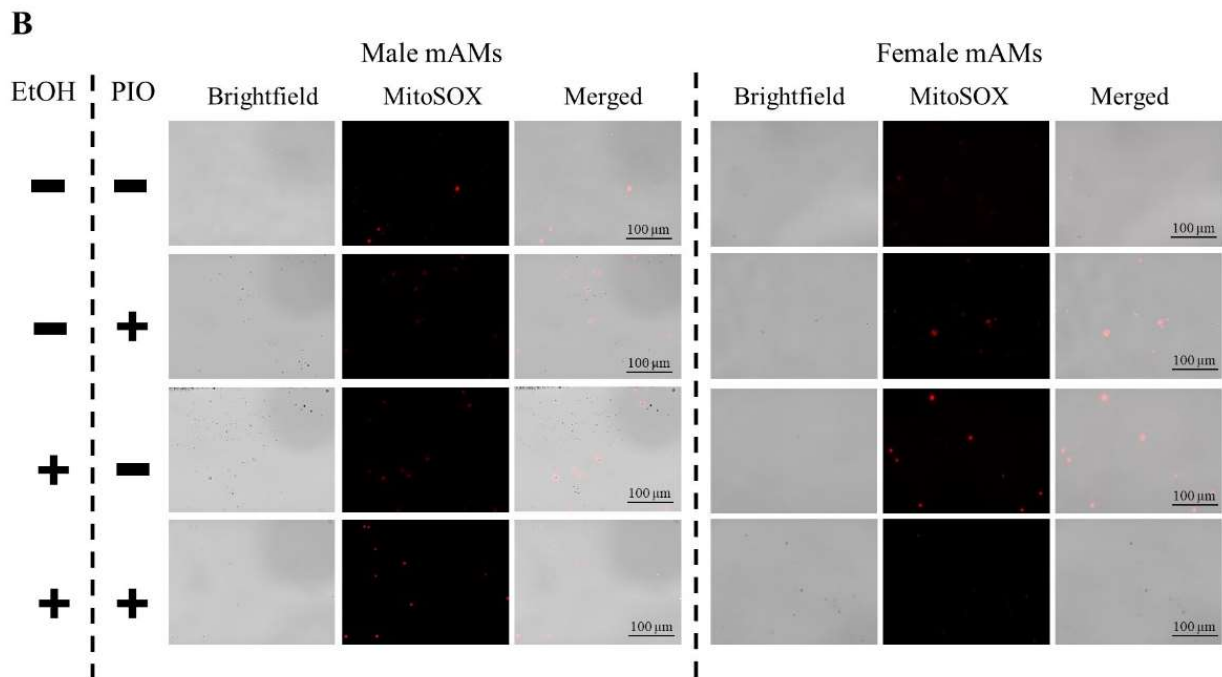
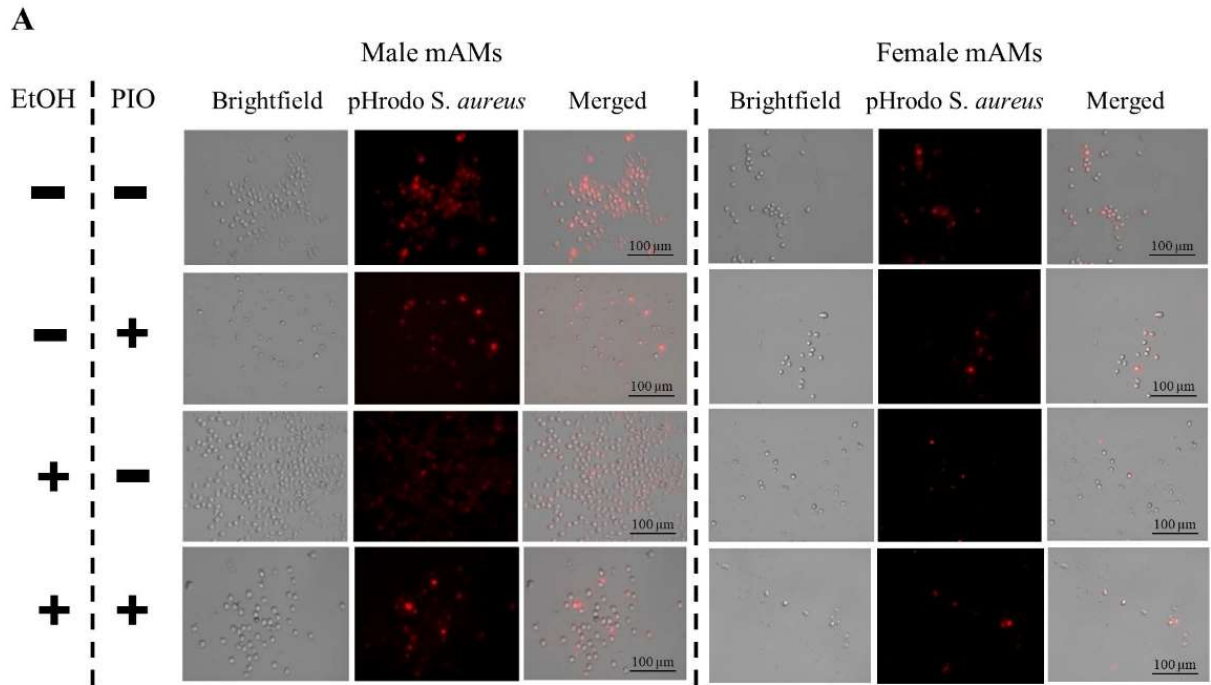
Supplemental Figures

Supplemental Fig. 3.2.1

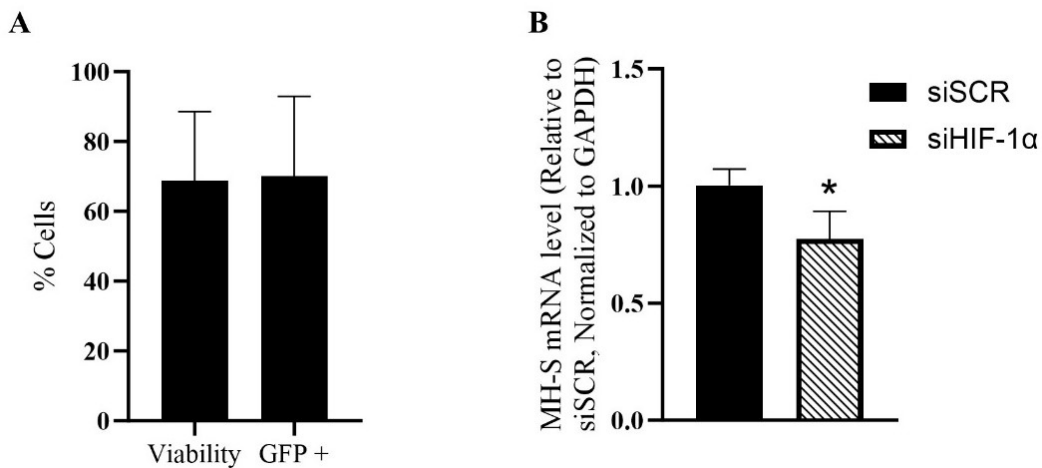


Supplemental Fig. 3.2.1: *Ex vivo* pioglitazone (PIO) in alveolar macrophages (hAM) isolated from people with alcohol use disorder (AUD) does not change proliferator-activated receptor gamma (PPAR γ) or superoxide dismutase 2 (SOD2) protein levels. A) hAMs (n=4) were isolated in sterile saline BAL fluid removal, red blood cell lysis with diH₂O, and culture in hAM media \pm PIO (AUD \pm PIO, 10 μ M, 24 h). Bars represented express mean \pm SD of RFUs / cell number of hAMs after staining for PPAR γ or SOD2, quantified from fluorescence microscopy at 20x (Students t-test).

Supplemental Fig. 3.2.2



Supplemental Fig. 3.2.2: Pioglitazone (PIO) improves phagocytic capacity and decreases mitochondrial superoxide in EtOH-fed mouse alveolar macrophages (mAMs). Representative images at 40x of mAMs isolated from EtOH-fed (20% w/v, 12 wks in drinking water) mice. **A)** Oral PIO treatment (10 mg / kg / day by oral gavage) improved phagocytic index measured via internalization of pHrodo-labeled *Staphylococcus aureus* in both male (n=9-10) and female (n=8-10) mAMs. Males had less phagocytic capacity relative to females for all groups. **B)** Oral PIO treatment decreased mitochondrial superoxide measured by MitoSOX in male (n=7-9) and female (n=4-5) mAMs.

Supplemental Fig. 3.2.3**S3: Knock down of hypoxia-inducible factor-1 alpha (HIF-1α) in MH-S cells. A)**

Viability and transfection of GFP reporter vector in MH-S using lipofectamine (n=2).

Knock down was confirmed with **B)** RT-qPCR for relative mRNA normalized to GAPDH

housekeeping gene (n=4) as previously reported. Bars represented express mean ± SD

(*p < 0.05 compared to siSCR, one-way t-test).

3.3 Conclusions

Overall, this chapter characterized AM bioenergetics under control and chronic EtOH exposure conditions. We found that EtOH induced a shift toward a glycolytic phenotype and away from mitochondrial generation of ATP using glucose and long chain fatty acids. Many of the alterations in metabolic phenotype could be reversed by decreased HIF-1 α or by activation of PPAR γ by pioglitazone. Further, loss of HIF-1 α and pioglitazone improved AM phagocytic index and oxidative stress in pre-clinical models of AUD. These results are indicative of a potential shared molecular mechanism affecting these transcription factors that potentiate a shifted AM phenotype. Since we did not see a complete reversal of the alcohol-induced AM phenotype, we hypothesize that the cause of AM dysfunction could be 1) multifaceted, and 2) upstream of altered HIF-1 α and PPAR γ activity.

A previous study by our group showed that alcohol induces oxidative stress and phagocytic dysfunction by miR-92a modification of NADPH oxidase 4, thus increasing oxidative species production⁵⁹. This suggests the importance in studying the epigenetic influence of alcohol exposure on AMs that should be further explored in the future. For example, alcohol drinking in non-human primates induced chromatin remodeling in AMs, but mechanisms of chromatin remodeling and the extent of gene transcription changes compared to alcohol-naïve AMs is still unclear. Additional to methylation and deacetylation of DNA histones which influence chromatin remodeling, post-translational modifications of proteins involved in redox homeostasis and mitochondrial metabolism are unexplored by our group. Two potential metabolic regulators that cause and can be affected by post-translational modifications include 5' adenosine monophosphate-

activated protein kinase and sirtuin 1. Both proteins are implicated in metabolic disorders¹⁸⁹, and their activity could explain the multifaceted nature of alcohol-induced disordered AM phenotype because of their many targets.

Chapter 4: Other Alterations in Pulmonary Cell Function due to Changes in Metabolism

Considering the substantial alveolar macrophage (AM) metabolic derangements observed during chronic alcohol use, we suspected that metabolism pathways beyond energy production could contribute toward immune cell deficiency. Since it is not yet known if reversing AM oxidative stress and metabolic phenotype improves AM function or decreases the risk of disease in people with alcohol use disorders (AUDs), we aimed to identify other targetable pathways that could influence AM function. Hyaluronic acid (HA) is an extracellular matrix polysaccharide that most cell types synthesize, but alveolar epithelial cells and resident macrophages also expel HA in the alveolar space. The hexosamine biosynthetic pathway, which branches from glycolysis (**Figure 4.1**) makes up the building blocks of HA. After HA synthesis by HA synthases (HAS) into high molecular weight HA (HMW HA), HA can signal to several different binding proteins referred to here as either HA binding proteins or hyaladherins. However, fragmentation of HMW HA into low molecular weight HA (LMW HA), or loss of fragmentation, can result in alternative signaling patterns to influence cellular functions (**Figure 4.2**). Although evidence suggests that epithelial, smooth muscle cell, and macrophage functions are each negatively influenced by oxidative stress and disordered extracellular matrix deposition, the influence of HA on these cell types during disease states is still unknown.

In chronic respiratory diseases, levels of LMW HA and leukocytes remain elevated, inflammation persists, and resident cells do not clear respiratory infections quickly, suggesting a possible pathological mechanism for prolonged bacterial

pneumonia. There is a lack of knowledge regarding how HAS, hyaluronidases (Hyal), or oxidative fragmentation factor into bacterial pneumonia clearance and if these pathways are valid therapeutic targets to ease persistent infections. Further, a co-author publication reveals a novel mechanism for altered HA dynamics in pulmonary vascular cells that should be investigated in other cells with similar phenotypes, like in AMs exposed to chronic alcohol.

This chapter includes a summary of my contributions to the alcohol and immunology field published in two conference reviews (Ch. 4.1), preliminary data used for those reviews, a review on how HA binding proteins may be involved in bacterial pneumonia pathogenesis, and a mechanism of HMW HA hyper synthesis during pulmonary hypertension that could be investigated in future studies in the context of chronic alcohol exposure.

Figure 4.1

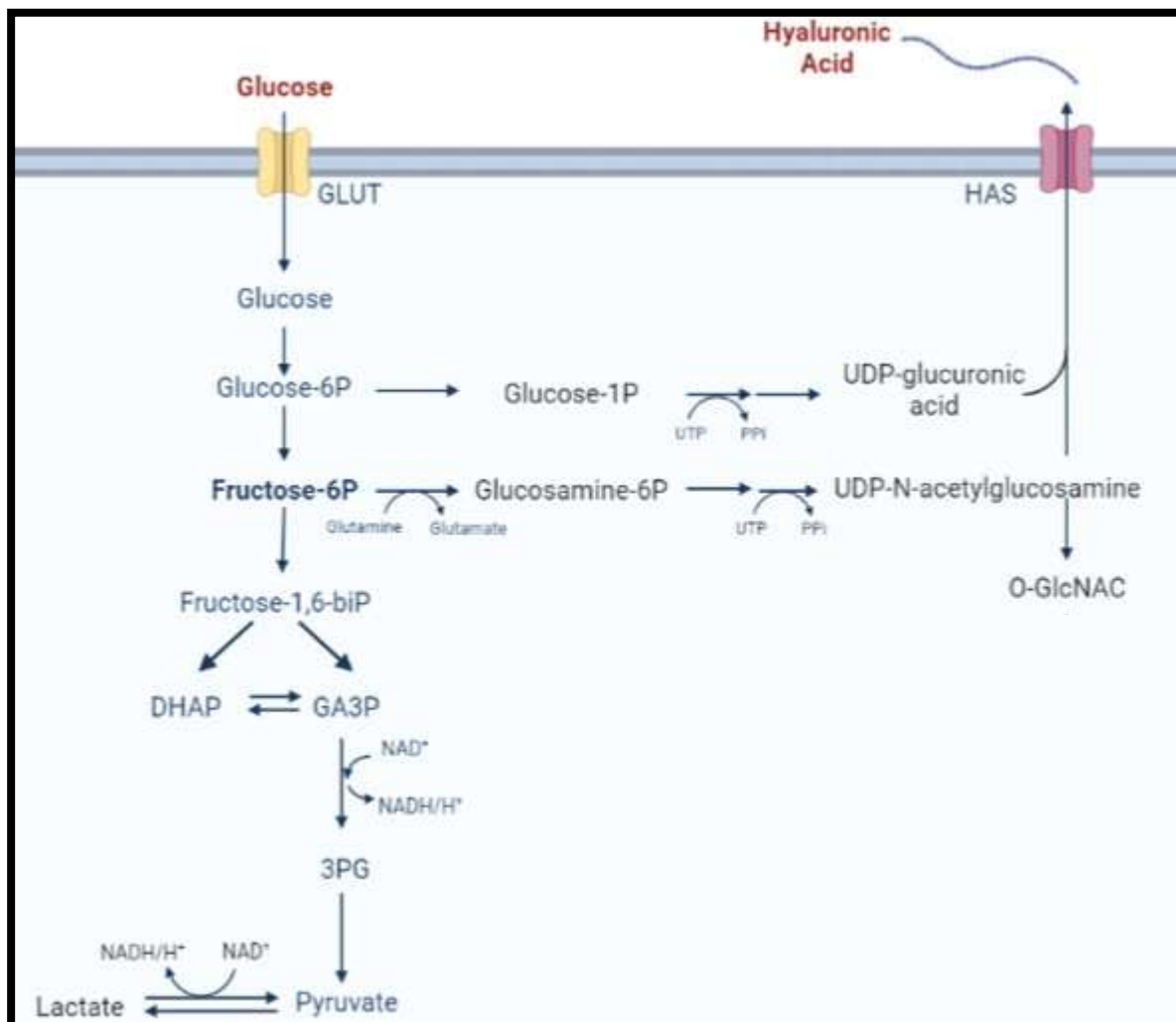


Figure 4.1: Simplified pathway of hyaluronic acid (HA) production from the hexosamine biosynthetic pathway. UDP-glucuronic acid and UDP-N-acetylglucosamine synthesized from glucose-6-phosphate (Glucose-6P) and fructose-6-phosphate (Fructose-6P), respectively. UDP-N-acetylglucosamine (UDP-GlcNAC) can modify proteins by O-GlcNAC, or for synthesis HA via HA synthase (HAS).

Figure 4.2

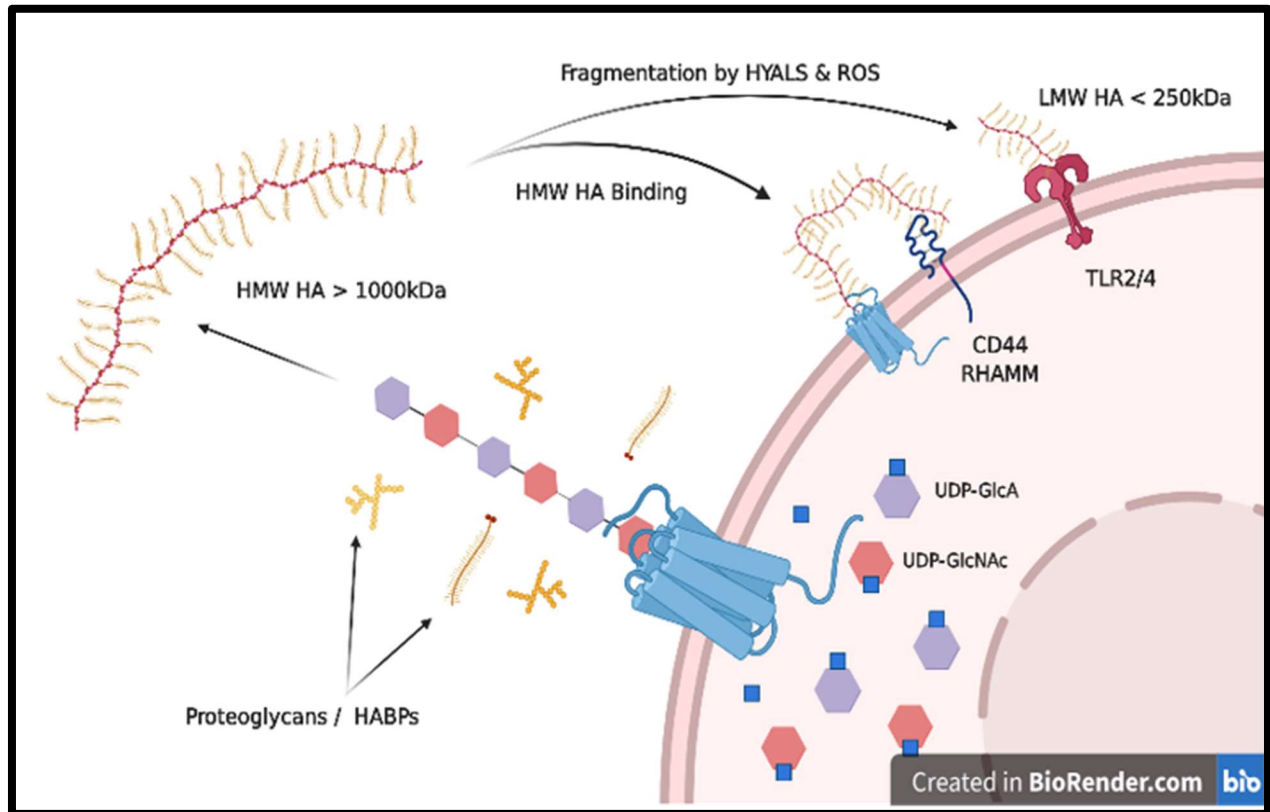


Figure 4.2: Simplified illustration of high and low molecular weight hyaluronic acid (HA) synthesis, fragmentation, and signaling. Several factors influence HA signaling including binding of proteoglycans, hyaluronic acid binding proteins (HABPs), and fragmentation by hyaluronidases (HYALs) or reactive oxygen species (ROS). Depending on the HA modification by other proteins or by changes in molecular weight, HA binds to alternate cell membrane proteins. In general, high molecular weight HA (HMW HA) signals through CD44 and Receptor for HA-mediated motility (RHAMM) while low molecular weight HA (LMW HA) signals through toll like receptors 2 or 4 (TLR2/4).

4.1 Hyaluronic Acid Dynamics Affect Alveolar Macrophage Mitochondrial and Phagocytic Function

Based on the relevant literature, I applied for a National Institute on Alcohol and Alcoholism (NIAAA) Ruth L. Kirschstein Predoctoral Individual National Research Service Award (F31) proposing to measure ethanol-induced changes in HA signaling and metabolism. NIAAA funded this grant proposal, and I started working on the proposed studies in September of 2021. The objective of the study was to investigate the underlying mechanisms of EtOH-induced AM phagocytic dysfunction due to intracellular and extracellular oxidative stress. These studies focused on EtOH-induced redox imbalance and its effect on HA synthesis, degradation, and inflammatory signaling in the AM. Mechanistic studies explored if perturbed HA synthesis, degradation, or signaling impacted mitochondrial function and energy metabolism. Our overarching hypothesis was that EtOH-induced oxidative stress and altered MT function impair AM phagocytic capabilities by modulating HA dynamics. I reported my findings from the course of these studies in multiple published reviews (PMC9974783 (Chapter 1 of this dissertation), PMC9994264 (Chapter 4.2.1), and PMC10330898 (Chapter 4.2.2)), and will be used as preliminary data for future manuscript generation.

4.1.1 Excerpt from: New Insights into the Mechanism of Alcohol-Mediated Organ Damage via its Impact on Immunity, Metabolism, and Repair Pathways: A Summary of the 2021 Alcohol and Immunology Research Interest Group (AIRIG) Meeting

Shanawaj Khair^{a,b,c,d}, Lisa A. Brennere^{f,g,h}, Michael Koval^{i,j}, Derrick Samuelson^k, Jessica A. Cucinello-Regland^l, Paige Anton^m, Mariann R. Pianoⁿ, Liz Simon^o, Kathryn Crotty^p, Farah Shariehq^r, Jeffrey B. Travers^s, Vaibhav Singh^t, Abigail Cannon^v, Adam Kim[†], Rebecca L. McCullough^m, Samantha M. Yeligar^p, Todd A. Wyatt^{k,u}, Rachel H. McMahan^{a,b}, Mashkoor A. Choudhry^{v,w}, Elizabeth J. Kovacs^{a,b,c,d,e*}

^aDepartment of Surgery, University of Colorado Denver, Anschutz Medical Campus, Aurora, CO, United States

^bAlcohol Research Program, University of Colorado Denver, Anschutz Medical Campus, Aurora, CO, United States

^cMolecular Biology Graduate Program, University of Colorado Denver, Anschutz Medical Campus, Aurora, CO, United States

^dMedical Scientist Training Program, University of Colorado Denver, Anschutz Medical Campus, Aurora, CO, United States

^eVA Rocky Mountain Mental Illness Research Education and Clinical Center, Rocky Mountain Regional Veterans Affairs (VA) Medical Center, Aurora, CO, United States

^fDepartment of Physical Medicine and Rehabilitation, University of Colorado Anschutz Medical Campus, Aurora, CO, United States

^gDepartment of Psychiatry and Neurology, University of Colorado Anschutz Medical Campus, Aurora, CO, United States

^hMilitary and Veteran Microbiome: Consortium for Research and Education, Aurora, CO, United States

ⁱDivision of Pulmonary, Allergy, Critical Care and Sleep Medicine, Department of Medicine, Emory University School of Medicine, Atlanta, GA, United States

^jDepartment of Cell Biology, Emory University School of Medicine, Atlanta, GA, United States

^kDepartment of Internal Medicine, University of Nebraska Medical Center, Omaha, NE, United States

^lDepartment of Physiology, Alcohol and Drug Abuse Center of Excellence, Louisiana State University Health Sciences Center, New Orleans, LA, United States

^mDepartment of Pharmaceutical Sciences, University of Colorado Denver, Anschutz Medical Campus, Aurora, CO, United States

ⁿCenter for Research Development and Scholarship, Vanderbilt University School of Nursing, Nashville, TN, United States

^oDepartment of Physiology, Comprehensive Alcohol HIV/AIDs Research Center, Louisiana State University Health Sciences Center, New Orleans, LA, United States

^pDivision of Pulmonary, Allergy, Critical Care, and Sleep Medicine, Department of Medicine, Atlanta Veterans Affairs Health Care System, Decatur, GA, United States

^qDepartment of Orthopedic Surgery and Rehabilitation, Loyola University Medical Center, Maywood, IL, United States

^rAlcohol Research Program, Loyola University Chicago Stritch School of Medicine, Maywood, IL, United States

^sWright State University, Dayton VAMC, Dayton, OH, United States

^tDepartment of Inflammation and Immunity, Cleveland Clinic, Cleveland, OH, United States

^uVeterans Affairs Nebraska-Western Iowa Health Care System, Omaha, NE, United States

^vAlcohol Research Program, Burn and Shock Trauma Research Institute, Department of Surgery, Loyola University Chicago Health Sciences Campus, Maywood, IL, United States

^wIntegrative Cell Biology Program, Loyola University Chicago Health Sciences Campus, Maywood, IL, United States

Full Citation: Khair, Shanawaj et al. “New insights into the mechanism of alcohol-mediated organ damage via its impact on immunity, metabolism, and repair pathways: A summary of the 2021 Alcohol and Immunology Research Interest Group (AIRIG) meeting.” *Alcohol (Fayetteville, N.Y.)* vol. 103 (2022): 1-7.

doi:10.1016/j.alcohol.2022.05.004

Funding: The authors would like to thank the National Institute on Alcohol Abuse and Alcoholism (NIAAA) and the Alcohol Research Programs at the University of Colorado Anschutz Medical Campus and Loyola University Chicago for financial support for the meeting. Support was also provided by the National Institutes of Health (NIH) under award numbers R13AA020768 (EJK/MAC), R21 AA026295 (EJK), R01 AT010005 (LAB), P50 AA024333 (LEN), U01AA026938 (LEN), R01 AA027456 (LEN), R01 AA025854 (MK), R01AA015566 (SE), R01AA025996 (SE), R01AA015566 (MR), U01AA013498 (MR), R00-AA026336 (DS), R21-AA021555 (JJC), R21 AA021225

(JJC), T32 GM08750 (MAC), T32 AA013527 (MAC), F31 AA028147 (JE), R01 HL062996 (JBT), and R01 ES031087 (JBT). The following authors were supported by grants from Veterans Affairs: I01 BX004335 (EJK), 1 I21 RX002232 (LAB), I01 BX005413 (TAW), IS1 BX004790 (DS), and 510 BX000853 (JBT). TAW is the recipient of a Research Career Scientist Award (IK6 BX003781) from the Department of Veterans Affairs. The authors would like to thank Dr. Vivian Gahtan, Chair of Loyola University Chicago's Department of Surgery, for supporting the meeting. In addition, we acknowledge the help of Renita Alis and Kim Stubbs from Loyola University Chicago and Debra Sartain and Victoria Bress from University of Colorado Denver Anschutz Medical Campus for logistical support. Lastly, we are grateful to Dr. H. Joe Wang from NIAAA for attending the scientific sessions remotely. This content is solely the responsibility of the authors and does not necessarily represent the official views of the NIH.

Abstract

On November 19th, 2021, the annual Alcohol and Immunology Research Interest Group (AIRIG) meeting was held at Loyola University Chicago Health Sciences Campus in Maywood, Illinois. The 2021 meeting focused on how alcohol misuse is linked to immune system derangements, leading to tissue and organ damage, and how this research can be translated into improving treatment of alcohol-related disease. This meeting was divided into three plenary sessions: the first session focused on how alcohol misuse affects different parts of the immune system, the second session presented research on mechanisms of organ damage from alcohol misuse, and the final session highlighted research on potential therapeutic targets for treating alcohol-mediated tissue damage. Diverse areas of alcohol research were covered during the meeting, from alcohol's effect on pulmonary systems and neuroinflammation to epigenetic changes, senescence markers, and microvesicle particles. These presentations yielded a thoughtful discussion on how the findings can lead to therapeutic treatments for people suffering from alcohol-related diseases.

Introduction

Alcohol misuse is a deadly yet preventable cause of death; annually, 95,000 people die in the United States from alcohol misuse, and 3 million people die worldwide¹⁶. Alcohol misuse is defined by excessive daily consumption, total consumption, or both, specifically daily consumption of more than 4 drinks per day for men or more than 3 drinks per day for women, or excess total consumption of more than 14 drinks per week for men or more than 7 drinks per week for women¹⁶. This disorder can lead to chronic health consequences, such as liver and digestive diseases, and increased susceptibility to infectious diseases, cancer, and cognitive decline, resulting in more than \$249 billion in economic costs in the United States¹⁷. While much progress has been made in investigating how alcohol misuse leads to these diseases, many questions remain unanswered surrounding alcohol-mediated tissue and organ injury and their impact on immune and inflammatory pathways. Thus, the 2021 AIRIG meeting was convened to highlight recent work on alcohol's impact on inflammation and the immune system, and the mechanisms by which this leads to organ damage.

Alcohol impairs alveolar macrophage mitochondrial bioenergetics and phagocytosis through changes in hyaluronic acid dynamics (Kathryn Crotty, PhD candidate in the laboratory of Dr. Samantha M. Yeligar, Emory University)

Kathryn Crotty, from Dr. Samantha Yeligar's laboratory, discussed their recent research exploring the role of the mechanism of alcohol-induced alveolar macrophage impairment. Excessive alcohol use augments the risk of pneumonia and acute respiratory distress syndrome, leading to increased morbidity and mortality. Alveolar macrophages (AM) are responsible for engulfing and clearing pathogens in the lower respiratory tract. However, *in vivo* mouse models have demonstrated that alcohol-induced mitochondria redox imbalance impairs the ability of AM to phagocytose pathogens^{50,59}. Oxidative stress also alters the molecular dynamics of the extracellular matrix polysaccharide, hyaluronic acid (HA), which has been implicated in pulmonary immunity and inflammation⁵⁶. *In vitro* experiments were performed using the MH-S mouse AM cell line, treated with or without 0.08% ethanol or 25 nM HA for 3 days. To delineate how ethanol affects HA, expression of key HA-binding and signaling proteins was measured by qRT-PCR and western blotting techniques. Ethanol-exposed AMs showed increased expression of mRNA and protein for both HA synthase 2 (HAS2), which is involved in high molecular weight HA (HMW HA, >1000 kD) synthesis, and cluster of differentiation 44 (CD44), which is involved in HA internalization and recycling. Mitochondrial bioenergetics and fuel flexibility were measured using an extracellular flux bioanalyzer. HMW HA impaired mitochondrial bioenergetics compared to untreated and low molecular weight HA- (LMW HA, <200 kD) treated MH-S cells. Ethanol and HMW HA altered basal respiration, mitochondria-linked ATP respiration, maximal respiration,

and spare respiratory capacity in MH-S cells. Overall, ethanol-induced changes in HA could alter mitochondrial bioenergetics and fuel metabolism through disrupted HA binding and signaling pathways. These data support modified HA dynamics as a mechanism for increased risk of respiratory infections in people with alcohol use disorders. Identifying the underlying mechanisms of HA dysregulation could potentially uncover novel targets for therapeutic intervention in alcohol-induced pulmonary immune dysfunction.

4.1.2 Excerpt from: Alcohol and Immunology: Mechanisms of Multi-Organ Damage. Summary of the 2022 Alcohol and Immunology Research Interest Group (AIRIG) Meeting

Rachel H. McMahan ^{a,b,*}, Paige Anton ^{b,c}, Leon G. Coleman ^d, Gail A.M. Cresci ^e, Fulton T. Crews ^d, Kathryn M. Crotty ^{f,g}, Marisa E. Luck ^h, Patricia E. Molina ⁱ, Vidula Vachharajani ^j, Joanne Weinberg ^k, Samantha M. Yeligar ^{f,g}, Mashkoo A. Choudhry ^h, Rebecca L. McCullough ^{b,c}, Elizabeth J. Kovacs ^{a,b,l,m}

^a Division of GI, Trauma, and Endocrine Surgery, Department of Surgery, University of Colorado Anschutz Medical Campus, Aurora, CO, United States

^b Alcohol Research Program, University of Colorado Anschutz Medical Campus, Aurora, CO, United States

^c Department of Pharmaceutical Sciences, University of Colorado Anschutz Medical Campus, Aurora, CO, United States

^d Department of Pharmacology, Bowles Center for Alcohol Studies, University of North Carolina at Chapel Hill School of Medicine, Chapel Hill, NC, United States

^e Departments of Pediatric Gastroenterology, Hepatology & Nutrition, Cleveland Clinic Children's Hospital and Inflammation & Immunity, Lerner Research Institute, Cleveland Clinic, Cleveland, OH, United States

^f Division of Pulmonary, Allergy, Critical Care and Sleep Medicine, Department of Medicine, Emory University, Atlanta, GA, United States

^g Atlanta Veterans Affairs Health Care System, Decatur, GA, United States

^h Alcohol Research Program, Burn & Shock Trauma Research Institute, Department of Surgery, Integrative Cell Biology Program, Stritch School of Medicine, Loyola University Chicago Health Sciences Division, Maywood, IL, United States

ⁱ Department of Physiology and Comprehensive Alcohol Research Center, Louisiana State University Health Sciences Center, New Orleans, LA, United States

^j Department of Inflammation and Immunity, Critical Care Medicine, Respiratory Institute, Lerner Research Institute, Cleveland Clinic Lerner College of Medicine of Case Western Reserve University, Cleveland, OH, United States

^k Department of Cellular & Physiological Sciences, Faculty of Medicine, University of British Columbia, Vancouver, British Columbia, Canada

^l Molecular Biology Graduate Program, University of Colorado Denver, Anschutz Medical Campus, Aurora, CO, United States

^m Rocky Mountain Regional Veterans Affairs Medical Center, Aurora, CO, United States

Full Citation: McMahan, Rachel H et al. "Alcohol and Immunology: Mechanisms of multi-organ damage. Summary of the 2022 alcohol and Immunology research interest group (AIRIG) meeting." *Alcohol (Fayetteville, N.Y.)* vol. 110 (2023): 57-63.

doi:10.1016/j.alcohol.2023.04.002

Funding: The authors would like to thank the National Institute on Alcohol Abuse and Alcoholism (NIAAA) and the Alcohol Research Programs at the University of Colorado Anschutz Medical Campus and Loyola University Chicago for financial support for the meeting. The authors would also like to thank the Society for Leukocyte Biology for hosting this satellite AIRIG meeting. Support was also provided by the National

Institutes of Health (NIH) under award numbers: R13 AA020768 (EJK/MAC), T32 AA007577 (PEM), P60AA009803 (PEM), R01AA026086 (SMY), R01 AA028043 (GAMC), R01 AA022460 (JW), U01 AA026108 (JW), T32 AA013527 (MAC/MEL), F30 DK123929 (MEL), K08 AA024829 (LGC), R01 AA028924 (LGC), R21 AA028599 (LGC), T32 ES029074 (PA), F31 AA030213 (PA), R00 AA025386 (RLM), T32 GM008602 (RAH), F31 AA029938 (KMC), R01 AA028763 (VV), R01 GM099807 (VV), U24 AA020024 (FTC), U01 AA020023 (FTC), U54 AA030463 (FTC), R01 AA015731 (MAC), R01 GM128242 (MAC), R01 AG018859 (EJK), R35 GM131831 (EJK), R21 AA026295 (EJK). EJK is the recipient of a Veterans Affairs Merit Award (I01 BX004335) from the Department of Veterans Affairs. LGC's research is supported by the Bowles Center for Alcohol Studies.

Abstract

On October 26th, 2022 the annual Alcohol and Immunology Research Interest Group (AIRIG) meeting was held as a satellite symposium at the annual meeting of the Society for Leukocyte Biology in Hawaii. The 2022 meeting focused broadly on the immunological consequences of acute, chronic, and prenatal alcohol exposure and how these contribute to damage in multiple organs and tissues. These included alcohol-induced neuroinflammation, impaired lung immunity, intestinal dysfunction, and decreased anti-microbial and anti-viral responses. In addition, research presented covered multiple pathways behind alcohol-induced cellular dysfunction, including mitochondrial metabolism, cellular bioenergetics, gene regulation, and epigenetics. Finally, the work presented highlighted potential biomarkers and novel avenues of treatment for alcohol-induced organ damage.

Hyaluronic acid characterization in alveolar macrophages during chronic alcohol use (Kathryn Crotty, PhD student in the laboratory of Dr. Samantha Yeligar, Emory University/Atlanta VA Health Care System).

Alcohol misuse increases the risk of pneumonia and acute respiratory distress syndrome, leading to increased morbidity and mortality rates⁴. AMs are responsible for clearing pathogens from the lower respiratory tract, but alveolar macrophages isolated from people with alcohol use disorders have phagocytic and mitochondrial dysfunction. It has been shown that the molecular dynamics of the extracellular matrix polysaccharide, hyaluronic acid (HA), and its signaling proteins are impacted by alcohol⁵⁶. *In vitro* experiments modeling acute and chronic alcohol consumption were performed using the MH-S mouse alveolar macrophage cell line or MLE-12 mouse alveolar epithelial cells. Compared to vehicle treated MH-S and MLE-12 cells, treatment with 0.08% ethanol decreased hyaluronic acid release at 24 h in both cell types, but was not sustained at 72 h. Additionally, protein levels of HA synthase 2, a major contributor to high molecular weight (>1000 kD) HA production in the lung, were unchanged at 24 h but increased at 72 h. C57BL/6J mice were given regular drinking water or 20% w/v ethanol in water for 12 weeks, then sacrificed for bronchoalveolar lavage, alveolar macrophage, alveolar epithelial type II cell, and lung tissue isolation. At this chronic alcohol exposure time point, only alveolar epithelial cells had increased HA release compared to control littermates. Finally, high molecular weight hyaluronic acid or vehicle was added to *in vitro* MH-S cell media for 72 h to quantify alterations in phagocytic capacity by *S. aureus* internalization or mitochondrial bioenergetic profile (basal respiration, mitochondria-linked ATP respiration, maximal respiration, and spare

respiratory capacity). Treatment with high molecular weight HA or ethanol reduced phagocytosis and mitochondrial bioenergetics compared to vehicle-treated cells. These studies demonstrate that changes in hyaluronic acid dynamics due to alcohol misuse impair AM phagocytic and mitochondrial function, and future studies will focus on elucidating how alcohol modifies the hexosamine biosynthetic pathway to disturb both hyaluronic acid metabolism and mitochondrial function to impact lung immunity.

The 2022 AIRIG meeting showcased a broad collection of talks focusing on alcohol's diverse effects on the inflammatory response in multiple tissues and organs, including neuroinflammation, impaired lung immunity, intestinal dysfunction, and heightened susceptibility to both viral and bacterial infection (**Table 4.1.2**).

Table 4.1.1: Summary of new findings related to alcohol-induced organ damage.

Table 1. Summary of new findings related to alcohol-induced organ damage.

Organ/Tissue	Effects of Alcohol
Immune Cells	↑SIRT2→ ↓Macrophage phagocytosis→ ↓Bacterial clearance ↓Myoblast differentiation, ↓Immune cell energetics→ ↑Viral replication
Brain	↑HMGB1, altered EV phenotype→ epigenetic modifications→ neuroimmune activation, ↓neurogenesis ↑NLRP3 activation in advanced age
Intestine	↓SCFA, ↓IL-27→ ↑Intestinal inflammation, ↓Intestinal barrier function→ ↑Neuroinflammation (via gut–brain axis)
Lung	Dysregulated Hyaluronic acid, ↑Oxidative Stress, ↓Mitochondrial Respiration→ ↓Alveolar macrophage function
Fetus	Altered fetal programming→ Neurodevelopmental delay, Unique cytokine profiles, ↑White blood cells, ↑Multi-organ adverse health outcomes

Abbreviations: SIRT2, deacetylase sirtuin 2; HMGB1, high mobility group box 1; EV, extracellular vesicle; NLRP3, NLR family pyrin domain containing 3; SCFA, short chain fatty acids; IL-27, interleukin (IL)-27; HA, Hyaluronic acid.

Summary

The 2021 and 2022 AIRIG meetings highlighted diverse work on alcohol's impact on various pathways, leading to cellular and tissue damage in multiple organs. Taken together, these data demonstrate how alcohol misuse impacts a wide variety of pathways in tissue and organ homeostasis, offering insight into several pathways for future studies. Overall, the meeting highlighted important advancements in our understanding of the widespread adverse effects of alcohol while underscoring important areas for future research. My contributions to these meetings included preliminary data indicating that dysregulated HA metabolism in the lung contributes toward a disrupted AM phenotype. Previous studies had not identified HA metabolism or signaling as a major influencer of AM phagocytosis or mitochondrial bioenergetics. Future studies may focus on furthering our understanding of these underlying mechanisms and further characterizing how alcohol-induced lung oxidative stress plays a role in HA metabolism that that could in turn influence AM phagocytic capacity.

4.2 Preliminary Data: Chronic Alcohol Exposure Increases Lung Hyaluronic Acid

To test our hypothesis that ethanol impacts HA metabolism and that differences in HA metabolism result in altered AM mitochondrial and phagocytic function, we used established murine *in vitro* and *in vivo* chronic EtOH consumption models to determine how HA modulates MT bioenergetics and AM phagocytosis, and how EtOH modulates HA dynamics. The role of HA in EtOH-induced AM dysfunction is unexplored and significant in delineating AM pathobiology relevant to EtOH-induced changes in cell metabolism. These studies could shift scientific and therapeutic paradigms by identifying perturbed HA dynamics as a mechanism of AM dysfunction. This project was an invaluable training opportunity and provided key insights into lung HA dynamics during chronic alcohol exposure.

Abstract

Introduction: Hyaluronic acid (HA) is a repeating disaccharide of variable molecular weight involved in structure, tissue repair, and immune defense all over the body. The building blocks of HA originate from the glycolytic pathway, however chronic alcohol exposure increases glycolysis in AMs, and this disrupted cellular metabolism has been linked to impaired AM function.

Methods: In lungs from peroxisome proliferator-activated receptor gamma (PPAR γ) knock out mice and a murine AM cell line, MH-S, qRT-PCR and western blot were used to measure levels of mRNA and proteins involved in HA metabolism and mitochondrial dynamics. ELISA-like assay was used on MH-S cells, lung cells from a mouse model of chronic EtOH ingestion, and bronchoalveolar lavage samples obtained from participants with AUDs to determine HA concentrations. Additionally, the effect of varying concentrations and molecular weights of HA on MH-S was assessed to investigate HA effect on AM MT bioenergetics, as measured using an extracellular flux bioanalyzer. Flow cytometry was used to measure AM phagocytosis of *Staphylococcus aureus*.

Results: EtOH and loss of PPAR γ similarly alter mRNAs related to mitochondrial function and HA metabolism (PPAR γ , TFAM, MFN2, DRP1, TLR2, and HAS2), and ethanol increases HAS2 and CD44 protein levels *in vitro*. EtOH increased HA concentration in bronchoalveolar lavage fluid and alveolar epithelial type II cells from mice fed EtOH in their drinking water and *in vitro* in MH-S cells exposed to chronic EtOH. AMs from mice and MH-S cells produced low concentrations of HA and HA concentration did not change due to EtOH in these cells. MH-S cells exhibit decreased MT respiration and phagocytic capacity in response to high concentrations of HA or

when exposed to high molecular weight HA, while lower concentration of low molecular weight HA increased phagocytic capacity.

Conclusions: Alcohol changes HA dynamics in AMs, and similar changes impair AM function independent of alcohol. One mechanism of impaired phagocytic capacity during chronic EtOH exposure may be through increased high molecular weight HA synthesis via increased glycolysis-derived precursors. Further studies are necessary to clarify the underlying mechanisms of increased HA synthesis and what role HA molecular weight plays during chronic alcohol misuse.

Introduction

A pattern of excessive alcohol consumption, termed alcohol use disorder (AUD)¹⁹⁰, is critical to study because alcohol misuse is linked to over 5 million annual deaths globally¹⁵, in part due to an increased risk of respiratory infections⁴² and acute respiratory distress syndrome (ARDS)⁴. Innate immune defense by alveolar macrophages (AM) in the lower respiratory tract is critical for the prevention of pulmonary diseases¹⁹¹, but alcohol misuse impairs the AM ability to phagocytose pathogens^{10,39,46,47} via increased cellular oxidative stress⁴⁸, mitochondrial (MT) redox imbalance^{49,50}, and impaired MT bioenergetics⁵⁹. Yet, the molecular mechanisms underlying impaired AM phagocytosis by alcohol misuse remains a fertile area for investigation^{10,46} and comprise the primary objective of this project: to elucidate if aberrant HA dynamics is a mechanism of alcohol-induced impairments in AM MT bioenergetics and phagocytosis.

AMs synthesize, degrade, and signal with the extracellular matrix polysaccharide hyaluronic acid (HA)¹⁹²⁻¹⁹⁴, but oxidant stress perturbs HA interactions with AM membrane proteins^{57,58,195} through altered HA molecular dynamics. High molecular weight HA (HMW HA, >1,000 kD) is produced predominantly by HA synthases (HAS) on the surface of alveolar epithelial type II cells in the uninflamed lung¹⁹⁶⁻¹⁹⁹. HA fragmentation occurs due to hyaluronidase (Hyal) activity²⁰⁰ and reactive oxygen species (ROS) during inflammation^{57,58} that non-specifically cleave glycosidic bonds within the polysaccharide²⁰⁰. In general, low molecular weight HA (LMW HA, <200 kD) signaling through HA binding proteins is pro-inflammatory, while HMW HA signaling is anti-inflammatory^{201,202}.

Chronic respiratory diseases, including ARDS, increase HA synthesis and LMW HA levels in the bronchoalveolar lavage (BAL) fluid of patients⁵⁶. Further, inflammation increases LMW HA levels^{199,201,203}, including during bacterial pneumonia^{204,205}, and decreases concomitantly with reductions in levels of leukocytes and inflammatory mediators during repair after lung injury^{199,206,207}. In mesenchymal stem cells, HA increases MT mass, MT DNA copy number, and MT biogenesis²⁰⁸, but little is known about how HA dynamics affect AM MT health markers or bioenergetics. HA uptake, HA degradation²⁰⁹⁻²¹¹, and activation of multiple signaling pathways in AM¹⁹³⁻¹⁹⁵ require HA binding proteins: CD44, receptor for HA mediated motility (RHAMM) and toll-like receptors 2 (TLR2) and 4 (TLR4). Interestingly LMW HA treatment in Kupffer cells isolated from ethanol (EtOH)-fed mice normalizes TLR signaling^{212,213} despite LMW HA having pro-inflammatory properties in other studies. Yet, LMW HA normalization of TLR signaling may indicate a therapeutic potential of targeting HA dynamics in treating alcohol-associated liver disease.

One proposed mechanism of EtOH-induced oxidative stress in AM includes loss of peroxisome proliferator-activated receptor gamma (PPAR γ) activity^{10,46,48}. Rosiglitazone and pioglitazone, PPAR γ agonists, improve EtOH-induced AM oxidative stress⁹, MT-derived ROS⁵⁹, and phagocytic dysfunction. Therefore, we examined the effect of PPAR γ and pioglitazone (PIO) on HA dynamics and related binding proteins. Understanding the impact of these extracellular perturbations in the HA profile on MT bioenergetics is critical to assessing the downstream effects on AM immune responses. Our overarching hypotheses are that EtOH impairs AM HA metabolism, and aberrant HA dynamics negatively impact MT function and phagocytic capabilities. If the results of

our studies support the hypotheses, then restoring homeostatic HA dynamics and inflammatory signaling may prevent lung injury and decrease the risk of respiratory infections in AUD individuals.

Methods & Materials

Human BAL samples: All procedures and data collection occurred at the Joseph Maxwell Cleland Atlanta Veterans Affairs Medical Center, Decatur, GA, United States, 30033 and reviewed and approved by the Atlanta Veterans Affairs Healthcare System Research and Development Committee and Emory University Institutional Review Boards. Otherwise healthy participants with and without AUDs were enrolled in research studies already including bronchoalveolar lavage (BAL) fluid collection via a standard bronchoscopy procedure (ClinicalTrials.gov Identifier: NCT03060772; discontinued due to the COVID-19 pandemic). Healthy controls were matched based on age, smoking status, and sex. Participants underwent a procedure under standard conscious sedation to instill isotonic saline into a sub-segment of the right middle lobe or lingula using a flexible fiberoptic bronchoscopy followed by 6 ~30 mL suction aliquots to obtain BAL fluid. Participants gave informed consent to all procedures performed and VA Pulmonary Disease Repository sample storage. Participants with AUDs took 30 mg of PIO once daily for 2-4 wks or no intervention, at which point bronchoscopy procedure was repeated. The effect of oral PIO on alveolar HA content was assessed in samples from the biorepository. Samples were aliquoted into 1.6 mL centrifuge tubes and stored at -80 °C with protease and phosphatase inhibitors until experimentation. Upon thawing, BAL samples were centrifuged at 1200 rpm for 5 min to separate cells or other debris from the lung fluid. BAL fluid was diluted 1:100 in sterile PBS for HA ELISA-like assay and protein normalization by BCA.

Animal Studies: All animal studies were performed in compliance with the Atlanta VA Health Care System Institutional Care and Use Committee and National

Institute of Health *Guide for the Care and Use of Laboratory Animals* guideline. Male Tie2-Cre PPAR γ $-/-$ mice were generated according to previously published work²¹⁴. Tie2-Cre PPAR γ $-/-$ mice should have only had PPAR γ knocked out in endothelial cells, however this proved to be a leaky model. Resident macrophages including AMs, Kupffer cells, microglia, and others develop almost exclusively from Tie2 expressing progenitor cells²¹⁵. Tie2-Cre PPAR γ $-/-$ mice and wild type mice were housed as previously described²¹⁴ and sacrificed for lung collection. Additionally, male C57BL/6J mice were housed and given ethanol or normal water as described in Chapter 3.2 (2 wk acclimation then 20% EtOH w/v for 10 wks). During the final 7 days of water or EtOH consumption, mice were given PIO (10 mg / kg / day, Cayman Chemicals, Ann Arbor, MI) in 100 μ L methylcellulose vehicle or methylcellulose vehicle alone by oral gavage^{46,113}. Mice were euthanized for tracheotomy and one lobe was tied off for alveolar epithelial type II cell (ATII) isolation as described previously²¹⁶. BAL procedure was done isolate mouse AMs (mAMs) as described in Chapter 3.2 and remaining BAL fluid was stored with protease and phosphatase inhibitors at -80 °C until experimentation. Half of the remaining mouse lungs were perfused, collected in protein lysis buffer, flash frozen in liquid nitrogen, and later transferred to -80 °C for storage. The other half was stored in RNA later for qRT-PCR. Isolated mAMs and ATII cells remained at 37 °C in a humidified, 5% CO₂ controlled incubator for 24 h before supernatant collection.

***In vitro* model of chronic EtOH exposure:** MH-S cells were cultured with and without EtOH (0.08%, 72 h) as described previously^{59,110}. For phagocytosis assays cells were treated with 10 or 1000 ng / mL of HA consisting of 10, 100, or 1000 kD (LifeCore Biomedical, Chaska, MN). For bioenergetics experiments, cells were treated with or

without LMW HA (25 nM of 10 kD HA, 72 h) or HMW HA (25 nM of 1000 kD HA, 72 h) dissolved in complete cell media. Bovine testes hyaluronidase or 4-methylumbelliferone (4-MU, M1381, Sigma, St. Louis, MO) were used to show decreased HA production measurable by HA ELISA-like assay.

qRT-PCR: Mouse lungs or MH-S cell pellets were taken and stored in RNA Later (Invitrogen, Waltham, MA) for preservation. Lungs were transferred to liquid nitrogen and pulverized by mortar and pestle for RNA isolation by TRIzol reagent (ThermoFisher Scientific, Rockford IL) and chloroform (200 μ L per 1 mL TRIzol). Similarly, RNA Later was removed from MH-S cell pellets and pellets were resuspended in TRIzol and chloroform. After vortex and 20 min centrifugation at 1200 rpm the aqueous layer from each sample was transferred to a new tube for precipitation (isopropanol and ethanol washes). RNA was quantified by nanodrop, diluted to 100 ng / μ L, and qRT-PCR was performed using iTaq Universal SYBR Green One-Step kit (Bio-Rad, Hercules, CA) on the Applied Biosystems 7500 Fast sequence detection system (ThermoFisher Scientific, Rockford IL). A full list of mouse primers is in **Table 4.2.1**, including GAPDH housekeeping gene.

Western blot: Control and EtOH treated cells were washed with PBS and lysed by protein lysis buffer with added protease and phosphatase inhibitors. Samples were prepared to a final concentration of 20-50 μ g as previously described¹¹⁰. After blocking, membranes were incubated with primary antibodies for GAPDH (G9545-100UL, 1:20,000, Sigma-Aldrich, St. Louis, MO), HAS1 (ab198846, 1:500, Abcam, Cambridge, England), HAS2 (sc-514737, 1:500, Santa Cruz, Dallas, TX), HAS3 (SAB2101015, 1:500, Sigma, Burlington, MA), Hyal1 (SAB2101113-100UL, 1:500, Sigma, Burlington,

MA), Hyal2 (ab68608, 1:500, Abcam, Cambridge, England), CD44 (ab157107, 1:1000, Abcam, Cambridge, England), TLR2 (ab213676, 1:1000, Abcam, Cambridge, England), or TLR4 (ab13556, 1:1000, Abcam, Cambridge, England) overnight at 4°C. Membranes were washed 3 times with TBST and incubated with 1:10,000 anti-rabbit or anti-mouse IRDye800CW Secondary Antibodies (926-32210 and 926-32211, Li-COR Biosciences, Lincoln, NE, United States) for 1 hour at room temperature. Odyssey Infrared Imaging System (LI-COR Biosciences) was used to image the membranes. Black and white representative membranes with CD44, HAS2, and GAPDH are shown in **Supplemental Fig. 4.2.1**. Image J software (NIH, Bethesda, MD, United States) was used to measure densitometry. HAS2 and CD44 protein values were normalized to GAPDH.

Hyaluronic acid enzyme-linked immunosorbent assay (ELISA)-like assay:

HA concentrations were assayed using the Aggrecan HA-binding protein (HABP) G1 Link-domain based ELISA-like assay (Quantikine, R&D Systems; Minneapolis, MN) according to manufacturer protocol. The ELISA was loaded with samples from MH-S cells, mouse lung, mouse BAL fluid, supernatant from mAMs, supernatant from ATII cells, or human BAL fluid. Optical density was taken at 450 nm (colorimetric signal) and 540 nm (background) in a standard plate reader (Omega, BMG LabTech; Ortenberg, Germany). Sample concentrations were analyzed according to manufacturer recommendation and normalized to ng protein determined by BCA assay. Samples with optical density exceeding the upper limit of linearity were diluted and repeated.

Hyaluronidase ELISA: Mouse BAL extracellular hyaluronidase expression was quantified using a Mouse Hyaluronidase (Sandwich ELISA) ELISA Kit (LS-F56345, LS

Bio, Shirley, MA) according to manufacturer protocol. BAL samples from male mice were centrifuged at 1200 rpm for 5 min to pellet cells and debris. Diluted BAL fluid (1:10) not including cells was used for the ELISA. Protein levels were normalized by BAL total protein measured by BCA assay.

Confocal microscopy: MH-S cells were stained using pHrodo-labeled *Staphylococcus aureus* as in Chapter 3.1 (Morris et al., 2022)¹¹⁰ and Chapter 3.2. Cells were washed 1x with PBS and incubated with 300 nM DAPI (D1306, Invitrogen, Waltham, MA) for 15 min. Cells were then washed twice more and fixed with 4% paraformaldehyde for 20 min. Samples were washed again and mounted with a coverslip for visualization. Images were taken at 60x on a Nikon A1R Inverted Confocal Microscope (Melville, NY) using a TRITC filter. Representative images display internalization of fluorescently labeled bacteria (**Supplemental Fig. 4.2.2, Top**).

Flow cytometry: After EtOH or HA exposure for 72 h, MH-S cells were washed and stained with pHrodo green *Staphylococcus aureus* using the flow cytometry assay for phagocytosis protocol according to manufacturer recommendations (P35382, ThermoFisher, Waltham, Massachusetts). Cells (>500,000 per group) were incubated with pHrodo *S. aureus* for 1 hour. On the last 15 minutes of pHrodo incubation 300 nM DAPI (D1306, Invitrogen, Waltham, MA) or Zombie NIR (423105, BioLegend, San Diego, CA) was added 1:1000 to stain for cells or dead cells. Finally, cells were washed twice, fixed with 4% paraformaldehyde for 20 min, and washed once more with 1x PBS, then resuspended in 500 μ L FACS buffer (PBS + 0.01% Sodium Azide + 1% fetal bovine serum). A BD Accuri C6 Plus Flow Cytometer (Franklin Lakes, NJ) was used to measure cell fluorescence for over 200,000 events. Gating was based zombie NIR

staining, as well as FSC/SSC plots to eliminate doublets and debris. Confirmation of cell staining and positive pHrodo signals is shown in **Supplemental Fig. 4.2.2 (bottom)**.

Results show mean pHrodo-FITC fluorescence relative to control cells \pm SEM.

Mitochondrial bioenergetics: Oxygen consumption rate and extracellular acidification rate were quantified using an extracellular flux analyzer (Agilent Seahorse XF, Santa Clara, CA). Mito Stress Test and ATP rate assays were done using the same preparation and inhibitors as in Chapter 3.2. MH-S cells were pre-treated for 72 h with HMW HA (1000kD, 1000 ng / mL), LMW HA (10 kD, 1000 ng / mL), or EtOH (0.08%).

Results

Chronic ethanol *in vitro* and knock out of PPAR γ *in vivo* alters transcription genes related to HA metabolism.

A previous study showed that EtOH alters mRNA levels of the MT proteins Tfam, Mfn2, Grp75, and Vdac in AMs after chronic EtOH exposure *in vitro* and in AMs from mice fed chronic EtOH *in vivo*⁵⁹. EtOH also increased glycolysis and oxidative stress related genes, Glut1, Glut4, HIF-1 α ¹¹⁰, and Nox4 *in vivo*¹¹³ and *in vitro*^{59,113}. Treatment with the PPAR γ ligand, PIO, improved mRNA levels of MT proteins and Nox4 after EtOH⁵⁹. Here we aimed to confirm some of these EtOH-induced changes *in vitro* and expand on the role of PPAR γ in transcription of these genes. Additionally, we were curious if EtOH or PPAR γ impacted HA metabolism and signaling (see Ch. 4.3), since = bacterial pneumonia^{204,205} and ARDS⁵⁶ increase HA content, and chronic alcohol consumption increases the risk for these disorders^{4,42}.

Using qRT-PCR, mRNA levels of several genes related to MT function, oxidative stress, and HA signaling and metabolism (**Figure 4.2.1, Top**) were measured in MH-S cells exposed to EtOH, or media control (Con). EtOH increased Glut4, Nox4, IL-1 β , Tlr2, Tlr4 and Has2. Additionally, we found that EtOH decreased PPAR γ , as confirmed previously⁴⁶. We were not able to determine significance for HIF-1 α , Mfn2, Drp1, and Tfam *in vitro* due to low sample sizes, but our trending results agree with findings seen previously⁵⁹. There were no significant changes in Vdac, Grp75, Glut1, IL-6, CD44, Rhamm, Hyal1, Hyal2, Has1, or Has3 levels. These results suggest that EtOH affects genes related to both MT function and HA metabolism.

In addition, lungs from mice with and without PPAR γ knock out (PPAR γ $-/-$ and Wild Type) were homogenized and RNA was isolated for qRT-PCR measurement of mRNA levels (**Figure 4.2.1, Bottom**). Fewer mRNA targets were quantified for mouse samples due to sample limitations. Lungs from Tie2-Cre PPAR γ $-/-$ mice had increased Drp1, Tlr2, CD44, and Has2 but decreased PPAR γ , Tfam, and Mfn2 relative to wild type mice. Since EtOH decreases PPAR γ in AMs, it is possible that the increase in Drp1, Tlr2 or 4, and Has2, and the loss of Tfam and Mfn2 are directly related to altered PPAR γ expression during EtOH exposure. However, other cell types in the lung are likely contributing toward differential mRNA expression *in vivo* compared to *in vitro* AMs. For example, PPAR γ $-/-$ lungs had increased CD44 but not EtOH-exposed MH-S cells; however, Has2 is increased in both models. These results led us to further investigate how EtOH and PPAR γ may impact HA synthesis.

AMs are not a major source of HA in the lung.

Since we hypothesized that EtOH alters AM HA metabolism, we checked HA synthase, hyaluronidase, and HA binding protein expression *in vitro*. EtOH increased HAS2 (producing HA > 1000 kD aka HMW HA) and CD44 levels while decreasing Hyal1 (**Figure 4.2.2A and Supplemental Fig. 4.2.1**), possibly indicating HMW HA hyper synthesis. CD44 internalizes HA for degradation^{209,210}, but can also form an anti-apoptotic coat on AMs¹⁹³ or influence immune cell phenotype via chitinase-3 like-protein-1 (CHI3L1)²¹⁷. We did not find any changes in HAS1 or HAS3, which primarily produces medium (200-1000 kD) or low (<200 kD) molecular weight HA (Fig. 4.2.2A). EtOH also did not alter cellular hyaluronidase 2 (membrane or secreted), or other binding proteins in AMs (TLR2 and TLR4).

EtOH did not significantly increase HA levels at any point during treatment *in vitro* compared to control (**Fig. 4.2.2B**) despite EtOH-associated increases in AM Has2 level. Negative controls, 4-methylumbelliferone (HA synthase inhibitor) and bovine testes hyaluronidase, were able to decrease or eliminate measurable HA (**Fig. 4.2.2B**). PPAR γ -/- in mouse lung and BAL fluid from mice given chronic EtOH significantly increased HA levels relative to wild type and control fed mice (**Fig. 4.2.2C,D**). Alveolar epithelial type II (ATII) cells isolated from EtOH-fed mice released significantly more HA than control-fed mice, but supernatants from isolated mouse AMs did not contain a quantifiable amount of HA (**Fig. 4.2.2D**). Since MH-S cells also contained little HA relative to cell numbers (>1x10⁶ MH-S cells and <1x10⁵ mAMs or ATII cells per sample), we determined that AMs do not contribute significantly to alveolar pools of HA *in vivo*. Previous studies showed that during chronic pulmonary diseases or in high oxidative stress environments, ROS or hyaluronidases fragment HA^{57,58,200}. While we did not see any change in cellular hyaluronidase expression, Fig. 4.2.2D does not include a measure of secreted Hyal2. To measure secreted hyaluronidase protein, a mouse hyaluronidase ELISA was used. EtOH increased hyaluronidase expression in mouse BAL fluid, which was attenuated by PIO treatment. PIO alone had no effect on hyaluronidase expression (**Fig. 4.2.2E**).

HA levels were also measured in human BAL fluid samples collected from participants with and without AUDs. Participants with AUDs received either two weeks of orally administered PIO (30 mg / day) or no PIO intervention. Healthy controls without AUD only received one bronchoscopy procedure (B1) while participants with AUD received one before and one after (B2 or AUD + PIO). Participants with AUDs had

slightly higher ($p=0.07$) levels of HA in their BAL fluid compared to healthy controls, and HA levels decreased after PIO treatment. Collectively, these results indicate that AMs do not contribute significantly to EtOH-induced increases in alveolar HA pools.

Additionally, molecular weight of HA may change due to EtOH based on hyaluronidase overexpression and redox imbalance^{49,50} in the alveolar space. PIO could be effective at restoring HA levels in people with AUDs, but it is still unknown whether the change in HA amount or molecular weight due to other alveolar cells may affect AM function.

High molecular weight hyaluronic acid (HMW HA) decreases AM phagocytosis and MT bioenergetics.

We aimed to determine if altered extracellular HA dynamics affect AM function. First, we confirmed that EtOH exposed MH-S cells have decreased levels of phagocytosis (**Fig 4.2.3A** and **Supplemental Fig. 4.2.2, Bottom**) This was important since the pHrodo kit with flow cytometry had not been used previously in the lab. Next, we repeated the flow cytometry procedure with MH-S cells incubated with varying HA concentrations and molecular weights. We found that, in general, LMW HA stimulated greater phagocytosis than control AMs, and HMW HA decreased phagocytic capacity (**Figure 4.2.3B**). Along with previous studies showing that LMW HA normalizes TLR signaling in resident liver macrophages^{212,213}, we agree that LMW HA is not always pro-inflammatory. Further, EtOH and HMW HA severely decreased MT respiration and total ATP production compared to LMW HA treated and control AMs (**Fig. 4.2.3C-E**).

Discussion

Altogether, chronic EtOH alters AM gene expression related to MT function and HA metabolism *in vitro*, however AMs are not a major contributor of HA in the alveolar space. Chronic EtOH consumption *in vivo* and in people with AUD increases HA content in BAL fluid, and a major contributor to alveolar HA pools are ATII cells. While EtOH increases HA levels, possibly by increasing HAS2 expression, secreted hyaluronidase levels are also increased. Yet, we were unable to quantify HA molecular weight from MH-S cells or mouse samples due to the high concentration of HA needed for carbohydrate electrophoresis. HA concentration, fragmentation, and signaling are implicated in chronic pulmonary inflammatory diseases including asthma^{218,219}, COPD/emphysema^{220,221}, and ARDS^{222,223}. Inflammation involves increased production of ROS that cleave HA^{57,58}. Further, oxidative stress increases Hyal expression in other systems^{224,225}. LMW HA (<200kD) undergoes a conformational change resulting in alternative clustering of HA binding proteins and differential signaling patterns^{195,226}. Although LMW HA normalizes TLR signaling in Kupffer cells after EtOH ingestion^{212,213}, how HA fragmentation impacts AM function has not been previously determined. Therefore, altered HA molecular weight due to fragmentation by oxidative species or hyaluronidase enzyme activity may influence lung cell functions.

Additionally, changes in alveolar HA may influence AM ability to phagocytose pathogens, potentially by decreasing AM MT respiration, but future studies are needed to determine mechanisms of HA signaling that would result in altered AM metabolism. Although the mechanism by which HA directly affects MT bioenergetics was not the focus of these initial proposed studies, ample evidence suggests that HA binding

proteins modulate oxidative phosphorylation²²⁷⁻²³⁰. Oxidative phosphorylation is the most efficient way for AM to generate large amounts of ATP for phagocytosis, but EtOH impairs MT membrane potential, ATP production, and MT bioenergetics in AM^{49,50,59}. Studies suggest that HA may affect other redox-sensitive MT effectors, such as PPAR γ coactivator 1 α (PGC1 α) or hypoxia-inducible factor 1 α (HIF1 α)^{178,206}, which are also implicated in alcohol-induced AM dysfunction during chronic alcohol use^{46,52,110}.

We also recognize that there are other HA binding proteins with relatively less expression in the lung that were unexplored. It is not fully known how HA binding proteins preferentially bind LMW or HMW HA. More so, previous literature has not been consistent in the definitions of LMW and HMW HA. I chose to use LMW HA as HA <200kDa and HMW HA >1000kDa because HA has a conformational change around 200kDa, and this change determines how HA binds to different surface receptors^{195,226}. Since people with AUD have increased risk for pneumonia, I expanded on this project by writing a review on how HA binding proteins, or hyaladherins, may be implicated in bacterial pneumonia pathophysiology, including how other cells may contribute towards disturbed AM function (**see Chapter 4.3**).

Tables & Figures

Table 4.2.1: Summary of mouse primers used for qRT-PCR used for mRNA detection of genes important for mitochondrial function and hyaluronic acid metabolism.

Name	Forward sequence (5' to 3')	Reverse sequence (3' to 5')
Peroxisome-proliferator activated receptor gamma (PPARγ)	<i>GAGTTCATGCTTGCAAGGATGC</i>	<i>CGATATCACTGGAGATCTCGCC</i>
Hypoxia-inducible factor-1 alpha (Hif-1α)	<i>CTCAAAGTCGGACAG</i>	<i>CCCTGCAGTAGGTTT</i>
Mitochondrial transcription factor 1B (Tfb1m)	<i>ATAGAGCCCAAGATCAAGCAG</i>	<i>GCACTGGAAGGCTGTTACA</i>
Mitochondrial transcription factor A (Tfam)	<i>CACCCAGATGCAAACTTTCA</i>	<i>CTGTGAGCAAGTATAAAG</i>
Mitofusin 2 (Mfn2)	<i>TCCTGGGCCCTAAGAATAGC</i>	<i>GAGAGGACGCTGAACCTGAT</i>
Dynamin-related protein 1 (Drp1)	<i>CAGGAATTGTTACGGTTCCCTAA</i>	<i>CCTGAATTAAGTTGTCCCGTGA</i>
Voltage dependent anion channel (Vdac)	<i>GGTACACTCAGACCCTAA</i>	<i>CACCCGCATTGACGTTCT</i>
75 kD glucose-related protein (Grp75)	<i>TCCTGTGTGGCTGTTATGGA</i>	<i>AGGGGTAGTTCTGGCACC</i>
Glucose transporter 4 (Glut4)	<i>AAAAGTGCCTGAAACCAGAG</i>	<i>TCACCTCCTGCTCTAAAAGG</i>
Glucose transporter 1 (Glut 1)	<i>CTCCTGCCCTGTTGTGTATAG</i>	<i>AAGGCCACAAAGCCAAAGAT</i>
NADPH oxidase 4 (NOX4)	<i>TGTTGGGCCTAGGATTGTGTT</i>	<i>AGGGACCTTCTGTGATCCTCG</i>
Interleukin 6 (IL-6)	<i>ACAACCACGGCCTTCCCTACTT</i>	<i>CACGATTTCCAGAGAACATGTG</i>
Interleukin 1 beta (IL-1β)	<i>AGTCTGCACAGTTCCCCAAC</i>	<i>TTAGGAAGACACGGGTTCCA</i>

Toll-like receptor 2 (Tlr2)	<i>TCTGGGCAGTCTTGAACATTT</i>	<i>AGAGTCAGGTGATGGATGTCG</i>
Toll-like receptor 4 (Tlr4)	<i>CAAGGGATAAGAACGCTGAGA</i>	<i>GCAATGTCTCTGGCAGGTGTA</i>
Cluster of differentiation 44 (cd44)	<i>AGCAGCGGCTCCACCATCGAGA</i>	<i>TCGGATCCATGAGTCACAGTG</i>
Receptor for hyaluronic acid-mediated motility (RHAMM)	<i>AGCAAGGATAGAGAAAGGGCTG</i>	<i>TGCAGACGAGCAGACAGTTC</i>
Hyaluronidase 2 (Hyal2)	<i>GCAGGACTAGGTCCCATCATC</i>	<i>TTCCATGCTACCACAAAGGGT</i>
Hyaluronidase 1 (Hyal1)	<i>TCATCGTGAACGTGACCAGT</i>	<i>GAGAGCCTCAGGATAACTTGGATG</i>
Hyaluronic acid synthase 3 (Has3)	<i>TGGACCCAGCCTGCACCATTG</i>	<i>CCCGCTCCACGTTGAAAGCCAT</i>
Hyaluronic acid synthase 2 (Has2)	<i>GAGCACCAAGGTTCTGCTTC</i>	<i>CTCTCCATACGGCGAGAGTC</i>
Hyaluronic acid synthase 1 (Has1)	<i>GAGGCCTGGTACAACCAAAAG</i>	<i>CTCAACCAACGAAGGAAGGAG</i>
Glyceraldehyde-3-phosphate dehydrogenase (Gapdh)	<i>GGATTTGGTCGTATTGGG</i>	<i>GGAAGATGGTGATGGGATT</i>

Figure 4.2.1

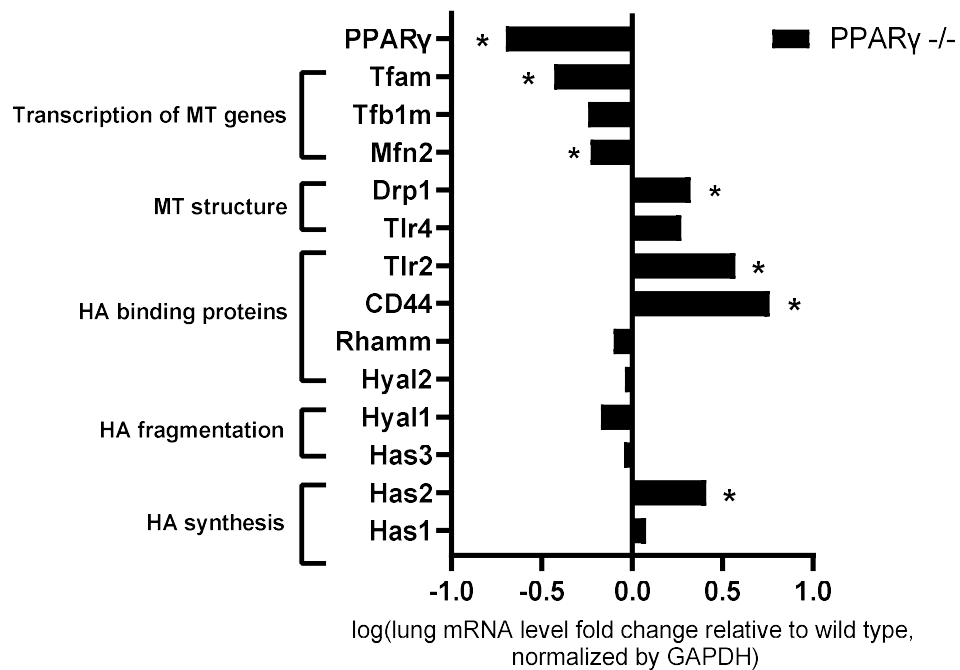
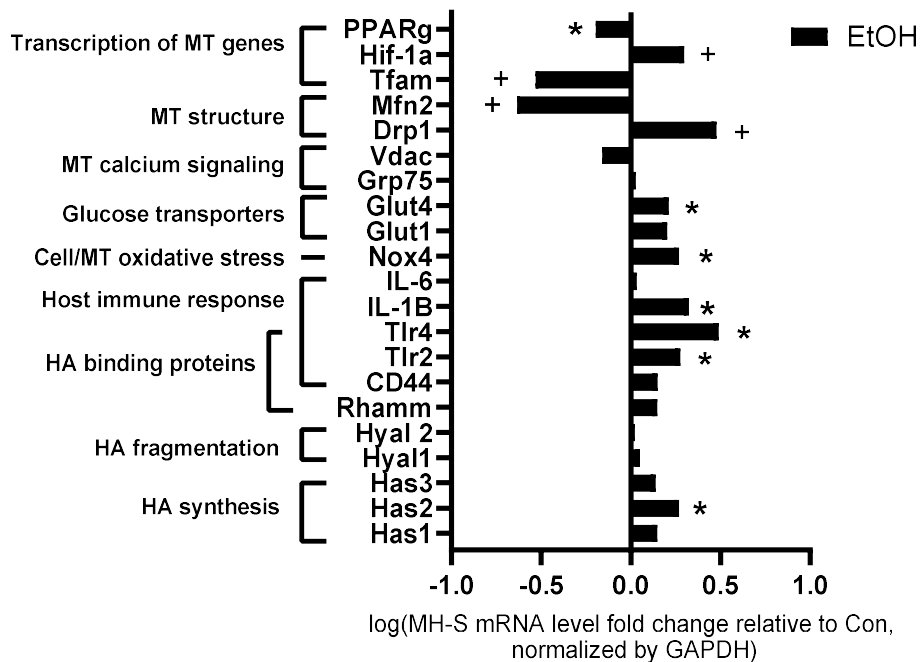


Figure 4.2.1: Effect of ethanol (EtOH) *in vitro* or peroxisome proliferator-activated receptor 1 gamma (PPAR γ) knock out *in vitro* in MH-S or *in vivo* mouse lungs on mRNAs associated with mitochondrial function and hyaluronic acid (HA) metabolism. A) EtOH increases glucose transporter 4 (Glut 4), NADPH oxidase 4 (Nox4), interleukin 1 beta (IL-1 β), Toll-like receptor 2 and 4 (Tlr2, Tlr4), and hyaluronic acid synthase 2 (Has2). EtOH decreases peroxisome proliferator-activated receptor gamma (PPAR γ). B) Lungs from Tie2-Cre PPAR γ $-/-$ mice had increased Drp1, Tlr2, CD44, and Has2 and decreased PPAR γ , Tfam, and Mfn2. *p < 0.05 vs. Control treated cells (n=3-16) or wild type mouse lung (n=3-4, students t-test). [†]n=1-2, no significance determined.

Figure 4.2.2

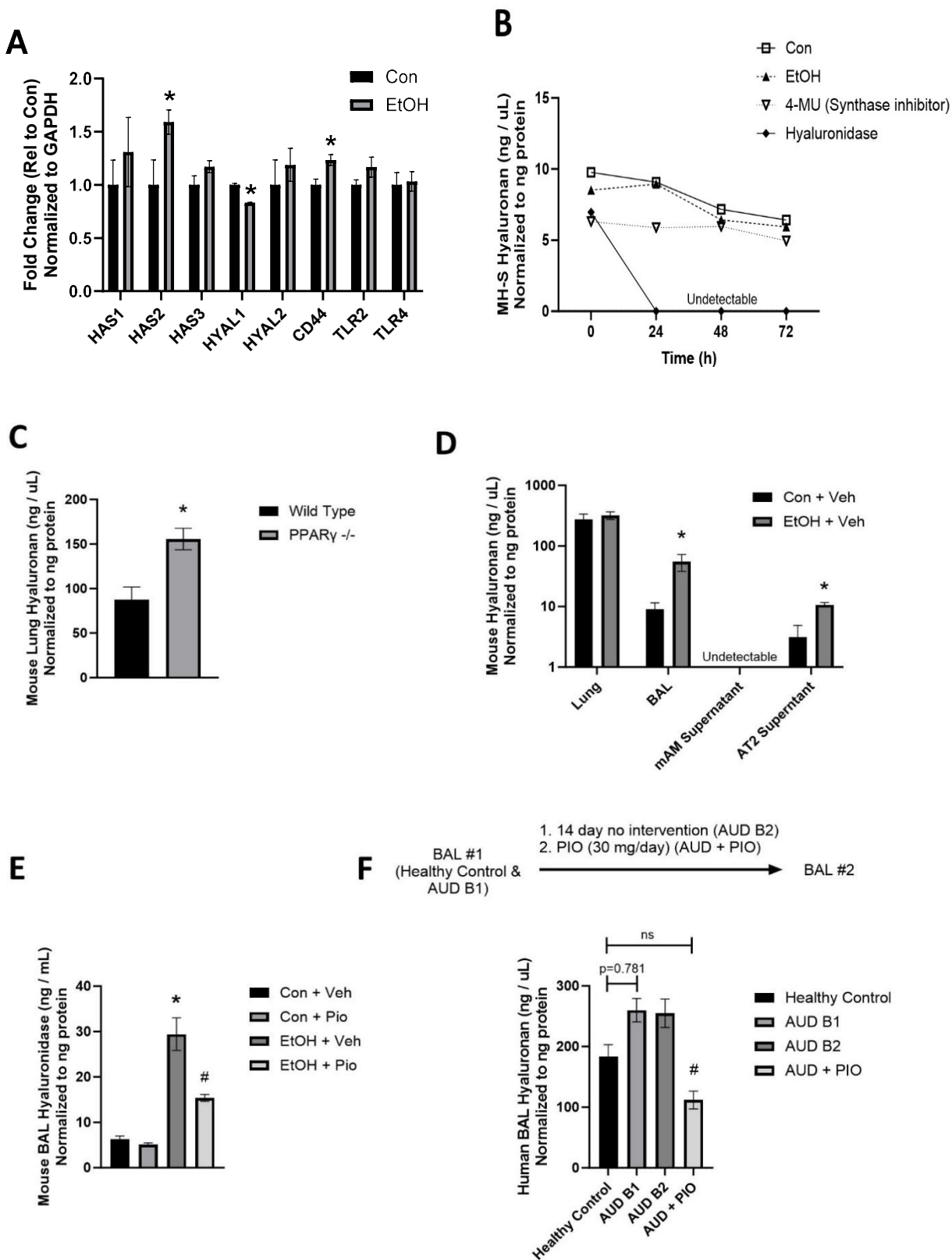


Figure 4.2.2: *In vitro* hyaluronic acid (HA)-related protein expression may influence HA release. A) EtOH increases hyaluronic acid synthase 2 (HAS2) and CD44 expression and decreases hyaluronidase 1 (HYAL1) *in vitro*. MH-S cells were cultured \pm 0.08% EtOH for 72 h (n=4-6) and lysed for western blotting by loading 20-50 μ g protein. Bars represent protein level means normalized to GAPDH \pm SEM. $p < 0.05$ vs. Con. **B)** HA concentration with hyaluronidase (20 nM) or 4-methylumbelliferone (1 μ M HA synthase inhibitor, 4-MU) **C-D)** HA concentration measured by HA ELISA-like assay in Tie2-Cre PPAR γ knock out mouse lung homogenates (n=3-5) and EtOH-fed and control-fed C57BL/6J mouse lung homogenates, bronchoalveolar lavage fluid, and supernatants from mouse alveolar macrophage and alveolar type II epithelial cells. **E)** Total hyaluronidase protein expression in BAL fluid measured by ELISA. Bars represent protein mean \pm SEM, n=3-4). **F)** HA concentration measured by HA ELISA-like assay in human BAL fluid from people with and without alcohol use disorders (n=7-9).

Figure 4.2.3

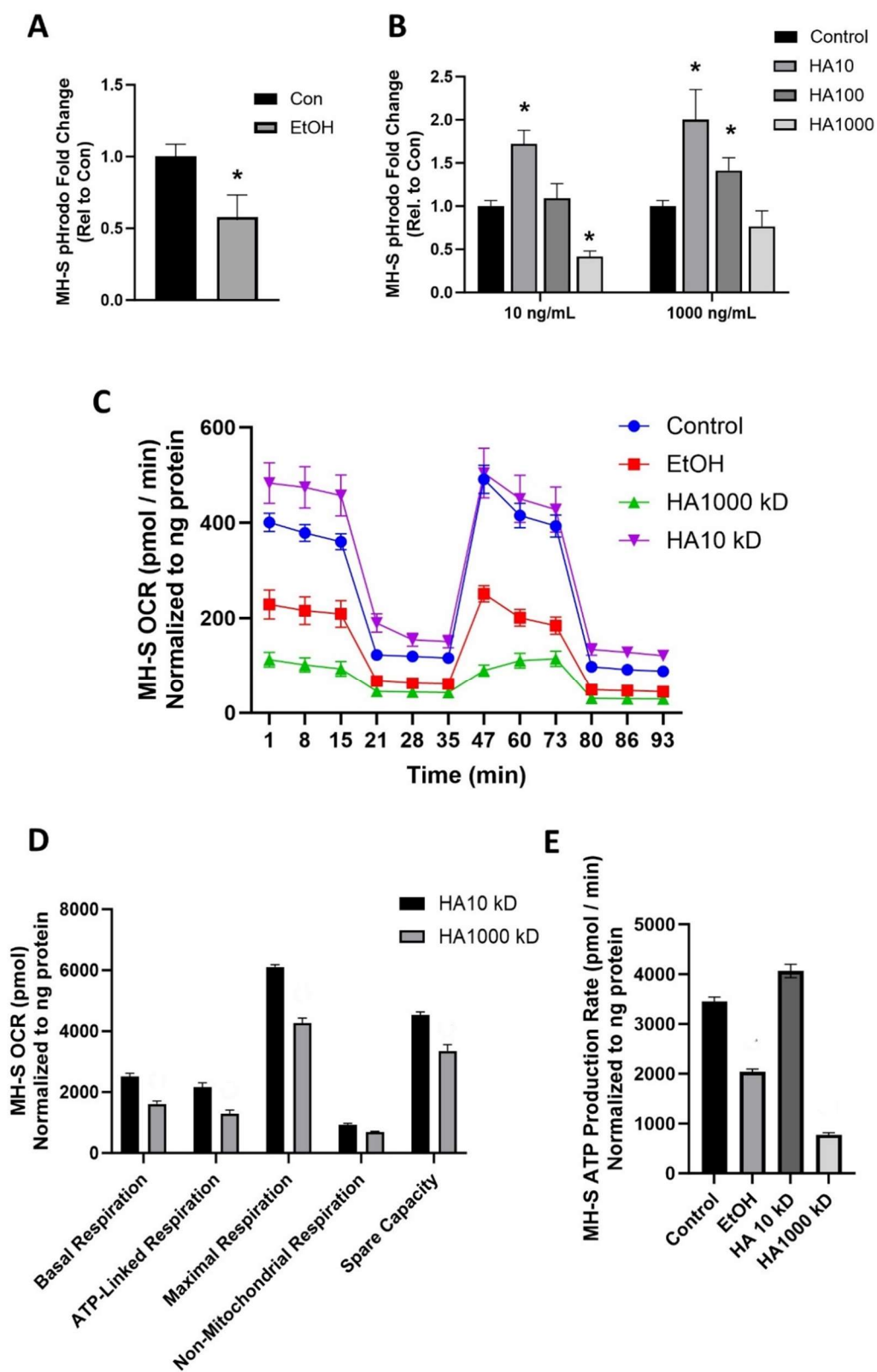
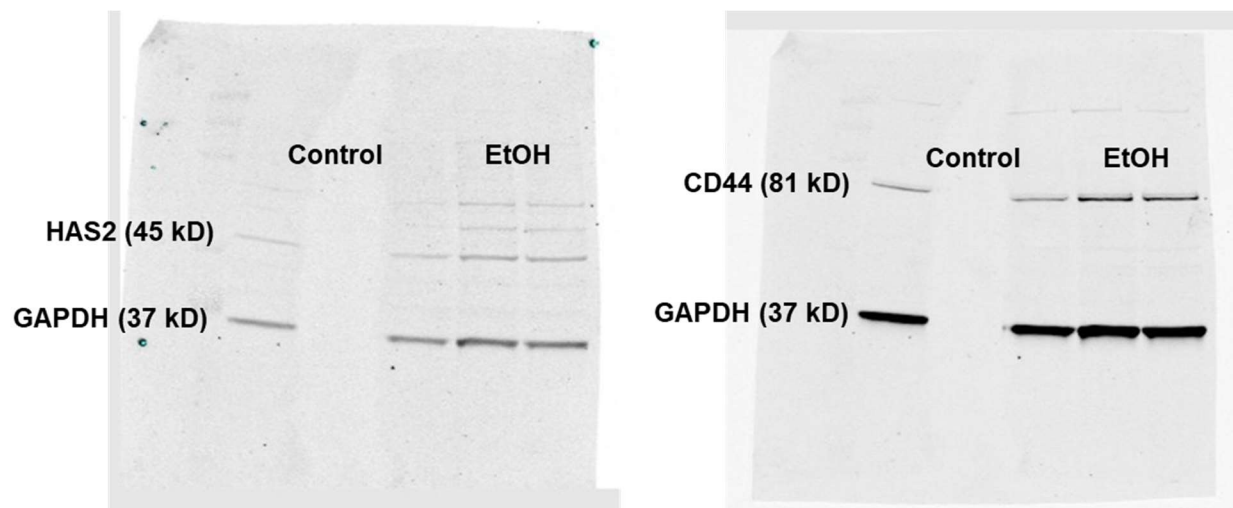


Figure 4.2.3: High molecular weight hyaluronic acid (HMW HA, 1000 kD)**decreases the AM phagocytosis and mitochondrial bioenergetic profile *in vitro*. A)**

Ethanol (EtOH) decreases MH-S cells phagocytosis as measured by internalization of fluorescently labeled *Staphylococcus aureus* and quantification by flow cytometry (n=7-8). **B)** HA molecular weight and concentration alters AM phagocytic capacity. HA10 kD (10 ng / mL or 1000 ng / mL, 72 h) improves phagocytosis but high molecular weight HA (10 ng / mL or 1000 ng / mL, 72 h, n=5) impairs phagocytosis. **C)** Seahorse XF Mito Stress Test assay was done to obtain a mitochondrial respiration profile (OCR profile). Oxygen consumption rate (OCR) was measured in response to 2 μ M oligomycin (Oligo), 0.5 μ M Carbonyl cyanide-p-trifluoromethoxyphenylhydrazone (FCCP), and 0.5 μ M rotenone and antimycin (R/A) in MH-S cells treated with EtOH (0.08%, 72 h), HA1000 kD (1000 ng / mL, 72 h), or HA10 kD (1000 ng / mL, 72 h). **D)** Basal respiration, ATP-linked respiration, maximal respiration, non-mitochondrial respiration, and spare capacity (n=2) determined using OCR profiles. **E)** Seahorse XF ATP rate assay was used to measure ATP production rate. EtOH and high molecular weight HA decreases total ATP levels *in vitro* (n=2). Bars represent fluorescence units or OCR means \pm SEM. OCR and ATP production is normalized to protein levels. *p < 0.05 relative to Con (students t-test or one-way ANOVA).

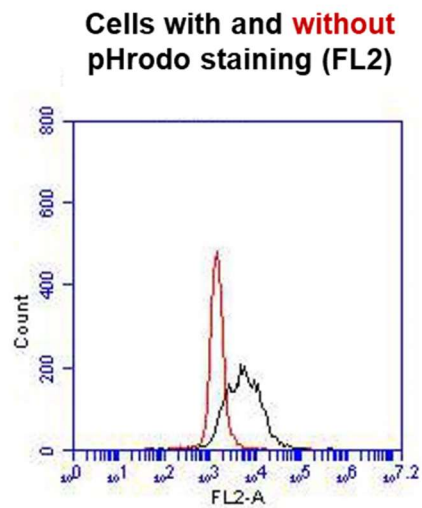
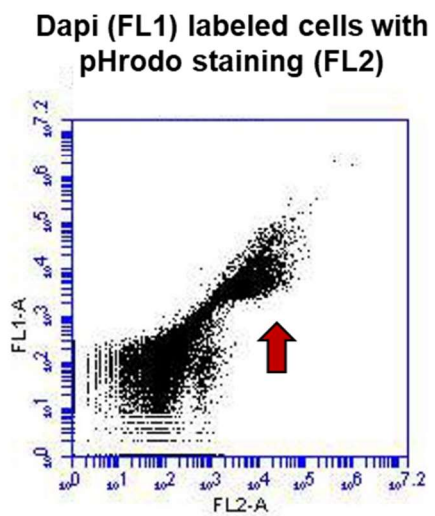
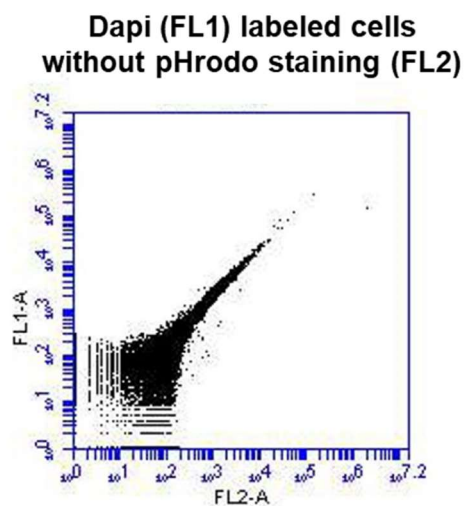
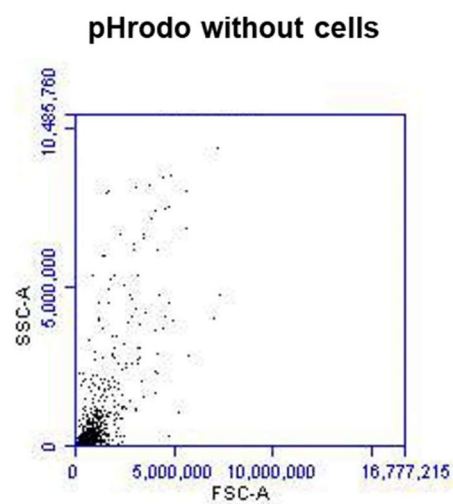
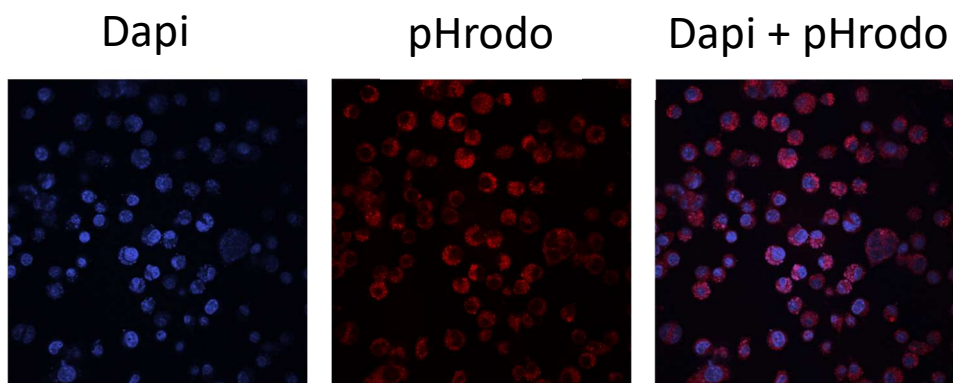
Supplemental Figures

Supplemental Figure 4.2.1



Supplemental Figure 4.2.1: Representative western blot membranes from control and ethanol (EtOH) treated MH-S cells. EtOH increases hyaluronic acid synthase 2 (HAS2) and CD44 levels *in vitro* (n=2), relative to GAPDH.

Supplemental Figure 4.2.2



Supplemental Figure 4.2.2: MH-S cell internalization of fluorescently labeled *Staphylococcus aureus*. A) Confocal imaging of MH-S cells stained with DAPI and pHrodo red *S. aureus*. **B-E)** Flow cytometry representative profiles of control buffer, MH-S cells without pHrodo staining, and with pHrodo staining.

4.3 Hyaladherins May be Implicated in Alcohol-Induced Susceptibility to Bacterial Pneumonia

Kathryn M. Crotty^{1,2} and Samantha M. Yeligar^{1,2*}

¹ Department of Medicine, Division of Pulmonary, Allergy, Critical Care and Sleep Medicine, Emory University, Atlanta, GA, United States

² Atlanta Veterans Affairs Health Care System, Decatur, GA, United States

***Correspondence:**

Kathryn M. Crotty: orcid.org/0000-0002-9461-4032

Samantha M. Yeligar: orcid.org/0000-0001-9309-0233, syeliga@emory.edu

Full Citation: Crotty KM, Yeligar SM. Hyaladherins May be Implicated in Alcohol-Induced Susceptibility to Bacterial Pneumonia. *Front Immunol.* 2022 May 12;13:865522. doi: 10.3389/fimmu.2022.865522. PMID: 35634317; PMCID: PMC9133445.

Author Contributions: KMC outlined and prepared the manuscript; SMY outlined and prepared the manuscript. All authors contributed to the article and approved the submitted version.

Funding: This work was supported in part by grants from: the National Institute on Alcohol Abuse and Alcoholism (F31AA029938) to KMC (ORCID ID: 0000-0002-9461-4032) and (R01AA026086) to SMY (ORCID ID: 0000-0001-9309-0233) as well as the National Institute of General Medical Sciences (T32GM008602) to Randy A. Hall. The contents of this report do not represent the views of the Department of Veterans Affairs or the US Government.

Abstract

Although the epidemiology of bacterial pneumonia and excessive alcohol use is well established, the mechanisms by which alcohol induces risk of pneumonia are less clear. Patterns of alcohol misuse, termed alcohol use disorders (AUD), affect about 15 million people in the United States. Compared to otherwise healthy individuals, AUDs increase the risk of respiratory infections and acute respiratory distress syndrome (ARDS) by 2-4-fold. Levels and fragmentation of hyaluronic acid (HA), an extracellular glycosaminoglycan of variable molecular weight, are increased in chronic respiratory diseases, including ARDS. HA is largely involved in immune-assisted wound repair and cell migration. Levels of fragmented, low molecular weight HA are increased during inflammation and decrease concomitant with leukocyte levels following injury. In chronic respiratory diseases, levels of fragmented HA and leukocytes remain elevated, inflammation persists, and respiratory infections are not cleared efficiently, suggesting a possible pathological mechanism for prolonged bacterial pneumonia. However, the role of HA in alcohol-induced immune dysfunction is largely unknown. This mini literature review provides insights into understanding the role of HA signaling in host immune defense following excessive alcohol use. Potential therapeutic strategies to mitigate alcohol-induced immune suppression in bacterial pneumonia and HA dysregulation are also discussed.

Keywords: hyaluronan, alcohol use disorder, pneumonia, hyaladherin, immunity

Introduction

Excessive alcohol use associated with alcohol use disorders (AUD) ¹⁹⁰ is linked to over 5 million annual deaths globally¹⁵, in part due to an increased risk of respiratory infections⁴² and acute respiratory distress syndrome (ARDS) ⁴. Pneumonia is a serious respiratory infection that is caused by at least one of several opportunistic bacteria, viruses, or fungi. Nearly 44,000 people die annually due to pneumonia in the United States, while another 1.5 million are hospitalized for pneumonia as a primary diagnosis¹⁶. Ethanol (EtOH) impairs mucociliary clearance in the upper airway^{40,41} and diminishes innate immune defense in the lower airway by impairing the ability of alveolar macrophages (AM) to phagocytose pathogens^{10,39,46,47}, such as bacterial pneumonia^{46,112}.

Upon pneumonia-associated microbial evasion of host immune defense mechanisms in the upper airway, microbial culture in the lower airways causes pneumonia. This mini review focuses on molecular mechanisms, such as that of hyaluronic acid (HA), that may be implicated in increased susceptibility to bacterial pneumonia during acute and chronic EtOH use. Modulation of HA metabolism, signaling, and intracellular communication that impact cellular immune functions during bacterial pneumonia may pave the way for future investigations on how alterations in the extracellular matrix may be exacerbated by excessive alcohol use.

Extracellular Matrix in the Lung

The extracellular matrix is a dynamic environment, rich with proteins, carbohydrates, and other significant structural molecules. In diseased states, additional matrix deposition results in diminished intracellular communication and progression to

fibrosis. AUD-associated risk of pneumonia and ARDS^{4,42} precedes pulmonary fibrosis and loss of function if unresolved⁵³.

Hyaluronic acid (HA), an extracellular matrix glycosaminoglycan, is essential for maintaining tissue structure, promoting cell survival, and regulating inflammation and leukocyte motility after pulmonary injury^{194,199,201,202,223,231}. Further, accumulation of HA fragments is associated with chronic pulmonary inflammation mediated by innate immune cells^{128,221,232-237}. Increased HA synthesis and fragmentation is commonly involved in pulmonary disease pathology including fibrotic diseases^{197,237-239}, excessive remodeling^{194,224,231,240}, and inflammation^{221,223,241-245}. In non-pathologic conditions, HA is expressed at very low concentrations in bronchoalveolar lavage fluid^{192,206} but is increased during pulmonary inflammation and pneumonia infections from *Klebsiella pneumoniae* and *Escherichia coli*^{204,246}.

Bacterial pneumonia clearance depends on dynamic, but regulated, HA metabolism and HA binding protein signaling^{204,244,246-248}. Regulation of HA size and signaling through cell surface immune receptors is necessary to mobilize leukocytes, including alveolar macrophages, for recognition and destruction of infectious pathogens in those with AUD. Remodeling after respiratory infections is crucial and involves a restoration of HA dynamics coinciding with decreases in bacterial colonization, inflammation, and leukocyte recruitment.

Hyaluronic Acid Signaling: Hyaladherins and Hyaluronic Acid-Protein Interactions

Hyaladherins are HA binding proteins that transmit changes in the extracellular matrix to cell signals for altered intra- or inter-immune cell function¹⁹⁴ through intermediate proteoglycans^{249,250} or by ionic HA binding to membrane proteins^{251,252}.

Although alcohol diminishes the ability of alveolar macrophages to recognize and clear pathogens, the role of HA on bacterial recognition during excessive alcohol use is largely unknown.

CD44 and CHI3L1: Cluster of differentiation 44 (CD44) is a hyaladherin that spans the cellular membrane, binds HA, and internalizes HA for lysosomal degradation by hyaluronidase enzymes^{209,210}. CD44 is the primary cell surface receptor for HA binding in lymphocytes²⁵³⁻²⁵⁵ and forms an anti-apoptotic coat of HA around alveolar macrophages¹⁹³. Therefore, CD44 is crucial for HA metabolism and signaling in leukocytes. Granulocyte macrophage colony stimulating factor (GM-CSF) and peroxisome proliferator-activated receptor gamma (PPAR γ) agonism induce expression of CD44 in monocytes that do not readily bind HA¹⁹³. However, chronic alcohol diminishes GM-CSF and PPAR γ ^{46,60} in primary alveolar macrophages, potentially decreasing their ability to form an anti-apoptotic HA coat for signaling with other hyaladherins.

Patients with eosinophilic pneumonia have high concentrations of CD44, HA, and interleukin-5 in their bronchoalveolar fluid. In contrast, CD44 deficient mice show decreased HA content after *Streptococcus pneumoniae* but increased HA in response to *Escherichia coli* infection²⁰⁴, suggesting that bacterial strains differentially influence host HA matrices. Yet, these studies do not address altered HA binding or signaling as mechanisms for worsened bacterial pneumonia. While altered CD44 expression following alcohol use may be one mechanism of bacterial pneumonia pathogenesis, altered HA molecular weight or indirect HA signaling may also impact inflammatory signaling and the innate immune response in leukocytes.

For indirect immune cell signaling, chitinase-3 like-protein-1 (CHI3L1) forms an intermediate bond between CD44 and HA²⁵⁶. Through HA binding to CHI3L1^{257,258}, lysosomal degradation of HA by CD44 internalization is inhibited. Thus, CHI3L1 indirectly inhibits HA uptake and degradation through CD44 mediated internalization, suggesting CHI3L1 as an important regulator of HA metabolism. CHI3L1 is expressed in macrophages, neutrophils and endothelial cells and is necessary for antigen response, oxidant injury response, inflammation, and macrophage phenotype in the lung²¹⁷. Alcohol and high CHI3L1 levels have been linked to the progression of liver injury and fibrosis²⁵⁹⁻²⁶¹, but not yet in alcohol and bacterial pneumonia.

In bacterial pneumonia, CHI3L1 activity promotes innate immune defenses by sensing oxidant stress, cytokines, growth factors and miRNAs in the extracellular environment. Patients hospitalized with pneumonia have increased levels of CHI3L1 in serum^{248,262,263}. Additionally, *S. pneumoniae* induces CHI3L1 expression, but mice lacking CHI3L1 have reduced bacterial clearance and enhanced mortality following *S. pneumoniae* infection²⁴⁷. These studies suggest CD44 and CHI3L1 as important regulators of innate immunity in the lung during bacterial pneumonia. Further, these studies provide CD44 and CHI3L1 as targetable mechanisms for treating bacterial pneumonia in those with AUD.

HA Heavy Chain Formation: Tumor necrosis factor-stimulated gene-6 (TSG-6) is secreted by immune cells²⁶⁴ and catalyzes inter- α -trypsin-inhibitor (I α I) heavy chain complex to HA through pentatraxin 3 (PTX3)²⁶⁵. Together, these molecular components generate a heavy chain HA matrix involved in airway inflammation²⁶⁶, hyperresponsiveness²⁶⁷⁻²⁷⁰ and toll-like receptor 4 (TLR4) mediated lung injury^{243,268},

possibly through PTX3 stimulation by TLR signaling²⁷¹. Ial attenuates lung injury in a porcine model of lipopolysaccharide (LPS)-induced sepsis²⁷², and PTX3 deficiency worsens LPS-induced lung injury. TSG-6 expression in cultured U-937 monocytes is enhanced by *Staphylococcus aureus* and *Chlamydia pneumoniae*²⁷³, suggesting enhanced expression in some strains of bacterial pneumonia. Further, PTX3 is involved in microbial recognition and innate immunity through recruitment of leukocytes and binding to *K. pneumoniae*, *Pseudomonas aeruginosa*, *Salmonella enterica*, *S. aureus*, *Neisseria meningitidis*, and *S. pneumoniae*²⁷⁴⁻²⁷⁶. Altogether, there is sufficient evidence for the role of heavy chain HA matrices in bacterial pneumonia, but further studies are needed to elucidate if PTX3 involvement in heavy chain HA formation is due to production by host or pathogen.

Little is known about heavy chain HA formation during excessive alcohol use. If heavy chain HA formation is involved in lung injury amelioration during bacterial pneumonia, disruptions in this process may lead to further lung injury and possibly sepsis. The risk of developing sepsis from pneumonia increases from 35% to 60% in people with AUD⁴. EtOH feeding to C57BL/6 mice significantly diminished survival rates and lung PTX3 expression in a model of sepsis, and delayed tumor necrosis factor alpha (TNF- α) level increases in plasma²⁷⁷. Similarly, in a binge drinking mouse model of gram-negative bacterial lung infection, plasma TNF- α was suppressed even while bacterial colonization was increased²⁷⁸. Overall, these studies suggest that sepsis after excessive alcohol use is not due to lack of inflammatory TNF- α signaling. Rather, alterations in PTX3 disrupt HA heavy matrix formation and may be a mechanism for deranged immune function in those with AUD.

Versican and TLRs: Lecticans are HA-binding proteoglycans, containing chondroitin sulfate side chains, that ionically bind to HA through clusters of positively charged amino acids forming the link domain^{252,255}. Little is known about how lecticans are impacted in bacterial pneumonia; however, levels of hyaluronan and the lectican, versican, increase during lung injury^{56,206,279}, perhaps by HA synthase regulation^{280,281}. Although rats exposed to fetal alcohol showed a decrease in synaptic versican²⁸², the role of versican in alcohol-induced lung derangements continues to be an active area of investigation.

TLRs bind to hyaladherins and are known mediators of the inflammatory response during bacterial pneumonia. Like HA, versican can act as a danger associated molecular pattern for TLR signaling in alveolar macrophages^{283,284}. Versican is augmented in the lungs of adult mice exposed to *P. aeruginosa* and upon TLR agonism²⁸⁵. Comparatively, conditional versican deficiency in myeloid cells reduced inflammatory cell recruitment to the lungs²⁸⁶. LPS stimulation of the TLR4/Trif pathway increases HA and versican levels in bone marrow derived macrophages *in vitro* and in murine alveolar macrophages^{246,286}, but there is a lack of similar studies with gram positive bacteria.

Defects in TLR signaling predispose an individual to immunodeficiency that can result in severe bacterial pneumonia²⁸⁷. Further, the versican receptors TLR2 and TLR4 are affected by excessive alcohol use. TLR2 and TLR4 do not bind HA but have been hypothesized to interact with HA through clustering of other matrix or membrane proteins and proteoglycans, like versican. Individuals with alcohol use disorders showed significant increases in TLR2; those with AUD and cannabis use exhibited significant

increases in TLR6²⁸⁸. No experimental groups had increased TLR4 expression in that study, but another study showed that alcohol exposure induced TLR4 endocytosis in alveolar macrophages, limiting TLR4 activity for the recognition of pathogens⁴⁶. These results suggest that TLR expression or signaling may compensate for impaired bacterial recognition in those who have AUD and bacterial pneumonia. Other membrane hyaladherins can also bind HA simultaneously to influence leukocyte phenotype²⁸⁹ and affect pro- or anti-inflammatory signaling depending on the binding protein. While it is not known if hyaluronan or any binding partners interact with the other TLRs, these studies identified multiple targets for therapeutic intervention.

RHAMM, HABP1 and HABP2: Receptor for HA mediated motility (RHAMM), and HA binding protein 1 and 2 (HABP1, HABP2) are expressed ubiquitously and have multiple binding partners, including HA^{290,291}. RHAMM contains putative binding domains for HA²⁹², but RHAMM is mainly expressed intracellularly^{291,293-295} to participate in signaling excluding HA. However, it is possible that HA binds to hyaladherins within the cell membrane because several hyaladherins are expressed intracellularly. Upon HA interaction with RHAMM, cell migration is promoted, influencing tissue remodeling or immune cell trafficking²⁹⁶. In mice, there is increased membrane expression of RHAMM following lung injury²⁹⁷. Further, RHAMM can compensate for CD44 through increased HA binding without increased RHAMM expression, indicating convergence of HA signaling pathways²⁹⁸.

RHAMM is implicated in acute lung injury²¹⁸, and alcohol use exacerbates acute lung injury^{4,10,45,53,222}. However, it is not yet known how alcohol consumption directly affects RHAMM in any organ system. Past work has shown that RHAMM and

transforming growth factor beta (TGFb) work collectively to promote cell motility²⁹⁹. Alcohol use inhibits inflammatory cytokines while stimulating TGFb, which acts as an inhibitory cytokine in human monocytes exposed to bacterial stimuli³⁰⁰. In contrast, some studies show that alcohol induces lung injury through proinflammatory pathways and promote fibrosis by stimulating TGFb1 activity^{132,301}. In alveolar macrophages, alcohol-induced oxidative stress through TGFb1 regulation of NADPH oxidases diminished alveolar macrophage function¹²⁹. Altogether, TGFb1 is clearly involved in immune dysfunction following alcohol use, but more information is necessary to conclude that changes in TGFb1 contribute to alterations in RHAMM signaling.

HABP1, also known as p32 or gC1qR, can be found at the cell surface with higher affinity for HA corresponding to ionic strength and acidic environments³⁰², and HA binding to HABP1 can inhibit HA degradation by *S. pneumoniae* hyaluronidases³⁰³. Bacteria express hyaluronidase proteins that degrade host HA matrices to allow for greater bacterial movement; thus, HABP1 activity is an endogenous antibacterial host defense. In humans, HABP1 assists in the regulation of HA metabolism in non-diseased states. While there is little known about HABP1's involvement in bacterial pneumonia, HABP1 activity is well described in cancer and mitochondrial biology. Alcohol exposure impairs alveolar macrophage ability to phagocytose pathogens^{10,39,46,47} via increased cellular oxidative stress⁴⁸, mitochondrial redox imbalance^{49,50}, and impaired mitochondrial bioenergetics⁵⁹. Mitochondrial HABP1 regulates oxidative phosphorylation^{304,305} by maintaining mitochondrial protein translation³⁰⁶, and cleavage of HABP1 by caspase-1 shifts cancer cell phenotype toward glycolysis³⁰⁷. In human lung cancers, HABP1 is highly expressed, leading to altered nuclear factor kappa B

(NFkB) activity and cell proliferation³⁰⁸, revealing a role for HABP1 in the lung microenvironment.

HABP2, also known as factor VII activating protease or plasma hyaluronan binding protein, is extracellular. High molecular weight HA inhibits HABP2's activity to maintain barrier integrity while low molecular weight HA prevents a leaky barrier^{309,310}. Normal barrier function prevents bacterial spread into the vasculature during bacterial pneumonia that would otherwise result in sepsis. Further, alcohol impairs pulmonary barrier function^{43,44}. In the lung, HABP2 may be involved in LPS-induced lung injury³¹⁰ and ARDS³¹¹ primarily through its role in modulating lung barrier integrity. In patients with ARDS, HABP2 levels and activity are increased in alveolar macrophage, epithelial, and endothelial cells³¹¹, and chronic alcohol use elevates the risk for ARDS⁴.

In vivo HABP2 silencing by small interfering RNA attenuated LPS-mediated lung injury and hyperpermeability, indicating a possible therapeutic strategy for bacterial pneumonia in those with AUD-induced barrier dysfunction. Additionally, HABP2 primarily binds to cell surface protease-activated receptors (PAR)³¹², and silencing of PAR1 and PAR3 can attenuate LPS-mediated barrier dysfunction³¹⁰. Mice with PAR2 genetic deletions exhibited severe lung inflammation, neutrophil accumulation, diminished macrophage, and neutrophil bacterial phagocytosis in a model of *P. aeruginosa*. These alterations were attenuated by PAR2 activation³¹³, indicating a possible role for HABP2 in bacterial pneumonia clearance. Other studies show similar roles for PARs in bacterial pneumonia pathology³¹³⁻³¹⁵; however, this mechanism needs to be further elucidated since HABP1 and the PARs each have multiple binding partners.

Discussion

This mini review addresses modulation of HA signaling by alcohol and bacterial pneumonia. CD44 and RHAMM are involved in HA metabolism, signaling, and intracellular communication. CHI3L1, Ial, TSG-6, PTX3, and versican all act as intermediates between HA and membrane signaling proteins, like CD44 and TLRs. Herein we also review how HA modulates cellular energy metabolism through HABP2 and intracellular signaling. Another hyaladherin, lymphatic vessel endothelial cell receptor 1 (LYVE-1), binds HA for immune cell motility and HA metabolism but was not discussed in detail due to its low expression in the lungs. Nevertheless, CD44 and LYVE-1 jointly assist in immune cell migration within the lymphatic system³¹⁶⁻³¹⁸ to traffic cells to the lungs during bacterial pneumonia. HA-hyaladherin interactions additionally assist with leukocyte motility. In summary, changes in the extracellular matrix impact cellular signaling in bacterial pneumonia that can be exacerbated by excessive alcohol use but there is still much to learn. Nevertheless, targeting hyaladherins may be a potential therapeutic strategy for mitigating lung injury in those with alcohol use disorders. These pathways have been summarized in **Figure 4.3.1**.

Controversies in the Hyaluronic Acid Field

Is increased HA production during lung disease pathological and does it need to be “fixed?” HA concentration increases, but average molecular weight decreases, in multiple pulmonary diseases involving immune dysfunction and inflammation. However, the mechanisms of HA signaling based on variations in molecular weight remain controversial in the field. Increased HA production appears to decrease leukocyte mobility and bacterial spread in pneumonia due to higher viscosity. However, increased HA production may aid in leukocyte motility through endogenous hyaladherins while preventing bacterial spread because of their lack of the same receptors.

Further, fragmented HA is thought to be pro-inflammatory while endogenous high molecular weight HA is anti-inflammatory^{203,235,242}. It is also clear that bacteria contain hyaluronidases to degrade host HA matrices, and fragmented HA can act as a danger associated molecular pattern for immune cell release of key immune factors. Our group has hypothesized that alcohol increases high molecular weight HA synthesis, thereby decreasing necessary proinflammatory signaling from fragmented HA. Alternatively, alcohol exposure may increase LMW HA rather than HMW HA, resulting in alternative immune signaling, thus the molecular weight of HA following chronic alcohol use will need to be determined in future studies. However, size classifications remain controversial in the field since “fragmented HA” or “low molecular weight HA” could range from HA chains of a few polysaccharides to 500 kD, and the mechanisms of HA immune signaling have yet to be fully elucidated. Future studies should be done to clarify the immune response of leukocytes to different sized HA polymers to confirm past results.

Therapeutic Potential

Although the risk of AUD individuals for getting sepsis and ARDS from pneumonia is approximately double that of non-AUD individuals⁴, treatment strategies are comparable between AUD and non-AUD individuals. There are several FDA approved modulators of HA or HA binding proteins that are available by prescription or as a clinical treatment; however, additional studies on HA modulation in bacterial pneumonia and alcohol are needed before therapeutic targeting of these pathways in people with AUD can take place. Targeting bacterial protein influence in host HA matrices and barrier dysfunction go hand-in-hand. As bacteria spread and host lung cell apoptosis persists, cellular barriers are broken down. Use of current small molecule inhibitors of bacterial hyaluronidases are insufficient as a therapeutic strategy because they have low specificity and potency. Bacteria contain some hyaluronidases that are different than those in humans. Therefore, upregulation of host defenses against bacterial hyaluronidases, like HABP1, may work as an alternative treatment to prevent uncontrolled bacterial proliferation.

Proposed mechanisms of EtOH-induced oxidative stress in alveolar macrophages include loss of PPAR γ activity^{10,46,48}, which is diminished following alcohol exposure^{46,48,60}. Rosiglitazone and pioglitazone, PPAR γ agonists, improve EtOH induced alveolar macrophage signaling from fragmented HA. However, size classifications remain controversial in the field. Future studies should be done to clarify the immune oxidative stress⁴⁷, mitochondrial-derived ROS⁵⁹, and dysfunctional phagocytosis and clearance of *K. pneumoniae*⁴⁶. Further, pioglitazone, reversed alcohol-induced derangements phagocytosis in alveolar macrophages^{46,48,60}. Because

mitochondrial derived ATP is necessary for high energy processes, like phagocytosis, impaired mitochondrial function is one explanation for why alcohol impairs alveolar macrophage phagocytic capacity. Identifying alcohol-induced mechanisms that impair HA signaling could further elucidate underlying mitochondrial dysfunction in alveolar macrophages.

In conclusion, AUDs increase the risk of respiratory infections and levels of the extracellular matrix component, HA, are increased in chronic respiratory diseases. HA signaling through hyaladherins are affected by alcohol use, which could modify inflammation and immune cell activity during bacterial pneumonia. The role of hyaladherins in alcohol-induced immune dysfunction is still largely unknown. This mini review highlights the necessity for future studies to provide insight into understanding the role of HA and its binding partners in host immune defense following excessive alcohol use.

Conflict of Interest: The authors declare that the research was conducted in the absence of any commercial or financial relationships that could be construed as a potential conflict of interest.

Publisher's Note: All claims expressed in this article are solely those of the authors and do not necessarily represent those of their affiliated organizations, or those of the publisher, the editors, and the reviewers. Any product that may be evaluated in this article, or claim that may be made by its manufacturer, is not guaranteed or endorsed by the publisher.

Copyright © 2022 Crotty and Yeligar. This is an open-access article distributed under the terms of the Creative Commons Attribution License (CC BY). The use, distribution or reproduction in other forums is permitted, provided the original author(s) and the copyright owner(s) are credited and that the original publication in this journal is cited, in accordance with accepted academic practice. No use, distribution or reproduction is permitted which does not comply with these terms.

Acknowledgements: The authors would like to acknowledge the Emory University Molecular and Systems Pharmacology Program and the Atlanta VA Health Care System for their continued support.

Figures

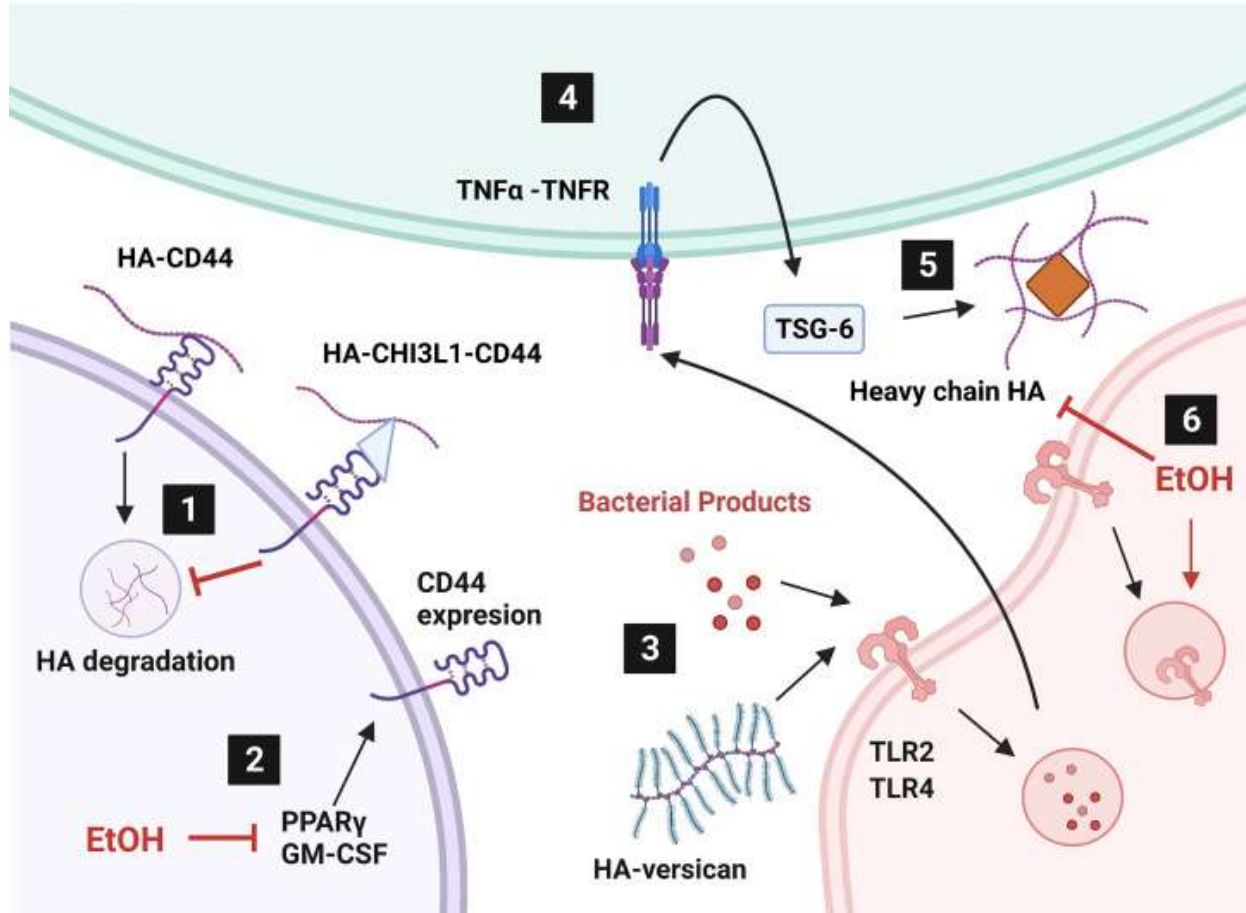


Figure 4.3.1: Alcohol affects hyaladherin signaling in the lung. 1) Internalization and degradation of hyaluronic acid (HA) is inhibited by overproduction of chitinase-3 like-protein-1 (CHI3L1). 2) Ethanol (EtOH) diminishes peroxisome proliferator activated receptor gamma (PPAR γ) and granulocyte-macrophage colony stimulating factor (GM-CSF) levels. 3) HA-versican competes with bacterial products for toll-like receptor (TLR) signaling. 4) TLR signaling induces tumor necrosis factor alpha (TNF- α) production. TNF- α stimulates TNF- α -stimulated gene-6 (TSG-6) expression. 5) TSG-6 catalyzes heavy chain HA matrix formation through pentatraxin 3 (PTX3, orange diamond). 6) EtOH induces TLR4 internalization and heavy chain formation by decreasing TNF- α . Created with BioRender.com.

4.4 Application of Hyaluronic Acid in Pulmonary Hypertension

I contributed to an additional co-author publication (PMC9676077) describing the implications of altered hyaluronic acid metabolism in pulmonary hypertension. Many of these findings are parallel to the preliminary data I have collected on changes in ethanol-induced hyaluronic acid metabolism. These results provide a possible mechanism by which HMW HA synthesis is promoted, which can be investigated in the context of alcohol misuse in future studies:

Pulmonary hypertension (PH) is a progressive disorder characterized by large-scale remodeling of the pulmonary vasculature mediated by enhanced pulmonary artery smooth muscle cell proliferation. Proposed treatments for PH to decrease vasoconstriction have been successful for some patients in reducing their mortality, but not in reversing their vascular remodeling. Vascular remodeling involving increased cell proliferation still leads to reduced quality of life because of decreased cardiac output, leading to dyspnea and cardiac fatigue. Targeting the mechanisms underlying vascular remodeling, involving smooth muscle cell proliferation, reduced apoptosis, and reduced mitochondrial bioenergetics could lead to future development of PH therapies.

PH is characterized by enhanced smooth muscle cell proliferation by resistance to apoptosis signals³¹⁹, increased mitochondrial-derived reactive oxygen species generation, and decreased mitochondrial function³²⁰. Pulmonary vascular remodeling is associated with metabolic imbalances³²¹, including altered mitochondrial number, fragmentation³²²⁻³²⁴, and a shift toward glycolysis-derived ATP production³²⁵. Additionally, in a rat model of PH, PASMCs had decreased mitochondrial function

caused by a loss in activity of the electron transport chain complexes, and increased levels of mitochondrial-derived ROS, membrane potential, and glycolysis³²⁶.

Another characteristic of pulmonary hypertension is hyper synthesis of the glycosaminoglycan, hyaluronic acid. In our collaboration with Dr. C. Michael Hart's lab, we aimed to see if high molecular weight hyaluronic acid (HMW HA) prevented human pulmonary artery smooth muscle cell (HPASMC) apoptosis induced by mitochondrial depolarization from carbonyl cyanide m-chlorophenyl hydrazone (CCCP). Apoptosis was confirmed via Annexin-V-FITC and propidium iodide (PI) detection by flow cytometry. After incubation with CCCP or vehicle control, HPASMCs were trypsinized and viable cell counts were collected before proceeding. HPASMCs were rinsed with 1X PBS, centrifuged, and resuspended with 500 μ L FACS buffer (PBS + 0.01% Sodium Azide + 1% fetal bovine serum). Cells were labeled with 50 mcg / mL of Annexin-V and PI. A BD Accuri C6 Plus Flow Cytometer (Franklin Lakes, NJ) was used to measure cell fluorescence for over 300,000 events. Gating was based on PI and zombie NIR staining, as well as FSC / SSC plots to eliminate debris. Final results show mean Annexin V-FITC fluorescence relative to uninduced controls.

We concluded that elevated levels of HMW HA induced apoptosis resistance. Overall, this manuscript showed that in pulmonary hypertension there is hyper synthesis of HMW HA by HA synthase 2, and this extracellular matrix phenotype promotes metabolic dysfunction and vascular remodeling^{224,327}. **Figure 4.4.1** shows my contribution toward this manuscript.

Figure 4.4.1

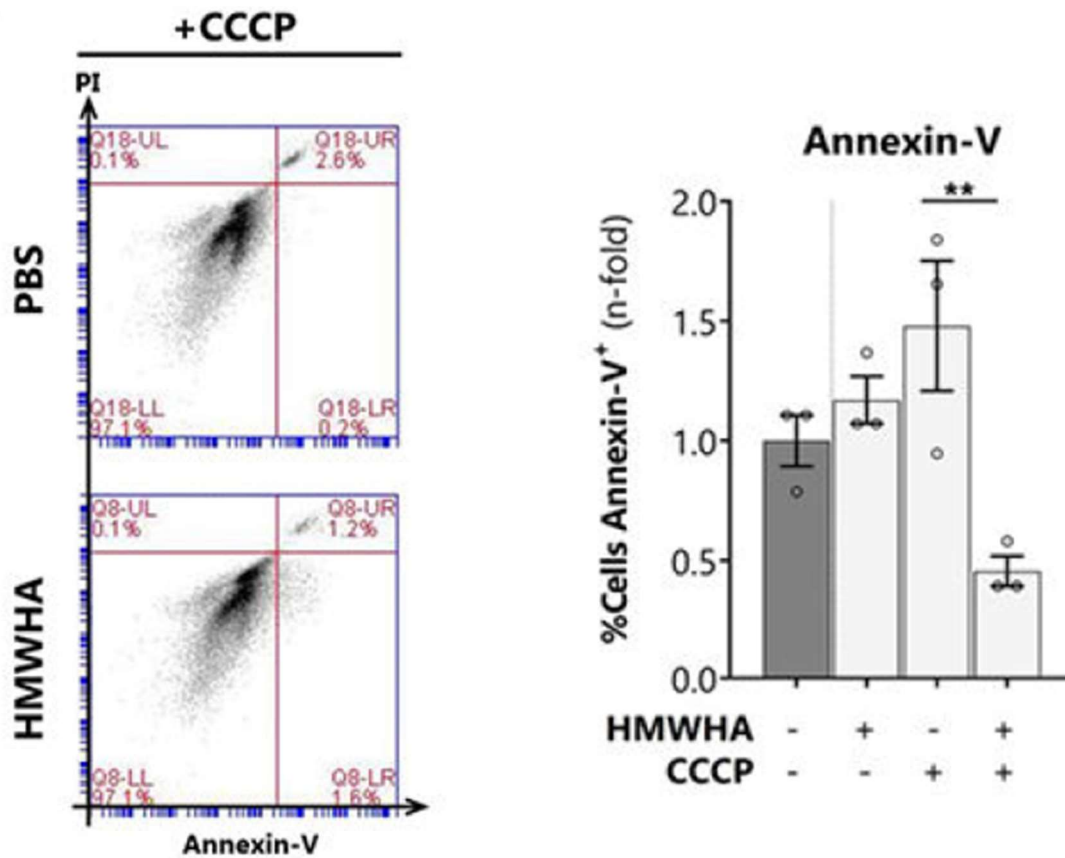


Figure 4.4.1: Measurement of human pulmonary artery smooth muscle cells (HPASMC) apoptosis Annexin-V staining, corresponding to intermediate-to-late apoptosis, determined by flow cytometry. Data expressed as mean \pm SEM **p < 0.01 by 2-way ANOVA of [HMW HA x CCCP].

4.4. Conclusions

Between 2020-2022, hyaluronic acid (HA) became a household name due to its use in skin care products, but HA is much more than an ingredient in hydrating facial serums. Our results and review of past studies show that changes in HA metabolism may be involved in pulmonary diseases involving pulmonary hypertension and community-acquired pneumonia. Several controversies were discussed, including the inaccessible technology required to measure low concentrations of HA and average HA molecular weight. Due to these limitations, I was unable to investigate the effect of disordered AM HA metabolism during chronic alcohol use. Ultimately, we determined that AMs do not contribute significantly to HA pools in the lung, but their function can be modified by external HA. This leads us to believe that HA produced by other cell types in the lung, such as alveolar type II epithelial cells, may affect AM functions, possibly leading to decreased AM mitochondrial respiration and phagocytic capacity.

Additionally, we were unable to measure HA molecular weight following chronic alcohol exposure in AMs, but previous studies clearly indicate that HA molecular weight can influence HA binding protein signaling (Chapter 4.3). HA molecular weight was measured in the lungs of mice in the paper by Tseng et al. (Chapter 4.4) but was not specifically measured in AMs. This manuscript provides a mechanism of HA hyper synthesis that could apply to chronic alcohol-induced hyper synthesis of HA (Chapter 4.2). HA binding protein 1 (HABP1), otherwise known as p32, could be a mechanism by which HMW HA diminishes mitochondrial function. Since HABP1 can be mitochondrial, signaling via HA-HABP1 interactions may provide a targetable mechanism for mitigating HMW HA-induced diminished mitochondrial respiration (Fig. 4.2.3 C-E). Future studies

are still needed to examine HA molecular weight during alcohol misuse, the role of alveolar type II epithelial cell's extracellular matrix on AMs, and if alcohol has an influence on disordered intracellular communication and mitochondrial functioning via changes in HA metabolism.

Chapter 5: Perspectives & Contributions Toward Other Fields

5.1 Perspectives

Known as the “powerhouse of the cell,” mitochondria are perhaps the most famous organelle. While this statement is certainly true, mitochondria are essential for determining cell function and fate. Mitochondria can move, divide, fuse, or self-destruct depending on cellular needs. In fact, these organelles can regulate cell signaling, division, or controlled cell death. Additionally, mitochondria are in nearly every human cell type, apart from red blood cells. Thus, any alteration in controlled mitochondrial biology has the potential to be catastrophic from the cellular to the organismal level.

Every cell type will have mitochondrial needs that differ, and these needs will change across the cell’s life cycle. It is thought that cells get 80% of their energy needed from oxidative phosphorylation in the mitochondria³²⁸, but this is an oversimplification. Many cells can switch metabolic phenotypes to drive energy production via glycolysis rather than oxidative phosphorylation. In 1927, Otto Warburg reported that tumors used between 5 and 35 times the amount of glucose as non-cancerous cells, and that lactic acid production correlated with glucose usage. Warburg’s observation indicated that tumors use fermentation rather than respiration for survival, but that fermentation was not necessary for survival. This phenomenon, known as the Warburg effect, is thought to be one characteristic of proliferating cancer cells³²⁹. However, we now know that non-cancerous cells also switch phenotypes and undergo the Warburg effect to drive division, such as during fetal development³³⁰ or immune cell proliferation^{331,332}. Further, cancerous cells do not need the Warburg effect to be proliferative, as tumors persist in the absence of glucose³²⁹. In fact, decreased aerobic respiration and glycolysis in

cancer cells may be a defense against harmful buildup of oxidative stress³³⁰.

Comparatively, cell senescence requires an alternative mitochondrial energy phenotype. Altogether, mitochondria are heterogeneous and require refined quality control mechanisms in non-pathologic cell types, and when these signals are disturbed, disease states arise.

In particular, our work heavily involved measuring mitochondrial respiration and several characteristics of mitochondrial bioenergetics including basal respiration, ATP-linked respiration, maximal respiration, spare respiratory capacity, and fuel flexibility. Cell growth or senescence can impact basal respiration and ATP-linked respiration and these bioenergetic measurements give researchers an idea of the cells' current mitochondrial phenotype. A lower or higher basal respiration or ATP-linked respiration may not be reason for concern but necessitates further investigation. However, an altered maximal respiration, spare respiratory capacity, or fuel flexibility could indicate a greater or impaired ability to shift energetic phenotype in a time of need. As is important with any scientific study, multiple measures of cellular metabolism or phenotype should be gathered to conclude how a particular treatment, condition, or disease affects cell function.

Immune cells are especially dependent on mitochondrial phenotypic changes to control activation state and inflammatory responses³³³. Immune cells have tissue-specific responses to inflammation and antigen presentation. While effector T cells prioritize glycolysis, memory and regulatory T cells rely more on fatty acid oxidation³³⁴. Further, canonically activated immune cells prefer the Warburg effect to oxidative phosphorylation^{331,332}. Additionally, immune cells rely on regulated MT-derived ROS,

which are not only a byproduct of the electron transport chain, but also serve as signaling molecules and defense against invading pathogens. Our studies so far have highlighted the role of alveolar macrophage oxidative stress and mitochondrial bioenergetics during chronic alcohol use, but because of the multifaceted role of mitochondria in controlling cell fate, there is much more still to be discovered. Similarly, we can use the effect of chronic alcohol exposure on AMs as an example to form future hypotheses surrounding mitochondrial dysfunction in other cell types. As the mitochondrial biology and immunometabolism fields grow, we must recognize and continue to challenge oversimplifications of complex cellular metabolism.

5.2 Collaborations & Contributions to Other Fields

Fortunately, during my time in the Yeligar lab, I was able to perform bioenergetics assays on primary and cultured human cells in order to contribute a piece to the complex puzzle that is cellular metabolism. Animal models can only go so far in modeling how human diseases progress, and when available, isolated human cells or organoids should be used to further develop therapeutics. This can include the use of primary or cultured human cells that do not require animal sacrifice for experimental testing. In particular, I was able to perform bioenergetics testing on human alveolar macrophages, human pulmonary artery smooth muscle cells, human aortic smooth muscle cells (Ch. 5.2.2), human antigen producing cells, and human embryonic kidney (HEK293T) cells (Ch. 5.2.1). This chapter briefly describes my contribution toward two submitted manuscripts (one accepted, PMC10259180) and the contributions to each respective field.

5.2.1 Regulator of G protein Signaling 14 Affects Mitochondrial Function in Human Embryonic Kidney 293T Cells

Regulator of G protein signaling 14 (RGS14) is an important modulator of neuronal excitability in the hippocampus and is protective against neuronal loss in temporal lobe epilepsy^{335,336}. Previously, loss of RGS14 in mice accelerated seizure activity and significantly altered gene expression of proteins involved in mitochondrial function and regulation of oxidative stress. In our collaboration with Dr. John Hepler, we aimed to see if RGS14 expression affected mitochondrial respiration in human embryonic kidney cells (HEK293T). HEK293 cells do not express RGS14, so expression was induced by plasmid transfection.

Excerpt from Harbin, et al.: Measurement of mitochondrial respiration using seahorse XF cell mitochondrial stress test in HEK293T cells.

“The measurement of mitochondrial respiration was performed as previously described with modifications⁵⁹. Briefly, HEK293T cells were cultured in Dulbecco’s essential medium (DMEM; Gibco, 11–995-040) supplemented with 10% fetal bovine serum and 1% penicillin/streptomycin and incubated at 37 °C, 5% CO₂ until the time of seeding or passaging. Cells were maintained by passaging every 2–3 days when cells reached 70–80% confluency. Mitochondrial respiration was evaluated using a XFe96 Extracellular Flux Analyzer (Agilent Seahorse Bioscience Inc., Billerica, MA) and Seahorse CF Cell Mito Stress Test Kit (Agilent, 103,015–100) according to manufacturer’s instructions. Briefly, cells were seeded into a Seahorse XFe96 microplate (Agilent, 103,794–100) at 15,000 cells/well and incubated for 24 h at 37 °C,

5% CO₂. FLAG-RGS14 or pcDNA3.1 (negative control) plasmids³³⁷. were transiently transfected using transfection medium DMEM supplemented with 5% FBS and 1% penicillin/streptomycin and polyethyleneimine (PEI) as the transfection reagent. Cells were then incubated for 24 h at 37 °C, 5% CO₂ to ensure adequate expression of both constructs. After transfection, cells were switched to Seahorse XF Base Medium supplemented with 1 mM l-glutamine, 5.5 mM d-glucose, and 2 mM sodium pyruvate (pH of 7.4) and equilibrated in this medium for 30 min. Oxygen consumption rate (OCR) was measured prior to and after sequential treatment with 1 μM oligomycin (mitochondrial complex V inhibitor), 0.5 μM carbonilcyanide p-trifluoromethoxyphenylhydrazone (FCCP) (ATP synthase inhibitor and proton uncoupler), and 0.5 μM rotenone/antimycin A (Complex I/III inhibitor). Basal respiration, mitochondrial ATP-linked respiration, maximal respiration, proton leak, spare respiratory capacity, and non-mitochondrial linked respiration were determined using the XF Wave 2.1 software. Cell lysates were collected in lysis buffer, and Pierce BCA assay was used to determine protein concentration. OCR values were normalized to HEK293T protein concentration in the same sample and were expressed as mean ± SEM. Western immunoblotting to confirm protein expression was performed as stated above using anti-FLAG HRP-conjugated antibody (Sigma Aldrich, A8592; 1:15,000) to verify transfection and expression of FLAG-RGS14.”

Mito Stress Test in these cells revealed that RGS14 slightly decreased baseline and maximal mitochondrial respiration without altering ATP-linked respiration or spare capacity (**Fig. 5.2.1**). These parameters will need to be reassessed in a neuronal cell line or in tissue from control and epileptic animal models with RGS14 knockout to

confirm the role of RGS14 in mitochondrial respiration. Overall, this manuscript (PMC10259180) demonstrated that RGS14 is neuroprotective in a mouse model of epilepsy, and that RGS14 may be involved in mitochondrial respiration and oxidative stress regulation pathways³³⁸.

Full Citation: Harbin, N H et al. "RGS14 limits seizure-induced mitochondrial oxidative stress and pathology in hippocampus." *Neurobiology of disease* vol. 181 (2023): 106128. doi:10.1016/j.nbd.2023.106128

Figure 5.2.1

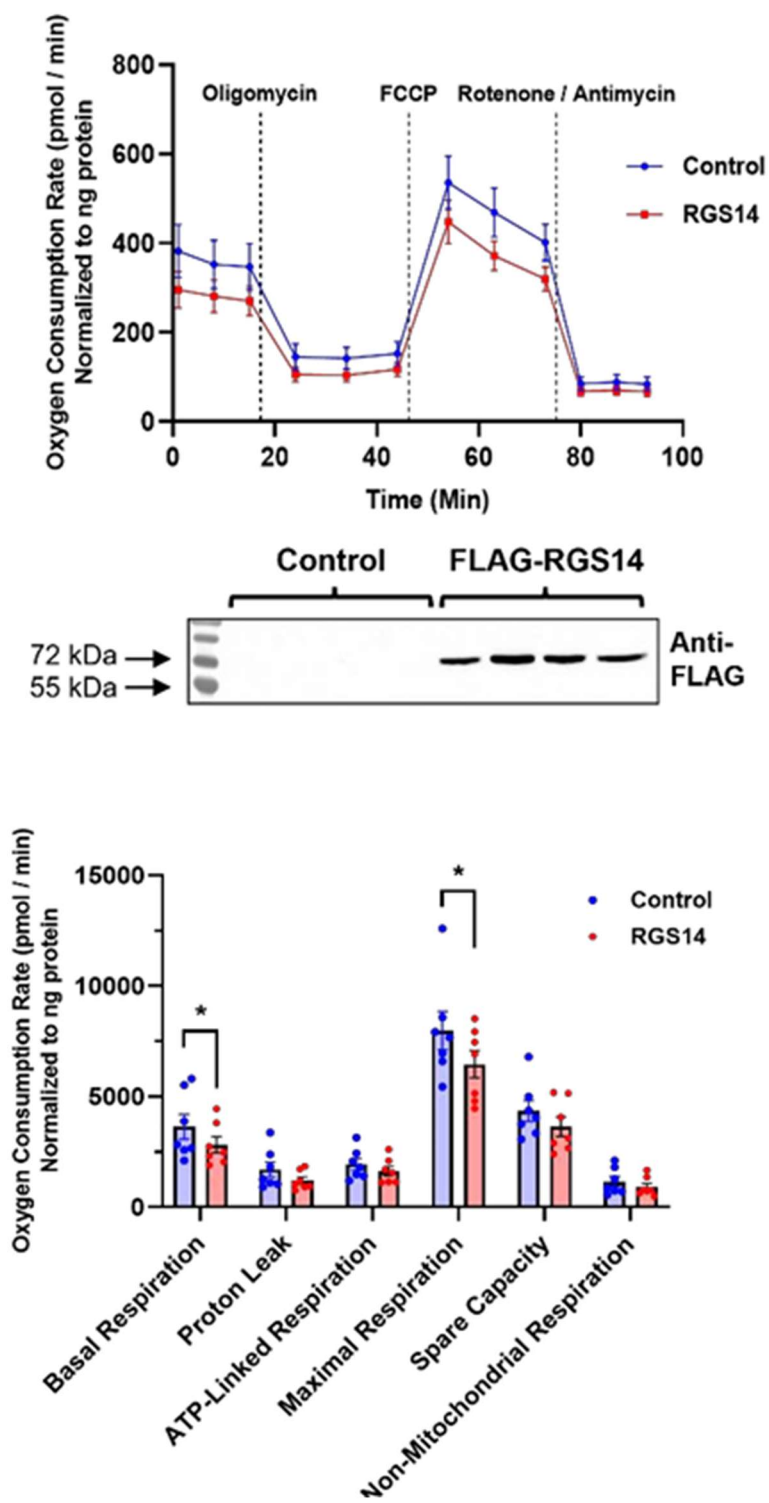


Figure 5.2.1: Regulator of G-protein signaling 14 (RGS14) decreases

mitochondrial respiration *in vitro*. Top left: Normalized oxygen consumption rate (OCR) plotted over time in HEK293T cells expressing pcDNA3.1 (control) or FLAG-RGS14 (RGS14, middle) during a mitochondrial stress test with injections of 2 μ M oligomycin, 0.5 μ M carbonyl cyanide-4-(trifluoromethoxy) phenylhydrazone (FCCP), and 0.5 μ M antimycin-A / rotenone. Measurements start at baseline and are followed by sequential treatments of cells with mitochondrial inhibitors oligomycin, FCCP, and rotenone/antimycin A. Bottom: Bar graphs summarizing the data obtained from the analysis of OCR profile (n=4-6).

5.2.2 Activation of ATP-Dependent Clp protease (ClpXP) Affects Mitochondrial Function in Human Aortic Smooth Muscle Cells

Aortic aneurisms are characterized by a structural remodeling of the vasculature whereby the vessel wall becomes increasingly thin until the point of rupture. Vascular smooth muscle cells have high plasticity and can maintain vessel structure by phenotypic and metabolic switching³³⁹. The ATP-dependent Clp protease (ClpXP) complex consists of a proteasome-like protease, ClpP, which degrades mitochondrial proteins with the help of a CLPX chaperone protein^{340,341}. In collaboration with Dr. Alejandra San Martin's lab, we aimed to see if ClpP activation by CLPX moderates a metabolic switch in human aortic smooth muscle cells. Overexpression of CLPX with an adenovirus (Ad_CLPX) decreased human aortic smooth muscle cell mitochondrial respiration including basal and ATP-linked respiration. Further, AD_CLPX shifted cells toward a more quiescent phenotype at baseline (**Figure 5.2.2**). Concomitantly, loss of ClpP using siRNAs decreased spare respiratory capacity and shifted cells toward a more glycolytic phenotype compared to scrambled control (**Figure 5.2.3**). Overall, the manuscript (in revision) shows that ClpXP can control the vascular phenotype and suppress aneurysm formation.

Figure 5.2.2

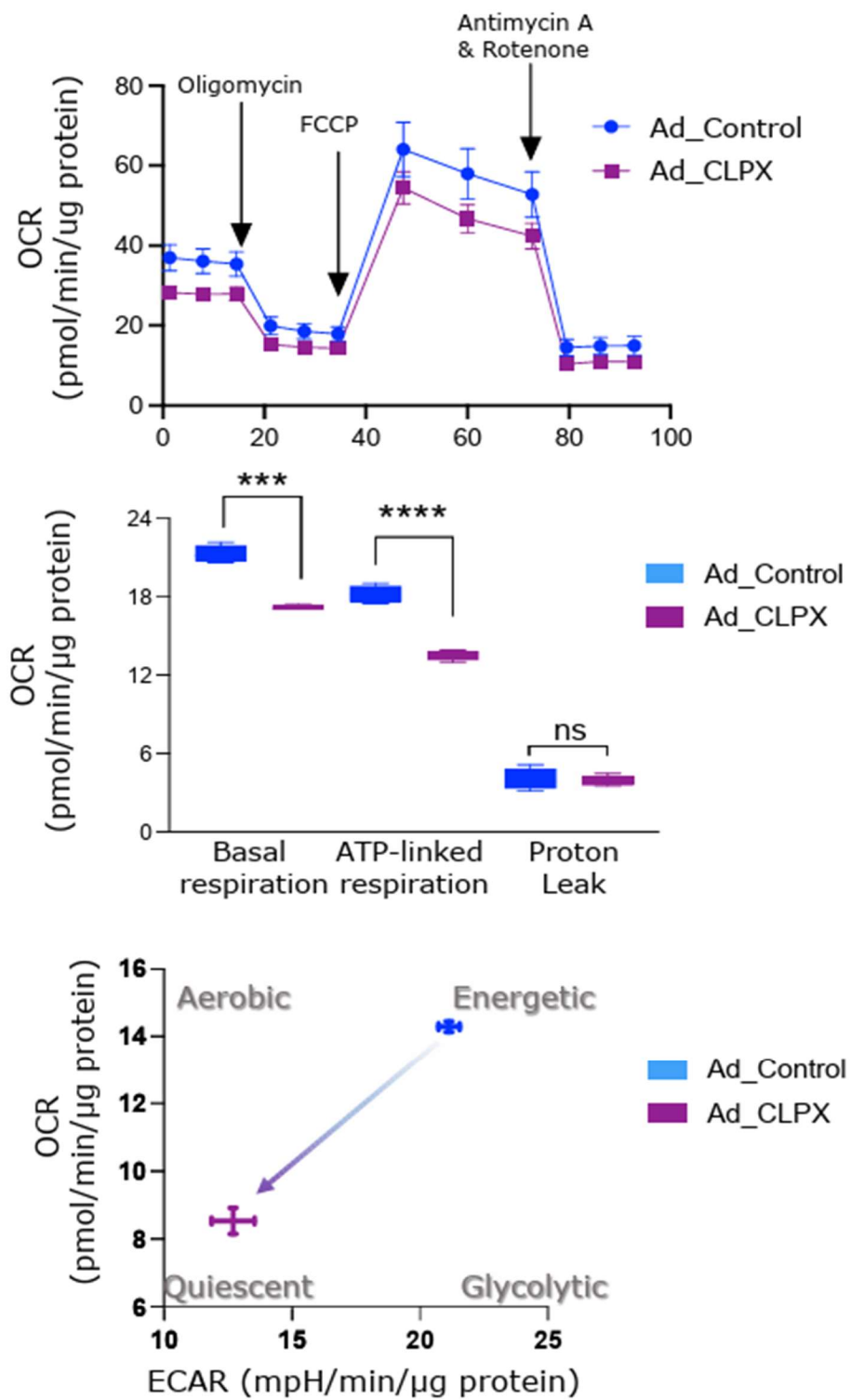


Figure 5.2.2: ClpXP chaperone protein (CLPX) decreases human aortic smooth muscle cell (HASMC) mitochondrial respiration and shifts cells toward a quiescent phenotype. Top: Profile of mitochondrial respiration over time in HASMCs expressing Ad_Control or Ad_CLPX. Basal OCR measurements were made, and 1 $\mu\text{g}/\text{mL}$ oligomycin, 1 μM carbonyl cyanide-4-(trifluoromethoxy) phenylhydrazone (FCCP), and 10 μM antimycin-A and 1 μM rotenone were then sequentially injected. Middle: Bar graphs summarizing the data obtained from the analysis of OCR profiles (basal corresponds to antimycin-A-inhibitable and ATP-linked corresponds to oligomycin-inhibitable). Bottom: Energy map showing the metabolic reprogramming induced by ClpXP gain-of-function. All data are presented as mean \pm SEM from three to six independent experiments. P values were calculated by non-paired t-test.

Figure 5.2.3

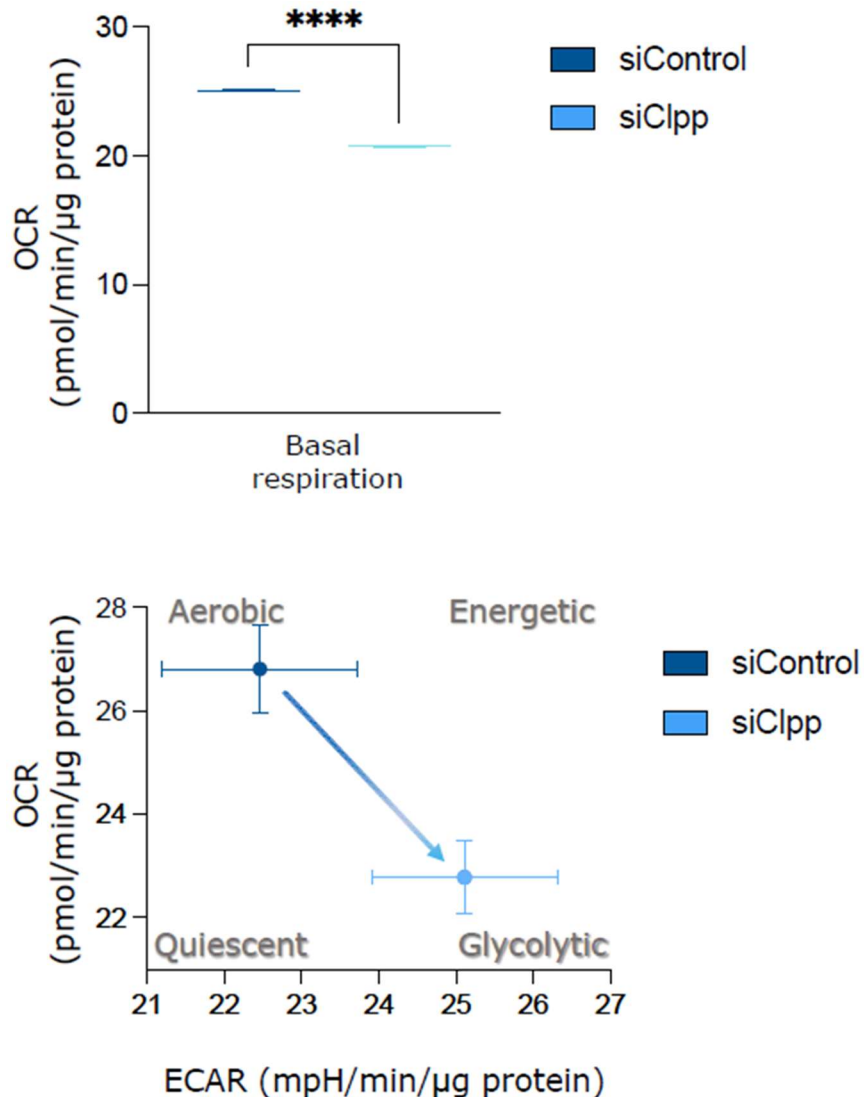


Figure 5.2.3: ATP-dependent Clp protease (ClpXP) loss-of-function inhibits respiration and induces glycolytic reprogramming in human aortic smooth muscle cell (HASMC). Top: Basal oxygen consumption rate measurements were made using a Seahorse analyzer in siControl and siClpx transfected HASMCs. Bottom: Energy map showing the metabolic glycolytic reprogramming induced by ClpXP loss-of-function. All data are presented as mean \pm SE from $n=15$. P values were calculated by non-paired t-test.

5.3 Conclusions

In combination with the previous chapters, oxidative stress and metabolic dysfunction are pathological phenotypic characteristics of cells that can lead to detrimental disorders in people. These two manuscripts highlighted in Chapter 5 agree that oxidative stress and metabolic dysfunction are central disease pathologies in temporal lobe epilepsy and aneurism formation. However, future studies will continue to uncover novel mechanisms of disease-associated metabolic dysfunction.

Chapter 6: Discussion & Future Directions

6.1 Discussion

In the United States, over 88,000 people die per year due to alcohol misuse³⁴², and alcohol-related healthcare costs add up to more than \$249 billion annually^{10,12}. Excessive ethanol (EtOH) use, associated with alcohol use disorders (AUD)¹⁹⁰, causes significant morbidity and mortality due to multi-organ dysfunction. The effects of chronic alcohol use are multifactorial and increase the risk of end-organ failure. Over the past four years of my time at Emory University, I have had the pleasure to attend conferences focused on how alcohol use leads to organ failure and how immune cell dysfunction contributes to injury. Common hot topics included how chronic or binge alcohol use impairs immune cell signaling or ability to respond to insult. In particular, alcohol disturbs pathogen recognition receptors (TLRs, etc.), inflammasome activation, chromatin reorganization, pro- and anti-inflammatory phenotypes, and loss of pathogen clearance systems (phagocytosis). Additionally, a hot topic in the field includes how alcohol use affects multi-organ cross talk, with a large focus on the gut microbiome and loss of barrier permeability across multiple organs. While I expect these subtopics within the field of alcohol and immunology to be fruitful in the future, the focus of this dissertation is on alveolar macrophage oxidative stress and metabolic dysfunction during chronic alcohol use.

In the lungs, EtOH misuse increases the risk of developing respiratory infections⁴² and acute respiratory distress syndrome (ARDS)⁴. Alveolar macrophages (AM) function as the first line of cellular defense against pathogens in the lower airway by coordinating immune responses¹⁹¹. Although previous studies have shown that EtOH

can impair AM phagocytosis due to increases in oxidative stress^{10,39,46,47}, the molecular mechanisms underlying these phenomena are largely unknown. The aim of this dissertation was to identify mechanisms of AM dysfunction and reveal new therapeutic targets for treating alcohol-induced lung injury and immune dysfunction during chronic alcohol use.

Chapters 2-4 included results gathered from AMs taken from Veterans with AUDs and non-AUD otherwise healthy control Veterans. Additionally, models of chronic alcohol exposure were used, including mice fed chronic alcohol in their drinking water compared to regular drinking water littermates and a murine AM cell line, MH-S. Overall, we expanded upon previously reported studies showing that EtOH exposed AMs have an altered metabolic phenotype and increased mitochondrial-derived oxidative stress relative to cells not exposed to EtOH. Chronic EtOH induced AM alternative metabolism and suppression of AM phagocytosis and clearance of *Staphylococcus aureus*, which is consistent with previous studies from our group. Additionally, we utilized three potential therapeutics to reverse functional deficits in AM. Zinc sulfate and S-adenosylmethionine (S-AMe) were used as antioxidant-aids to target EtOH-induced cellular and mitochondrial oxidative stress. S-AMe is a precursor to glutathione and was used due to the poor bioavailability of glutathione in humans, while zinc acts as a cofactor for antioxidant enzymes. An FDA-approved drug used for type II diabetes, pioglitazone (PIO), decreased oxidative stress and reversed alterations in the AM metabolic phenotype by acting as an agonist for PPAR γ , which plays a key role in mitochondrial function and in decreasing HIF-1 α levels (Ch. 3.1 and 3.2). The reversal in phenotype

resulted in a shift back toward oxidative phosphorylation rather than glycolysis for energy production.

Our results showed that oral zinc for two weeks in participants with AUDs was able to decrease cellular and mitochondrial-derived oxidative stress but did not improve phagocytosis. Chapters 2 and 3.2 contained samples from the same clinical trial (ExZACTO; ClinicalTrials.gov identifier: NCT01899521), meaning that within this group of people with AUDs, oral zinc sulfate and *ex vivo* PIO decreased AM oxidative stress. Pre-clinical studies administering zinc or glutathione to mice *in vivo* or AMs isolated from people with AUDs *ex vivo*, however, did show improvements in overall AM phagocytic capacity and redox homeostasis. I expect that many factors influenced these negative clinical trial results. First, the study was under-powered considering the variability of the participant population. Participants were matched for several factors (sex, smoking status, and age), but the cohort of participants had a wide range of co-morbidities, including people with pulmonary disorders (sleep apnea, pleural effusion, pulmonary embolism, COPD), and metabolic disorders (hypothyroidism, pancreatitis, diabetes) (**Table 3.2.1**). Further, over half of the participants were regular smokers, and smoking further impairs AM function^{343,344}, which may not be reversible by decreasing oxidative stress alone.

Smoking cigarettes acts as a 'second hit' for people with AUDs, and consistent with our human population (**Tables 2.1** and **3.2.1**), most people who drink alcohol also smoke³⁴⁵. Inherently, it would be wrong to only study alcohol misuse without including other environmental factors. For example, smoking and alcohol use together may cause a toxic buildup of aldehydes where only one environmental exposure may not³⁴⁶, thus

decreasing lung immunity by multiple mechanisms^{41,346,347}. The large number of smokers in the studies presented here does, however, confound our results. We do not know if zinc or SAME affected AM oxidative stress or phagocytic index in the non-smoking or smoking populations differently or if these supplements would be effective in one population over another.

Interestingly, we did not see a correlation between cellular or mitochondrial oxidative stress in people with AUDs (**Figure 2.8**). Since AM phagocytosis was not correlated in people with AUDs, and targeting oxidative stress with zinc or SAME did not improve AM phagocytosis, next we aimed to reverse AM metabolic derangements using the PPAR γ ligand, PIO. PPAR γ is a nuclear receptor that heterodimerizes with retinoid X receptors to regulate gene transcription^{178,348}. PPAR γ is well known for its role in fatty acid and glucose metabolism and ligands are effective in decreasing disease severity in multiple metabolic disorders³⁴⁹. Here we show that chronic EtOH exposure decreases the ability of AMs to metabolize mitochondrial fuels (glucose, glutamine, and long chain fatty acids) for efficient ATP production. ATP is important to AM phagocytosis because key proteins involved in recognition, uptake, degradation, and clearance of pathogens require ATP. For example, pathogen degradation requires an ATP-dependent transporter to acidify phagolysosomes³⁵⁰.

PIO was able to reverse many of the alterations in mitochondrial respiration driven by chronic EtOH exposure in AMs, including a Warburg-like effect whereby oxidative phosphorylation was diminished and glycolysis was ramped up. A previous study highlighted in Chapter 3.1 suggests that the EtOH-dependent phenotype could be explained by stabilization of HIF-1 α , but in Chapter 3.2 we show that knock down of

HIF-1 α was not able to reverse all of the metabolic derangements dependent on EtOH exposure *in vitro* (**Figure 3.2.4**). Indirect activity of PPAR γ in decreasing oxidative stress (**Figures 3.2.1D, 3.2.2B**)^{46,59,60,110} may explain partial reversal by PIO of metabolic derangements caused by EtOH-induced HIF-1 α activity. In turn, less HIF-1 α activity would decrease glucose transporters and glycolysis proteins that are upregulated during EtOH exposure, and the appearance of the Warburg effect would decrease without fully reversing AM metabolic dysfunction.

EtOH decreases GSH which promotes increased NADPH oxidase (NOX) enzyme activity¹¹². NOX enzymes use NADPH to reduce oxygen to superoxide in AM and contribute significantly to oxidative stress during chronic alcohol misuse^{59,112,113,351,352}. NOX4 expression induced by NOX1 and NOX2 activation causes phagocytic dysfunction in AMs¹¹³, and EtOH promotes NOX protein translation by post-translational mechanisms^{59,353}. Epigenetic mechanisms of alcohol-dependent changes in genome expression include methylation and deacetylation of histones to reorganize chromatin structure, and thus altering transcription factor access to promoter regions on DNA³⁵⁴. Additionally, several non-coding micro RNAs (miRNAs) have been implicated in increased NOX protein expression by suppressing transcription factor activity^{59,353}. Further, epigenetic remodeling is dependent on the metabolic state of cells since enzymes necessary for remodeling often require NAD, ATP, acetyl CoA, or S-adenosylmethionine (SAMe)³⁵⁴. However, alcohol metabolism decreases availability of these substrates³⁵⁴, leading to further disruption of the already disordered genome.

Once there is redox imbalance in the lung, oxidant sensitive protein activity is enhanced. We have shown that one such protein, HIF-1 α , is necessary for the shift

toward glycolytic phenotype during EtOH exposure in mouse AMs (**Chapter 3.1**)¹¹⁰ and is in part responsible for decreased mitochondrial pyruvate oxidation (**Fig. 3.2.4**). PIO pharmacologically reverses post-translational alterations leading to oxidative stress and metabolic dysfunction^{59,353}. The reversal of these post-translational alterations is enough to improve AM phagocytosis during chronic EtOH exposure^{59,60,110,353}. Yet, chromatin reorganization and post-translational modifications by miRNAs very likely negatively affect AM function in ways still undiscovered. For example, the molecular mechanisms underlying disturbed hyaluronic acid metabolism during chronic alcohol misuse are still unknown.

One characteristic of EtOH-induced metabolic dysfunction discovered here is hyper synthesis of hyaluronic acid (HA) by alveolar epithelial type II (ATII) cells. ATII cells are responsible for maintaining gas exchange in alveoli by production of surfactant and maintenance of the epithelial barrier. Chronic alcohol disrupts surfactant and barrier integrity due to loss of glutathione, loss of zinc, and increased NADPH oxidase activity and signaling^{43,116,117,120,352,355,356}. Additionally, alveolar epithelial cell HA deposition allows for immune cell motility, and past studies reported that AM interactions with the extracellular matrix play a role in lung injury repair and regulation of inflammation^{194,223,245}. AMs were expected to have altered HA production considering a glycolytic shift during chronic EtOH exposure because HA is synthesized from glycolysis intermediates. We found that AMs produce significantly less HA compared to ATII cells, and that chronic alcohol use in humans and chronic EtOH feeding in mice increased HA levels in bronchoalveolar fluid without altering AM-dependent HA synthesis (**Figure 4.2.2**). To determine the effect of excess alveolar HA on AM function we treated AMs

with excess HA at varied concentrations and molecular weights. Surprisingly, we found that high molecular weight HA decreased AM phagocytosis (**Figure 4.2.3**) and mitochondrial respiration relative to vehicle treated and low molecular weight HA treated cells.

Hyaluronidases and ROS fragment high molecular weight into low molecular weight HA^{57,58,200}. Based on these previous studies, we expected that AMs and ATII cells exposed to EtOH would have lower molecular weight HA than cells without EtOH, since EtOH increases oxidative stress (**Figure 3.2.2B**)^{46,49,50,59,113,357} and hyaluronidase expression in BAL fluid (**Figure 4.2.2E**). Since AMs produce so little HA, techniques to measure HA molecular weight were near impossible to perform. Future studies may be effective in measuring HA molecular weight from total lung homogenates, bronchoalveolar lavage fluid, or cultured ATII supernatants. Since ATII cells produce more HA than AMs (**Fig. 4.2.2D**) and altered extracellular HA concentration and molecular weight influence AM function (**Fig. 4.2.3 B-E**), studies that focus on intracellular communication may be more fruitful until techniques to measure low concentration polysaccharide molecular weight are more sensitive.

6.2 Future Directions

The studies presented included several limitations that could be addressed in future work. One consideration that I did not account for *in vitro* was the unique exposure of alveolar cells rapidly changing oxygen and carbon dioxide levels due to pulmonary respiration. Further, controlling for EtOH evaporation without starving the cells of oxygen over time was a challenge, and does not reflect how EtOH exposure occurs in the lungs. AMs were found to have high baseline oxygen consumption rates compared to vascular cells (Chapters 2 and 5), possibly due to higher mitochondrial content³⁵⁸, and were observed to look unhealthy when not exposed to filtered air flow. These factors likely could explain why there are subtle differences between mAM and MH-S cell metabolism (Chapter 3.2).

Further, alveolar macrophage populations are not homogeneous in mitochondrial bioenergetics or phagocytic capacity. Heterogeneous macrophage populations are apparent in these studies in the ability of cells to shift from a quiescent to energetic phenotype (Fig. 3.1.10) and the wide range of internalization and clearance of *Staphylococcus aureus* (Supplemental Fig. 4.2.2). In future studies, sorting macrophage populations following chronic EtOH exposure may help to identify why some AMs have decreased phagocytic capacity while others do not. One specific possibility is due to the loss of PPAR γ in phagocytosis-low populations and maintenance of PPAR γ levels in phagocytosis-high populations. Similarly, AM PPAR γ levels in nuclear and cytosolic fractions could be correlated with phagocytic abilities following pioglitazone treatment in EtOH-exposed cells. The Yeligar lab or other groups could perform these experiments

with a focus on PPAR γ or other proteins of interest (HIF-1 α , NOX4, SOD2, etc.) via flow cytometry or fluorescence microscopy.

Additionally, measuring reactive oxygen species using fluorescent probes is sometimes reportedly nonspecific, and there are more accurate techniques for measuring mitochondrial and cellular oxidative stress³⁵⁹. In fact, if molecular probes, like MitoSOX and DCFH-DA, were able to react with all reactive oxygen species, this would end up impairing cellular function because cells would no longer have physiological amounts of oxidative species. In turn, signaling by oxidative species would be impaired, thereby altering cellular function. More reliable measurements of superoxide include reduction of cytochrome c³⁵¹ or spin trapping followed by electron paramagnetic (spin) resonance (EPR)³⁶⁰ using recombinant SOD as a negative control. Otherwise, MitoSOX or other probe staining should be followed by liquid chromatography mass spectrometry (LC-MS) to confirm accumulation of the fluorescent byproduct. A recent *Nature Metabolism* review outlines limitations of commonly used redox sensitive probes, proper controls, and more sensitive methods for measuring oxidative species³⁵⁹. In future studies, isolated AM oxidative stress after alcohol exposure should be confirmed using these methods.

Another limitation of these studies was the minimal number of AMs that were isolated from mice, and the insufficient sample size in humans and mice to compare males and females. Often when designing these studies, we needed to optimize the usage of mAMs, which required pooling cells or omitting experiments that could have strengthened our findings. Subsequent animal experiments should fill these holes by increasing sample sizes of MT fuel flexibility and ATP production in mAMs. Further,

mouse and human studies should increase sample sizes for phagocytic index, oxidative stress measurements, and bioenergetics assays to compare differences between male and females. Considering that there were sex-dependent differences in mAM phagocytic index, we expect that mAM MT bioenergetics and human AM phagocytic index may differ between sexes, but low sample sizes and low power contributed toward us not finding sex-specific differences.

The clinical significance of these projects would be improved by examining how alcohol exposure impacts intracellular crosstalk in the alveolar space and if PIO remains effective in a model of bacterial pneumonia. As mentioned previously, examining crosstalk between different cell types and between organ systems is a novel area with much left to discover. Chronic alcohol use increases barrier permeability in multiple systems^{44,74,111}, allowing for leakage of unwanted molecules or proteins into unwanted spaces. Along with alcohol use, bacterial pneumonia also impairs barrier function, leading to detrimental lung damage in the form of ARDS or sepsis (infection of the blood stream)³⁶¹. Implementation of *in vitro* and *in vivo* models of chronic alcohol use and a common cause of community acquired pneumonia (*Streptococcus pneumoniae*, *Klebsiella pneumonia*, or *Staphylococcus aureus*) ± antibacterial agents (erythromycin or doxycycline) ± PIO could reveal if AM responses are improved in the presence of alcohol. Alternatively, PIO efficacy with first pass antibiotics + PIO could be compared to less common antibiotic treatments. For example, comparing erythromycin + PIO to a high dose respiratory fluoroquinolone or a combination of oral beta-lactam and macrolide, as is recommended for people with AUDs³⁶². Following pneumonia pathogenesis and treatments, AM oxidative stress, MT bioenergetics, and phagocytic

index could then be compared to determine if PIO would potentially be effective in people with AUDs who present to the hospital with community acquired pneumonia.

Finally, much work will need to be done to end the stigma against thiazolidinediones, like PIO, especially if PIO can increase the efficacy of antibiotics to clear pneumonias in people with AUDs. Chapter 3.2 briefly mentions the controversy surrounding PPAR γ ligands as drugs. Historically, thiazolidinediones caused liver, kidney, and cardiac toxicity, which eventually lead to the removal of troglitazone from the United States market. Rosiglitazone and pioglitazone are still FDA approved; however, rosiglitazone has increased risk for toxicity compared to pioglitazone¹⁸⁵⁻¹⁸⁸, and therefore is contraindicated in people with AUDs who may have multi-organ damage. Considering the low risk of organ toxicity, PIO use may be more beneficial at lower doses or in the short term. Future pre-clinical and clinical trials going forward should consider these risks before subjecting animals or humans with and without AUDs to potentially harmful treatments.

In summary, this dissertation describes an altered metabolic phenotype in alveolar macrophages exposed to chronic alcohol and the use of agents targeting cellular oxidative stress and transcription of metabolic genes to in part reverse the observed alcohol-induced phenotype. Yet, the effect of chronic alcohol use is not identical across diverse groups of people, organ systems, or cell types. Likewise, redox homeostasis and metabolic control differ within heterogeneous populations of cells of the same type. However, oxidative stress and mitochondrial dysfunction are at the center of several diseases, and immunometabolism is a promising field for discoveries in medicine to be made.

References

- 1 Basham, W. R. On the Effects of Alcohol, or Spirit-Drinking, in Diseases of the Liver: Delivered at Westminster Hospital. *Atlanta Med Surg J* **6**, 731-743 (1861).
- 2 William Osler, T. M. *The principles and practice of medicine :designed for the use of practitioners and students of medicine*. Eighth Edition edn, (Appleton and Company, 1892).
- 3 Saitz, R., Ghali, W. A. & Moskowitz, M. A. The impact of alcohol-related diagnoses on pneumonia outcomes. *Arch Intern Med* **157**, 1446-1452 (1997).
- 4 Moss, M. *et al*. Chronic alcohol abuse is associated with an increased incidence of acute respiratory distress syndrome and severity of multiple organ dysfunction in patients with septic shock. *Crit Care Med* **31**, 869-877 (2003).
<https://doi.org/10.1097/01.CCM.0000055389.64497.11>
- 5 Goss, C. H. *et al*. Cost and incidence of social comorbidities in low-risk patients with community-acquired pneumonia admitted to a public hospital. *Chest* **124**, 2148-2155 (2003). <https://doi.org/10.1378/chest.124.6.2148>
- 6 Seitz, H. K. *et al*. Alcoholic liver disease: from pathophysiology to therapy. *Alcohol Clin Exp Res* **29**, 1276-1281 (2005).
<https://doi.org/10.1097/01.alc.0000171896.37022.f7>
- 7 Moss, M. Epidemiology of sepsis: race, sex, and chronic alcohol abuse. *Clin Infect Dis* **41 Suppl 7**, S490-497 (2005). <https://doi.org/10.1086/432003>
- 8 Jerrells, T. R. *et al*. Association of chronic alcohol consumption and increased susceptibility to and pathogenic effects of pulmonary infection with respiratory

- syncytial virus in mice. *Alcohol* **41**, 357-369 (2007).
<https://doi.org/10.1016/j.alcohol.2007.07.001>
- 9 Mehta, A. J. & Guidot, D. M. Alcohol abuse, the alveolar macrophage and pneumonia. *Am J Med Sci* **343**, 244-247 (2012).
<https://doi.org/10.1097/MAJ.0b013e31823ede77>
- 10 Yeligar, S. M. *et al.* Alcohol and lung injury and immunity. *Alcohol* **55**, 51-59 (2016). <https://doi.org/10.1016/j.alcohol.2016.08.005>
- 11 White, A. M., Castle, I. P., Powell, P. A., Hingson, R. W. & Koob, G. F. Alcohol-Related Deaths During the COVID-19 Pandemic. *JAMA* **327**, 1704-1706 (2022).
<https://doi.org/10.1001/jama.2022.4308>
- 12 Sacks, J. J., Gonzales, K. R., Bouchery, E. E., Tomedi, L. E. & Brewer, R. D. 2010 National and State Costs of Excessive Alcohol Consumption. *Am J Prev Med* **49**, e73-e79 (2015). <https://doi.org/10.1016/j.amepre.2015.05.031>
- 13 Substance & (SAMHSA), A. a. M. H. S. A. 2019 National Survey on Drug Use and Health (NSDUH). Table 5.4A – Alcohol Use Disorder in Past Year among Persons Aged 12 or Older, by Age Group and Demographic Characteristics: Numbers in Thousands, 2018 and 2019.
(<https://www.samhsa.gov/data/sites/default/files/reports/rpt29394/NSDUHDetailedTabs2019/NSDUHDetTabsSect5pe2019.htm>).
- 14 Substance & (SAMHSA), A. a. M. H. S. A. 2021 National Survey on Drug Use and Health (NSDUH). Table 5.6A – Alcohol Use Disorder in Past Year: Among People Aged 12 or Older; by Age Group and Demographic Characteristics, Numbers in Thousands,

- 2021.(<https://www.samhsa.gov/data/sites/default/files/reports/rpt39441/NSDUHDetailedTabs2021/NSDUHDetailedTabs2021/NSDUHDetTabsSect5pe2021.htm>).
- 15 Organization, W. H. Global status report on alcohol and health. *World Health Organization, Geneva* (2018).
- 16 Centers for Disease Control and Prevention, N. C. f. H. S. U. C. o. D.-o. C. W. O. D., released in 2020. Data are from the Multiple Cause of Death Files, 1999-2019, as compiled from data provided by the 57 vital statistics jurisdictions through the Vital Statistics Cooperative Program. Accessed at <http://wonder.cdc.gov/ucd-icd10.html> on Sep 9, 2021 7:39:39 PM.
- 17 Bouchery, E. E., Harwood, H. J., Sacks, J. J., Simon, C. J. & Brewer, R. D. Economic costs of excessive alcohol consumption in the U.S., 2006. *Am J Prev Med* **41**, 516-524 (2011). <https://doi.org/10.1016/j.amepre.2011.06.045>
- 18 Gray, J. I. & Farber, D. L. Tissue-Resident Immune Cells in Humans. *Annu Rev Immunol* **40**, 195-220 (2022). <https://doi.org/10.1146/annurev-immunol-093019-112809>
- 19 de la Monte, S. M. & Kril, J. J. Human alcohol-related neuropathology. *Acta Neuropathol* **127**, 71-90 (2014). <https://doi.org/10.1007/s00401-013-1233-3>
- 20 Coleman, L. G., Jr., Zou, J. & Crews, F. T. Microglial-derived miRNA let-7 and HMGB1 contribute to ethanol-induced neurotoxicity via TLR7. *J Neuroinflammation* **14**, 22 (2017). <https://doi.org/10.1186/s12974-017-0799-4>
- 21 Crews, F. T. *et al.* Neuroimmune Function and the Consequences of Alcohol Exposure. *Alcohol Res* **37**, 331-341, 344-351 (2015).

- 22 Henriques, J. F. *et al.* Microglia and alcohol meet at the crossroads: Microglia as critical modulators of alcohol neurotoxicity. *Toxicol Lett* **283**, 21-31 (2018).
<https://doi.org/10.1016/j.toxlet.2017.11.002>
- 23 Crews, F. T., Qin, L., Sheedy, D., Vetreno, R. P. & Zou, J. High mobility group box 1/Toll-like receptor danger signaling increases brain neuroimmune activation in alcohol dependence. *Biol Psychiatry* **73**, 602-612 (2013).
<https://doi.org/10.1016/j.biopsych.2012.09.030>
- 24 Alfonso-Loeches, S., Pascual-Lucas, M., Blanco, A. M., Sanchez-Vera, I. & Guerri, C. Pivotal role of TLR4 receptors in alcohol-induced neuroinflammation and brain damage. *J Neurosci* **30**, 8285-8295 (2010).
<https://doi.org/10.1523/JNEUROSCI.0976-10.2010>
- 25 Pascual, M., Balino, P., Alfonso-Loeches, S., Aragon, C. M. & Guerri, C. Impact of TLR4 on behavioral and cognitive dysfunctions associated with alcohol-induced neuroinflammatory damage. *Brain Behav Immun* **25 Suppl 1**, S80-91 (2011). <https://doi.org/10.1016/j.bbi.2011.02.012>
- 26 Asquith, M. *et al.* Chronic ethanol consumption modulates growth factor release, mucosal cytokine production, and microRNA expression in nonhuman primates. *Alcohol Clin Exp Res* **38**, 980-993 (2014). <https://doi.org/10.1111/acer.12325>
- 27 Bala, S. *et al.* Circulating microRNAs in exosomes indicate hepatocyte injury and inflammation in alcoholic, drug-induced, and inflammatory liver diseases. *Hepatology* **56**, 1946-1957 (2012). <https://doi.org/10.1002/hep.25873>

- 28 Coleman, L. G. The emerging world of subcellular biological medicine: extracellular vesicles as novel biomarkers, targets, and therapeutics. *Neural Regen Res* **17**, 1020-1022 (2022). <https://doi.org/10.4103/1673-5374.324846>
- 29 Crenshaw, B. J. *et al.* Alcohol Modulates the Biogenesis and Composition of Microglia-Derived Exosomes. *Biology (Basel)* **8** (2019). <https://doi.org/10.3390/biology8020025>
- 30 Montesinos, J., Alfonso-Loeches, S. & Guerri, C. Impact of the Innate Immune Response in the Actions of Ethanol on the Central Nervous System. *Alcohol Clin Exp Res* **40**, 2260-2270 (2016). <https://doi.org/10.1111/acer.13208>
- 31 Crews, F. T., Zou, J. & Coleman, L. G., Jr. Extracellular microvesicles promote microglia-mediated pro-inflammatory responses to ethanol. *J Neurosci Res* **99**, 1940-1956 (2021). <https://doi.org/10.1002/jnr.24813>
- 32 Keyes, K. M. Age, Period, and Cohort Effects in Alcohol Use in the United States in the 20th and 21st Centuries: Implications for the Coming Decades. *Alcohol Res* **42**, 02 (2022). <https://doi.org/10.35946/arcr.v42.1.02>
- 33 Keyes, K. M. Alcohol use in older adult US population: trends, causes and consequences. *Alcohol* (2022). <https://doi.org/10.1016/j.alcohol.2022.05.005>
- 34 Tevik, K. *et al.* Mortality in older adults with frequent alcohol consumption and use of drugs with addiction potential - The Nord Trondelag Health Study 2006-2008 (HUNT3), Norway, a population-based study. *PLoS One* **14**, e0214813 (2019). <https://doi.org/10.1371/journal.pone.0214813>

- 35 Franceschi, C. *et al.* Inflamm-aging. An evolutionary perspective on immunosenescence. *Ann N Y Acad Sci* **908**, 244-254 (2000).
<https://doi.org/10.1111/j.1749-6632.2000.tb06651.x>
- 36 Frank, M. G., Barrientos, R. M., Watkins, L. R. & Maier, S. F. Aging sensitizes rapidly isolated hippocampal microglia to LPS *ex vivo*. *J Neuroimmunol* **226**, 181-184 (2010). <https://doi.org/10.1016/j.jneuroim.2010.05.022>
- 37 Meier, P. & Seitz, H. K. Age, alcohol metabolism and liver disease. *Curr Opin Clin Nutr Metab Care* **11**, 21-26 (2008).
<https://doi.org/10.1097/MCO.0b013e3282f30564>
- 38 Lucey, M. R., Hill, E. M., Young, J. P., Demo-Dananberg, L. & Beresford, T. P. The influences of age and gender on blood ethanol concentrations in healthy humans. *J Stud Alcohol* **60**, 103-110 (1999).
<https://doi.org/10.15288/jsa.1999.60.103>
- 39 Greenberg, S. S. *et al.* Ethanol inhibits lung clearance of *Pseudomonas aeruginosa* by a neutrophil and nitric oxide-dependent mechanism, *in vivo*. *Alcohol Clin Exp Res* **23**, 735-744 (1999).
- 40 Price, M. E. *et al.* Loss of cAMP-dependent stimulation of isolated cilia motility by alcohol exposure is oxidant-dependent. *Alcohol* **80**, 91-98 (2019).
<https://doi.org/10.1016/j.alcohol.2018.09.010>
- 41 Wyatt, T. A., Gentry-Nielsen, M. J., Pavlik, J. A. & Sisson, J. H. Desensitization of PKA-stimulated ciliary beat frequency in an ethanol-fed rat model of cigarette smoke exposure. *Alcohol Clin Exp Res* **28**, 998-1004 (2004).
<https://doi.org/10.1097/01.alc.0000130805.75641.f4>

- 42 Baker, R. C. & Jerrells, T. R. Recent developments in alcoholism:immunological aspects. *Recent Dev Alcohol* **11**, 249-271 (1993).
- 43 Burnham, E. L., Brown, L. A., Halls, L. & Moss, M. Effects of chronic alcohol abuse on alveolar epithelial barrier function and glutathione homeostasis. *Alcohol Clin Exp Res* **27**, 1167-1172 (2003).
<https://doi.org/10.1097/01.ALC.0000075821.34270.98>
- 44 Pelaez, A., Bechara, R. I., Joshi, P. C., Brown, L. A. & Guidot, D. M. Granulocyte/macrophage colony-stimulating factor treatment improves alveolar epithelial barrier function in alcoholic rat lung. *Am J Physiol Lung Cell Mol Physiol* **286**, L106-111 (2004). <https://doi.org/10.1152/ajplung.00148.2003>
- 45 Liang, Y., Yeligar, S. M. & Brown, L. A. Chronic-alcohol-abuse-induced oxidative stress in the development of acute respiratory distress syndrome. *ScientificWorldJournal* **2012**, 740308 (2012).
<https://doi.org/10.1100/2012/740308>
- 46 Yeligar, S. M., Mehta, A. J., Harris, F. L., Brown, L. A. & Hart, C. M. Peroxisome Proliferator-Activated Receptor gamma Regulates Chronic Alcohol-Induced Alveolar Macrophage Dysfunction. *Am J Respir Cell Mol Biol* **55**, 35-46 (2016).
<https://doi.org/10.1165/rcmb.2015-0077OC>
- 47 Baughman, R. P. & Roselle, G. A. Surfactant deficiency with decreased opsonic activity in a guinea pig model of alcoholism. *Alcohol Clin Exp Res* **11**, 261-264 (1987). <https://doi.org/10.1111/j.1530-0277.1987.tb01303.x>
- 48 Wagner, M. C., Yeligar, S. M., Brown, L. A. & Michael Hart, C. PPARgamma ligands regulate NADPH oxidase, eNOS, and barrier function in the lung

- following chronic alcohol ingestion. *Alcohol Clin Exp Res* **36**, 197-206 (2012).
<https://doi.org/10.1111/j.1530-0277.2011.01599.x>
- 49 Liang, Y., Harris, F. L., Jones, D. P. & Brown, L. A. S. Alcohol induces mitochondrial redox imbalance in alveolar macrophages. *Free Radic Biol Med* **65**, 1427-1434 (2013). <https://doi.org/10.1016/j.freeradbiomed.2013.10.010>
- 50 Liang, Y., Harris, F. L. & Brown, L. A. Alcohol induced mitochondrial oxidative stress and alveolar macrophage dysfunction. *Biomed Res Int* **2014**, 371593 (2014). <https://doi.org/10.1155/2014/371593>
- 51 Kumar, V. Pulmonary Innate Immune Response Determines the Outcome of Inflammation During Pneumonia and Sepsis-Associated Acute Lung Injury. *Front Immunol* **11**, 1722 (2020). <https://doi.org/10.3389/fimmu.2020.01722>
- 52 Morris, N. L. & Yeligar, S. M. Role of HIF-1alpha in Alcohol-Mediated Multiple Organ Dysfunction. *Biomolecules* **8** (2018). <https://doi.org/10.3390/biom8040170>
- 53 Sueblinvong, V. *et al.* Chronic alcohol ingestion primes the lung for bleomycin-induced fibrosis in mice. *Alcohol Clin Exp Res* **38**, 336-343 (2014).
<https://doi.org/10.1111/acer.12232>
- 54 Lewis, S. A. *et al.* Profiling of extracellular vesicle-bound miRNA to identify candidate biomarkers of chronic alcohol drinking in nonhuman primates. *Alcohol Clin Exp Res* **46**, 221-231 (2022). <https://doi.org/10.1111/acer.14760>
- 55 Rhoades, N. S. *et al.* Functional, transcriptional, and microbial shifts associated with healthy pulmonary aging in rhesus macaques. *Cell Rep* **39**, 110725 (2022).
<https://doi.org/10.1016/j.celrep.2022.110725>

- 56 Hallgren, R., Samuelsson, T., Laurent, T. C. & Modig, J. Accumulation of hyaluronan (hyaluronic acid) in the lung in adult respiratory distress syndrome. *Am Rev Respir Dis* **139**, 682-687 (1989).
<https://doi.org/10.1164/ajrccm/139.3.682>
- 57 Parsons, B. J. Free radical studies of components of the extracellular matrix: contributions to protection of biomolecules and biomaterials from sterilising doses of ionising radiation. *Cell Tissue Bank* **19**, 201-213 (2018).
<https://doi.org/10.1007/s10561-017-9650-5>
- 58 Rees, M. D., Kennett, E. C., Whitelock, J. M. & Davies, M. J. Oxidative damage to extracellular matrix and its role in human pathologies. *Free Radic Biol Med* **44**, 1973-2001 (2008). <https://doi.org/10.1016/j.freeradbiomed.2008.03.016>
- 59 Morris, N. L., Harris, F. L., Brown, L. A. S. & Yeligar, S. M. Alcohol induces mitochondrial derangements in alveolar macrophages by upregulating NADPH oxidase 4. *Alcohol* **90**, 27-38 (2021).
<https://doi.org/10.1016/j.alcohol.2020.11.004>
- 60 Yeligar, S. M., Mehta, A. J., Harris, F. L., Brown, L. A. S. & Hart, C. M. Pioglitazone Reverses Alcohol-Induced Alveolar Macrophage Phagocytic Dysfunction. *J Immunol* (2021). <https://doi.org/10.4049/jimmunol.2000565>
- 61 Gao, R. *et al.* Sirt1 restrains lung inflammasome activation in a murine model of sepsis. *Am J Physiol Lung Cell Mol Physiol* **308**, L847-853 (2015).
<https://doi.org/10.1152/ajplung.00274.2014>

- 62 Grassme, H., Carpinteiro, A., Edwards, M. J., Gulbins, E. & Becker, K. A. Regulation of the inflammasome by ceramide in cystic fibrosis lungs. *Cell Physiol Biochem* **34**, 45-55 (2014). <https://doi.org/10.1159/000362983>
- 63 Piantadosi, C. A. & Suliman, H. B. Mitochondrial Dysfunction in Lung Pathogenesis. *Annu Rev Physiol* **79**, 495-515 (2017). <https://doi.org/10.1146/annurev-physiol-022516-034322>
- 64 Kane, C. J. & Drew, P. D. Inflammatory responses to alcohol in the CNS: nuclear receptors as potential therapeutics for alcohol-induced neuropathologies. *J Leukoc Biol* **100**, 951-959 (2016). <https://doi.org/10.1189/jlb.3MR0416-171R>
- 65 Mandrekar, P., Catalano, D., Jeliaskova, V. & Kodys, K. Alcohol exposure regulates heat shock transcription factor binding and heat shock proteins 70 and 90 in monocytes and macrophages: implication for TNF-alpha regulation. *J Leukoc Biol* **84**, 1335-1345 (2008). <https://doi.org/10.1189/jlb.0407256>
- 66 Muralidharan, S. *et al.* Moderate alcohol induces stress proteins HSF1 and hsp70 and inhibits proinflammatory cytokines resulting in endotoxin tolerance. *J Immunol* **193**, 1975-1987 (2014). <https://doi.org/10.4049/jimmunol.1303468>
- 67 Choudhury, A. *et al.* Inhibition of HSP90 and Activation of HSF1 Diminish Macrophage NLRP3 Inflammasome Activity in Alcohol-Associated Liver Injury. *Alcohol Clin Exp Res* **44**, 1300-1311 (2020). <https://doi.org/10.1111/acer.14338>
- 68 Ratna, A. *et al.* Myeloid Endoplasmic Reticulum Resident Chaperone GP96 Facilitates Inflammation and Steatosis in Alcohol-Associated Liver Disease. *Hepatol Commun* **5**, 1165-1182 (2021). <https://doi.org/10.1002/hep4.1713>

- 69 Drouin, M., Saenz, J. & Chiffolleau, E. C-Type Lectin-Like Receptors: Head or Tail in Cell Death Immunity. *Front Immunol* **11**, 251 (2020).
<https://doi.org/10.3389/fimmu.2020.00251>
- 70 Kim, A., Bellar, A., McMullen, M. R., Li, X. & Nagy, L. E. Functionally Diverse Inflammatory Responses in Peripheral and Liver Monocytes in Alcohol-Associated Hepatitis. *Hepatol Commun* **4**, 1459-1476 (2020).
<https://doi.org/10.1002/hep4.1563>
- 71 Zhou, H. *et al.* IRAKM-Mincle axis links cell death to inflammation: Pathophysiological implications for chronic alcoholic liver disease. *Hepatology* **64**, 1978-1993 (2016). <https://doi.org/10.1002/hep.28811>
- 72 Yang, A. M. *et al.* Intestinal fungi contribute to development of alcoholic liver disease. *J Clin Invest* **127**, 2829-2841 (2017). <https://doi.org/10.1172/JCI90562>
- 73 Starkel, P., Leclercq, S., de Timary, P. & Schnabl, B. Intestinal dysbiosis and permeability: the yin and yang in alcohol dependence and alcoholic liver disease. *Clin Sci (Lond)* **132**, 199-212 (2018). <https://doi.org/10.1042/CS20171055>
- 74 Starkel, P. & Schnabl, B. Bidirectional Communication between Liver and Gut during Alcoholic Liver Disease. *Semin Liver Dis* **36**, 331-339 (2016).
<https://doi.org/10.1055/s-0036-1593882>
- 75 Samuelson, D. R. *et al.* Pulmonary immune cell trafficking promotes host defense against alcohol-associated Klebsiella pneumonia. *Commun Biol* **4**, 997 (2021).
<https://doi.org/10.1038/s42003-021-02524-0>

- 76 Sommer, F., Anderson, J. M., Bharti, R., Raes, J. & Rosenstiel, P. The resilience of the intestinal microbiota influences health and disease. *Nat Rev Microbiol* **15**, 630-638 (2017). <https://doi.org/10.1038/nrmicro.2017.58>
- 77 Maccioni, L., Leclercq, I. A., Schnabl, B. & Starkel, P. Host Factors in Dysregulation of the Gut Barrier Function during Alcohol-Associated Liver Disease. *Int J Mol Sci* **22** (2021). <https://doi.org/10.3390/ijms222312687>
- 78 Shah, N. J., Royer, A. & John, S. in *StatPearls* (2022).
- 79 Isselbacher, K. J. & Greenberger, N. J. Metabolic Effects of Alcohol on the Liver. *N Engl J Med* **270**, 403-410 CONCL (1964).
- 80 Lieber, C. S. Hepatic and metabolic effects of alcohol. *Gastroenterology* **50**, 119-133 (1966).
- 81 Lieber, C. S. Fatty liver, cirrhosis, and metabolic effects related to problem drinking. *Psychiatr Res Rep Am Psychiatr Assoc* **24**, 119-131 (1968).
- 82 Li, F., McClain, C. J. & Feng, W. Microbiome dysbiosis and alcoholic liver disease(☆). *Liver Res* **3**, 218-226 (2019).
<https://doi.org/10.1016/j.livres.2019.09.001>
- 83 Bishehsari, F. *et al.* Alcohol and Gut-Derived Inflammation. *Alcohol Res* **38**, 163-171 (2017).
- 84 Hartmann, P., Chu, H., Duan, Y. & Schnabl, B. Gut microbiota in liver disease: too much is harmful, nothing at all is not helpful either. *Am J Physiol Gastrointest Liver Physiol* **316**, G563-G573 (2019). <https://doi.org/10.1152/ajpgi.00370.2018>

- 85 Mutlu, E. A. *et al.* Colonic microbiome is altered in alcoholism. *Am J Physiol Gastrointest Liver Physiol* **302**, G966-978 (2012).
<https://doi.org/10.1152/ajpgi.00380.2011>
- 86 Yan, A. W. *et al.* Enteric dysbiosis associated with a mouse model of alcoholic liver disease. *Hepatology* **53**, 96-105 (2011). <https://doi.org/10.1002/hep.24018>
- 87 Hendriks, T. & Schnabl, B. Indoles: metabolites produced by intestinal bacteria capable of controlling liver disease manifestation. *J Intern Med* **286**, 32-40 (2019). <https://doi.org/10.1111/joim.12892>
- 88 Roager, H. M. & Licht, T. R. Microbial tryptophan catabolites in health and disease. *Nat Commun* **9**, 3294 (2018). <https://doi.org/10.1038/s41467-018-05470-4>
- 89 Zelante, T. *et al.* Tryptophan catabolites from microbiota engage aryl hydrocarbon receptor and balance mucosal reactivity via interleukin-22. *Immunity* **39**, 372-385 (2013). <https://doi.org/10.1016/j.immuni.2013.08.003>
- 90 Hendriks, T. *et al.* Bacteria engineered to produce IL-22 in intestine induce expression of REG3G to reduce ethanol-induced liver disease in mice. *Gut* **68**, 1504-1515 (2019). <https://doi.org/10.1136/gutjnl-2018-317232>
- 91 Gupta, N. M., Deshpande, A. & Rothberg, M. B. Pneumonia and alcohol use disorder: Implications for treatment. *Cleve Clin J Med* **87**, 493-500 (2020).
<https://doi.org/10.3949/ccjm.87a.19105>
- 92 Jong, G. M., Hsiue, T. R., Chen, C. R., Chang, H. Y. & Chen, C. W. Rapidly fatal outcome of bacteremic *Klebsiella pneumoniae* pneumonia in alcoholics. *Chest* **107**, 214-217 (1995). <https://doi.org/10.1378/chest.107.1.214>

- 93 Ray, K. Manipulating the gut microbiota to combat alcoholic hepatitis. *Nat Rev Gastroenterol Hepatol* **17**, 3 (2020). <https://doi.org/10.1038/s41575-019-0246-3>
- 94 Gao, B. *et al.* Functional Microbial Responses to Alcohol Abstinence in Patients With Alcohol Use Disorder. *Front Physiol* **11**, 370 (2020). <https://doi.org/10.3389/fphys.2020.00370>
- 95 Cheng, M. *et al.* Gut Microbiota Is Involved in Alcohol-Induced Osteoporosis in Young and Old Rats Through Immune Regulation. *Front Cell Infect Microbiol* **11**, 636231 (2021). <https://doi.org/10.3389/fcimb.2021.636231>
- 96 Tripathi, D. *et al.* Alcohol enhances type 1 interferon-alpha production and mortality in young mice infected with *Mycobacterium tuberculosis*. *PLoS Pathog* **14**, e1007174 (2018). <https://doi.org/10.1371/journal.ppat.1007174>
- 97 Llopis, M. *et al.* Intestinal microbiota contributes to individual susceptibility to alcoholic liver disease. *Gut* **65**, 830-839 (2016). <https://doi.org/10.1136/gutjnl-2015-310585>
- 98 Perez, J. C. Fungi of the human gut microbiota: Roles and significance. *Int J Med Microbiol* **311**, 151490 (2021). <https://doi.org/10.1016/j.ijmm.2021.151490>
- 99 Day, A. W. & Kumamoto, C. A. Gut Microbiome Dysbiosis in Alcoholism: Consequences for Health and Recovery. *Front Cell Infect Microbiol* **12**, 840164 (2022). <https://doi.org/10.3389/fcimb.2022.840164>
- 100 Bartoletti, M. *et al.* Epidemiology and outcomes of bloodstream infection in patients with cirrhosis. *J Hepatol* **61**, 51-58 (2014). <https://doi.org/10.1016/j.jhep.2014.03.021>

- 101 Hartmann, P. *et al.* Dynamic Changes of the Fungal Microbiome in Alcohol Use Disorder. *Front Physiol* **12**, 699253 (2021).
<https://doi.org/10.3389/fphys.2021.699253>
- 102 Lang, S. *et al.* Intestinal Fungal Dysbiosis and Systemic Immune Response to Fungi in Patients With Alcoholic Hepatitis. *Hepatology* **71**, 522-538 (2020).
<https://doi.org/10.1002/hep.30832>
- 103 Lang, S. *et al.* Changes in the fecal bacterial microbiota associated with disease severity in alcoholic hepatitis patients. *Gut Microbes* **12**, 1785251 (2020).
<https://doi.org/10.1080/19490976.2020.1785251>
- 104 Dunn, W. & Shah, V. H. Pathogenesis of Alcoholic Liver Disease. *Clin Liver Dis* **20**, 445-456 (2016). <https://doi.org/10.1016/j.cld.2016.02.004>
- 105 Peltier, M. R. *et al.* Sex differences in stress-related alcohol use. *Neurobiol Stress* **10**, 100149 (2019). <https://doi.org/10.1016/j.ynstr.2019.100149>
- 106 Breslow, R. A., Castle, I. P., Chen, C. M. & Graubard, B. I. Trends in Alcohol Consumption Among Older Americans: National Health Interview Surveys, 1997 to 2014. *Alcohol Clin Exp Res* **41**, 976-986 (2017).
<https://doi.org/10.1111/acer.13365>
- 107 Teeters, J. B., Lancaster, C. L., Brown, D. G. & Back, S. E. Substance use disorders in military veterans: prevalence and treatment challenges. *Subst Abuse Rehabil* **8**, 69-77 (2017). <https://doi.org/10.2147/SAR.S116720>
- 108 SAMHSA, C. f. B. H. S. a. Q. 2021 National Survey on Drug Use and Health. Table 5.6A—Alcohol use disorder in past year: among people aged 12 or older;

- by age group and demographic characteristics, numbers in thousands, 2021. (2021).
- 109 Aderem, A. & Underhill, D. M. Mechanisms of phagocytosis in macrophages. *Annu Rev Immunol* **17**, 593-623 (1999).
<https://doi.org/10.1146/annurev.immunol.17.1.593>
- 110 Morris, N. L., Michael, D. N., Crotty, K. M., Chang, S. S. & Yeligar, S. M. Alcohol-Induced Glycolytic Shift in Alveolar Macrophages Is Mediated by Hypoxia-Inducible Factor-1 Alpha. *Front Immunol* **13**, 865492 (2022).
<https://doi.org/10.3389/fimmu.2022.865492>
- 111 Sadikot, R. T., Bedi, B., Li, J. & Yeligar, S. M. Alcohol-induced mitochondrial DNA damage promotes injurious crosstalk between alveolar epithelial cells and alveolar macrophages. *Alcohol* **80**, 65-72 (2019).
<https://doi.org/10.1016/j.alcohol.2018.08.006>
- 112 Yeligar, S. M., Harris, F. L., Hart, C. M. & Brown, L. A. Glutathione attenuates ethanol-induced alveolar macrophage oxidative stress and dysfunction by downregulating NADPH oxidases. *Am J Physiol Lung Cell Mol Physiol* **306**, L429-441 (2014). <https://doi.org/10.1152/ajplung.00159.2013>
- 113 Yeligar, S. M., Harris, F. L., Hart, C. M. & Brown, L. A. Ethanol induces oxidative stress in alveolar macrophages via upregulation of NADPH oxidases. *J Immunol* **188**, 3648-3657 (2012). <https://doi.org/10.4049/jimmunol.1101278>
- 114 Karaye, I. M., Maleki, N., Hassan, N. & Yunusa, I. Trends in Alcohol-Related Deaths by Sex in the US, 1999-2020. *JAMA Netw Open* **6**, e2326346 (2023).
<https://doi.org/10.1001/jamanetworkopen.2023.26346>

- 115 Yeh, M. Y., Burnham, E. L., Moss, M. & Brown, L. A. Non-invasive evaluation of pulmonary glutathione in the exhaled breath condensate of otherwise healthy alcoholics. *Respir Med* **102**, 248-255 (2008).
<https://doi.org/10.1016/j.rmed.2007.09.005>
- 116 Brown, L. A., Ping, X. D., Harris, F. L. & Gauthier, T. W. Glutathione availability modulates alveolar macrophage function in the chronic ethanol-fed rat. *Am J Physiol Lung Cell Mol Physiol* **292**, L824-832 (2007).
<https://doi.org/10.1152/ajplung.00346.2006>
- 117 Moss, M. *et al.* The effects of chronic alcohol abuse on pulmonary glutathione homeostasis. *Am J Respir Crit Care Med* **161**, 414-419 (2000).
<https://doi.org/10.1164/ajrccm.161.2.9905002>
- 118 Holguin, F., Moss, I., Brown, L. A. & Guidot, D. M. Chronic ethanol ingestion impairs alveolar type II cell glutathione homeostasis and function and predisposes to endotoxin-mediated acute edematous lung injury in rats. *J Clin Invest* **101**, 761-768 (1998). <https://doi.org/10.1172/JCI1396>
- 119 Mehta, A. J. *et al.* Zinc supplementation restores PU.1 and Nrf2 nuclear binding in alveolar macrophages and improves redox balance and bacterial clearance in the lungs of alcohol-fed rats. *Alcohol Clin Exp Res* **35**, 1519-1528 (2011).
<https://doi.org/10.1111/j.1530-0277.2011.01488.x>
- 120 Joshi, P. C., Mehta, A., Jabber, W. S., Fan, X. & Guidot, D. M. Zinc deficiency mediates alcohol-induced alveolar epithelial and macrophage dysfunction in rats. *Am J Respir Cell Mol Biol* **41**, 207-216 (2009). <https://doi.org/10.1165/rcmb.2008-0209OC>

- 121 Mehta, A. J., Yeligar, S. M., Elon, L., Brown, L. A. & Guidot, D. M. Alcoholism causes alveolar macrophage zinc deficiency and immune dysfunction. *Am J Respir Crit Care Med* **188**, 716-723 (2013). <https://doi.org/10.1164/rccm.201301-0061OC>
- 122 Brown, S. D., Gauthier, T. W. & Brown, L. A. Impaired terminal differentiation of pulmonary macrophages in a Guinea pig model of chronic ethanol ingestion. *Alcohol Clin Exp Res* **33**, 1782-1793 (2009). <https://doi.org/10.1111/j.1530-0277.2009.01017.x>
- 123 Schulz, K. F., Altman, D. G., Moher, D. & Group, C. CONSORT 2010 Statement: updated guidelines for reporting parallel group randomized trials. *Open Med* **4**, e60-68 (2010).
- 124 Obianyo, O. *et al.* Metabolic Consequences of Chronic Alcohol Abuse in Non-Smokers: A Pilot Study. *PLoS One* **10**, e0129570 (2015). <https://doi.org/10.1371/journal.pone.0129570>
- 125 Bray, T. M. & Bettger, W. J. The physiological role of zinc as an antioxidant. *Free Radic Biol Med* **8**, 281-291 (1990). [https://doi.org/10.1016/0891-5849\(90\)90076-u](https://doi.org/10.1016/0891-5849(90)90076-u)
- 126 Rennard, S. I., Bitterman, P. B. & Crystal, R. G. Response of the lower respiratory tract to injury. Mechanisms of repair of the parenchymal cells of the alveolar wall. *Chest* **84**, 735-739 (1983). <https://doi.org/10.1378/chest.84.6.735>
- 127 Cantin, A. M., Hubbard, R. C. & Crystal, R. G. Glutathione deficiency in the epithelial lining fluid of the lower respiratory tract in idiopathic pulmonary fibrosis. *Am Rev Respir Dis* **139**, 370-372 (1989). <https://doi.org/10.1164/ajrccm/139.2.370>

- 128 Cantin, A. M., Larivee, P. & Begin, R. O. Extracellular glutathione suppresses human lung fibroblast proliferation. *Am J Respir Cell Mol Biol* **3**, 79-85 (1990).
<https://doi.org/10.1165/ajrcmb/3.1.79>
- 129 Brown, S. D. & Brown, L. A. Ethanol (EtOH)-induced TGF-beta1 and reactive oxygen species production are necessary for EtOH-induced alveolar macrophage dysfunction and induction of alternative activation. *Alcohol Clin Exp Res* **36**, 1952-1962 (2012). <https://doi.org/10.1111/j.1530-0277.2012.01825.x>
- 130 Park, M. K. *et al.* The Protective Role of Glutathione on Zinc-Induced Neuron Death after Brain Injuries. *Int J Mol Sci* **24** (2023).
<https://doi.org/10.3390/ijms24032950>
- 131 Wiseman, D. A., Sharma, S. & Black, S. M. Elevated zinc induces endothelial apoptosis via disruption of glutathione metabolism: role of the ADP translocator. *Biometals* **23**, 19-30 (2010). <https://doi.org/10.1007/s10534-009-9263-y>
- 132 Sueblinvong, V. *et al.* TGFbeta1 mediates alcohol-induced Nrf2 suppression in lung fibroblasts. *Alcohol Clin Exp Res* **38**, 2731-2742 (2014).
<https://doi.org/10.1111/acer.12563>
- 133 Lauver, D. A., Kaissarian, N. M. & Lucchesi, B. R. Oral pretreatment with liposomal glutathione attenuates reperfusion injury in rabbit isolated hearts. *J Cardiovasc Pharmacol* **61**, 233-239 (2013).
<https://doi.org/10.1097/FJC.0b013e31827c0f02>
- 134 Alcoholism, N. I. o. A. A. a. *Alcohol Facts and Statistics*,
<<https://www.niaaa.nih.gov/alcohol-health/overview-alcohol-consumption/alcohol-facts-and-statistics>> (

- 135 Brown, L. A., Harris, F. L., Ping, X. D. & Gauthier, T. W. Chronic ethanol ingestion and the risk of acute lung injury: a role for glutathione availability? *Alcohol* **33**, 191-197 (2004). <https://doi.org/10.1016/j.alcohol.2004.08.002>
- 136 Chaudhry, R. & Varacallo, M. in *StatPearls* (2023).
- 137 Ros, S. & Schulze, A. Balancing glycolytic flux: the role of 6-phosphofructo-2-kinase/fructose 2,6-bisphosphatases in cancer metabolism. *Cancer Metab* **1**, 8 (2013). <https://doi.org/10.1186/2049-3002-1-8>
- 138 Gong, Y. *et al.* Blockage of glycolysis by targeting PFKFB3 alleviates sepsis-related acute lung injury via suppressing inflammation and apoptosis of alveolar epithelial cells. *Biochem Biophys Res Commun* **491**, 522-529 (2017). <https://doi.org/10.1016/j.bbrc.2017.05.173>
- 139 Hu, K. *et al.* Caloric Restriction Mimetic 2-Deoxyglucose Alleviated Inflammatory Lung Injury via Suppressing Nuclear Pyruvate Kinase M2-Signal Transducer and Activator of Transcription 3 Pathway. *Front Immunol* **9**, 426 (2018). <https://doi.org/10.3389/fimmu.2018.00426>
- 140 Liu, W., Shen, S. M., Zhao, X. Y. & Chen, G. Q. Targeted genes and interacting proteins of hypoxia inducible factor-1. *Int J Biochem Mol Biol* **3**, 165-178 (2012).
- 141 Miska, J. *et al.* HIF-1alpha Is a Metabolic Switch between Glycolytic-Driven Migration and Oxidative Phosphorylation-Driven Immunosuppression of Tregs in Glioblastoma. *Cell Rep* **27**, 226-237 e224 (2019). <https://doi.org/10.1016/j.celrep.2019.03.029>

- 142 Wang, T. *et al.* HIF1alpha-Induced Glycolysis Metabolism Is Essential to the Activation of Inflammatory Macrophages. *Mediators Inflamm* **2017**, 9029327 (2017). <https://doi.org/10.1155/2017/9029327>
- 143 Del Rey, M. J. *et al.* Hif-1alpha Knockdown Reduces Glycolytic Metabolism and Induces Cell Death of Human Synovial Fibroblasts Under Normoxic Conditions. *Sci Rep* **7**, 3644 (2017). <https://doi.org/10.1038/s41598-017-03921-4>
- 144 Blum, J. I., Bijli, K. M., Murphy, T. C., Kleinhenz, J. M. & Hart, C. M. Time-dependent PPARgamma Modulation of HIF-1alpha Signaling in Hypoxic Pulmonary Artery Smooth Muscle Cells. *Am J Med Sci* **352**, 71-79 (2016). <https://doi.org/10.1016/j.amjms.2016.03.019>
- 145 Wu, G. *et al.* Hypoxia Exacerbates Inflammatory Acute Lung Injury via the Toll-Like Receptor 4 Signaling Pathway. *Front Immunol* **9**, 1667 (2018). <https://doi.org/10.3389/fimmu.2018.01667>
- 146 Cho, S. J., Moon, J. S., Lee, C. M., Choi, A. M. & Stout-Delgado, H. W. Glucose Transporter 1-Dependent Glycolysis Is Increased during Aging-Related Lung Fibrosis, and Phloretin Inhibits Lung Fibrosis. *Am J Respir Cell Mol Biol* **56**, 521-531 (2017). <https://doi.org/10.1165/rcmb.2016-0225OC>
- 147 Katada, R. *et al.* Expression of aquaporin-4 augments cytotoxic brain edema after traumatic brain injury during acute ethanol exposure. *Am J Pathol* **180**, 17-23 (2012). <https://doi.org/10.1016/j.ajpath.2011.09.011>
- 148 He, Z. *et al.* Adipose tissue hypoxia and low-grade inflammation: a possible mechanism for ethanol-related glucose intolerance? *Br J Nutr* **113**, 1355-1364 (2015). <https://doi.org/10.1017/S000711451500077X>

- 149 Yun, J. W. *et al.* Binge alcohol promotes hypoxic liver injury through a CYP2E1-HIF-1alpha-dependent apoptosis pathway in mice and humans. *Free Radic Biol Med* **77**, 183-194 (2014). <https://doi.org/10.1016/j.freeradbiomed.2014.08.030>
- 150 Yuan, Y., Hilliard, G., Ferguson, T. & Millhorn, D. E. Cobalt inhibits the interaction between hypoxia-inducible factor-alpha and von Hippel-Lindau protein by direct binding to hypoxia-inducible factor-alpha. *J Biol Chem* **278**, 15911-15916 (2003). <https://doi.org/10.1074/jbc.M300463200>
- 151 Woods, P. S. *et al.* Tissue-Resident Alveolar Macrophages Do Not Rely on Glycolysis for LPS-induced Inflammation. *Am J Respir Cell Mol Biol* **62**, 243-255 (2020). <https://doi.org/10.1165/rcmb.2019-0244OC>
- 152 Yeligar, S. M., Machida, K. & Kalra, V. K. Ethanol-induced HO-1 and NQO1 are differentially regulated by HIF-1alpha and Nrf2 to attenuate inflammatory cytokine expression. *J Biol Chem* **285**, 35359-35373 (2010). <https://doi.org/10.1074/jbc.M110.138636>
- 153 Kang, H., Park, Y. K. & Lee, J. Y. Nicotinamide riboside, an NAD(+) precursor, attenuates inflammation and oxidative stress by activating sirtuin 1 in alcohol-stimulated macrophages. *Lab Invest* **101**, 1225-1237 (2021). <https://doi.org/10.1038/s41374-021-00599-1>
- 154 Herold, S., Mayer, K. & Lohmeyer, J. Acute lung injury: how macrophages orchestrate resolution of inflammation and tissue repair. *Front Immunol* **2**, 65 (2011). <https://doi.org/10.3389/fimmu.2011.00065>
- 155 Papandreou, I., Cairns, R. A., Fontana, L., Lim, A. L. & Denko, N. C. HIF-1 mediates adaptation to hypoxia by actively downregulating mitochondrial oxygen

- consumption. *Cell Metab* **3**, 187-197 (2006).
<https://doi.org/10.1016/j.cmet.2006.01.012>
- 156 Fischer, M., You, M., Matsumoto, M. & Crabb, D. W. Peroxisome proliferator-activated receptor alpha (PPARalpha) agonist treatment reverses PPARalpha dysfunction and abnormalities in hepatic lipid metabolism in ethanol-fed mice. *J Biol Chem* **278**, 27997-28004 (2003). <https://doi.org/10.1074/jbc.M302140200>
- 157 Blomstrand, R., Kager, L. & Lantto, O. Studies on the ethanol-induced decrease of fatty acid oxidation in rat and human liver slices. *Life Sci* **13**, 1131-1141 (1973). [https://doi.org/10.1016/0024-3205\(73\)90380-9](https://doi.org/10.1016/0024-3205(73)90380-9)
- 158 Correnti, J. M. *et al.* Ethanol and C2 ceramide activate fatty acid oxidation in human hepatoma cells. *Sci Rep* **8**, 12923 (2018). <https://doi.org/10.1038/s41598-018-31025-0>
- 159 Sutliff, R. L., Kang, B. Y. & Hart, C. M. PPARgamma as a potential therapeutic target in pulmonary hypertension. *Ther Adv Respir Dis* **4**, 143-160 (2010).
<https://doi.org/10.1177/1753465809369619>
- 160 Lee, K. S. *et al.* Peroxisome proliferator activated receptor-gamma modulates reactive oxygen species generation and activation of nuclear factor-kappaB and hypoxia-inducible factor 1alpha in allergic airway disease of mice. *J Allergy Clin Immunol* **118**, 120-127 (2006). <https://doi.org/10.1016/j.jaci.2006.03.021>
- 161 SAMHSA, C. f. B. H. S. a. Q. 2021 National Survey on Drug Use and Health. Table 5.6A—Alcohol use disorder in past year: among people aged 12 or older; by age group and demographic characteristics, numbers in thousands. (2021).

- 162 White, A. M., Slater, M. E., Ng, G., Hingson, R. & Breslow, R. Trends in Alcohol-Related Emergency Department Visits in the United States: Results from the Nationwide Emergency Department Sample, 2006 to 2014. *Alcohol Clin Exp Res* **42**, 352-359 (2018). <https://doi.org/10.1111/acer.13559>
- 163 Sarkar D, J. M., Wang HJ. Alcohol and the Immune System. *Alcohol Res* **37**, 153-155 (2015).
- 164 Bagasra, O., Howeedy, A. & Kajdacsy-Balla, A. Macrophage function in chronic experimental alcoholism. I. Modulation of surface receptors and phagocytosis. *Immunology* **65**, 405-409 (1988).
- 165 Wallaert, B., Aerts, C., Colombel, J. F. & Voisin, C. Human alveolar macrophage antibacterial activity in the alcoholic lung. *Am Rev Respir Dis* **144**, 278-283 (1991). <https://doi.org/10.1164/ajrccm/144.2.278>
- 166 Standiford, T. J. & Danforth, J. M. Ethanol feeding inhibits proinflammatory cytokine expression from murine alveolar macrophages ex vivo. *Alcohol Clin Exp Res* **21**, 1212-1217 (1997).
- 167 Nunnari, J. & Suomalainen, A. Mitochondria: in sickness and in health. *Cell* **148**, 1145-1159 (2012). <https://doi.org/10.1016/j.cell.2012.02.035>
- 168 Malnassy, G. *et al.* Inhibition of Abelson Tyrosine-Protein Kinase 2 Suppresses the Development of Alcohol-Associated Liver Disease by Decreasing PPARgamma Expression. *Cell Mol Gastroenterol Hepatol* **16**, 685-709 (2023). <https://doi.org/10.1016/j.jcmgh.2023.07.006>

- 169 Hunninghake, G. W., Gadek, J. E., Kawanami, O., Ferrans, V. J. & Crystal, R. G. Inflammatory and immune processes in the human lung in health and disease: evaluation by bronchoalveolar lavage. *Am J Pathol* **97**, 149-206 (1979).
- 170 Song, K. *et al.* Chronic ethanol consumption by mice results in activated splenic T cells. *J Leukoc Biol* **72**, 1109-1116 (2002).
- 171 Yeligar, S. M. *et al.* Dysregulation of Alveolar Macrophage PPARgamma, NADPH Oxidases, and TGFbeta(1) in Otherwise Healthy HIV-Infected Individuals. *AIDS Res Hum Retroviruses* **33**, 1018-1026 (2017).
<https://doi.org/10.1089/AID.2016.0030>
- 172 Antony, V. B., Godbey, S. W., Hott, J. W. & Queener, S. F. Alcohol-induced inhibition of alveolar macrophage oxidant release in vivo and in vitro. *Alcohol Clin Exp Res* **17**, 389-393 (1993). <https://doi.org/10.1111/j.1530-0277.1993.tb00781.x>
- 173 Libon, C., Forestier, F., Cotte-Laffitte, J., Labarre, C. & Quero, A. M. Effect of acute oral administration of alcohol on superoxide anion production from mouse alveolar macrophages. *J Leukoc Biol* **53**, 93-98 (1993).
<https://doi.org/10.1002/jlb.53.1.93>
- 174 Wichmann, M. W., Zellweger, R., DeMaso, C. M., Ayala, A. & Chaudry, I. H. Enhanced immune responses in females, as opposed to decreased responses in males following haemorrhagic shock and resuscitation. *Cytokine* **8**, 853-863 (1996). <https://doi.org/10.1006/cyto.1996.0114>
- 175 Pittet, J. F. *et al.* Estrogen Alleviates Sex-Dependent Differences in Lung Bacterial Clearance and Mortality Secondary to Bacterial Pneumonia after

- Traumatic Brain Injury. *J Neurotrauma* **38**, 989-999 (2021).
<https://doi.org/10.1089/neu.2020.7327>
- 176 Rastrelli, G. *et al.* Low testosterone levels predict clinical adverse outcomes in SARS-CoV-2 pneumonia patients. *Andrology* **9**, 88-98 (2021).
<https://doi.org/10.1111/andr.12821>
- 177 Wigger, G. W. *et al.* Alcohol impairs recognition and uptake of Mycobacterium tuberculosis by suppressing toll-like receptor 2 expression. *Alcohol Clin Exp Res* **46**, 2214-2224 (2022). <https://doi.org/10.1111/acer.14960>
- 178 Ahmadian, M. *et al.* PPARgamma signaling and metabolism: the good, the bad and the future. *Nat Med* **19**, 557-566 (2013). <https://doi.org/10.1038/nm.3159>
- 179 Forman, B. M., Chen, J. & Evans, R. M. The peroxisome proliferator-activated receptors: ligands and activators. *Ann N Y Acad Sci* **804**, 266-275 (1996).
<https://doi.org/10.1111/j.1749-6632.1996.tb18621.x>
- 180 Nobs, S. P. & Kopf, M. PPAR-gamma in innate and adaptive lung immunity. *J Leukoc Biol* **104**, 737-741 (2018). <https://doi.org/10.1002/JLB.3MR0118-034R>
- 181 Fernández-Checa, J. C. Alcohol-induced liver disease: when fat and oxidative stress meet. *Ann Hepatol* **2**, 69-75 (2003).
- 182 Gao, B. & Bataller, R. Alcoholic liver disease: pathogenesis and new therapeutic targets. *Gastroenterology* **141**, 1572-1585 (2011).
<https://doi.org/10.1053/j.gastro.2011.09.002>
- 183 Seitz, H. K. *et al.* Alcoholic liver disease. *Nat Rev Dis Primers* **4**, 16 (2018).
<https://doi.org/10.1038/s41572-018-0014-7>

- 184 Slovinisky, W. S., Shaghghi, H., Para, R., Romero, F. & Summer, R. Alcohol-induced lipid dysregulation impairs glycolytic responses to LPS in alveolar macrophages. *Alcohol* **83**, 57-65 (2020).
<https://doi.org/10.1016/j.alcohol.2019.08.009>
- 185 Scheen, A. J. Thiazolidinediones and liver toxicity. *Diabetes Metab* **27**, 305-313 (2001).
- 186 Xu, B., Xing, A. & Li, S. The forgotten type 2 diabetes mellitus medicine: rosiglitazone. *Diabetol Int* **13**, 49-65 (2022). <https://doi.org/10.1007/s13340-021-00519-0>
- 187 Graham, D. J. *et al.* Risk of acute myocardial infarction, stroke, heart failure, and death in elderly Medicare patients treated with rosiglitazone or pioglitazone. *JAMA* **304**, 411-418 (2010). <https://doi.org/10.1001/jama.2010.920>
- 188 Hsiao, F. Y., Hsieh, P. H., Huang, W. F., Tsai, Y. W. & Gau, C. S. Risk of bladder cancer in diabetic patients treated with rosiglitazone or pioglitazone: a nested case-control study. *Drug Saf* **36**, 643-649 (2013). <https://doi.org/10.1007/s40264-013-0080-4>
- 189 Zimmermann, A. *et al.* Metabolic control of mitophagy. *Eur J Clin Invest*, e14138 (2023). <https://doi.org/10.1111/eci.14138>
- 190 Association, A. P. Diagnostic and Statistical Manual of Mental Disorders. 5th ed. *American Psychiatric Association; Arlington, VA* (2013).
- 191 Hussell, T. & Bell, T. J. Alveolar macrophages: plasticity in a tissue-specific context. *Nat Rev Immunol* **14**, 81-93 (2014). <https://doi.org/10.1038/nri3600>

- 192 Underhill, C. B., Nguyen, H. A., Shizari, M. & Culty, M. CD44 positive macrophages take up hyaluronan during lung development. *Dev Biol* **155**, 324-336 (1993). <https://doi.org/10.1006/dbio.1993.1032>
- 193 Dong, Y. *et al.* The survival of fetal and bone marrow monocyte-derived alveolar macrophages is promoted by CD44 and its interaction with hyaluronan. *Mucosal Immunol* **11**, 601-614 (2018). <https://doi.org/10.1038/mi.2017.83>
- 194 Johnson, P., Arif, A. A., Lee-Sayer, S. S. M. & Dong, Y. Hyaluronan and Its Interactions With Immune Cells in the Healthy and Inflamed Lung. *Front Immunol* **9**, 2787 (2018). <https://doi.org/10.3389/fimmu.2018.02787>
- 195 Weigel, P. H. Planning, evaluating and vetting receptor signaling studies to assess hyaluronan size-dependence and specificity. *Glycobiology* **27**, 796-799 (2017). <https://doi.org/10.1093/glycob/cwx056>
- 196 Abbadi, A., Lauer, M., Swaidani, S., Wang, A. & Hascall, V. Hyaluronan Rafts on Airway Epithelial Cells. *J Biol Chem* **291**, 1448-1455 (2016). <https://doi.org/10.1074/jbc.M115.704288>
- 197 Liang, J. *et al.* Hyaluronan and TLR4 promote surfactant-protein-C-positive alveolar progenitor cell renewal and prevent severe pulmonary fibrosis in mice. *Nat Med* **22**, 1285-1293 (2016). <https://doi.org/10.1038/nm.4192>
- 198 Weigel, P. H. & DeAngelis, P. L. Hyaluronan synthases: a decade-plus of novel glycosyltransferases. *J Biol Chem* **282**, 36777-36781 (2007). <https://doi.org/10.1074/jbc.R700036200>
- 199 Teder, P. *et al.* Resolution of lung inflammation by CD44. *Science* **296**, 155-158 (2002). <https://doi.org/10.1126/science.1069659>

- 200 Stern, R. & Jedrzejewski, M. J. Hyaluronidases: their genomics, structures, and mechanisms of action. *Chem Rev* **106**, 818-839 (2006).
<https://doi.org/10.1021/cr050247k>
- 201 Jiang, D., Liang, J. & Noble, P. W. Hyaluronan as an immune regulator in human diseases. *Physiol Rev* **91**, 221-264 (2011).
<https://doi.org/10.1152/physrev.00052.2009>
- 202 Jiang, D., Liang, J. & Noble, P. W. Hyaluronan in tissue injury and repair. *Annu Rev Cell Dev Biol* **23**, 435-461 (2007).
<https://doi.org/10.1146/annurev.cellbio.23.090506.123337>
- 203 Petrey, A. C. & de la Motte, C. A. Hyaluronan, a crucial regulator of inflammation. *Front Immunol* **5**, 101 (2014). <https://doi.org/10.3389/fimmu.2014.00101>
- 204 Wang, Q., Teder, P., Judd, N. P., Noble, P. W. & Doerschuk, C. M. CD44 deficiency leads to enhanced neutrophil migration and lung injury in Escherichia coli pneumonia in mice. *Am J Pathol* **161**, 2219-2228 (2002).
[https://doi.org/10.1016/S0002-9440\(10\)64498-7](https://doi.org/10.1016/S0002-9440(10)64498-7)
- 205 van der Windt, G. J. *et al.* CD44 deficiency is associated with increased bacterial clearance but enhanced lung inflammation during Gram-negative pneumonia. *Am J Pathol* **177**, 2483-2494 (2010). <https://doi.org/10.2353/ajpath.2010.100562>
- 206 Nettelbladt, O. & Hallgren, R. Hyaluronan (hyaluronic acid) in bronchoalveolar lavage fluid during the development of bleomycin-induced alveolitis in the rat. *Am Rev Respir Dis* **140**, 1028-1032 (1989).
<https://doi.org/10.1164/ajrccm/140.4.1028>

- 207 Aya, K. L. & Stern, R. Hyaluronan in wound healing: rediscovering a major player. *Wound Repair Regen* **22**, 579-593 (2014).
<https://doi.org/10.1111/wrr.12214>
- 208 Solis, M. A. *et al.* Hyaluronan Upregulates Mitochondrial Biogenesis and Reduces Adenosine Triphosphate Production for Efficient Mitochondrial Function in Slow-Proliferating Human Mesenchymal Stem Cells. *Stem Cells* **34**, 2512-2524 (2016). <https://doi.org/10.1002/stem.2404>
- 209 Culty, M., Nguyen, H. A. & Underhill, C. B. The hyaluronan receptor (CD44) participates in the uptake and degradation of hyaluronan. *J Cell Biol* **116**, 1055-1062 (1992). <https://doi.org/10.1083/jcb.116.4.1055>
- 210 Culty, M., O'Mara, T. E., Underhill, C. B., Yeager, H., Jr. & Swartz, R. P. Hyaluronan receptor (CD44) expression and function in human peripheral blood monocytes and alveolar macrophages. *J Leukoc Biol* **56**, 605-611 (1994).
<https://doi.org/10.1002/jlb.56.5.605>
- 211 Poon, G. F. *et al.* Hyaluronan Binding Identifies a Functionally Distinct Alveolar Macrophage-like Population in Bone Marrow-Derived Dendritic Cell Cultures. *J Immunol* **195**, 632-642 (2015). <https://doi.org/10.4049/jimmunol.1402506>
- 212 Saikia, P. *et al.* Hyaluronic acid 35 normalizes TLR4 signaling in Kupffer cells from ethanol-fed rats via regulation of microRNA291b and its target Tollip. *Sci Rep* **7**, 15671 (2017). <https://doi.org/10.1038/s41598-017-15760-4>
- 213 Saikia, P. *et al.* MicroRNA 181b-3p and its target importin alpha5 regulate toll-like receptor 4 signaling in Kupffer cells and liver injury in mice in response to ethanol. *Hepatology* **66**, 602-615 (2017). <https://doi.org/10.1002/hep.29144>

- 214 Kleinhenz, J. M. *et al.* Disruption of endothelial peroxisome proliferator-activated receptor-gamma reduces vascular nitric oxide production. *Am J Physiol Heart Circ Physiol* **297**, H1647-1654 (2009).
<https://doi.org/10.1152/ajpheart.00148.2009>
- 215 Gomez Perdiguero, E. *et al.* Tissue-resident macrophages originate from yolk-sac-derived erythro-myeloid progenitors. *Nature* **518**, 547-551 (2015).
<https://doi.org/10.1038/nature13989>
- 216 Chen, J., Chen, Z., Narasaraju, T., Jin, N. & Liu, L. Isolation of highly pure alveolar epithelial type I and type II cells from rat lungs. *Lab Invest* **84**, 727-735 (2004). <https://doi.org/10.1038/labinvest.3700095>
- 217 Zhao, T., Su, Z., Li, Y., Zhang, X. & You, Q. Chitinase-3 like-protein-1 function and its role in diseases. *Signal Transduct Target Ther* **5**, 201 (2020).
<https://doi.org/10.1038/s41392-020-00303-7>
- 218 Liang, J. *et al.* Role of hyaluronan and hyaluronan-binding proteins in human asthma. *J Allergy Clin Immunol* **128**, 403-411 e403 (2011).
<https://doi.org/10.1016/j.jaci.2011.04.006>
- 219 Petrigli, G. & Allegra, L. Aerosolised hyaluronic acid prevents exercise-induced bronchoconstriction, suggesting novel hypotheses on the correction of matrix defects in asthma. *Pulm Pharmacol Ther* **19**, 166-171 (2006).
<https://doi.org/10.1016/j.pupt.2005.03.002>
- 220 Klagas, I. *et al.* Decreased hyaluronan in airway smooth muscle cells from patients with asthma and COPD. *Eur Respir J* **34**, 616-628 (2009).
<https://doi.org/10.1183/09031936.00070808>

- 221 Papakonstantinou, E. *et al.* COPD Exacerbations Are Associated With Proinflammatory Degradation of Hyaluronic Acid. *Chest* **148**, 1497-1507 (2015).
<https://doi.org/10.1378/chest.15-0153>
- 222 Esposito, A. J., Bhatraju, P. K., Stapleton, R. D., Wurfel, M. M. & Mikacenic, C. Hyaluronic acid is associated with organ dysfunction in acute respiratory distress syndrome. *Crit Care* **21**, 304 (2017). <https://doi.org/10.1186/s13054-017-1895-7>
- 223 Noble, P. W. & Jiang, D. Matrix regulation of lung injury, inflammation, and repair: the role of innate immunity. *Proc Am Thorac Soc* **3**, 401-404 (2006).
<https://doi.org/10.1513/pats.200604-097AW>
- 224 Tseng, V. *et al.* Extracellular Superoxide Dismutase Regulates Early Vascular Hyaluronan Remodeling in Hypoxic Pulmonary Hypertension. *Sci Rep* **10**, 280 (2020). <https://doi.org/10.1038/s41598-019-57147-7>
- 225 Krupkova, O. *et al.* Expression and activity of hyaluronidases HYAL-1, HYAL-2 and HYAL-3 in the human intervertebral disc. *Eur Spine J* **29**, 605-615 (2020).
<https://doi.org/10.1007/s00586-019-06227-3>
- 226 Weigel, P. H. & Baggenstoss, B. A. What is special about 200 kDa hyaluronan that activates hyaluronan receptor signaling? *Glycobiology* **27**, 868-877 (2017).
<https://doi.org/10.1093/glycob/cwx039>
- 227 Rajasagi, M. *et al.* Anti-CD44 induces apoptosis in T lymphoma via mitochondrial depolarization. *J Cell Mol Med* **14**, 1453-1467 (2010).
<https://doi.org/10.1111/j.1582-4934.2009.00909.x>

- 228 McGarry, T. *et al.* Resolution of TLR2-induced inflammation through manipulation of metabolic pathways in Rheumatoid Arthritis. *Sci Rep* **7**, 43165 (2017).
<https://doi.org/10.1038/srep43165>
- 229 Zhang, Y., Shan, P., Srivastava, A., Li, Z. & Lee, P. J. Endothelial Stanniocalcin 1 Maintains Mitochondrial Bioenergetics and Prevents Oxidant-Induced Lung Injury via Toll-Like Receptor 4. *Antioxid Redox Signal* **30**, 1775-1796 (2019).
<https://doi.org/10.1089/ars.2018.7514>
- 230 Fernandez, S. & Cordoba, M. Hyaluronic acid-induced capacitation involves protein kinase C and tyrosine kinase activity modulation with a lower oxidative metabolism in cryopreserved bull sperm. *Theriogenology* **122**, 68-73 (2018).
<https://doi.org/10.1016/j.theriogenology.2018.09.005>
- 231 Jiang, D. *et al.* Regulation of lung injury and repair by Toll-like receptors and hyaluronan. *Nat Med* **11**, 1173-1179 (2005). <https://doi.org/10.1038/nm1315>
- 232 Cantor, J., Ma, S. & Turino, G. A pilot clinical trial to determine the safety and efficacy of aerosolized hyaluronan as a treatment for COPD. *Int J Chron Obstruct Pulmon Dis* **12**, 2747-2752 (2017). <https://doi.org/10.2147/COPD.S142156>
- 233 Gebe, J. A. *et al.* Modified High-Molecular-Weight Hyaluronan Promotes Allergen-Specific Immune Tolerance. *Am J Respir Cell Mol Biol* **56**, 109-120 (2017). <https://doi.org/10.1165/rcmb.2016-0111OC>
- 234 Haserodt, S., Aytekin, M. & Dweik, R. A. A comparison of the sensitivity, specificity, and molecular weight accuracy of three different commercially available Hyaluronan ELISA-like assays. *Glycobiology* **21**, 175-183 (2011).
<https://doi.org/10.1093/glycob/cwq145>

- 235 Sokolowska, M. *et al.* Low molecular weight hyaluronan activates cytosolic phospholipase A2alpha and eicosanoid production in monocytes and macrophages. *J Biol Chem* **289**, 4470-4488 (2014).
<https://doi.org/10.1074/jbc.M113.515106>
- 236 Stern, R., Asari, A. A. & Sugahara, K. N. Hyaluronan fragments: an information-rich system. *Eur J Cell Biol* **85**, 699-715 (2006).
<https://doi.org/10.1016/j.ejcb.2006.05.009>
- 237 Vistejnova, L. *et al.* Low molecular weight hyaluronan mediated CD44 dependent induction of IL-6 and chemokines in human dermal fibroblasts potentiates innate immune response. *Cytokine* **70**, 97-103 (2014).
<https://doi.org/10.1016/j.cyto.2014.07.006>
- 238 Buonpensiero, P. *et al.* Hyaluronic acid improves "pleasantness" and tolerability of nebulized hypertonic saline in a cohort of patients with cystic fibrosis. *Adv Ther* **27**, 870-878 (2010). <https://doi.org/10.1007/s12325-010-0076-8>
- 239 Savani, R. C. *et al.* A role for hyaluronan in macrophage accumulation and collagen deposition after bleomycin-induced lung injury. *Am J Respir Cell Mol Biol* **23**, 475-484 (2000). <https://doi.org/10.1165/ajrcmb.23.4.3944>
- 240 Vaday, G. G. *et al.* Combinatorial signals by inflammatory cytokines and chemokines mediate leukocyte interactions with extracellular matrix. *J Leukoc Biol* **69**, 885-892 (2001).
- 241 Bollyky, P. L. *et al.* Cutting edge: high molecular weight hyaluronan promotes the suppressive effects of CD4+CD25+ regulatory T cells. *J Immunol* **179**, 744-747 (2007). <https://doi.org/10.4049/jimmunol.179.2.744>

- 242 Johnson, C. G. *et al.* High molecular weight hyaluronan ameliorates allergic inflammation and airway hyperresponsiveness in the mouse. *Am J Physiol Lung Cell Mol Physiol* **315**, L787-L798 (2018).
<https://doi.org/10.1152/ajplung.00009.2018>
- 243 Li, Z., Potts-Kant, E. N., Garantziotis, S., Foster, W. M. & Hollingsworth, J. W. Hyaluronan signaling during ozone-induced lung injury requires TLR4, MyD88, and TIRAP. *PLoS One* **6**, e27137 (2011).
<https://doi.org/10.1371/journal.pone.0027137>
- 244 McKallip, R. J., Ban, H. & Uchakina, O. N. Treatment with the hyaluronic Acid synthesis inhibitor 4-methylumbelliferone suppresses LPS-induced lung inflammation. *Inflammation* **38**, 1250-1259 (2015).
<https://doi.org/10.1007/s10753-014-0092-y>
- 245 Wight, T. N. *et al.* Interplay of extracellular matrix and leukocytes in lung inflammation. *Cell Immunol* **312**, 1-14 (2017).
<https://doi.org/10.1016/j.cellimm.2016.12.003>
- 246 Chang, M. Y. *et al.* A rapid increase in macrophage-derived versican and hyaluronan in infectious lung disease. *Matrix Biol* **34**, 1-12 (2014).
<https://doi.org/10.1016/j.matbio.2014.01.011>
- 247 Dela Cruz, C. S. *et al.* Chitinase 3-like-1 promotes *Streptococcus pneumoniae* killing and augments host tolerance to lung antibacterial responses. *Cell Host Microbe* **12**, 34-46 (2012). <https://doi.org/10.1016/j.chom.2012.05.017>
- 248 Nordenbaek, C. *et al.* YKL-40, a matrix protein of specific granules in neutrophils, is elevated in serum of patients with community-acquired pneumonia requiring

- hospitalization. *J Infect Dis* **180**, 1722-1726 (1999).
<https://doi.org/10.1086/315050>
- 249 Neame, P. J., Christner, J. E. & Baker, J. R. Cartilage proteoglycan aggregates. The link protein and proteoglycan amino-terminal globular domains have similar structures. *J Biol Chem* **262**, 17768-17778 (1987).
- 250 Zimmermann, D. R. & Ruoslahti, E. Multiple domains of the large fibroblast proteoglycan, versican. *EMBO J* **8**, 2975-2981 (1989).
- 251 Goldstein, L. A. *et al.* A human lymphocyte homing receptor, the hermes antigen, is related to cartilage proteoglycan core and link proteins. *Cell* **56**, 1063-1072 (1989). [https://doi.org/10.1016/0092-8674\(89\)90639-9](https://doi.org/10.1016/0092-8674(89)90639-9)
- 252 Kohda, D. *et al.* Solution structure of the link module: a hyaluronan-binding domain involved in extracellular matrix stability and cell migration. *Cell* **86**, 767-775 (1996). [https://doi.org/10.1016/s0092-8674\(00\)80151-8](https://doi.org/10.1016/s0092-8674(00)80151-8)
- 253 Aruffo, A., Stamenkovic, I., Melnick, M., Underhill, C. B. & Seed, B. CD44 is the principal cell surface receptor for hyaluronate. *Cell* **61**, 1303-1313 (1990).
[https://doi.org/10.1016/0092-8674\(90\)90694-a](https://doi.org/10.1016/0092-8674(90)90694-a)
- 254 Miyake, K., Underhill, C. B., Lesley, J. & Kincade, P. W. Hyaluronate can function as a cell adhesion molecule and CD44 participates in hyaluronate recognition. *J Exp Med* **172**, 69-75 (1990). <https://doi.org/10.1084/jem.172.1.69>
- 255 Toole, B. P. Hyaluronan and its binding proteins, the hyaladherins. *Curr Opin Cell Biol* **2**, 839-844 (1990). [https://doi.org/10.1016/0955-0674\(90\)90081-o](https://doi.org/10.1016/0955-0674(90)90081-o)
- 256 Geng, B. *et al.* Chitinase 3-like 1-CD44 interaction promotes metastasis and epithelial-to-mesenchymal transition through beta-catenin/Erk/Akt signaling in

- gastric cancer. *J Exp Clin Cancer Res* **37**, 208 (2018).
<https://doi.org/10.1186/s13046-018-0876-2>
- 257 Malinda, K. M., Ponce, L., Kleinman, H. K., Shackelton, L. M. & Millis, A. J. Gp38k, a protein synthesized by vascular smooth muscle cells, stimulates directional migration of human umbilical vein endothelial cells. *Exp Cell Res* **250**, 168-173 (1999). <https://doi.org/10.1006/excr.1999.4511>
- 258 Nishikawa, K. C. & Millis, A. J. gp38k (CHI3L1) is a novel adhesion and migration factor for vascular cells. *Exp Cell Res* **287**, 79-87 (2003).
[https://doi.org/10.1016/s0014-4827\(03\)00069-7](https://doi.org/10.1016/s0014-4827(03)00069-7)
- 259 Lee, D. H. *et al.* Chitinase-3-like-1 deficiency attenuates ethanol-induced liver injury by inhibition of sterol regulatory element binding protein 1-dependent triglyceride synthesis. *Metabolism* **95**, 46-56 (2019).
<https://doi.org/10.1016/j.metabol.2019.03.010>
- 260 Nojgaard, C. *et al.* Serum levels of YKL-40 and PIIINP as prognostic markers in patients with alcoholic liver disease. *J Hepatol* **39**, 179-186 (2003).
[https://doi.org/10.1016/s0168-8278\(03\)00184-3](https://doi.org/10.1016/s0168-8278(03)00184-3)
- 261 Johansen, J. S. *et al.* Serum YKL-40 is increased in patients with hepatic fibrosis. *J Hepatol* **32**, 911-920 (2000). [https://doi.org/10.1016/s0168-8278\(00\)80095-1](https://doi.org/10.1016/s0168-8278(00)80095-1)
- 262 Kronborg, G. *et al.* Serum level of YKL-40 is elevated in patients with *Streptococcus pneumoniae* bacteremia and is associated with the outcome of the disease. *Scand J Infect Dis* **34**, 323-326 (2002).
<https://doi.org/10.1080/00365540110080233>

- 263 Ostergaard, C., Johansen, J. S., Benfield, T., Price, P. A. & Lundgren, J. D. YKL-40 is elevated in cerebrospinal fluid from patients with purulent meningitis. *Clin Diagn Lab Immunol* **9**, 598-604 (2002). <https://doi.org/10.1128/cdli.9.3.598-604.2002>
- 264 Milner, C. M., Tongsoongnoen, W., Rugg, M. S. & Day, A. J. The molecular basis of inter-alpha-inhibitor heavy chain transfer on to hyaluronan. *Biochem Soc Trans* **35**, 672-676 (2007). <https://doi.org/10.1042/BST0350672>
- 265 Salustri, A. *et al.* PTX3 plays a key role in the organization of the cumulus oophorus extracellular matrix and in in vivo fertilization. *Development* **131**, 1577-1586 (2004). <https://doi.org/10.1242/dev.01056>
- 266 Stober, V. P. *et al.* TNF-stimulated gene 6 promotes formation of hyaluronan-inter-alpha-inhibitor heavy chain complexes necessary for ozone-induced airway hyperresponsiveness. *J Biol Chem* **292**, 20845-20858 (2017). <https://doi.org/10.1074/jbc.M116.756627>
- 267 Garantziotis, S. *et al.* Hyaluronan mediates ozone-induced airway hyperresponsiveness in mice. *J Biol Chem* **284**, 11309-11317 (2009). <https://doi.org/10.1074/jbc.M802400200>
- 268 Garantziotis, S. *et al.* TLR4 is necessary for hyaluronan-mediated airway hyperresponsiveness after ozone inhalation. *Am J Respir Crit Care Med* **181**, 666-675 (2010). <https://doi.org/10.1164/rccm.200903-0381OC>
- 269 Lazrak, A. *et al.* Hyaluronan mediates airway hyperresponsiveness in oxidative lung injury. *Am J Physiol Lung Cell Mol Physiol* **308**, L891-903 (2015). <https://doi.org/10.1152/ajplung.00377.2014>

- 270 Swaidani, S. *et al.* TSG-6 protein is crucial for the development of pulmonary hyaluronan deposition, eosinophilia, and airway hyperresponsiveness in a murine model of asthma. *J Biol Chem* **288**, 412-422 (2013).
<https://doi.org/10.1074/jbc.M112.389874>
- 271 Balhara, J. *et al.* PTX3 Deficiency Promotes Enhanced Accumulation and Function of CD11c(+)CD11b(+) DCs in a Murine Model of Allergic Inflammation. *Front Immunol* **12**, 641311 (2021). <https://doi.org/10.3389/fimmu.2021.641311>
- 272 Jourdain, M. *et al.* Effects of N omega-nitro-L-arginine methyl ester on the endotoxin-induced disseminated intravascular coagulation in porcine septic shock. *Crit Care Med* **25**, 452-459 (1997). <https://doi.org/10.1097/00003246-199703000-00014>
- 273 Mandi, Y. *et al.* The Opposite Effects of Kynurenic Acid and Different Kynurenic Acid Analogs on Tumor Necrosis Factor-alpha (TNF-alpha) Production and Tumor Necrosis Factor-Stimulated Gene-6 (TSG-6) Expression. *Front Immunol* **10**, 1406 (2019). <https://doi.org/10.3389/fimmu.2019.01406>
- 274 Bottazzi, B. *et al.* The long pentraxin PTX3 as a link among innate immunity, inflammation, and female fertility. *J Leukoc Biol* **79**, 909-912 (2006).
<https://doi.org/10.1189/jlb.1005557>
- 275 Deban, L., Jaillon, S., Garlanda, C., Bottazzi, B. & Mantovani, A. Pentraxins in innate immunity: lessons from PTX3. *Cell Tissue Res* **343**, 237-249 (2011).
<https://doi.org/10.1007/s00441-010-1018-0>

- 276 Presta, M., Camozzi, M., Salvatori, G. & Rusnati, M. Role of the soluble pattern recognition receptor PTX3 in vascular biology. *J Cell Mol Med* **11**, 723-738 (2007). <https://doi.org/10.1111/j.1582-4934.2007.00061.x>
- 277 Kasuda, S., Kudo, R., Yuui, K., Sakurai, Y. & Hatake, K. Acute ethanol intoxication suppresses pentraxin 3 expression in a mouse sepsis model involving cecal ligation and puncture. *Alcohol* **64**, 1-9 (2017). <https://doi.org/10.1016/j.alcohol.2017.04.003>
- 278 Jimenez, V. M., Jr., Settles, E. W., Currie, B. J., Keim, P. S. & Monroy, F. P. Persistence of *Burkholderia thailandensis* E264 in lung tissue after a single binge alcohol episode. *PLoS One* **14**, e0218147 (2019). <https://doi.org/10.1371/journal.pone.0218147>
- 279 Hallgren, O. *et al.* Altered fibroblast proteoglycan production in COPD. *Respir Res* **11**, 55 (2010). <https://doi.org/10.1186/1465-9921-11-55>
- 280 Evanko, S. P., Potter-Perigo, S., Johnson, P. Y. & Wight, T. N. Organization of hyaluronan and versican in the extracellular matrix of human fibroblasts treated with the viral mimetic poly I:C. *J Histochem Cytochem* **57**, 1041-1060 (2009). <https://doi.org/10.1369/jhc.2009.953802>
- 281 Chang, M. Y. *et al.* Versican is produced by Trif- and type I interferon-dependent signaling in macrophages and contributes to fine control of innate immunity in lungs. *Am J Physiol Lung Cell Mol Physiol* **313**, L1069-L1086 (2017). <https://doi.org/10.1152/ajplung.00353.2017>
- 282 Elibol, B., Beker, M., Jakubowska-Dogru, E. & Kilic, U. Fetal alcohol and maternal stress modify the expression of proteins controlling postnatal

- development of the male rat hippocampus. *Am J Drug Alcohol Abuse* **46**, 718-730 (2020). <https://doi.org/10.1080/00952990.2020.1780601>
- 283 Wang, W. *et al.* Ligation of TLR2 by versican: a link between inflammation and metastasis. *Arch Med Res* **40**, 321-323 (2009).
<https://doi.org/10.1016/j.arcmed.2009.04.005>
- 284 Zhang, Z., Miao, L. & Wang, L. Inflammation amplification by Versican: the first mediator. *Int J Mol Sci* **13**, 6873-6882 (2012).
<https://doi.org/10.3390/ijms13066873>
- 285 Snyder, J. M., Washington, I. M., Birkland, T., Chang, M. Y. & Frevert, C. W. Correlation of Versican Expression, Accumulation, and Degradation during Embryonic Development by Quantitative Immunohistochemistry. *J Histochem Cytochem* **63**, 952-967 (2015). <https://doi.org/10.1369/0022155415610383>
- 286 Kang, I. *et al.* Versican Deficiency Significantly Reduces Lung Inflammatory Response Induced by Polyinosine-Polycytidylic Acid Stimulation. *J Biol Chem* **292**, 51-63 (2017). <https://doi.org/10.1074/jbc.M116.753186>
- 287 Currie, A. J. *et al.* Primary immunodeficiency to pneumococcal infection due to a defect in Toll-like receptor signaling. *J Pediatr* **144**, 512-518 (2004).
<https://doi.org/10.1016/j.jpeds.2003.10.034>
- 288 Bailey, K. L. *et al.* Alcohol and cannabis use alter pulmonary innate immunity. *Alcohol* **80**, 131-138 (2019). <https://doi.org/10.1016/j.alcohol.2018.11.002>
- 289 Wight, T. N., Kang, I. & Merrilees, M. J. Versican and the control of inflammation. *Matrix Biol* **35**, 152-161 (2014). <https://doi.org/10.1016/j.matbio.2014.01.015>

- 290 D'Souza, M. & Datta, K. Evidence for naturally occurring hyaluronic acid binding protein in rat liver. *Biochem Int* **10**, 43-51 (1985).
- 291 Turley, E. A., Noble, P. W. & Bourguignon, L. Y. Signaling properties of hyaluronan receptors. *J Biol Chem* **277**, 4589-4592 (2002).
<https://doi.org/10.1074/jbc.R100038200>
- 292 Yang, B., Zhang, L. & Turley, E. A. Identification of two hyaluronan-binding domains in the hyaluronan receptor RHAMM. *J Biol Chem* **268**, 8617-8623 (1993).
- 293 Assmann, V., Jenkinson, D., Marshall, J. F. & Hart, I. R. The intracellular hyaluronan receptor RHAMM/IHABP interacts with microtubules and actin filaments. *J Cell Sci* **112 (Pt 22)**, 3943-3954 (1999).
- 294 Entwistle, J., Hall, C. L. & Turley, E. A. HA receptors: regulators of signalling to the cytoskeleton. *J Cell Biochem* **61**, 569-577 (1996).
[https://doi.org/10.1002/\(sici\)1097-4644\(19960616\)61:4<569::aid-jcb10>3.0.co;2-b](https://doi.org/10.1002/(sici)1097-4644(19960616)61:4<569::aid-jcb10>3.0.co;2-b)
- 295 Lynn, B. D., Turley, E. A. & Nagy, J. I. Subcellular distribution, calmodulin interaction, and mitochondrial association of the hyaluronan-binding protein RHAMM in rat brain. *J Neurosci Res* **65**, 6-16 (2001).
<https://doi.org/10.1002/jnr.1122>
- 296 Sherman, L., Sleeman, J., Herrlich, P. & Ponta, H. Hyaluronate receptors: key players in growth, differentiation, migration and tumor progression. *Curr Opin Cell Biol* **6**, 726-733 (1994). [https://doi.org/10.1016/0955-0674\(94\)90100-7](https://doi.org/10.1016/0955-0674(94)90100-7)

- 297 Zaman, A. *et al.* Expression and role of the hyaluronan receptor RHAMM in inflammation after bleomycin injury. *Am J Respir Cell Mol Biol* **33**, 447-454 (2005). <https://doi.org/10.1165/rcmb.2004-0333OC>
- 298 Nedvetzki, S. *et al.* RHAMM, a receptor for hyaluronan-mediated motility, compensates for CD44 in inflamed CD44-knockout mice: a different interpretation of redundancy. *Proc Natl Acad Sci U S A* **101**, 18081-18086 (2004). <https://doi.org/10.1073/pnas.0407378102>
- 299 Samuel, S. K. *et al.* TGF-beta 1 stimulation of cell locomotion utilizes the hyaluronan receptor RHAMM and hyaluronan. *J Cell Biol* **123**, 749-758 (1993). <https://doi.org/10.1083/jcb.123.3.749>
- 300 Szabo, G., Mandrekar, P., Girouard, L. & Catalano, D. Regulation of human monocyte functions by acute ethanol treatment: decreased tumor necrosis factor-alpha, interleukin-1 beta and elevated interleukin-10, and transforming growth factor-beta production. *Alcohol Clin Exp Res* **20**, 900-907 (1996). <https://doi.org/10.1111/j.1530-0277.1996.tb05269.x>
- 301 Kaphalia, L. & Calhoun, W. J. Alcoholic lung injury: metabolic, biochemical and immunological aspects. *Toxicol Lett* **222**, 171-179 (2013). <https://doi.org/10.1016/j.toxlet.2013.07.016>
- 302 Jha, B. K. *et al.* pH and cation-induced thermodynamic stability of human hyaluronan binding protein 1 regulates its hyaluronan affinity. *J Biol Chem* **279**, 23061-23072 (2004). <https://doi.org/10.1074/jbc.M310676200>

- 303 Yadav, G. *et al.* Evidence for inhibitory interaction of hyaluronan-binding protein 1 (HABP1/p32/gC1qR) with *Streptococcus pneumoniae* hyaluronidase. *J Biol Chem* **284**, 3897-3905 (2009). <https://doi.org/10.1074/jbc.M804246200>
- 304 Fogal, V. *et al.* Mitochondrial p32 protein is a critical regulator of tumor metabolism via maintenance of oxidative phosphorylation. *Mol Cell Biol* **30**, 1303-1318 (2010). <https://doi.org/10.1128/MCB.01101-09>
- 305 Muta, T., Kang, D., Kitajima, S., Fujiwara, T. & Hamasaki, N. p32 protein, a splicing factor 2-associated protein, is localized in mitochondrial matrix and is functionally important in maintaining oxidative phosphorylation. *J Biol Chem* **272**, 24363-24370 (1997). <https://doi.org/10.1074/jbc.272.39.24363>
- 306 Yagi, M. *et al.* p32/gC1qR is indispensable for fetal development and mitochondrial translation: importance of its RNA-binding ability. *Nucleic Acids Res* **40**, 9717-9737 (2012). <https://doi.org/10.1093/nar/gks774>
- 307 Sunderhauf, A. *et al.* GC1qR Cleavage by Caspase-1 Drives Aerobic Glycolysis in Tumor Cells. *Front Oncol* **10**, 575854 (2020). <https://doi.org/10.3389/fonc.2020.575854>
- 308 Sun, Y. J., Shi, G. H., Zhao, W. W. & Zheng, S. Y. HABP1 promotes proliferation and invasion of lung adenocarcinoma cells through NFkappaB pathway. *Neoplasma* (2021). https://doi.org/10.4149/neo_2021_210904N1271
- 309 Sumiya, J. *et al.* Isolation and characterization of the plasma hyaluronan-binding protein (PHBP) gene (HABP2). *J Biochem* **122**, 983-990 (1997). <https://doi.org/10.1093/oxfordjournals.jbchem.a021861>

- 310 Mambetsariev, N. *et al.* Hyaluronic Acid binding protein 2 is a novel regulator of vascular integrity. *Arterioscler Thromb Vasc Biol* **30**, 483-490 (2010).
<https://doi.org/10.1161/ATVBAHA.109.200451>
- 311 Wygrecka, M., Markart, P., Fink, L., Guenther, A. & Preissner, K. T. Raised protein levels and altered cellular expression of factor VII activating protease (FSAP) in the lungs of patients with acute respiratory distress syndrome (ARDS). *Thorax* **62**, 880-888 (2007). <https://doi.org/10.1136/thx.2006.069658>
- 312 Byskov, K., Etscheid, M. & Kanse, S. M. Cellular effects of factor VII activating protease (FSAP). *Thromb Res* **188**, 74-78 (2020).
<https://doi.org/10.1016/j.thromres.2020.02.010>
- 313 Moraes, T. J. *et al.* Role of PAR2 in murine pulmonary pseudomonal infection. *Am J Physiol Lung Cell Mol Physiol* **294**, L368-377 (2008).
<https://doi.org/10.1152/ajplung.00036.2007>
- 314 Kager, L. M. *et al.* Overexpression of the endothelial protein C receptor is detrimental during pneumonia-derived gram-negative sepsis (Melioidosis). *PLoS Negl Trop Dis* **7**, e2306 (2013). <https://doi.org/10.1371/journal.pntd.0002306>
- 315 Schouten, M., van't Veer, C., Roelofs, J. J., Levi, M. & van der Poll, T. Protease-activated receptor-1 impairs host defense in murine pneumococcal pneumonia: a controlled laboratory study. *Crit Care* **16**, R238 (2012).
<https://doi.org/10.1186/cc11910>
- 316 Johnson, L. A. *et al.* Dendritic cells enter lymph vessels by hyaluronan-mediated docking to the endothelial receptor LYVE-1. *Nat Immunol* **18**, 762-770 (2017).
<https://doi.org/10.1038/ni.3750>

- 317 Banerji, S. *et al.* LYVE-1, a new homologue of the CD44 glycoprotein, is a lymph-specific receptor for hyaluronan. *J Cell Biol* **144**, 789-801 (1999).
<https://doi.org/10.1083/jcb.144.4.789>
- 318 Jackson, D. G. Leucocyte Trafficking via the Lymphatic Vasculature-Mechanisms and Consequences. *Front Immunol* **10**, 471 (2019).
<https://doi.org/10.3389/fimmu.2019.00471>
- 319 Green, D. E. *et al.* Peroxisome proliferator-activated receptor- γ enhances human pulmonary artery smooth muscle cell apoptosis through microRNA-21 and programmed cell death 4. *Am J Physiol Lung Cell Mol Physiol* **313**, L371-L383 (2017). <https://doi.org/10.1152/ajplung.00532.2016>
- 320 Yeligar, S. M. *et al.* PPAR γ Regulates Mitochondrial Structure and Function and Human Pulmonary Artery Smooth Muscle Cell Proliferation. *Am J Respir Cell Mol Biol* **58**, 648-657 (2018). <https://doi.org/10.1165/rcmb.2016-0293OC>
- 321 Paulin, R. & Michelakis, E. D. The metabolic theory of pulmonary arterial hypertension. *Circ Res* **115**, 148-164 (2014).
<https://doi.org/10.1161/CIRCRESAHA.115.301130>
- 322 Bonnet, S. *et al.* An abnormal mitochondrial-hypoxia inducible factor-1 α -Kv channel pathway disrupts oxygen sensing and triggers pulmonary arterial hypertension in fawn hooded rats: similarities to human pulmonary arterial hypertension. *Circulation* **113**, 2630-2641 (2006).
<https://doi.org/10.1161/CIRCULATIONAHA.105.609008>

- 323 Fijalkowska, I. *et al.* Hypoxia inducible-factor1alpha regulates the metabolic shift of pulmonary hypertensive endothelial cells. *Am J Pathol* **176**, 1130-1138 (2010). <https://doi.org/10.2353/ajpath.2010.090832>
- 324 Marsboom, G. *et al.* Dynamin-related protein 1-mediated mitochondrial mitotic fission permits hyperproliferation of vascular smooth muscle cells and offers a novel therapeutic target in pulmonary hypertension. *Circ Res* **110**, 1484-1497 (2012). <https://doi.org/10.1161/CIRCRESAHA.111.263848>
- 325 Blum, J. I., Bijli, K. M., Murphy, T. C., Kleinhenz, J. M. & Hart, C. M. Time-dependent PPAR γ Modulation of HIF-1 α Signaling in Hypoxic Pulmonary Artery Smooth Muscle Cells. *Am J Med Sci* **352**, 71-79 (2016). <https://doi.org/10.1016/j.amjms.2016.03.019>
- 326 Rafikov, R. *et al.* Complex I dysfunction underlies the glycolytic switch in pulmonary hypertensive smooth muscle cells. *Redox Biol* **6**, 278-286 (2015). <https://doi.org/10.1016/j.redox.2015.07.016>
- 327 Tseng, V. *et al.* 3'UTR shortening of HAS2 promotes hyaluronan hyper-synthesis and bioenergetic dysfunction in pulmonary hypertension. *Matrix Biol* **111**, 53-75 (2022). <https://doi.org/10.1016/j.matbio.2022.06.001>
- 328 Wang, Y. *et al.* The role of mitochondrial dynamics in disease. *MedComm* (2020) **4**, e462 (2023). <https://doi.org/10.1002/mco2.462>
- 329 Warburg, O., Wind, F. & Negelein, E. The Metabolism of Tumors in the Body. *J Gen Physiol* **8**, 519-530 (1927). <https://doi.org/10.1085/jgp.8.6.519>

- 330 Antico Arciuch, V. G., Elguero, M. E., Poderoso, J. J. & Carreras, M. C. Mitochondrial regulation of cell cycle and proliferation. *Antioxid Redox Signal* **16**, 1150-1180 (2012). <https://doi.org/10.1089/ars.2011.4085>
- 331 Ferraro, E., Germano, M., Mollace, R., Mollace, V. & Malara, N. HIF-1, the Warburg Effect, and Macrophage/Microglia Polarization Potential Role in COVID-19 Pathogenesis. *Oxid Med Cell Longev* **2021**, 8841911 (2021). <https://doi.org/10.1155/2021/8841911>
- 332 De Santa, F., Vitiello, L., Torcinaro, A. & Ferraro, E. The Role of Metabolic Remodeling in Macrophage Polarization and Its Effect on Skeletal Muscle Regeneration. *Antioxid Redox Signal* **30**, 1553-1598 (2019). <https://doi.org/10.1089/ars.2017.7420>
- 333 Breda, C. N. S., Davanzo, G. G., Basso, P. J., Saraiva Camara, N. O. & Moraes-Vieira, P. M. M. Mitochondria as central hub of the immune system. *Redox Biol* **26**, 101255 (2019). <https://doi.org/10.1016/j.redox.2019.101255>
- 334 Pearce, E. L. & Pearce, E. J. Metabolic pathways in immune cell activation and quiescence. *Immunity* **38**, 633-643 (2013). <https://doi.org/10.1016/j.immuni.2013.04.005>
- 335 Lee, S. E. *et al.* RGS14 is a natural suppressor of both synaptic plasticity in CA2 neurons and hippocampal-based learning and memory. *Proc Natl Acad Sci U S A* **107**, 16994-16998 (2010). <https://doi.org/10.1073/pnas.1005362107>
- 336 Harbin, N. H., Bramlett, S. N., Montanez-Miranda, C., Terzioglu, G. & Hepler, J. R. RGS14 Regulation of Post-Synaptic Signaling and Spine Plasticity in Brain. *Int J Mol Sci* **22** (2021). <https://doi.org/10.3390/ijms22136823>

- 337 Shu, F. J., Ramineni, S., Amyot, W. & Hepler, J. R. Selective interactions between Gi alpha1 and Gi alpha3 and the GoLoco/GPR domain of RGS14 influence its dynamic subcellular localization. *Cell Signal* **19**, 163-176 (2007). <https://doi.org/10.1016/j.cellsig.2006.06.002>
- 338 Harbin, N. H. *et al.* RGS14 limits seizure-induced mitochondrial oxidative stress and pathology in hippocampus. *Neurobiol Dis* **181**, 106128 (2023). <https://doi.org/10.1016/j.nbd.2023.106128>
- 339 Petsophonsakul, P. *et al.* Role of Vascular Smooth Muscle Cell Phenotypic Switching and Calcification in Aortic Aneurysm Formation. *Arterioscler Thromb Vasc Biol* **39**, 1351-1368 (2019). <https://doi.org/10.1161/ATVBAHA.119.312787>
- 340 Mabanglo, M. F. & Houry, W. A. Recent structural insights into the mechanism of ClpP protease regulation by AAA+ chaperones and small molecules. *J Biol Chem* **298**, 101781 (2022). <https://doi.org/10.1016/j.jbc.2022.101781>
- 341 Baker, T. A. & Sauer, R. T. ClpXP, an ATP-powered unfolding and protein-degradation machine. *Biochim Biophys Acta* **1823**, 15-28 (2012). <https://doi.org/10.1016/j.bbamcr.2011.06.007>
- 342 CDC– fact sheets: “alcohol use and health–alcohol”. *Centers for Disease Control and Prevention; Atlanta, GA* (2018).
- 343 Plowman, P. N. The pulmonary macrophage population of human smokers. *Ann Occup Hyg* **25**, 393-405 (1982). <https://doi.org/10.1093/annhyg/25.4.393>
- 344 Martin, R. R. Cigarette smoking and human pulmonary macrophages. *Hosp Pract* **12**, 97-104 (1977). <https://doi.org/10.1080/21548331.1977.11707193>

- 345 Romberger, D. J. & Grant, K. Alcohol consumption and smoking status: the role of smoking cessation. *Biomed Pharmacother* **58**, 77-83 (2004).
<https://doi.org/10.1016/j.biopha.2003.12.002>
- 346 Osna, N. A. *et al.* Second hits exacerbate alcohol-related organ damage: an update. *Alcohol Alcohol* **56**, 8-16 (2021). <https://doi.org/10.1093/alcalc/agaa085>
- 347 Gaydos, J. *et al.* Alcohol abuse and smoking alter inflammatory mediator production by pulmonary and systemic immune cells. *Am J Physiol Lung Cell Mol Physiol* **310**, L507-518 (2016). <https://doi.org/10.1152/ajplung.00242.2015>
- 348 Hernandez-Quiles, M., Broekema, M. F. & Kalkhoven, E. PPARgamma in Metabolism, Immunity, and Cancer: Unified and Diverse Mechanisms of Action. *Front Endocrinol (Lausanne)* **12**, 624112 (2021).
<https://doi.org/10.3389/fendo.2021.624112>
- 349 Wagner, N. & Wagner, K. D. The Role of PPARs in Disease. *Cells* **9** (2020).
<https://doi.org/10.3390/cells9112367>
- 350 Mindell, J. A. Lysosomal acidification mechanisms. *Annu Rev Physiol* **74**, 69-86 (2012). <https://doi.org/10.1146/annurev-physiol-012110-142317>
- 351 Nauseef, W. M. Detection of superoxide anion and hydrogen peroxide production by cellular NADPH oxidases. *Biochim Biophys Acta* **1840**, 757-767 (2014).
<https://doi.org/10.1016/j.bbagen.2013.04.040>
- 352 Downs, C. A. *et al.* Ethanol alters alveolar fluid balance via Nadph oxidase (NOX) signaling to epithelial sodium channels (ENaC) in the lung. *PLoS One* **8**, e54750 (2013). <https://doi.org/10.1371/journal.pone.0054750>

- 353 Yeligar, S. M., Harris, F. L., Brown, L. A. S. & Hart, C. M. Pharmacological reversal of post-transcriptional alterations implicated in alcohol-induced alveolar macrophage dysfunction. *Alcohol* **106**, 30-43 (2023).
<https://doi.org/10.1016/j.alcohol.2022.10.003>
- 354 Zakhari, S. Alcohol metabolism and epigenetics changes. *Alcohol Res* **35**, 6-16 (2013).
- 355 Alli, A. A. *et al.* Chronic ethanol exposure alters the lung proteome and leads to mitochondrial dysfunction in alveolar type 2 cells. *Am J Physiol Lung Cell Mol Physiol* **306**, L1026-1035 (2014). <https://doi.org/10.1152/ajplung.00287.2013>
- 356 Downs, C. A., Trac, D., Brewer, E. M., Brown, L. A. & Helms, M. N. Chronic alcohol ingestion changes the landscape of the alveolar epithelium. *Biomed Res Int* **2013**, 470217 (2013). <https://doi.org/10.1155/2013/470217>
- 357 Polikandriotis, J. A. *et al.* Chronic ethanol ingestion increases superoxide production and NADPH oxidase expression in the lung. *Am J Respir Cell Mol Biol* **34**, 314-319 (2006). <https://doi.org/10.1165/rcmb.2005-0320OC>
- 358 Asayama, K. *et al.* Immunolocalization of cellular glutathione peroxidase in adult rat lungs and quantitative analysis after postembedding immunogold labeling. *Histochem Cell Biol* **105**, 383-389 (1996). <https://doi.org/10.1007/BF01463659>
- 359 Murphy, M. P. *et al.* Guidelines for measuring reactive oxygen species and oxidative damage in cells and in vivo. *Nat Metab* **4**, 651-662 (2022).
<https://doi.org/10.1038/s42255-022-00591-z>
- 360 Halliwell, B. G. J. M. C. *Free Radicals in Biology and Medicine 5th edn.*

- 361 Long, M. E., Mallampalli, R. K. & Horowitz, J. C. Pathogenesis of pneumonia and acute lung injury. *Clin Sci (Lond)* **136**, 747-769 (2022).
<https://doi.org/10.1042/CS20210879>
- 362 Regunath, H. & Oba, Y. in *StatPearls* (2023).